Title
Functional connectivity in a circuit that mediates song learning and behavior

Author
Kimpo, Rhea R.

Publication Date
2000

Peer reviewed|Thesis/dissertation

Functional Connectivity in a Circuit that Mediates Song Learning and Behavior

by

Rhea R. Kimpo

DISSERTATION

Submitted in partial satisfaction of the requirements for the degree of

DOCTOR OF PHILOSOPHY

in

Neuroscience

in the

GRADUATE DIVISION

of the

UNIVERSITY OF CALIFORNIA SAN FRANCISCO

Date University Librarian

Degree Conferred: .....

ACKNOWLEDGEMENTS

I thank Allison Doupe for being a great advisor and a true mentor to me. I have learned a great deal from her, and I will undoubtedly continue to do so. Allison's tireless commitment to my graduate education enabled me to accomplish many daunting tasks. Her devotion and enthusiasm for science also made my tenure in her lab very exciting and stimulating. Allison's critical thinking has continually challenged me to raise my level of scientific understanding. Her belief that I could do so has provided me with the inspiration and conviction to be a good scientist. If I were given the chance to do my thesis work all over, I would still choose to work with her.

I was also extraordinarily fortunate to have worked with Frederic Theunissen. I truly enjoyed working with him, and I thank him for his willingness to share his expertise and knowledge. He always gave very thoughtful and instructive answers to my questions, for which I am truly appreciative.

I would like to acknowledge the insightful advice that I received from my thesis committee: Stephen Lisberger (chair), Allison Doupe, Christoph Schreiner, Michael Stryker, and Yang Dan. They provided me with different excellent point of views regarding my work. I believe that my thesis improved considerably as a result of their guidance and scientific wisdom.

I also thank Charlotte Boettiger, Gabriela Carrillo, Mimi Kao and Michele Solis, my fellow graduate students in the Doupe Lab, for their camaraderie and friendship. Their readiness to share their experience and to dispense advice helped me navigate through graduate school. I also thank them for their willingness to share their scientific knowledge, from which many enjoyable discussions ensued. I am especially thankful for Charlotte's and Mimi's interest in my work. They have contributed to my understanding of my research, and how my results relate to their own studies.

I am also grateful for the scientific discussions and advice from the other members of the Doupe Lab: Michael Brainard, Neal Hessler, Katherine Moortgat, Cooper Roddey,

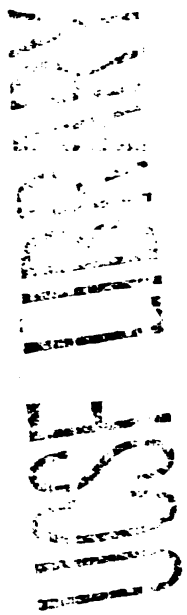

Kamal Sen, Todd Troyer, and Brian Wright. My research was much improved from the thorough scrutiny of the Doupe Lab members. I want to specifically thank Michael Brainard, Cooper Roddey, Kamal Sen, and Todd Troyer for their invaluable comments which broadened my understanding of my work.

I would like to acknowledge the love and support of my parents, Ramon and Ruth Kimpo; without them, graduate school would have been very difficult. They have given me the strength and courage to accomplish whatever I set my sights on. Moreover, they have provided me with the opportunity to study in this country, for which I am eternally grateful. They are, without a doubt, my true heroes.

Finally, I thank the person who completes me, Benedict Gallardo. His love and devotion has taken me through many happy and trying times, from UC Berkeley to UC San Francisco. I always appreciated his scientific opinion about my work, which helped me view my research in a different light. I look forward to our lifelong collaboration.

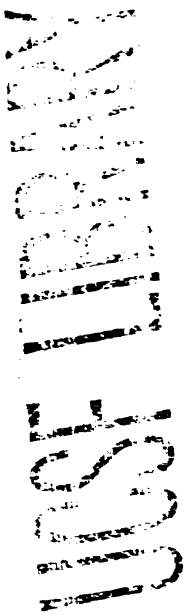

The text of Chapter 2 is a reprint of the material as it appears in *Neuron*. The co-author listed (Allison J. Doupe) directed and supervised the research that forms the basis for the dissertation.

Functional Connectivity in a Circuit that Mediates Song Learning and Behavior

by

Rhea R. Kimpo

ABSTRACT

The song system mediates song learning and behavior in songbirds. It has two functionally distinct pathways: the motor pathway, which is essential for song production, and the anterior forebrain pathway (AFP), which is necessary during song learning. One hypothesized role of the AFP is to mediate the auditory feedback that is crucial for song learning, through its projection to the motor pathway. Consistent with this hypothesis, AFP neurons are auditory and selective for the bird's own song (BOS) in adults that have completed learning. The neural interactions between the song pathways may therefore reveal the processes that underlie song learning and behavior. To investigate these neural interactions, we studied the induction of an immediate early gene (IEG) product, analyzed the cross-covariance and coherency of simultaneously recorded activity, and compared simultaneously recorded auditory responses in these two pathways.

The induction of an IEG product in adults revealed that the activity of two populations of neurons in the motor pathway is associated with song production, suggesting a role in song maintenance. Cross-covariance and coherency analyses showed robust correlated activity between LMAN, the output nucleus of the AFP, and its target pre-motor nucleus, RA. The direct LMAN-RA correlated activity was stronger in adults than juveniles, even though adults have completed song learning. We detected correlated activity between indirectly connected nuclei, suggesting that functional connectivity in the song system involves a highly interconnected network of neurons. Correlated activity between some song nuclei was variable, indicating that the functional connectivity may have several states. The timing and strength of LMAN-RA correlated activity changed significantly with age, consistent with these changes being important for song learning. Selectivity in RA reflected

those of its afferent nuclei in distinct ways, and increased with age, suggesting that this selectivity plays a role in song learning.

The complex neural interactions in the song system highlight the importance of studying simultaneous activity of nuclei within the song system. These neural interactions may underlie the processes by which the song system mediates song learning and behavior.

Stephen G. Lisberger

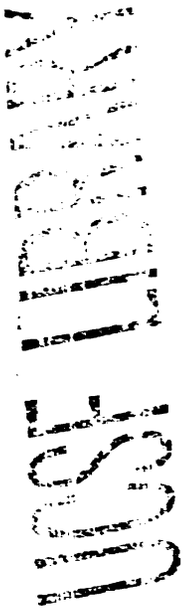

TABLE OF CONTENTS

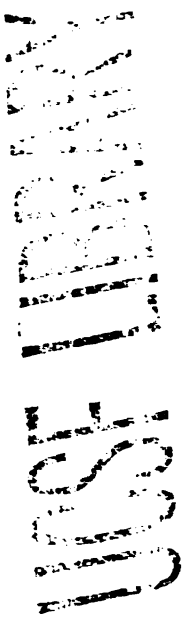

LIST OF TABLES

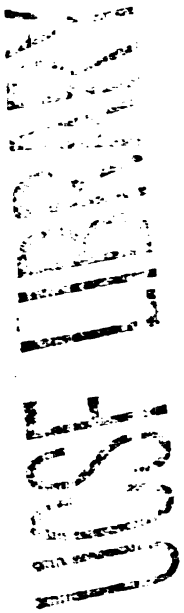

LIST OF FIGURES

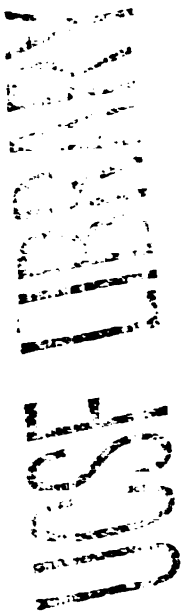

Chapter 1:

Background and Experimental Rationale

Understanding the neural basis of learning and memory is a central question in neuroscience. Birdsong provides an excellent model for studying the neural processes that underlie learning. It is a natural behavior that is learned during the first few months of life, and involves precise coordination of the vocal musculature and respiratory apparatus. Song learning in birds also has many parallels with human speech (Doupe and Kuhl, 1999), and may therefore provide insight into general neural processes that mediate learning of vocalizations. Indeed, the avian groups that learn their vocalizations, which are songbirds (Passeriformes), parrots (Psittaciformes), and hummingbirds (Trochiliformes), are the only readily accessible animal models for learned vocalizations. The singing behavior of these birds is well described by decades of behavioral research, providing a wealth of information upon which neuroscience experiments can be based. Moreover, discrete neural structures that are unique to birds that learn how to vocalize have been identified (Nottebohm et al, 1976). This network of neural structures, called the song system, mediates song learning. Consistent with their role in song learning, these structures are absent in birds that vocalize but do not learn their vocalizations (Kroodsma and Konishi, 1991). Studies of the neural interactions within the song system could reveal processes that may underlie song learning in songbirds. In this thesis, three different approaches were employed to investigate these neural interactions: the induction of an immediate early gene, the correlation of simultaneous activity in intact animals, and the comparison of selectivity of auditory responses between song nuclei and across development.

Auditory experience is crucial for song learning

Birdsong, like human speech, requires normal auditory experience in order for learning to progress normally. Song learning occurs in two phases, during the first few months of life. During the first or "sensory" phase, the juvenile bird listens to and memorizes the tutor song. Isolation of young birds during the sensory phase leads to abnormal vocalizations (Eales, 1985, 1987; Morrison and Nottebohm, 1993). The sensory

phase is followed by the sensorimotor phase, in which the juvenile initially sings rambling songs, called plastic songs. Plastic songs are lower in amplitude, have poor syllable morphology and variable syllable sequence between renditions (Immelmann, 1969). The juvenile bird gradually matches its vocalizations to a memorized copy of its tutor song. During this sensorimotor phase, the juvenile bird needs to hear itself sing in order to learn to produce its song properly. Birds deafened prior to or during this stage produce abnormal songs (Konishi, 1965; Price, 1979). As the bird reaches adulthood, the song becomes "crystallized", that is, the song has well-defined syllables and a highly stereotyped sequence of syllables. These behavioral results strongly suggest that there are neural processes for the initial memorization of song, and for later matching of song to an internal song model.

Song learning in zebra finches (*Taeniopygia guttata*) is less protracted than in some songbirds, and the sensory and sensorimotor phases overlap (Figure 1-1a). For zebra finches, the sensory phase of song learning begins around post-hatch day 5-10, and lasts until days 60-65. The sensorimotor phase in zebra finches is from around post-hatch day 35, when juvenile birds begin to vocalize, to days 90-100, when zebra finches reach adulthood. At this age, zebra finches produce a crystallized song that does not change over time under normal conditions. Studies have shown, however, that zebra finches require auditory feedback to maintain their adult crystallized song. Absent or altered auditory feedback in adult zebra finches results in the gradual degradation of the adult song (Williams and McKibben, 1992; Nordeen and Nordeen, 1992; Williams and Mehta, 1999; Woolley and Rubel, 1999; Leonardo and Konishi, 1999; Brainard and Doupe, 2000; Lombardino and Nottebohm, 2000). The onset and rate of deterioration of the crystallized adult song has been shown to be age-dependent (Lombardino and Nottebohm, 2000). The behavioral experiments on adults zebra finches suggest that the neural processes that mediate song learning may be also be involved in the maintenance and plasticity of song in adults.

Brain structures that mediate song behavior

The brain structures that mediate song learning in songbirds are organized into a network of nuclei, known as the song system (Figure 1-1b). These structures were first identified by a combination of behavioral and anatomical techniques (Nottebohm et al, 1976). The song system is composed of two pathways, the descending motor pathway for song and the anterior forebrain pathway (AFP). The descending motor pathway includes HVc (abbreviation used as a proper name), the robust nucleus of the archistriatum (RA), and the tracheosyringeal portion of the hypoglossal nucleus (nXIIts). Additional nuclei including nucleus interfacialis (NIf), nucleus Uvaeformis of the thalamus (Uva), and the medial portion of the magnocellular nucleus of the anterior neostriatum are likely to form part of the entire motor pathway for song, but their role is less well understood (Nottebohm et al, 1982; McCasland, 1987; Williams and Vicario, 1993; Vates et al, 1997). The nuclei in the AFP, which include Area X, the medial portion of the dorsolateral nucleus of the thalamus (DLM), and the lateral portion of the magnocellular nucleus of the anterior neostriatum (LMAN), form a feed-forward loop from HVc to RA. HVc innervates both RA and Area X, the first nucleus in the chain of nuclei in the AFP, while LMAN, the output nucleus of the AFP, directly innervates RA. Thus, these two pathways converge onto nucleus RA.

Behavioral and electrophysiological studies provide some knowledge about the function of these nuclei in song behavior. Lesions in either HVc or RA at any time during the bird's life result in degraded song, or in some cases, complete absence of singing (Nottebohm et al, 1976; Simpson and Vicario, 1990). This indicates that these structures are required for song production throughout the bird's life. Consistent with this, HVc and RA exhibit an increase in activity that precedes the production of syllables, as recorded in awake singing birds (McCasland, 1987; Yu and Margoliash, 1996). The nuclei in the AFP, on the other hand, are necessary during song learning. Lesions in either LMAN or Area X of juveniles undergoing learning result in abnormal song (Bottjer, 1984; Sohrabji et al, 1990;

Scharff and Nottebohm, 1991), while lesions of LMAN in adults with normal song have no effect on song production (Bottjer et al, 1984; Nordeen and Nordeen, 1992). Recent studies show that LMAN is necessary for vocal plasticity, even in adults. Lesions in LMAN prevent the gradual changes of adult crystallized song that result from altered or absence of auditory feedback, or late learning (Morrison and Nottebohm, 1993; Williams and Mehta, 1999; Brainard and Doupe, 2000). Evidence of singing related activity in LMAN and Area X (Hessler and Doupe, 1999a; b) also supports the idea that the AFP is still involved in the song behavior of adults.

Consistent with the crucial role of auditory experience during song learning, the nuclei of the song system exhibit auditory responsiveness. Auditory input enters the song system at HVc and NIf through connections from Field L, the avian homologue of the primary auditory cortex in mammals (Fortune and Margoliash; 1995; Vates et al, 1996). The nuclei in both the motor pathway and the AFP exhibit auditory responses that are selective for the bird's own song in adults (Margoliash 1985, 1986; Volman, 1993; Doupe and Konishi, 1991; Vicario and Yohay, 1993; Maekawa and Uno, 1996; Theunissen and Doupe, 1998), although all nuclei do not exhibit the same degree of selectivity. For example, a comparison of the selectivity of Area X and LMAN units in adults indicates that LMAN exhibits a higher degree of selectivity (Doupe, 1997). Moreover, the selectivity for the bird's own song emerges during song learning; this has been shown for HVc, LMAN and Area X neurons. In juvenile birds undergoing sensory learning, LMAN, Area X and HVc neurons respond equally to the tutor's song, and songs of other adult conspecifics (birds of the same species) (Volman, 1993; Doupe, 1997; Doupe and Solis, 1997). However, at around the time when the juvenile bird begins vocalizing, the neurons in these nuclei become selective for bird's own song, or in some cases the tutor song, or respond equally to both (Volman, 1993; Solis and Doupe, 1997).

These behavioral and electrophysiological experiments provide some information about the function of the song system; however, studying a number of these nuclei

simultaneously would shed light on how these nuclei may interact with each other. For example, identifying which networks of neurons in the song system are active during passive stimulation or during singing would help elucidate the sites of neuronal processing that are specifically correlated with these different aspects of birdsong. In chapter 2, we employed the anatomical detection of Fos induction, an immediate early gene product, to identify networks of neurons that are specifically active during auditory stimulation, or during singing, in adult male zebra finches. Immediate early gene induction has been widely used as a marker for neuronal activity (Hunt et al, 1987; Morgan and Curran, 1988; Rusak et al, 1990; Sagar et al, 1988; Sharp et al, 1993; Jurgens et al, 1996; Sherin et al, 1996). Moreover, Fos induction could shed light on the molecular mechanisms that underlie song behavior, since Fos is a transcription factor. Its expression indicates the transduction of neuronal activity into a cascade of gene expression in the neuron. We found that two specific populations of neurons are active by this assay during singing in adult zebra finches: the RA-projecting neurons of HVc, and RA neurons. The singing-induced Fos expression in these neurons proved to be tightly associated with the motor act of singing, and not necessarily the auditory feedback during singing.

The AFP is necessary during learning

Studies show that LMAN, the output nucleus of the AFP, is likely to participate in the acquisition of sensory information necessary for song learning. The best evidence for this is that during sensory acquisition in zebra finches, silencing LMAN activity with a glutamate receptor antagonist impairs tutor song copying (Basham et al, 1996). In addition, birds that are acoustically isolated exhibit the capacity to acquire new syllables well past the end of the sensory period (Eales 1985, 1987; Morrison and Nottebohm ,1993). In these cases, LMAN activity is required for the acquisition of new syllables in isolated birds, although these experiments do not distinguish between a role in sensory or motor learning of new syllables. Consistent with a role in song learning, LMAN axons in RA are present at

the time when sensory learning is occurring, while HVc axons are absent (Akutagawa and Konishi, 1994; Mooney and Rao, 1994). Similarly, neurons in LMAN at this age are responsive to auditory stimulation by the tutor and conspecific songs. These experiments suggest that LMAN mediates the acquisition of sensory information during the sensory phase, and may thus contain information about the tutor song.

LMAN also appears to play a role in sensorimotor learning. LMAN lesions in juveniles at the onset of sensorimotor learning result in an arrested state of the plastic song. The number of syllables decreases rapidly after silencing LMAN, and an apparent loss of variability of plastic songs is observed (Bottjer et al, 1984; Scharff and Nottebohm, 1991). In one study, a slight further degradation of the arrested plastic song occurred after silencing LMAN activity in juveniles (Bottjer et al, 1984). These studies suggest that LMAN is necessary for vocal plasticity in juveniles. During singing in juvenile birds, the induction of an immediate early gene, Zenk, has also been observed in LMAN and Area X (Jin and Clayton, 1997). This indicates that both nuclei are active during singing of plastic songs in juveniles. Indeed, the activity in LMAN of juveniles is modulated during singing (Hessler, unpublished observations). Consistent with a role in sensorimotor learning, LMAN contains neurons that are selective for the bird's own song, the tutor song, or that respond equally to both (Solis and Doupe, 1997). LMAN neurons are thus well suited to mediate the auditory feedback that is necessary during song learning (Nordeen and Nordeen, 1992; Doupe, 1997). In particular, LMAN may evaluate the similarity of the current plastic song to the memorized copy of the tutor song, and send error signals to RA that would guide learning in the motor pathway for song (Troyer et al, 2000a, b; Brainard and Doupe, 2000).

Neurons in RA are candidate sites of plasticity during song learning

RA is the point of convergence of the two functionally distinct pathways of the song system, the motor pathway and the AFP, and may thus be an important site of neural

plasticity during song learning. Individual RA neurons receive input from both HVc and LMAN (Canady et al, 1988; Mooney and Konishi, 1991; Mooney, 1992), providing a location where both inputs may interact. Developmental studies show that RA neurons receive LMAN inputs first, and only later receive HVc inputs; this is consistent with the postulated roles of the two pathways in song learning (Mooney and Rao, 1994; Akutagawa and Konishi, 1994). LMAN synapses in RA are present early in life, during sensory learning and at a time when LMAN is required for sensory acquisition of the tutor song. HVc, which is necessary for song production, innervates RA at around the time when the bird begins to vocalize. During sensorimotor learning, both LMAN and HVc inputs are present in RA, and can thus modulate the activity in RA (Herrmann and Arnold, 1991; Mooney and Rao, 1994; Akutagawa and Konishi, 1994; Mooney, 1992; Kittelberger and Mooney, 1999; Spiro et al, 1999).

The neuronal activity of RA must be modulated during song learning, since RA controls the motor expression of song. RA sends axons to the tracheosyringeal portion of the hypoglossal nucleus, which contains motorneurons that innervate the vocal musculature (Nottebohm et al, 1976; Vicario, 1991). RA also sends axons to brainstem nuclei that control the respiratory apparatus of the bird (Nottebohm et al, 1976; Wild, 1993). RA neurons can therefore coordinate the rhythm of breathing and production of sounds during singing. Stimulation of RA in singing birds disrupt the ongoing syllable, indicating that neurons in RA have fine control of the vocalizations involved in singing (Vu et al, 1994). Indeed, the pattern of RA activity in awake singing birds is unique and consistent for each syllable (Yu and Margoliash, 1996). Complex vocalizations that are similar to song syllables can be elicited by stimulation of RA in a quiescent bird (Vicario and Simpson, 1995).

The neural interactions between AFP and motor pathway nuclei may reveal processes that underlie learning

Few studies have focused on neural interactions between song nuclei in the song system. Because RA is a primary site of plasticity during song learning, the modulation of RA activity by its afferents is of particular interest. Slice preparations show that the LMAN and HVc synapses in RA neurons are both excitatory (Kubota and Saito, 1991; Mooney and Konishi, 1991; Mooney, 1992). When LMAN and HVc axons that synapse onto the same RA neuron are stimulated simultaneously, the excitatory post-synaptic potentials from each input sum up almost linearly (Mooney and Konishi, 1991; Mooney, 1992). However, slice experiments do not have the benefit of an intact song system, nor of a physiological state of neuronal activity. In adults, the auditory responsiveness of RA neurons depends critically on HVc activity, while LMAN activity is not necessary (Doupe and Konishi, 1991; Vicario and Yohay, 1993). This suggests that LMAN input in RA may no longer be functional in adults. However, behavioral studies on late learning and the deterioration of crystallized songs in adults indicate that LMAN is necessary for vocal plasticity in adults (Morrison and Nottebohm, 1993; Williams and Mehta, 1999; Brainard and Doupe, 2000). This suggests that LMAN activity may still modulate the activity in RA, even in adults. Slice experiments, and the studies of auditory responsiveness, are therefore inadequate assays for determining the neural interactions between song nuclei within an intact song system.

Understanding the neural interactions between song nuclei would help elucidate the neural processes underlying song learning and behavior. One way to assay neural interaction between neurons is to measure the correlation of activity, which can be calculated from their simultaneously recorded spontaneous or evoked activity. This also provides a measurement of the potential functional connectivity between two neural areas. Thus, measuring the correlation of activity between song nuclei should shed light on the structure of the functional connectivity within the song system, and how information may be processed within the song system. For example, one can infer whether the functional connectivity within the song system is arranged in parallel channels of connectivity, or in a highly interconnected network of neurons. Moreover, one can also determine whether

LMAN and RA are still functionally connected in adults, as suggested by behavioral experiments. In chapter 3, we describe the neural interactions between LMAN, RA and HVc of adult birds, as measured by the correlated activity between these nuclei. As described in chapter 3, the correlation of activity between indirectly connected nuclei suggests that the functional connectivity within the song system involves broad divergent and reconvergent connectivity between song nuclei, and extensive intrinsic connectivity within some nuclei. Moreover, activity in LMAN and RA is significantly correlated, and has two components: one that is due to the common input of HVc to LMAN and HVc, and the other that is due to the direct projection from LMAN to RA.

Because song learning occurs during post-hatch development, studies on the correlation of activity of song nuclei in juveniles may elucidate neural processes that are specifically involved in song learning. In particular, it would be important to determine whether the functional connectivity within the song system of juveniles is different from that in adults. Developmental changes in the functional connectivity would highlight how the song system may process information differently during learning, compared to when learning is completed. Features of the correlated activity, such as its timing and strength, that are different between juvenile and adults may be those that are crucial for song learning. For example, it would be of interest to determine if LMAN and RA are more strongly correlated in juveniles than adults, since LMAN is necessary for song learning in juveniles and not required for normal song production in adults. In chapter 4, we describe the correlation of activity between LMAN, RA and/or HVc in juveniles, using simultaneously recorded activity from any two nuclei. We found that the functional connectivity of the song system in juveniles is similar to that observed in adults. However, in contrast to our expectation, we found that the direct correlated activity between LMAN and RA was slower in timing and weaker in strength than that of adults. Thus, the strength and timing of the direct LMAN-RA correlated activity may affect the learning that occurs in the motor pathway for song.

Comparison of auditory responses between nuclei

The degree of selectivity for the bird's own song over other acoustic stimuli is not the same for Area X and LMAN in adults (Doupe, 1997). This suggests that selectivity of auditory responses may be processed differently as auditory information is passed onto downstream nuclei. Thus, comparing the selectivity of auditory responses between song nuclei may shed light on the neural interactions within the song system. Of particular interest is the selectivity of responses of RA neurons, and that of its input neurons, LMAN and HVc. It is unknown whether selectivity for the bird's own song in RA also emerges during development, as observed for its afferent nuclei, HVc and LMAN. Moreover, a direct comparison of the selectivity of RA, LMAN and HVc in juveniles would indicate whether selectivity in RA is more similar to that of one input nucleus, or shares characteristics with both nuclei. A similar comparison of the selectivity of RA, LMAN and HVc neurons in adults would also show whether similarities and differences in selectivity between these three nuclei change over development. In chapter 5, we compare the selectivity of simultaneously recorded responses from LMAN and RA, and in some cases HVc, of juvenile and adult birds. We found that at both ages, selectivity in RA is similar in some ways to LMAN, and other ways to HVc selectivity. However, in both juveniles and adults, LMAN had a higher degree of selectivity for the bird's own song, and exhibited inhibitory responses more frequently, than did RA or HVc. RA neurons responded in an inhibitory manner more frequently in adults than in juveniles, and in this sense became more similar to LMAN. Experiments that would directly test the contribution of LMAN and HVc to the selectivity of responses in RA are outlined in chapter 6 (Future Directions).

In summary, this thesis studied the neural interactions between LMAN, RA and HVc in the song system of juveniles and adults. Immediate early gene induction in the song system indicated that the HVc to RA pathway may be the molecular site of plasticity for song maintenance in adults. The correlation of activity within the song system suggested

that the functional connectivity in the song system involves a highly interconnected network of neurons. Such a system may be useful during song learning, and for maintaining adult crystallized songs. Moreover, developmental studies showed that slow temporal characteristics of the direct LMAN-RA correlated activity are correlated with learning, and may therefore be crucial for song learning. Finally, a comparison of auditory responses and selectivity between LMAN, RA and HVc suggested that both afferent nuclei influence RA activity. The complexity of the neural interactions that we observed highlights the importance of studying multiple nuclei in the song system simultaneously, in order to understand how the song system mediates song learning and behavior.

Figure 1-1. a) Timeline of song learning in zebra finches b) Diagram of the anatomy of song system. The descending motor pathway for song includes HVc, RA, nxIIts, and respiratory nuclei (shown in black). Area X, DLM, and LMAN (open symbols) form the anterior forebrain pathway (AFP), which is a feed-forward loop that indirectly connects HVc to RA.

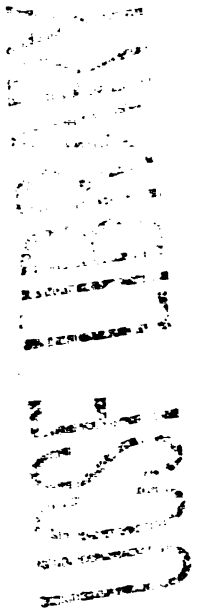

Figure 1-1

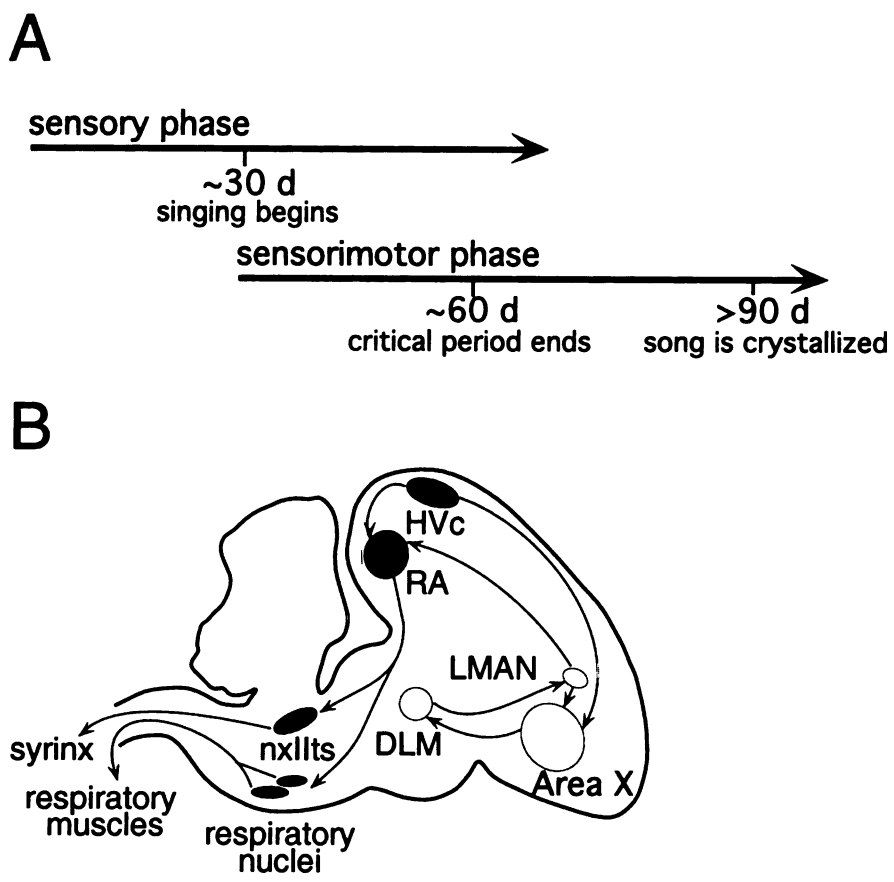
A
sensory phase
~30 d
singing begins
sensorimotor phase
~60 d
critical period ends
>90 d
song is crystallized
B
HVc
RA
LMAN
DLM
Area X
nxIIts
syrinx
respiratory muscles
respiratory nuclei

Chapter 2:

FOS is Induced by Singing in Distinct Neural Populations in a Motor Network

ABSTRACT

Mechanisms underlying the learned vocal behavior of songbirds were studied by examining expression of the protein product of the immediate early gene c-fos (Fos) in zebra finches. Auditory stimuli including the bird's own song did not induce Fos in the song system. In contrast, the motor act of singing induced Fos in two song sensorimotor nuclei, HVc and RA. This induction was independent of auditory feedback, since it occurred in deafened birds that sang. Double-labeling studies demonstrated that only one of the two sets of projection neurons in HVc expressed singing-related Fos. The motor-driven induction of Fos identifies functionally distinct cell populations in a network for singing, and may point to sites of cellular plasticity necessary for song maintenance.

INTRODUCTION

Birdsong is a complex learned behavior, with the potential to reveal how the brain learns and performs sensorimotor tasks. Young songbirds must initially hear and memorize a tutor song, and later use auditory feedback from their own vocalizations to learn to produce a copy of the memorized song (Konishi, 1965; Marler, 1970). By adulthood, songbirds in many species have developed a central motor pattern generator for song and are less dependent on auditory feedback than juvenile birds for normal vocal production, but in some species adults require continued hearing for maintenance of their stable adult song (Konishi, 1965; Nordeen and Nordeen, 1992). The neural mechanisms underlying singing and song learning must therefore involve both sensory and motor processing and their interaction.

The set of brain nuclei known as the song system (Fig. 2-1) is essential for birdsong learning and production. Lesion and electrophysiological studies of this vocal control system have begun to elucidate the neural mechanisms underlying song. The descending sensorimotor pathway, which includes the song nuclei HVc (the acronym is used here as the proper name, as proposed by Fortune and Margoliash, 1995), the robust nucleus of the archistriatum (RA; Fig. 2-1), and the tracheosyringeal portion of the hypoglossal nucleus (nXIIts), is essential for normal song production throughout life (Nottebohm et al., 1976; Vu et al., 1994). A number of other song nuclei play a role in singing, including nucleus uvaeformis (Uva), nucleus interfacialis (NIf), and the dorsomedial nucleus of the intercollicularis (DM; McCasland, 1987; Williams and Vicario, 1993). HVc and RA contain premotor neurons active during singing, as well as auditory neurons strongly responsive to presentation of the bird's own song (McCasland, 1987; Yu and Margoliash, 1996; Margoliash, 1983, 1986; Doupe and Konishi, 1991; Vicario and Yohay, 1993). A second discrete circuit of song nuclei is the anterior forebrain pathway (AFP), consisting of Area X (X), the medial portion of the dorsolateral nucleus of the thalamus (DLM), and the lateral portion of the magnocellular nucleus of the anterior

neostriatum (LMAN; Bottjer et al., 1989; Okuhata and Saito, 1987). Unlike the motor pathway, the AFP is not required for adult song production, but is essential during song learning (Bottjer et al., 1984; Sohrabji et al., 1990; Scharff and Nottebohm, 1991; Morrison & Nottebohm, 1993); neurons in this pathway also respond to acoustic presentation of the bird's own song (Doupe and Konishi, 1991; Doupe, 1997).

Little is known about the molecular mechanisms involved in singing and song learning. The expression of immediate early genes (IEGs) could provide a molecular approach to the investigation of song. In many systems IEGs are transiently expressed, initiating a cascade of gene expression, in response to various extracellular stimuli, including depolarization, neurotransmitters, and growth factors (Sheng and Greenberg, 1990; Morgan and Curran, 1991). They are useful markers of neuronal activation *in vivo*, capable of revealing the physiological stimuli that initiate gene transcription (Morgan and Curran, 1988; Hunt et al., 1987; Rusak et al., 1990) and of anatomically identifying whole networks of neurons involved in a physiological process (Sagar et al., 1988; Sharp et al, 1993; Jürgens et al., 1996; Sherin et al., 1996). Moreover, IEGs have been implicated in the long-term gene expression essential for neuronal plasticity and learning (e.g. Cole et al., 1989; Sheng and Greenberg, 1990; Anokhin et al., 1991) and could therefore point to cellular sites of plasticity in the song system.

The importance of hearing throughout song learning and the presence of song-responsive neurons at all ages suggests that IEGs might be activated in the song system by sounds, especially song. Indeed, presentation of birdsong induces mRNA for a zinc finger protein IEG, known as ZENK, in a number of telencephalic auditory areas that are indirect sources of input to the song system (Mello at al., 1992, Mello and Clayton, 1994); similar results were seen with a canary homologue of c-jun (Nastiuk et al., 1994). However, ZENK induction in response to song has not been observed within the nuclei of the song system itself, despite well described auditory responses throughout this system (Margoliash, 1983,

1986, Margoliash and Fortune, 1992; Doupe and Konishi, 1991; Vicario and Yohay, 1993; Volman, 1993, 1996; Doupe, 1997).

The lack of ZENK induction in song nuclei in response to song presentation raised the possibility that a different set of IEGs might be involved in transcriptional regulation in the song system. We therefore looked for expression of the structurally different IEG c-fos (Sheng and Greenberg, 1990; Morgan and Curran, 1991) in the zebra finch song system, using immunohistochemical labeling with an antibody to the protein product of c-fos (Fos). The results presented here demonstrate that, like ZENK, Fos was not induced in the song system by presentation of birdsong. It was strongly induced, however, in the two sensorimotor song nuclei HVc and RA when adult birds sang. To distinguish between sensory and motor activation of Fos, we analyzed Fos induction in deafened birds induced to sing. Robust Fos immunoreactivity was also found in HVc and RA of these birds, indicating that gene expression was elicited by the motor activity of singing and was independent of auditory feedback and sensorimotor matching. Moreover, double-labeling of the projection neurons in HVc with Fos immunohistochemical staining and retrograde tracers revealed that only one of the two known populations of HVc projection neurons, the neurons projecting to RA, expressed singing-related Fos.

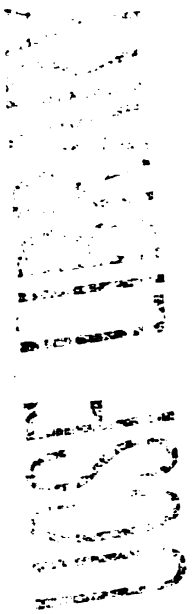

MATERIALS and METHODS

All birds were adult (≥ 120 days old) male zebra finches (*Taeniopygia guttata*) obtained from a local breeder or from our own breeding colony.

Passive Auditory Stimulation. Birds were isolated individually in sound attenuation chambers at least 15 hours before the experiment, and then presented with playback of either conspecific songs or broadband noise bursts for 50 minutes and perfused immediately; in one case a bird received only 15 min of stimulation and was perfused 15 minutes after the end of this period. A sequence of four songs (approximate duration of each song was 1-2 sec) or broadband noise bursts of 2 sec duration played at 2-3 second intervals was broadcast (average intensity 70 dB SPL) twice every minute, followed by 20 seconds of silence. In 3 cases conspecific songs included the bird's own song. Any vocalizations during the stimulation period were recorded or noted. Tape recordings were analyzed for the amount of time spent singing and for the time of occurrence of singing.

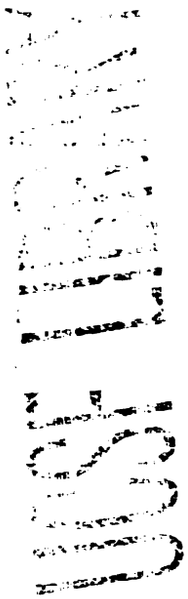

The time period of 50 min for observing Fos protein induction was chosen because, in general, c-fos messenger RNA expression begins within minutes after an effective stimulus and is maximal by 30 min in many systems (e.g. Kornhauser et al., 1992); Fos protein expression is abundant 15-30 min after gene expression starts (Kruijer et al, 1984, 1985; Curran and Morgan, 1985). In our experiments birds initiated singing on average 1min 39sec after the start of the 50 min session (range 0-7min 53sec).

Female-Induced Singing in Deaf and Hearing Birds. In experiments that included deaf birds, singing was induced by presenting female finches. Birds were deafened by bilateral cochlear removal as described by Konishi (1965). Deafening was performed under Equithesin or isofluorane anesthesia 3-5 days (n=8) or 364-500 days (n=2) before the experiment.

The hearing and deaf birds were isolated and stimulated individually in sound attenuation chambers as described above; in a small number of experiments, 4-5 birds, each

in individual cages but not in sound chambers, were tested in a room away from the colony in which they had been placed at least 15 hours before the experiment. Songs of birds that were stimulated in this experimental set-up were previously recorded for identification purposes. In both types of set-up, singing was induced by placing one or multiple females in the male's cage or in a neighboring cage at the start of a 50 minute session. Vocalizations were recorded using microphones. All tape recordings were later analyzed for amount and occurrence in time of singing. Birds were perfused at the end of the 50 minute session.

Birds that were exposed to female birds in order to induce singing clearly attended and acted aroused, as evidenced by non-vocal courtship behavior, i.e. approaching the female, beak wiping and tail-twisting (Morris, 1970), and in many cases by singing. To test for the effects of arousal without singing, singing was actively prevented in three birds. This was done during the entire 50 min session by distracting the bird with a hand movement near the cage each time singing was about to start, as indicated by vocalization of introductory notes which almost always initiate song (Price, 1979).

Fos Immunohistochemistry. Birds were perfused intracardially with 0.025M phosphate-buffered (PB) 0.9% saline or lactated Ringers followed by 4% paraformaldehyde (PFA) in PB. Some brains were post-fixed in 4% PFA for 2-4.5 hours. Brains were cryoprotected by sinking in 30% sucrose-PFA or 30% sucrose-PB at 4°C and cut coronally into 40μm thick sections using a freezing microtome; sections were collected in PB. Every third section was used for Fos immunohistochemistry and adjacent sections were Nissl-stained. To minimize variability in staining attributable to the histological procedure rather than to the behavior of the birds, brain sections of all birds observed in each experiment were processed in a single batch. Each individual experiment usually included 4-5 birds, and always spanned a range of times spent singing, including little or no time singing, and in experiments on hearing, included both hearing and deaf birds. This ensured that all procedures including reaction time were identical for the different behavioral conditions. Free floating sections were

processed immunohistochemically for Fos protein using an anti-chicken Fos IgG (kind gift of Dr. Peter Sharp); this antibody was raised against a chicken c-fos peptide sequence, and on Western blots labels a band with the expected molecular weight of Fos (47-50kD; Sharp et al., 1995). The standard avidin-biotin peroxidase protocol (Vectastain, Vector Laboratories, Burlingame, CA) was used to visualize the antibody, except that the avidin-biotin complex (ABC) solution was used at half concentration. Sections were washed in Tris-phosphate buffer (0.01M Tris in 0.01M PB and 0.9% Saline, with 0.05% Thimerosal; TPBS) containing 0.3% Triton X-100 (Triton) and 1% normal goat serum (NGS; Antibodies, Inc., Davis, CA), incubated in 5% NGS diluted in TPBS with 0.3% Triton for 1 hr, and then in rabbit anti-chicken Fos IgG (1:10,000-1:15,000 diluted in TPBS containing 0.3% Triton and 1% NGS; optimal antibody concentration was determined in early experiments by titration) overnight. The secondary antibody was diluted in TPBS containing 0.3% Triton and 1% NGS, and the ABC in TPBS containing only 0.3% Triton. Peroxidase was visualized using diaminobenzidine (DAB, Sigma) with nickel intensification, and glucose oxidase to generate hydrogen peroxide. Brain sections were mounted on slides and examined in the light microscope. Observers were blind to the amount of time each bird sang and whether the birds were deaf or not. Fos immunoreactive material was evenly distributed in the nuclei of cells.

Control experiments were performed to examine the specificity of the Fos antibody. In one experiment, a second set of brain sections was incubated in an excess of the Fos peptide (against which the Fos antibody was raised) along with the Fos antibody: no Fos staining was seen in the peptide-blocked sections, although Fos staining in the unblocked sections was normal. Moreover, in all Fos immunohistochemistry experiments, Fos antibody was omitted from some sections. Only low levels of non-specific staining were observed in these sections.

Quantification of Fos-immunoreactive (IR) cells. The quantitative analysis was done only on birds that had been stimulated for 50 minutes with conspecific songs or female finches and whose vocalizations had been recorded during the stimulation period. The number of Fos-IR cells / mm^2 in HVc, RA and an area in the neostriatum directly underneath HVc (Neo) of approximately equal size to HVc was determined for each bird, using a computer-assisted image analysis system (NIH Image). Images of brain sections containing HVc and RA were captured at 4x with a CCD camera and converted to digital images in which each pixel was assigned a value from 0 to 255. Care was taken to ensure that each digitized image spanned close to the full range of gray values without saturation of either black or white. Using NIH Image, Fos-IR cells in HVc, RA, and Neo in each section were counted by setting a size range for cellular nuclei (in pixels) and a threshold level for staining intensity. The threshold level, which included all dark gray and black stained cells, was set to be the same for each set of brains processed simultaneously for Fos immunohistochemistry; in practice the threshold was similar even for different sets of brains (usually 180-185 pixels; range 170-195). Counting was done blind to the amount of time spent singing and to whether the bird was deaf or not. The areas of HVc, RA and Neo in each section were also measured. When the boundaries of HVc or RA were unclear from the immunostained sections, the adjacent Nissl section was examined. Overstained sections were excluded from the analysis. In a small number of sections (n=6/56 nuclei), there was patchy background staining that prevented accurate computer counting; in these cases dark gray and black stained Fos positive cells were handcounted under a light microscope.

Retrograde labeling of projection neurons in HVc. To identify which population of HVc neurons (i.e. RA-projecting or Area X-projecting) was expressing Fos, we carried out retrograde labeling experiments. Cholera toxin B subunit (List Biological Laboratories, Inc., Campbell, CA) was pressure injected (700-1000nl, 30-60 psi) unilaterally into Area X 3-4 days before the stimulation experiment (n=3); similarly, fluorogold (Fluorochrome, Inc.,

Engelwood, CO) was pressure injected (approximately 360nl, 5-10 psi) unilaterally in RA 5-6 days before the experiment (n=2). Area X was located using stereotaxic coordinates, while RA was found using stereotaxic coordinates and its characteristic spontaneous activity in electrophysiological recordings. As described previously, song was induced by tape stimulation for 50 minutes using conspecific songs. Fos immunohistochemistry was performed first, using nickel-intensified DAB (staining cell nuclei gray to black), followed by immunohistochemical staining for the retrograde tracer using the standard avidin-biotin peroxidase (Vectastain, Vector Laboratories) protocol, with the ABC solution used at half concentration, and DAB alone (staining cells brown). Sections for cholera toxin B subunit immunohistochemistry were washed in TPBS containg 0.3% Triton and 1% normal horse serum (NHS; Antibodies, Inc.) and incubated in 5% NHS in TPBS containing 0.3% NHS. Goat anti-cholera toxin IgG (List Biological Laboratories, Inc., Campbell, CA) was used at 1:30,000 dilution and the secondary antibody, biotinylated mouse anti-goat IgG (Pierce), was used at 1:5,000 dilution; both were diluted in TPBS containing 0.3% Triton and 1% NHS. Sections for fluorogold immunohistochemistry were washed in TPBS containing 0.3% Triton and 1% NGS, incubated in 5% or 10% NGS diluted in the same buffer, and then in 1:10,000 or 1:7,500 dilution of Fos antibody. Rabbit anti-flurogold IgG (Chemicon, Temecula, CA) diluted in TPBS containing 0.3% Triton and 10% NGS at 1:30,000 was gently mixed for 1 hour at RT before being added to the sections. The secondary antibody, biotinylated goat anti-rabbit IgG (Vectastain, Vector Laboratories) was used at the recommended concentration and diluted in TPBS containing 0.3% Triton and 1% NGS.

Cells were considered to be double-labeled only if they met the following criteria: (1) Fos-IR and retrograde tracer were co-localized within the same neuron, within the same focal plane, and with good alignment of the boundaries of the nuclear and cytoplasmic staining, and (2) the neuron was well-filled by the retrograde tracer so that the neuronal soma was well defined.

RESULTS

Lack of Fos induction by auditory stimulation

A small number of Fos-immunoreactive (IR) cells was consistently seen in hyperstriatum ventrale, hippocampus, and non-song system areas of the neostriatum of all songbirds examined. However, presentation of taped auditory stimuli caused no induction of Fos protein within song nuclei of adult male zebra finches that listened and did not sing throughout the 50 min stimulation period (n = 9). These nuclei included HVc and RA (Fig. 2-2a, b) as well as the other song motor areas Uva, NIf, DM, and nXIIts (Fig. 2-1; data not shown). The nuclei of the anterior forebrain also did not express Fos in response to song presentation (Fig. 2-2 e,g). We attempted to induce Fos expression with several different types of acoustic stimuli, including conspecific songs (n=4) and broad band noise bursts (n=5). In 3 experiments, the conspecific songs included the bird's own song (presented 30-100 times at 12-15 sec intervals over a period of 30-50 min). In these cases, HVc was also found to have no or few Fos -IR cells, even though neurons in HVc of awake birds respond vigorously to playback of the bird's own song (McCasland and Konishi, 1981).

Stimulation with song also did not elicit an increase in Fos staining, compared to birds that did not hear song, in other forebrain auditory regions, including areas that show induction of ZENK in response to the same method of song presentation: the caudomedial neostriatum (NCM), the shelf underlying HVc, and the cup around RA (Mello et al., 1992).

Induction of Fos in singing birds

In contrast to the birds that were quiet during song presentation, birds that countersang during the 50 min of taped song stimulation exhibited marked induction of Fos immunostaining in the two sensorimotor song nuclei HVc and RA (n = 11; Fig. 2-2c, d). The pattern of Fos staining in HVc and RA was consistent with specific labeling of the Fos antigen (see Experimental Procedures).

Other song nuclei that play a role in singing, specifically NIf, Uva, DM, and the motor nucleus nXIIts, showed no consistent Fos induction with singing. In particular, nXIIts and Uva were never seen to express Fos, while DM and NIf had a small number of faint Fos-IR cells in one bird that sang very robustly (6 min 45 sec total in 50 min); however, another bird that sang almost identically (6 min 24 sec, during similar intervals of the 50 min session) showed no such induction. Similarly, although one singer showed faint induction of a small number of cells in the nuclei of the AFP, in general, no Fos-IR cells were found in Area X (Fig. 2-2h), DLM (not shown) and LMAN (Fig. 2-2f) of birds that countersang to presentation of conspecific songs and had strong Fos induction in HVc and RA.

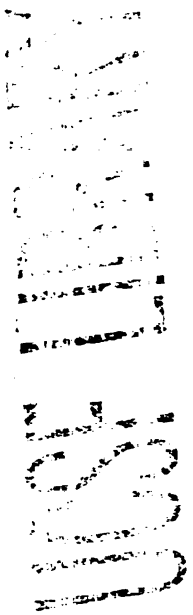

Fos is induced by the motor act of singing

To determine whether induction of Fos in HVc and RA in singing birds was due to the motor act of singing or to the auditory feedback from the bird's own voice, we examined Fos expression in normal and deafened singing birds. We deafened birds by bilateral cochlear removal and induced birds to sing by presentation of female finches. Deaf birds included animals that were deafened 3-5 days prior to the Fos experiment (n=8), and thus had normal song, as well as birds deafened more than one year before the experiment (n=2), that therefore had greatly degraded songs (Nordeen and Nordeen, 1992). As in the song playback experiments, the observation period lasted 50 min and birds were then immediately perfused. In all deaf birds (n=10) and hearing birds (n=11), Fos induction in HVc and RA was again associated with the act of singing (Fig. 2-3).

None of the singers in these experiments expressed Fos in any other song motor nuclei or in the AFP, whether they were hearing or deaf. As with tape stimulated birds, Fos staining was consistently found in most of the neostriatum, as well as in the hyperstriatum ventrale and hippocampus of both deaf and hearing birds. One important difference between these experiments and the auditory stimulation experiments is that, since singing

could not be triggered with acoustic stimuli in deaf birds, all birds were induced to sing by exposure to female finches. The presence of females alone did not account for the Fos induction in the song system, however, since birds that saw females and clearly became aroused but did not sing showed no induction of Fos in HVc and RA. In three birds we also tested for the effects of strong arousal without singing by actively distracting the birds each time they initiated singing. Although this prevented full singing, attempts to sing and other courtship behaviors continued unabated throughout the session. These birds also showed no Fos induction in the song system. In general, however, more Fos-IR cells were observed in the caudal neostriatum and in the archistriatum surrounding RA (including the archistriatum, pars dorsalis; Johnson et al, 1995) in birds that were induced to sing by exposure to females rather than by tape stimulation, regardless of whether the bird sang or not and regardless of the bird's hearing status. This is evident for instance in Fig. 2-3a (open arrow) and Fig. 2-3b (closed arrow). This may be due to arousal upon seeing the females, since it has been shown using 2-deoxyglucose that the activity in caudal neo- and archistriatum increases with arousal (Bischof et al, 1986, 1988).

The number of Fos-IR cells in HVc and RA was related to whether the bird sang. We measured the duration of singing during the 50 min observation period and classified birds as either poor singers (< 20 sec of singing in 50 min; range 0-16 sec, mean 4.7 sec; n=7 for hearing birds, n=3 for deaf) or robust singers (>20 sec in 50 min; range 21-405 sec, mean 146. 4 sec; n=12 for hearing birds, n=7 for deaf). We then counted the numbers of strongly Fos-IR cells per mm^2 in HVc and RA in all birds, as well as in a non-song area from the neostriatum underlying HVc (Neo); all of these measurements were done blind both to the amount of singing and to the hearing status of the birds (see Experimental Procedures). The number of Fos-IR cells was greater in song nuclei of robust singers than of poor singers (Fig. 2-4a). Although there was a slightly lower mean total number of Fos-IR cells in HVc and RA of deaf birds compared to hearing birds, this difference was not significant, and was likely due to the fact that deaf birds rarely sang for as long as hearing

birds. We performed two-way analyses of variance of the number of Fos-IR cells/mm^2 in HVc, RA, and Neo, with singing category (poor / robust) and hearing status (deaf / hearing) as the factors. In the control area Neo, there was no significant effect of singing on Fos induction ($F_{1,23}$=0.582, p=0.45). In contrast, there was a significant effect of singing on Fos expression in both HVc and RA (HVc: $F_{1,24}$=9.67, p<.005, RA: $F_{1,25}$=4.95, p<.036), consistent with the idea that singing-associated Fos induction is specific to the song system. In all three areas measured, hearing status had no significant effect of its own (HVc: $F_{1,24}$=0.83, p=0.37; RA: $F_{1,24}$=0.47, p=0.49; Neo: $F_{1,24}$=0.01, p=0.94) and had no significant interaction with singing (HVc: $F_{1,24}$=1.16, p=.29; RA: $F_{1,25}$=.74, p=.396; Neo: $F_{1,24}$=0.02, p=0.88). This confirms that, as in the song playback experiments, acoustic stimuli did not influence Fos induction. Therefore, the increased gene expression in HVc and RA in singing birds reflected the motor act of singing rather than auditory feedback from song.

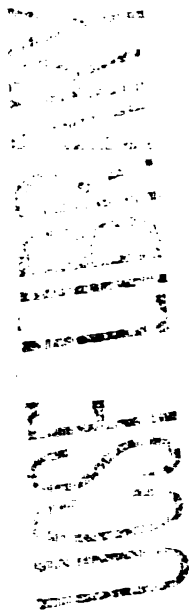

The amount of Fos expression in HVc, RA, and Neo was further correlated with the amount of time spent singing (Fig. 2-4b). Correlations between the total time a bird sang during the 50 min and the number of Fos-IR cells/mm^2 were significant for both HVc and RA (R=0.589, p<.0008 for HVc, R=0.684, p<0.0001 for RA; Pearson correlation coefficients), but not for Neo (R=0.132, p=0.516).

Functional segregation of two populations of projection neurons in HVc

HVc is both a sensory and a premotor nucleus and contains two separate but densely interconnected populations of projection neurons: those projecting to the next premotor nucleus RA and those projecting to Area X in the AFP. Both populations of projection neurons respond to song playback in anesthetized birds (Doupe and Konishi, 1991; Vicario and Yohay, 1993), but it is not clear whether both populations are equally involved in singing. The strong Fos immunoreactivity associated with singing in HVc provided a method for addressing this question. We retrogradely labeled projection neurons in HVc with cholera toxin or fluorogold from one or the other of the two known

targets of HVc and then induced singing. With this approach we could identify the Fos-IR neurons that projected to X or RA. We found no X-projecting HVc cells expressing Fos in 3 birds that sang robustly. Fig. 2-5a shows the typically large cholera toxin-filled Area X projection neurons in HVc, with unstained nuclei, surrounded by numerous smaller Fos-IR nuclei. In contrast to the large X-projecting neurons, many fluorogold-filled RA-projecting neurons throughout HVc contained Fos-IR nuclei (Fig. 2-5b, n=2 birds). These neurons had the smaller soma size expected of RA-projection neurons in HVc (Sohrabji et al., 1989). HVc also contained Fos-IR cells that were not labeled with retrograde tracer: these cells might simply not have been backfilled, but might also represent interneurons activated to induce Fos during singing. In the striatum one of the changes elicited by chronic exposure to cocaine is a dramatic increase in the number of interneurons showing Fos induction (Moratalla et al., 1996). We did not quantify the percentage of cells double-labeled, because this would depend on the numbers of cells filled and the number of Fos-IR cells, both of which vary independently from bird to bird. By our criteria, however (see Experimental Procedures), there were no clearly Fos-IR X-projecting neurons but numerous Fos-IR RA-projecting cells in all singing birds examined. This indicates that these interconnected HVc neuronal populations differ functionally in their roles during singing.

DISCUSSION

Our findings demonstrate that, despite the importance of hearing in song learning and maintenance in zebra finches, auditory activation does not induce Fos expression in any song nuclei. In contrast, the motor act of singing strongly induces the expression of Fos protein in two song sensorimotor nuclei, even in the complete absence of auditory input and sensorimotor matching. In addition, the double-labeling study revealed that only one of the two populations of projection neurons in HVc, the cells projecting to RA, exhibits induction of Fos-IR in response to singing: this indicates a functional segregation of neurons within a highly interconnected motor network and may point to particular sites of cellular plasticity in song maintenance.

The cellular consequences of neuronal activation by singing and song playback must differ

These results provide a striking example of the fact that neuronal activation alone does not lead to gene transcription (e.g. Sagar and Sharp, 1990; Labiner et al., 1993; Chergui et al., 1996). Although HVc neurons in awake birds respond strongly to presentation of the bird's own song (McCasland and Konishi, 1981), multiple presentations of the bird's song in these experiments did not induce Fos expression in HVc. In contrast, singing strongly induced Fos expression. The activity of HVc and RA during this motor behavior must differ in crucial ways from passive sensory activation of these nuclei. One difference may be that the level of neuronal depolarization in HVc and RA is simply much greater during singing than during listening: chronic recordings from the HVc of singing birds show sustained depolarization of many neurons, including a maintained increase in firing of neurons for several seconds before and after song (McCasland, 1987; Yu and Margoliash, 1996). In contrast, neural activity in HVc during song playback occurs only during the stimulus (McCasland and Konishi, 1981). A dependence of IEG expression on the amount of depolarization has been seen in many systems (e.g. Cole et al., 1989). Numerous studies *in vivo* and *in vitro* also suggest that increased intracellular calcium

(often via NMDA receptors) is a critical step linking sustained depolarization to gene transcription (Chergui et al., 1996; Labiner et al., 1993; Cole et al., 1989; Greenberg et al., 1986; Morgan and Curran, 1986). Both HVc and RA neurons are known to be part of local circuits densely interconnected via glutamate and especially NMDA receptors (Vu and Lewicki, 1994; Perkel, 1995). Singing-associated depolarization in these nuclei may result in NMDA receptor activation and sufficient calcium influx to induce gene activation.

Whatever the mechanism underlying the Fos induction seen here, it is closely linked to singing, because we observed a significant correlation between the amount of time spent singing and the number of Fos-positive cells induced. Although this correlation was significant, it was only moderate, perhaps because in behavioral experiments such as these the exact amount of stimulation is not under the experimenter's control. In our study robust singers initiated singing on average by 1 min 39 sec into the 50 min observation period but continued to sing at different intervals thereafter. Therefore the same total amount of time spent singing might vary in its effectiveness in inducing Fos, depending on the time between singing bouts and the end of the observation period, when birds were perfused. Despite this source of variability, however, the number of Fos-expressing cells was still significantly associated with the total time birds spent singing.

We also did not see consistent Fos-labeling with song playback or singing in Field L, the forebrain primary auditory area, although Fos has been elicited by auditory stimuli in the primary auditory cortex of mammals (Zuschratter et al., 1995). In those studies Fos was induced with tone bursts or narrow band stimuli; the complexity and varying nature of the auditory stimuli used in our playback studies, however, may not elicit optimal activation of neurons in the tonotopically organized primary auditory areas.

The same stimuli activate different IEGs in different areas of the songbird brain

The induction of Fos was different from that of the IEG ZENK in that there was no clear induction of Fos by song playback in the caudomedial neostriatum (NCM), in the

outer layers of the field L complex, nor in the auditory areas immediately surrounding HVc and RA (Mello et al., 1992, Mello and Clayton, 1994), although Fos shared with ZENK its lack of induction in the song system by auditory stimulation. Recent work also shows singing-related ZENK mRNA induction in the song system of canaries, but again not in areas identical to those expressing Fos: the anterior forebrain nuclei, especially Area X, show ZENK induction as well as HVc and RA (Jarvis and Nottebohm, 1996). This difference from Fos could be due to experimental conditions, to a species difference, or to different requirements for expression of various IEGs in the song system. Other studies also indicate that different IEGS can be induced by different stimuli, or may show differing sensitivity to the same stimuli (Sheng and Greenberg, 1990; Nastiuk et al., 1994). Induction of distinct combinations of IEGs in particular song brain areas could endow cells with a variety of long-term cellular responses to the same physiological activation.

The motor act of singing induces gene expression in areas critical to song production

The fact that Fos was induced in HVc and RA in both deaf and hearing finches that sang clearly reveals a link between motor activation and gene expression; the auditory feedback inevitably present in normal singing birds is not required for Fos induction. IEGs are often induced in the intact nervous system in response to external sensory stimuli or neuromodulators, but direct electrical stimulation of motor cortical or vocal motor areas can also induce Fos throughout motor pathways (Sagar et al., 1988; Wan et al., 1992; Jürgens et al., 1996). Fos induction in the song system during singing, however, is one of the most striking examples to date of spontaneous motor behavior inducing gene transcription and translation in a coordinated network of neurons.

Although other brain areas are involved in the motor act of singing, including Uva, NIf, the midbrain nucleus DM, and the motor nucleus nXIIts (McCasland, 1987; Williams and Vicario, 1993), these regions showed no consistent Fos induction with singing. They

may have a higher threshold for Fos induction or may be less active during vocalization than HVc and RA. NIf and Uva for instance seem to play a role in coordinating singing rather than representing the direct premotor commands for song (Williams and Vicario, 1993; Vu et al., 1994). The nucleus nXIIts, which contains the motor neurons that innervate the muscles of the vocal organ, is undoubtedly very active during singing. The fact that it exhibits no Fos induction further supports the idea that Fos expression in the song system does not simply reflect neuronal firing. Instead, Fos induction may require a more specific activation in the two nuclei which may be critical for the generation of the song pattern (Vu et al., 1994; Yu and Margoliash, 1996). In addition, HVc and RA are the only song motor nuclei with clear evidence of convergent auditory and motor inputs (Kelley and Nottebohm, 1979; McCasland and Konishi, 1981; Mooney, 1991; Doupe and Konishi, 1991): perhaps Fos is induced specifically in cells that integrate sensorimotor signals.

In our experiments Fos was also not consistently expressed in the AFP. Little is known about the activity of this pathway in awake birds, and the AFP may simply be less active during singing. However, the lack of Fos induction may also be correlated with the fact that the AFP is not required for song production in adult zebra finches (Bottjer et al., 1984; Sohrabji et al., 1990; Scharff and Nottebohm, 1991; Morrison & Nottebohm, 1993). The AFP is essential for song learning, but zebra finches are "closed" learners, that is, they do not normally learn song in adulthood. The observation that Fos was not induced by singing in the AFP of adult zebra finches, while ZENK was induced in the AFP of singing canaries, birds that are "open" learners (Jarvis and Nottebohm, 1996), might reflect the differential capacity to learn new song in adulthood of these two species.

Fos induction during singing may indicate active maintenance of stable song

What is the possible significance and function of the gene induction during singing in adult birds? IEGs are often proposed to mediate specific long-term responses to external stimuli, including modifications underlying neuronal plasticity. For instance, it has recently

been shown that Fos expression is elevated in association with motor skill learning and synaptic growth, and not simply with increased motor activity, in a rat motor cortical system in which activity and learning could be dissociated (Kleim et al., 1996). Yet adult zebra finches do not normally exhibit motor plasticity, singing the same unchanging song throughout adulthood (Nordeen and Nordeen, 1992). Thus, IEGs may function non-specifically, by regulating the expression of "housekeeping" genes involved in the increased cellular metabolism elicited by singing. Such a non-specific role has not been ruled out in many instances of IEG induction (Sheng and Greenberg, 1990).

On the other hand, adult zebra finches can change their song: if adult finches are deafened or subjected to disruptions of the peripheral vocal system, song quality changes and gradually deteriorates (Nordeen and Nordeen, 1992; Williams and McKibben, 1992). This suggests that some active maintenance of song is required even in adulthood, and may involve a comparison between auditory feedback and what the bird expected to hear, in order to strengthen or adjust the motor output. It is clear from our study that Fos expression does not depend on how well the intended song output and the auditory feedback match, since Fos is equally induced in both deaf and hearing birds, and in birds with normal and deteriorated song. It is nonetheless intriguing that Fos induction is seen only in HVc and RA: much of the learning of the song motor pattern likely occurs in these nuclei, and they are plausible sites for a sensorimotor matching process, since they are both premotor and auditory (Kelley and Nottebohm, 1979; McCasland and Konishi, 1981; Margoliash, 1983, 1986; McCasland, 1987; Yu and Margoliash, 1996; Doupe and Konishi, 1991; Vicario and Yohay, 1993). The restriction of Fos induction to these nuclei could indicate a role for this IEG in maintenance of song by auditory feedback, and might thus identify the cells undergoing active stabilization of singing-related synapses. For instance, Fos induction might be a prerequisite to a neuron's changing in response to auditory feedback. By this hypothesis, however, Fos expression would not be an "instructive" signal, but would be a "permissive" factor for song plasticity.

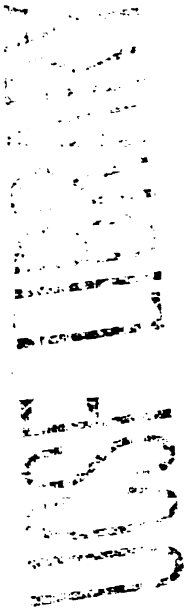

Functional segregation of neuronal populations in a network

Double-labeling with Fos immunohistochemistry and retrograde tracers revealed that only the RA-projecting neurons in HVc exhibited singing-driven Fos induction. The RA- and X-projecting neurons in HVc are intermingled within the nucleus and densely interconnected via glutamate receptors, and in anesthetized birds exhibit remarkably similar neurophysiological responses to song, as judged by their outputs in X and RA (Doupe and Konishi, 1991; Vicario and Yohay, 1993). Electrophysiological studies in singing birds have not yet been able to distinguish between these two sets of neurons (McCasland and Konishi, 1981; McCasland, 1987; Yu and Margoliash, 1996). Our results therefore provide the first direct evidence that these HVc projection neurons are functionally distinct: in singing birds only the neurons projecting to the downstream motor nucleus RA had the appropriate activity to induce Fos. Our results also raise the possibility that the X-projecting neurons are not involved in any long-term plasticity that might result from Fos induction. Other data suggest that X-projecting neurons in HVc are more stable than RA-projecting neurons as well: although new neurons are added in adulthood to HVc, they are added only to the RA-projecting or interneuronal populations (Alvarez-Bullya et al., 1988, 1992; Kirn and Nottebohm, 1993).

In this study we have demonstrated marked induction of the transcriptional regulator Fos during the performance of a stable but learned behavior. Our results suggest that active molecular mechanisms are involved in either maintenance of cells after pronounced singing-related activity, or in stabilizing and regulating song neurons and their connections in adult birds. The differential expression of Fos in subsets of neurons indicates that genetic mechanisms are selectively engaged by different pathways in the song system, and suggests that dissection of the cellular and molecular consequences of singing will further elucidate how a neuronal circuit mediates a complex sensorimotor task.

Figure 2-1 Schematic Diagram of the Song System.

The descending sensorimotor pathway, which is essential for singing throughout a bird's life, includes HVc, the robust nucleus of the archistriatum (RA) and the tracheosyringeal portion of the hypoglossal nucleus (nXIIts), a motor nucleus that controls the muscles of the syrinx, the bird's vocal organ. The anterior forebrain pathway (hatched areas), which is required during learning, consists of Area X, the medial portion of the dorsolateral nucleus of the thalamus (DLM) and the lateral portion of the magnocellular nucleus of the anterior neostriatum (LMAN). The dorsomedial nucleus of the intercollicularis (DM), nucleus interfacialis (NIf) and the thalamic nucleus uvaeformis (Uva) all play a role in singing. The field L complex (L) is the source of auditory inputs to the song system.

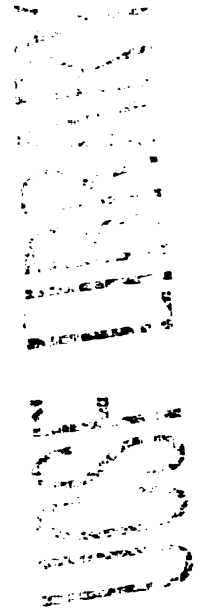

Figure 2-1

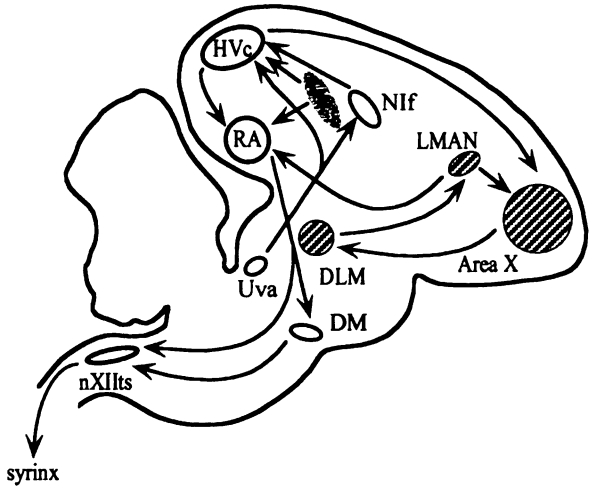

Figure 2-2 Singing Induces Expression of Fos in HVc and RA of Male Adult Zebra Finches.

Panels A, B, E, and G show coronal sections of song nuclei of a bird that was stimulated with conspecific songs for 50 minutes but did not countersing. No significant Fos induction was detected in HVc, RA, LMAN and Area X. Panels C, D, F, and H show song nuclei of a bird that was stimulated in the same manner, but countersang to the playback of conspecific songs for a total of 6min 24sec. HVc (C) and RA (D) contain numerous Fos immunoreactive cells, while LMAN (F) and Area X (H) do not exhibit detectable Fos protein. The bird began singing 1 min into the 50 min stimulation period and was perfused immediately after the session. Scale bar in D represents 200μm for panels A-D; in H, 200μm for panels E-H; medial is to the right in all sections.

Figure 2-2

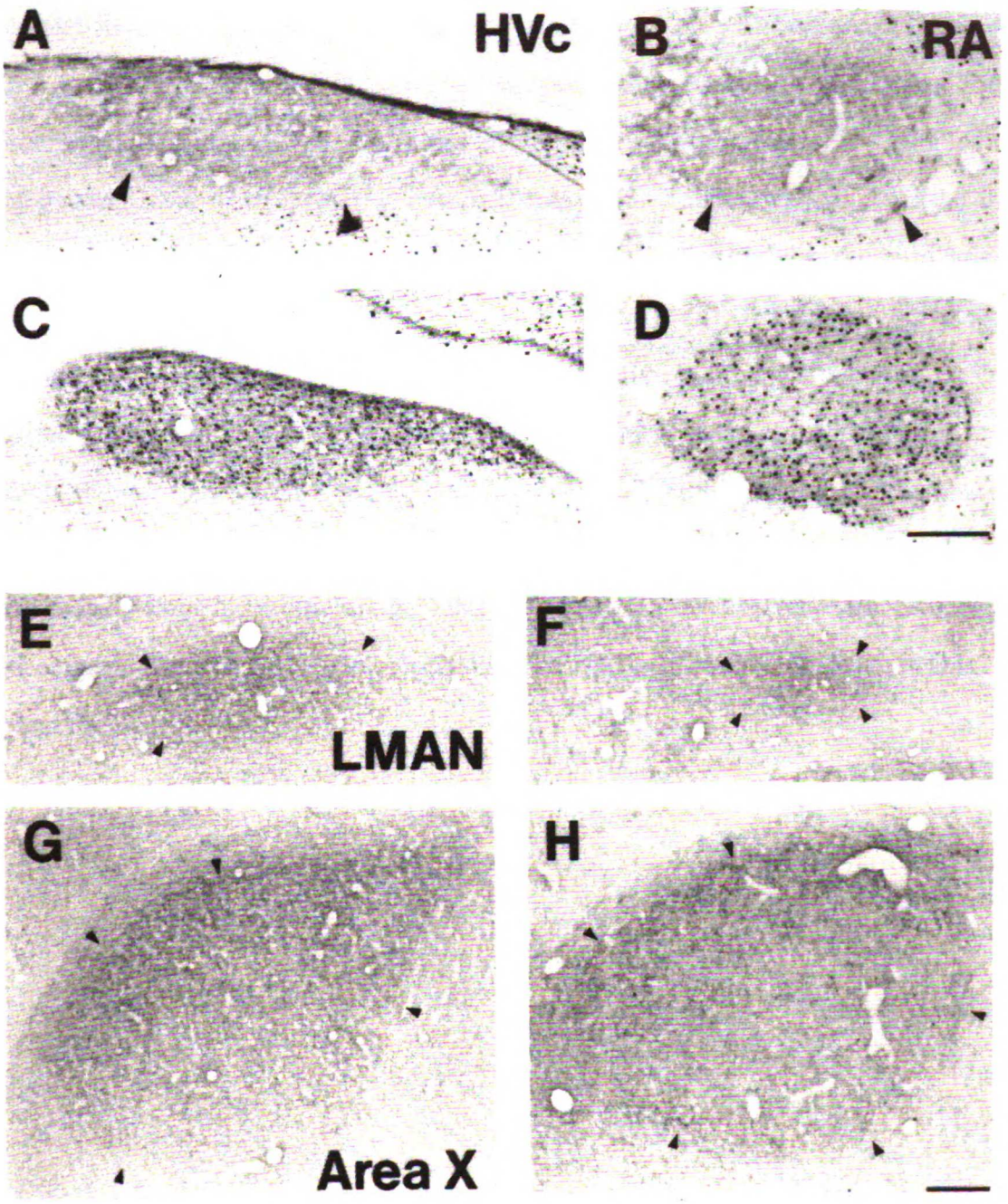

Figure 2-3 Singing-associated Fos Expression in HVc and RA Reflects the Motor Act of Singing.

HVc (A) and RA (B) of a hearing bird induced to sing during a 50 minute session by presentation of female finches. Many Fos-immunoreactive (IR) cells were detected in HVc and RA. The bird began singing as soon as the session started and sang for a total of 2min 16sec. HVc (C) and RA (D) of a deaf bird that began singing immediately and sang for a total of 2min 28sec when exposed to female finches during a 50min session. As in the hearing bird, HVc and RA contained numerous Fos-IR cells. The bird was deafened 3 days before the experiment. In both deaf and hearing birds, exposure to females in order to elicit singing induced more Fos-IR cells in the caudal neostriatum (open arrow points to examples) and in the archistriatum surrounding RA (arrow points to examples) than in tape stimulated birds. The relatively caudal sections of HVc in (A) and (C) illustrate that the caudomedial portion of HVc, a thinner and more densely packed area of the nucleus that runs medially along the ventricle (e.g. Nordeen et al., 1987), also exhibits Fos induction with singing. Sections are coronal, medial is to the right in all photos. Scale bar in D is 200μm for (A-D).

Figure 2-3

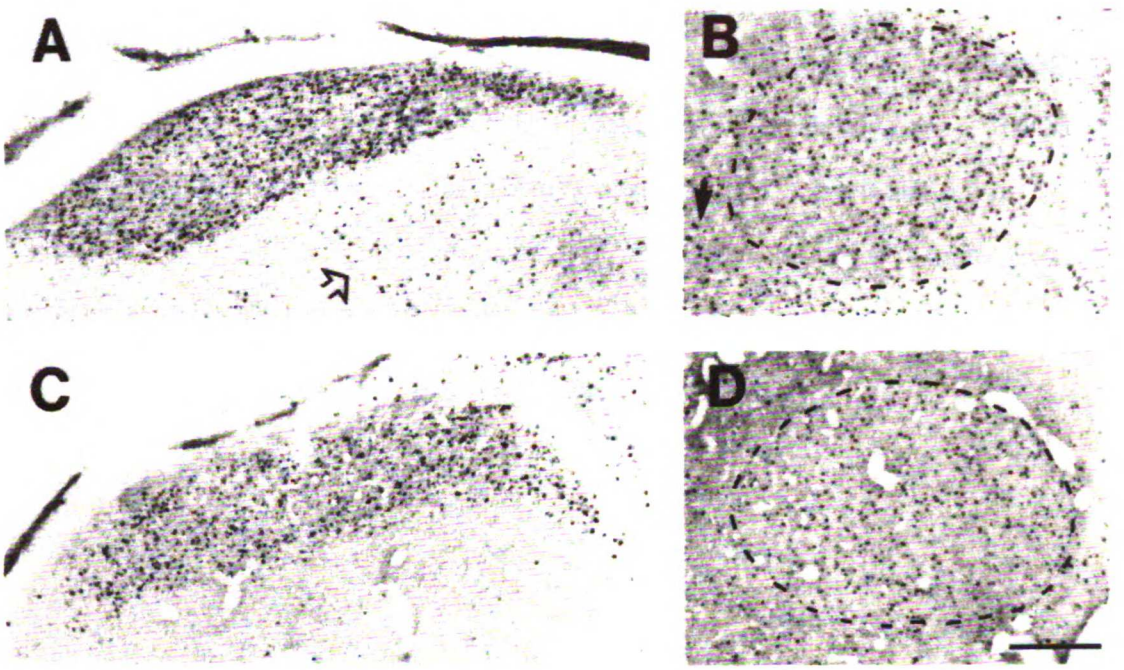

Figure 2-4 The Amount of Fos Expression in HVc and RA is Correlated with the Amount of Time Spent Singing.

(A) Histograms show mean number of Fos-immunoreactive (IR) cells/mm^2 in HVc, RA and a control area, Neo (see Experimental Procedures) of poor singers (<20sec of singing) and robust singers (21-405sec of singing), in deaf (white bars) and hearing birds (black bars). Error bars indicate standard errors. (B) Scattergrams plot the mean number of Fos-IR cells/mm^2 in HVc, RA, and Neo of each bird against the total number of seconds the bird sang during the 50min session. Lines represent the best least-squares fit to the data.

Figure 2-4

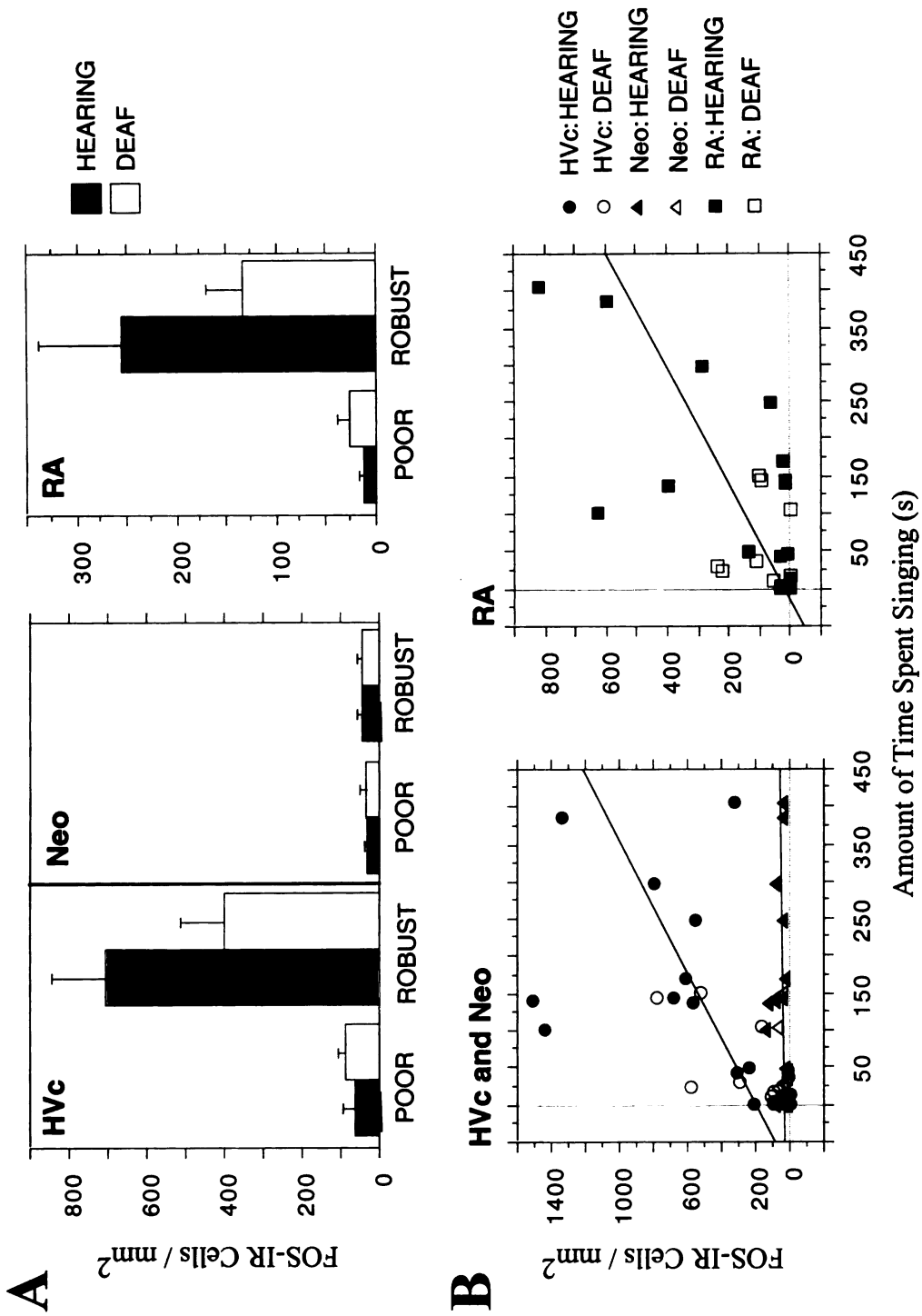
A
FOS-IR Cells / mm2
HVc
Neo
RA
HEARING
DEAF
POOR
ROBUST
B
HVc and Neo
RA
HVc: HEARING
HVc: DEAF
Neo: HEARING
Neo: DEAF
RA: HEARING
RA: DEAF
Amount of Time Spent Singing (s)

Figure 2-5 RA-projecting Neurons in HVc Express Singing-related Fos, while Area X-projecting Neurons Do Not.

(A) Retrogradely labeled Area X-projecting neurons within HVc (brown, arrows point to some examples) do not express singing-related Fos (arrowhead points to an example of a Fos-IR nucleus without cytoplasmic retrograde tracer). Cholera toxin B subunit was injected into the ipsilateral Area X 3 days before the experiment. Singing was induced by playback of conspecific songs for 50min. (B) Numerous retrogradely labeled RA-projecting HVc neurons (brown) express singing-associated Fos (arrows point to some examples). Fluorogold was injected into the ipsilateral RA 6 days before the experiment. The stimulation paradigm was the same as in (A). Scale bar in B is 50μm for (A and B).

Figure 2-5

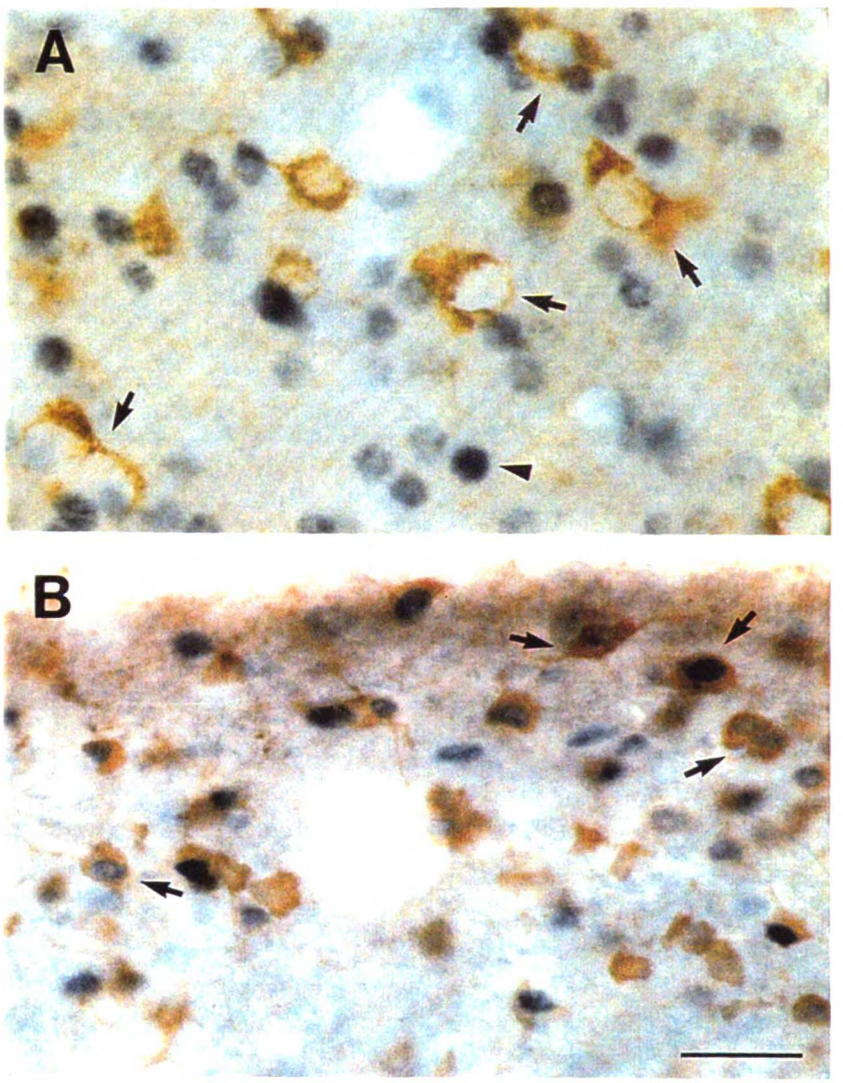

Chapter 3:

Functional Connectivity in a Circuit Dedicated to Song Learning

ABSTRACT

The anterior forebrain pathway (AFP) in songbirds may mediate the auditory feedback that is necessary for song learning and production. The output nucleus of the AFP, the lateral portion of magnocellular nucleus of the neostriatum (LMAN), sends direct projections to the robust nucleus of the archistriatum (RA), a pre-motor nucleus that controls the expression of song. Very little is known, however, about how LMAN modulates the activity of RA in an intact animal. To understand the neural interaction between LMAN and RA, we simultaneously recorded the activity of LMAN, RA, and in some cases, HVc, the source of afferents to both the AFP and RA, in anesthetized adult zebra finches.

Cross-covariance and coherency analysis revealed robust correlated activity between LMAN and RA. The majority of the pairs of LMAN-RA sites exhibited correlated activity with two components. One component, in which the probability of RA firing increased after LMAN spikes, is consistent with a correlation reflecting the direct projection from LMAN to RA. This suggests that LMAN plays a role in the song behavior of adults, in contrast to a previous hypothesis that the AFP becomes less functional in adults.

The second component of LMAN-RA correlated activity indicates an increase in RA firing probability before LMAN spikes, and most likely reflects the common input to these two nuclei from HVc. We tested this hypothesis in two ways. We recorded directly from HVc as well as LMAN and RA, and found that the activity of HVc was robustly correlated not only with the activity of its direct output, RA, but also with the activity of LMAN, even though HVc and LMAN are only indirectly connected. Second, we found that silencing HVc activity greatly diminished the second component of the LMAN-RA correlated activity, and only slightly affected the LMAN-RA correlation due to the direct interaction of LMAN with RA. Both the strong correlation between HVc-LMAN activity, and the LMAN-RA correlated activity that reflects HVc common input, suggest that correlated activity in the AFP is maintained over multiple synapses, across indirectly connected areas. Thus, the

functional connectivity in the AFP may involve divergent and reconvergent connections between song nuclei, and extensive intrinsic connections within each song nucleus.

Finally, the strength and timing of the 'common input' LMAN-RA correlated activity was variable between pairs of LMAN and RA sites, and corresponded well with the strength and timing of HVc-LMAN correlated activity in the same birds. This suggests that the neural interaction between AFP nuclei is physiologically modulated, and may reflect the state of the animal's song plasticity or behavior. Investigation of the neural interaction between song nuclei may therefore elucidate the process by which the AFP mediates song learning and behavior.

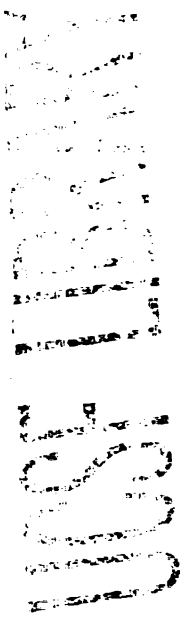

INTRODUCTION

Birdsong is a complex behavior that is learned during post-hatch development. A highly specialized and discrete set of brain areas found only in songbirds, called the song system, mediates song learning and expression of song. It is composed of two functionally distinct circuits: the motor pathway and the anterior forebrain pathway (AFP; Fig. 3-1a). The motor pathway includes the nucleus HVc (abbreviation used here as the proper name), which directly innervates another forebrain nucleus, the robust nucleus of the archistriatum (RA). RA then projects to motor neurons involved in the control of vocal and respiratory musculature (Nottebohm et al, 1976; Vicario, 1993; Wild, 1993). HVc and RA are required for song production throughout the bird's life (Nottebohm et al, 1976, Simpson and Vicario, 1990). The AFP, on the other hand, is crucial for song learning: lesions in the AFP nuclei of juveniles have been shown to disrupt song learning, while lesions in the AFP of normal adults have no effect on song production (Bottjer et al, 1984; Sohrabji et al, 1990; Scharff and Nottebohm, 1991). The first nucleus in the AFP, Area X, receives input from HVc, and the output nucleus of the AFP, the lateral portion of the magnocellular nucleus of the neostriatum (LMAN), sends direct projections to RA. Thus, the AFP forms an indirect loop from HVc to RA. Despite the established anatomical connections between the song system nuclei, little is known about how the AFP modulates the activity of the motor pathway in an intact animal.

Song learning occurs in two phases, both of which depend critically on hearing. During the first, "sensory", phase, a juvenile bird listens to and memorizes a tutor song. This is followed by the "sensorimotor phase", in which the juvenile produces variable and rambling songs that it gradually matches to the memorized tutor song (Immelman, 1969). By the time the bird reaches adulthood, the song is crystallized into a stable pattern of well defined song syllables. Juvenile songbirds deprived of either a tutor song or the auditory feedback of their own voice produce abnormal songs (Konishi, 1965; Price, 1979). Even crystallized song continues to depend on auditory feedback, although to a lesser extent than

during learning, since deafening or altering the auditory feedback in adult birds results in gradual degradation of their crystallized song (Nordeen and Nordeen, 1992; Williams and McKibben, 1992; Williams and Mehta, 1999; Leonardo and Konishi, 1998; Brainard and Doupe, 2000).

Consistent with the importance of auditory experience and feedback for song behavior, neurons in the song system of adults exhibit auditory responses that are highly selective for the bird's own song (Margoliash and Konishi, 1985; Margoliash, 1986; Okuhata and Saito, 1987; Doupe and Konishi, 1991; Volman, 1993; Vicario and Yohay, 1993). Moreover, this selectivity emerges during the course of song learning (Volman, 1993; Doupe, 1997; Solis and Doupe, 1997). The auditory response properties of the AFP neurons have led to the hypothesis that the anterior forebrain pathway may mediate the auditory feedback that is necessary for song learning (Doupe, 1993; Nordeen and Nordeen, 1992). Specifically, the AFP may transmit an evaluation of how well the bird's own song matches the memorized tutor song to the motor pathway at the level of RA, and in this way, guide song learning (Troyer et al 1996; 2000a; b; Doya and Sejknowski, 1995; Brainard and Doupe, 2000).

By this hypothesis, the neurons in RA, which receive excitatory synapses from both LMAN and HVc, are important sites of plasticity during song learning (Williams, 1989; Kubota and Saito, 1991; Mooney and Konishi, 1991; Mooney, 1992). As song learning is completed, however, the influence of LMAN on RA has been thought to be abolished. Around the time when LMAN lesions no longer disrupt normal song learning, a large number of LMAN axons retract from RA (Hermann and Arnold, 1991). By adulthood, HVc input to RA appears to have become more important than LMAN input: HVc activity is sufficient to confer auditory responsiveness in RA, while LMAN activity is not necessary for RA auditory responses (Doupe and Konishi, 1991; Vicario and Yohay, 1993).

Recent behavioral experiments, however, suggest that the AFP still has a role in song plasticity in adult birds, similar to its function in juveniles. Although lesions of the AFP in

adults have no effect on normal song production, lesions of adult LMAN largely prevent changes in crystallized song that result from late learning, tracheosyringeal nerve sections or deafening (Morrison and Nottebohm, 1993; Williams and McKibben, 1999; Brainard and Doupe, 2000). Thus, investigation of anatomical connectivity and of the source of auditory responsiveness may not be adequate assays for determining the neural interaction between song nuclei.

Therefore, to investigate the functional neural interaction between the AFP and the motor pathway, we recorded simultaneously from LMAN, RA and/or HVc nuclei in anesthetized, adult zebra finches, both during spontaneous and song evoked activity. We found that the correlated activity between LMAN and RA that likely reflects the direct LMAN to RA projection was very strong. This is consistent with a role for AFP in adult song plasticity, and contrasts with the idea that LMAN's role in birdsong behavior is abolished as song learning is completed. Surprisingly, we also observed correlated activity suggesting that activity between indirectly connected song nuclei, such as HVc and LMAN, was robustly correlated as well. This suggests that the functional connectivity of the song system allows correlated activity to be maintained across multiple synapses. Thus, a possible model for the functional connectivity of the song system involves broad divergent and reconvergent connectivity between song nuclei, and extensive intrinsic connections within song nuclei. Finally, we found that the correlation of activity within the AFP was variable in magnitude and timing, suggesting that the functional connectivity in the song system is physiologically modulated.

MATERIALS AND METHODS

Animals and Song Recording. Data were collected from 21 adult male zebra finches (>120d days, post-hatch) raised in our breeding colony. Until 55-60 days of age, the birds were housed in individual cages with their parents and siblings from the same clutch and visually isolated from other zebra finches (conspecifics) in order to limit their learning to the male parent (Immelman, 1969; Eales, 1987; Williams, 1990). At 55-60 days of age, the birds were housed in cages with conspecific males of similar age. Before the experiment, adult birds, and their tutors if available, were placed individually in a sound-attenuated chamber, and their songs were tape-recorded using a sound-triggered recording system. A bird's tutor, which is typically its father, is the adult male that provided the model song during the bird's sensory learning period (15 to 55 days of age). Tapes were scanned by playback, and after scanning 10-20 songs, the typical song of each bird was digitized and entered into a SPARC IPX computer.

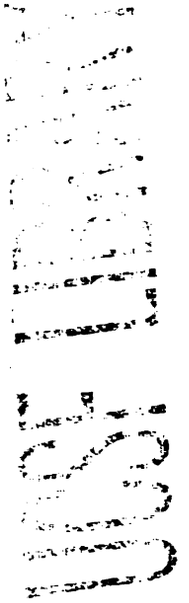

Surgery. At least two days before the experiment, birds were anesthetized with 20-30µl of Equithesin (i.m.; 0.85g chloral hydrate, 0.21g pentobarbital. 0.42g $MgSO_4$, 2.2ml 100% ethanol, and 8.6ml propylene glycol to a total volume of 20ml with water) and placed in a setreotaxic head holder. An area of the skin was removed to expose the skull, and stereotaxic head coordinates relative to the bifurcation of the midsagittal sinus were used to locate song nuclei. The top layer of skull was removed around these areas and ink marks were placed at the coordinates. Because HVc is directly above RA in the head position used, the stereotaxic head coordinates used for locating RA were chosen so that the path of RA recording electrode avoided HVc. This was accomplished by having the RA electrode approach the skull from the rear at a 45 degree angle, thus entering the brain ventral to HVc. A metal post was fixed on the skull using dental cement (Dentsply, Milford, DE).

On the day of the experiment, birds were anesthetized with a 20% solution of urethane in water (50-75µl, i.m., Sigma, St. Louis, MO; administered in three injections at

20-30 minute intervals). The head was immobilized by attaching the metal post to a holder. Body temperature was monitored and stabilized at 37-40 degrees Fahrenheit using a temperature controller (FHC, Brunswick, ME). A parylene coated tungsten (1.0-2.0 MΩ; AM Systems, Everett, WA), or glass coated platinum-iridium electrode (1.0-3.0 MΩ; Ainsworth, Wellford, UK) was positioned above each mark indicating the location of a song nucleus. The second layer of skull was removed around each marked area, the dura opened, and the electrode lowered.

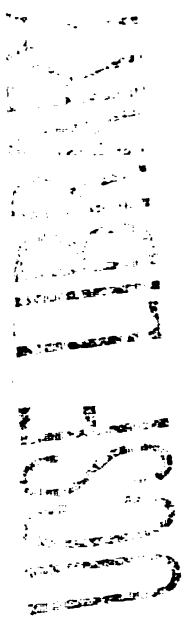

Auditory Stimuli and Presentation. The complete stimulus set included the bird's own song (BOS), its tutor song, brothers' songs, conspecific songs, songs of other species (heterospecific songs: songs from bengalese finches, white crown, song and field sparrows), a 100 msec broad-band white noise and 300 msec pure tone bursts (1 and 2 kHz). The set also included versions of the BOS and tutor song whose temporal order had been manipulated: these included songs presented in reverse, where each syllable and the entire sequence of syllables are reversed, and songs in reverse order, where only the sequence of syllables is reversed. In some trials, no stimulus was played and only spontaneous activity was collected.

Because the primary goal of the work was to study the correlation of activity between song nuclei, not all stimulus types were presented to each recording site. A subset of the stimulus set was consistently used across all sites: the BOS, tutor song and a 100 msec broad band white noise burst. When possible the following stimuli were presented: the BOS and tutor song in reverse and reverse order, 1-3 songs of brothers, 1-3 conspecific songs, 1-3 heterospecific songs, and at least one pure tone burst. Most trials (10-368) were devoted to the BOS while (5-80) trials each of the other stimuli were presented.

The duration of song stimuli varied from 1.2 - 2.6s. All song stimuli were filtered with a high pass filter at 300-700 Hz and a low pass filter at 8 kHz, and normalized to an average root mean square amplitude of 70dB. The bird was placed in a double-walled

anechoic sound-attenuated chamber (Acoustic Systems, Austin, TX), with auditory stimuli presented from a calibrated speaker 23 cm away from the bird. The frequency-response in the chamber was flat (±6 dB) within the range of 500Hz to 10.5 kHz. The speaker was calibrated to broadcast sound with a maximum intensity level of 75dB. Stimuli were presented in an interleaved fashion with 6 to 8 seconds of inter-stimulus interval to prevent habituation of neuronal activity. In some experiments, the stimuli were presented in a randomized, interleaved fashion.

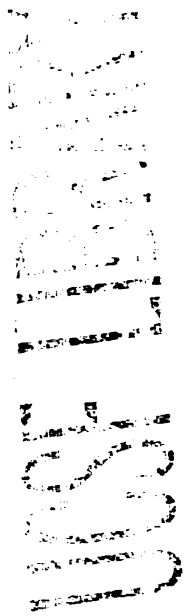

Electrophysiology. *LMAN and RA simultaneous recording* LMAN and RA extracellular activity were recorded simultaneously. The neuronal signals were amplified and filtered between 300 Hz and 10 kHz through separate channels. Using a window discriminator (FHC), small clusters (2-5 units) or single units were isolated, and their spike arrival times recorded in the computer using a data collection software developed by Michael Lewicki and Larry Proctor (California Institute of Technology), and Frederic Theunissen (UCSF). LMAN and RA were identified by their characteristic spontaneous activity (Solis and Doupe, 1997; Doupe, 1997; Vicario and Yohay, 1993), and recordings were made whenever this activity was encountered to test for the presence of auditory responses. Multiple and single units were defined to be auditory when the average firing rate during at least one stimulus type was significantly different ($p<.05$, paired student's t-test) than the spontaneous firing rate collected during a period of 2 seconds immediately before stimulus onset. Search stimuli included BOS, tutor song, and a broad band white noise burst. Data for each stimulus were displayed as raster plots and summed peri-stimulus time histograms (30 msec bin width) for 5-10 trials. Stability of the recording sites were monitored by observing the waveforms displayed on oscilloscopes and the spontaneous firing rates. Trials where the neuronal activity was not stable were discarded. Electrolytic lesions were made at particular recording sites to serve as guides for locating the rest of the recording sites.

At the end of the experiment, birds were deeply anesthetized with Metofane, and perfused intracardially with 0.9% saline or Lactated Ringer's and 3.7% Formalin in .025M Phosphate buffer. Brains were post-fixed in Formalin, and sliced into 40 μm sections. Every other section was mounted on glass slides, and Nissl or Silver stained. Stained sections were examined under light microscopy, and recording sites were reconstructed based on the stereotaxic coordinates of the lesions.

Three electrode recording. In some LMAN-RA experiments, an additional parylene-coated tungsten electrode (1.0-2.0 MΩ, AM systems) was positioned above HVc coordinates. Extracellular neuronal activity of small clusters (2-5 units) of HVc, LMAN and RA activity were recorded either simultaneously or in a pair-wise manner (in initial experiments, due to limitations of the recording set-up). Pair-wise recordings involved recording from two nuclei at a time, without moving the electrodes, such that the recordings were always made from the same HVc, LMAN and RA sites. HVc neuronal activity was recorded as described above for LMAN and RA, and was identified based on its characteristic spontaneous activity.

Inactivation experiments. To determine the effect of disrupting HVc activity on the correlation of activity between LMAN and RA, HVc activity at and around the recording site was silenced using 2mM kynurenate, a glutamate receptor antagonist (180 ηl-5μl, pH 7.4, with 10% biotin dextran amine (BDA; Molecular Probes, Eugene, OR) and Pontamine Sky Blue (BDH Lab Supplies, England) in 0.1M Phosphate buffer). HVc, LMAN and RA activity were recorded simultaneously, as described earlier, before, during and after infusing kynurenate into HVc. All recordings were extracellular, and from small clusters of units (2-5 units).

An injection/recording electrode that consisted of a double barreled glass electrode pulled to 20-35μm tip size, to which a parylene coated tungsten electrode (1.0-2.0 MΩ, AM Systems) was glued with epoxy and dental resin (3M Dental Products, St. Paul, MN) was positioned above and lowered into HVc. The tips of the glass and tungsten electrodes were

5-40μm apart in depth, and 10-150 μm apart in the horizontal axis. In some experiments, a parylene coated tungsten electrode (1.0-2.0 MΩ) was first used to locate HVc, and then replaced with the injection/recording electrode. The kynurenate solution was delivered by manual pressure injection using a Hamilton syringe attached to a calibrated micromanipulator (Sutter Instruments, Novato, CA). The amount injected was also monitored by the level of the solution relative to calibration marks made on the glass electrode or polyethylene tubing that attached the electrode to the pressure injector.

When all recording sites were auditory to at least one stimulus type, the responses were characterized by presenting different types of stimuli to establish a baseline of correlated activity between the three nuclei. In cases where the HVc tungsten electrode was replaced with an injection/recording electrode, activity in all three sites was re-characterized to ensure that the sites had not changed or were not damaged. When the baseline correlated activity between LMAN and RA showed two narrow peaks (see results; Figure 3-2b, inset), kynurenate was injected slowly and in small amounts (over 13-43 minutes) while simultaneously recording from HVc, LMAN and RA (n=3). Recording of neuronal activity was continued for 1.5-2.5 hours after the start of kynurenate injection. At the end of the experiment, birds were sacrificed and their brains processed as described earlier. In addition, the brain sections were processed for BDA to visualize the approximate spread of kynurenate.

Data Analysis. To be included in the data set for analysis, the pairs or triplets of recording sites were all required to be auditory. The locations of the recording sites used for data analysis were also confirmed to be in the corresponding song nucleus.

Correlated activity. To quantify how well the activity of two nuclei was correlated, the cross-covariance (Aertsen et al, 1989) and coherency functions (Brillinger et al, 1976; Rosenberg et al, 1989) of the activity in one nucleus relative to the activity in another nucleus were calculated with the aid of a mathematical software Matlab v5.2 (The

Mathworks, Inc., Natick, MA). Both cross-covariance and coherency functions were calculated for two time intervals: during the stimulus presentation of the BOS (evoked activity), and during 2 seconds of spontaneous activity before stimulus onset. For the spontaneous activity, all trials with different stimuli were merged. In a small number of cases (n=1 for multi-unit and n=2 for single unit activity), however, the spontaneous activity from BOS trials showed significant coherency peaks that were not significant in the spontaneous activity from all trials. These coherency peaks derived during spontaneous activity from BOS trials were included in the analysis because, on average, the spontaneous coherency peaks from BOS trials were not significantly different from those from merged trials (with respect to peak and overall strength, time delay and width; see below).

To calculate the cross-covariance, the cross-correlation function was calculated, and then the shuffled cross-correlation was subtracted from it. The cross-correlation (Cross(τ_κ)) (Perkel et al, 1967; Moore et al, 1970) of a spike train (r(t)) relative to a second spike train (s(t)) as a function of τ_κ (time delay relative to spikes in s(t)) is given by

$$Cross(\tau_K) = \frac{1}{N}\sum_{i=1}^{N}\frac{1}{T}\int_0^T s_i(t)r_i(t+\tau)dt$$

where N is the number of trials, and T is the time interval being studied.
In practice, the data were binned in 10msec time windows and the cross-correlation function was calculated using the discrete version

$$Cross(\tau_K) = \frac{1}{N}\sum_{i=1}^{N}\frac{1}{T}\frac{1}{dt}\sum_{j=1}^{T_n} s_i(t_j)r_i(t_j+\tau_K)$$

where dt = 10 msec and T_n is the number of bins in the interval being studied.

To remove features that are influenced by an event that repeats itself identically for all trials, which is usually the stimulus, we subtracted the shuffled cross-correlation from the raw cross-correlation, thereby removing any stimulus triggered effects on the cross-correlation (Perkel et al, 1967; Palm et al, 1988; Aertsen et al, 1989). The shuffled cross-correlation was

calculated by correlating trial (i) with trial (i+1). This correlation also takes into account the expected mean firing rate of r(t), and so subtracting the shuffled cross-correlation from the raw cross-correlation gives the cross-covariance function (Aertsen et al, 1989).

A possible source of cross-covariance between the activity of two neurons that does not reflect the neuronal interaction between these neurons is the temporal structure of firing within each neuron. For example, a spike in neuron A triggers a spike in neuron B; however, neuron A has a high probability of firing again once it has fired an action potential. Hence, the second spike in neuron A would also be correlated to the spike in neuron B that was triggered by the first spike from neuron A. To take this type of correlation into account, we calculated the coherency function (Brillinger et al, 1976; Rosenberg et al, 1989). The coherency function includes normalization of the cross-covariance function by the temporal structure of firing within each site (the auto-covariance of each spike train) and therefore excludes any secondary effects in the correlated activity between two areas that may arise from the nature of firing activity within each area. The coherency function is thus a better estimate of the association of firing between two recording sites than the cross-covariance function. .

The coherency function of activity r(t) in one nucleus relative to the activity s(t) of another nucleus is given by:

$$Coherency_{rs}(\lambda) = \frac{f_{rs}(\lambda)}{\sqrt{f_{rr}(\lambda) f_{ss}(\lambda)}}$$

where $f_{rs}(\lambda)$ is the the Fast Fourier Transform (FFT) of the cross-covariance function of r(t) relative to spikes in s(t), and $f_{rr}(\lambda)$ and $f_{ss}(\lambda)$ are the FFT of the auto-covariance of r(t) and s(t), respectively. The auto-covariance functions were calculated in the same manner as the cross-covariance, except that each spike train was correlated with itself. The inverse FFT of the coherency function was calculated for plotting purposes. The coherency function ranges from -1 to +1 and is a measure of association between two processes, with ± 1 indicating perfect linear prediction of r(f) based on knowledge of s(f) and 0 indicating that knowledge of s(f) was ineffectual in the linear prediction of r(f).

The standard error of our estimate of the cross-covariance and coherency functions were calculated using a bootstrap re-sampling method called Jackknife (Thomson and Chave, 1991). This has the advantage of not making any assumptions on the nature of the spike train probability distributions, whereas the analytical technique of determining the standard error assumes that the firing rates have a normal distribution and that r(t) and s(t) are independent. The Jackknife method involves re-sampling the data set, but with a different single trial omitted each time, thus creating a 'pseudo' data set with N values (where N = number of trials in the original data set) whose variance can be measured. The Jackknife variance is obtained using Tukey's formula:

$$variance\{F(\tau_K)\} = \frac{N-1}{N}\sum_{j=1}^{N}[F_j(\tau_K) - F_{mean}(\tau_K)]^2$$

where $F_j(\tau_K)$ is the correlation function when the *jth* sample is deleted, and $F_{mean}(\tau_K)$ is the mean of all the $F_j(\tau_K)$ correlation functions. The Jackknife variance of a cross-covariance function was estimated by the calculating the variance of N (number of trials) values of the shuffled cross-covariance, where one pair of trials was deleted each time. The Jackknife variance of a coherency function was calculated from N (number of trials) values of coherency functions that were derived from shuffled cross-covariance functions: one pair of trials was deleted at a time, the shuffled cross-covariance was calculated, and then normalized by the auto-covariance of both spike trains to obtain the coherency function.

To measure parameters of the cross-covariance and coherency functions, we fitted both functions with 3 Gaussian functions: first, all the data points from τ_κ = -1000 to 1000 ms (outside region), except for the central region (τ_κ = -100 to 100 ms), were fitted with one Gaussian, and then the central region minus the fit of the outside region was fitted with two Gaussians (for example, see Fig. 3-2a). For LMAN-RA coherency functions, however, the Gaussian fits of the outside region had amplitudes close to zero during both spontaneous and evoked activity (for multi-unit activity, mean=.006$\pm$.017, n=80 and for single units,

mean=.007±.016, n=40). Thus, only the central region of LMAN-RA coherency functions were fitted with Gaussians (for example, see Fig. 3-2b). For the same reason, the same fitting method was applied to HVc-RA and HVc-LMAN coherency functions. The amplitude of the peak of each Gaussian, its time delay and half-width at 61% amplitude (specifically, $amplitude \times e^{-1/2}$) were measured (Fig. 3-1b). The strength of correlation was assessed in two ways: (1) the peak strength, defined as the maximum coherency and equivalent to the peak amplitude, and (2) the overall strength, defined as the total coherency over all time delays (τ) and calculated as $amplitude \times width$ (area under the peak). Because the data were binned in 10 ms time windows, the amplitude, time delay and width were directly measured from the data in cases when the width of a peak was less than 10 ms. These measurements were used to confirm or replace the parameters obtained from the Gaussian fit. Goodness of fit was estimated by calculating the regression between the fit and actual data points (an R^2 value), but also assessed by visual inspection. An R^2 value > 0.7 was considered a good fit. Fits that clearly were off were thrown out. To be considered a significant peak, the amplitude of the peak was required to be greater than three times the square root of the corresponding Jackknife variance (Jackknife noise), which is a 99% confidence level. To ascertain that the central region had two separate peaks, the separation of the peaks (difference between time delays) had to be greater than the sum of their widths. This model fit the cross-covariance and coherency functions with 2 peaks in the central region well (coherency: multi-unit, R^2= .93±.04, single unit, R^2= .91±.07; cross-covariance: multi-unit, R^2= .94±.05; single unit, R^2= .90±.05), but in some cases the data did not have two well-separated peaks. These cases included three different types of functions: (1) functions where only one of the two peaks was significant, (2) functions with peaks did not meet our criteria for separation and (3) functions that showed only one peak. Only the last type of coherency functions was considered to have a true single peak, and the central regions of these functions were re-fit with one Gaussian.

To determine the changes in correlated LMAN and RA activity before and after disrupting HVc activity (see Inactivation Experiments above), the coherency functions during

spontaneous activity for trials before and during silencing of HVc activity using kynurenate were calculated. Kynurenate trials were defined as trials collected after the start of kynurenate injection, with stable spontaneous firing rates before stimulus presentation, which typically began 6-17 minutes after the start of the kynurenate injection. Coherency peaks for pre- and kynurenate activity were fitted with Gaussian functions as described above. In order to quantify the changes in the coherency function in one case where a peak from the pre-kynurenate coherency function disappeared in the kynurenate trials due to the manipulation, a "peak" with the same time delay as its corresponding pre-kynurenate peak was chosen and fitted with a Gaussian.

Selectivity. The selectivity of auditory responses in LMAN, RA and HVc was described using a metric d' (Green and Swets, 1996) that quantifies the ability of neurons to discriminate between stimulus A and B. Preference for stimulus A over stimulus B was calculated as follows:

$$d'_{A-B} = \frac{2(\overline{RS}_A - \overline{RS}_B)}{\sqrt{\sigma_A^2 + \sigma_B^2}}$$

where $\overline{RS}_A$ and $\overline{RS}_B$ are the mean response strengths to stimulus A and B, respectively and σ^2 is the variance of the mean RS. The response strength was measured as the firing rate during stimulus presentation minus the spontaneous firing rate during two seconds before stimulus onset. Neurons were considered selective for a stimulus type if their $d'_{A-B} > 0.5$ or $d'_{A-B} < -0.5$. A value of $d'_{A-B} > 0.5$ indicated that the neurons preferred stimulus A over stimulus B, while $d'_{A-B} < -0.5$ indicated the opposite.

Two types of selectivity were examined, song selectivity and BOS order selectivity (Margoliash, 1986; Doupe, 1997; Solis and Doupe, 1997). To describe song selectivity, we compared the auditory responses to the BOS and another song type, either the tutor song, brothers' songs or conspecific songs. To determine BOS order selectivity, we calculated the d′ between responses to the BOS presented in forward order and reverse or reverse order.

Topographical alignment of LMAN and RA recording sites. LMAN projections to RA are topographically organized in 3 broad compartments with considerable overlap at the boundaries (Johnson et al, 1995). Using Nissl and Silver stains of the sections encompassing LMAN and RA, we identified each recording site as being approximately well within or on the boundaries between these three compartments. The topographical alignment of the pairs of recording sites was then rated as follows: (3) excellent, when the LMAN compartment(s) where the LMAN recording site was located sends projections to the RA compartment(s) where the RA recording site was located; (2) fair, when the LMAN compartment(s) with the LMAN recording site was adjacent to the LMAN compartment that projects to the RA compartment(s) that contained the RA recording site; and (1) poor, when the LMAN compartment with the LMAN recording site was not adjacent to the LMAN compartment that sends projections to the RA compartment where the RA recording site was located.

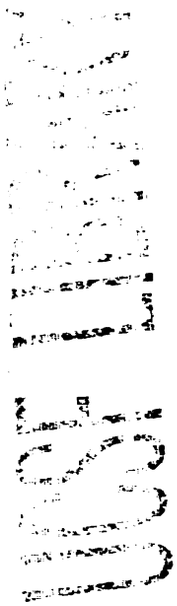

RESULTS

Correlated activity between LMAN and RA

We recorded simultaneously from LMAN and RA of anesthetized adult zebra finches (Figure 3-1a), collecting activity from 40 pairs of multi-unit auditory LMAN-RA neurons (2-5 units at each site, n=15 birds) and 20 single unit auditory pairs (n=6 birds). All LMAN and RA sites were selective for BOS, responding more strongly to BOS than to songs of other adult zebra finches (CON; see Methods). The mean d' values for BOS response relative to CON response ($d'_{BOS-CON}$) for LMAN single and multi-unit sites were 1.37±.48 and 1.76±.67, respectively, and for RA single and multi-unit sites, 1.91±1.00 and 2.26±.96, respectively. LMAN and RA sites also exhibited BOS order selectivity, preferring the BOS played in normal order over temporally altered versions of BOS such as reverse BOS (REV; see Methods). For LMAN single and multi-unit sites, the mean d' values for BOS response relative to reverse BOS response ($d'_{BOS-REV}$) were 1.95±.66 and 2.03±.84, respectively; for RA single and multi-unit sites, the mean $d'_{BOS-REV}$ were 2.13±.23 and 2.93±1.18, respectively. These results are similar to those shown in earlier studies (Doupe and Konishi, 1991; Doupe, 1997; Solis and Doupe, 1997; Vicario and Yohay, 1993).

To measure the relationship between activity in LMAN and RA, we calculated the cross-covariance and coherency functions of RA activity relative to LMAN spikes, for data collected during spontaneous activity preceding all stimuli, and during evoked activity in response to the BOS. For both of these functions, correlations due to events that occurred identically across all trials (usually, the stimulus) were removed by subtracting the shuffled cross-correlation from the raw cross-correlation (see Methods). We fitted the data with Gaussian functions and measured the following parameters of the observed peaks (Fig. 3-1b): a) time delay relative to LMAN spikes at time delay = 0, b) half-width ('width') at 61% amplitude (*amplitude x* $e^{-1/2}$), c) peak strength, which is the strength at the peak time delay and equivalent to the amplitude, and d) overall strength, which is the strength over all time delays and calculated as the area under the peak (*amplitude x width*). A peak was considered

significant if its amplitude was greater than 3X our estimate of the standard error, and if the Gaussian function fit from which it was derived had a goodness of fit value (R^2) that was greater than 0.70 (see Methods). Both the cross-covariance and coherency functions revealed strong correlated activity between LMAN and RA, as indicated by significant positive peaks in the cross-covariance plots (cross-covariograms; Figure 3-2a) and coherency plots (Figure 3-2b). Twenty six out of 40 (65%) LMAN-RA pairs exhibited at least one significant peak in their cross-covariograms during spontaneous activity, while 22/40 (55%) LMAN-RA pairs displayed at least one significant peak during evoked activity. Using the coherency analysis, we found that 29/40 (72.5%) of the LMAN-RA pairs exhibited at least one significant coherency peak during spontaneous activity, while 22/40 (55%) exhibited at least one significant coherency peak during evoked activity.

The positive peaks in the cross-covariograms of LMAN-RA spontaneous multi-unit activity exhibited two different widths: narrow and wide. The presence of a wide peak was assessed by how well all data points, except those with time delays between -100 and 100 msec, were fit by a single Gaussian function (goodness of fit value, R^2). An $R^2 > .70$ was considered a good fit. With this criterion, 20/40 (50%) LMAN-RA pair sites exhibited wide peaks during spontaneous activity, although only 15 of these peaks were significant. The mean width of the significant wide peaks during spontaneous activity was 353.16$\pm$135.46 msec (Figure 3-2a, 3-3a), while the mean width of the significant narrow peaks was 18.61$\pm$9.96 msec (n=24/40 pairs; Fig. 3-2a, 3-3a). During evoked activity, however, only 2/40 (5%) LMAN-RA pairs exhibited wide peaks in their the cross-covariograms and none of these peaks were significant, while 22/40 pairs exhibited narrow peaks with a mean width of 14.41$\pm$6.67 msec (Figure 3-3b).

The coherency plots, on the other hand, exhibited only significant narrow peaks (Figure 3-2b). The narrow peaks observed in the LMAN-RA coherency functions will be described in the following sections. The mean R^2 values for the wide peaks were 0.19$\pm$.20 (range, 1.61×10^{-4} - 0.61; n=40) during spontaneous activity, and 0.03$\pm$.05 (range, 5.53×10^{-8}

- 0.27; n=40) during evoked activity, indicating the lack of wide peaks in the coherency functions. Moreover, the mean amplitudes of the putative wide peaks were close to zero: the mean amplitude was 0.01+.02 (n=40) during spontaneous activity and 0.003+.004 (n=40) during evoked activity. Thus, we only fitted the data between -100 and 100 msec with Gaussian functions.

The coherency function is obtained by normalizing the cross-covariance by the auto-correlation of firing both within LMAN and RA (Rosenberg et al; also see Methods). Hence, the elimination of the wide correlation peak by this normalization suggests that the long time scale correlation between LMAN and RA activity is largely due to the temporal structure of spontaneous firing within LMAN and RA. Because the coherency function provides a normalized estimate of the correlation of activity between LMAN and RA, and gave similar results to the cross-covariance analysis (except for the elimination of the wide peak reported above), from here on we will focus on the results derived from the coherency analysis.

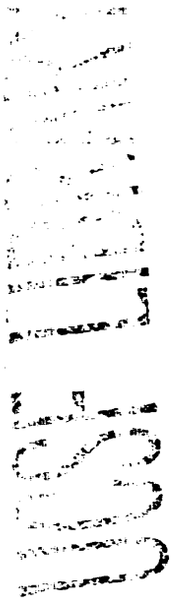

To be certain that the LMAN-RA correlations observed were not an artifact of the multi-unit recordings, we examined the coherency functions of RA single unit activity relative to spikes from single LMAN neurons (n=22 single unit LMAN-RA pairs). As was observed for multi-unit data, the LMAN-RA coherency functions for single unit data did not exhibit wide peaks (Fig. 3-4), as evinced by the low mean goodness of fit values (R^2) during spontaneous (0.15$\pm$.16. n=22) and evoked activity (.03$\pm$.04, n=22). Similarly, the coherency functions of LMAN-RA single unit activity showed only significant narrow peaks: 13/22 (59%) and 7/22 (32%) LMAN-RA unit pairs had at least one significant narrow peak during spontaneous and evoked activity, respectively. This indicates that LMAN and RA activity are correlated at the single unit level, and it is unlikely that the coherency peaks derived from multi-unit activity recordings are artefactual.

Narrow peaks observed in coherency functions. Examination of the narrow peaks in the coherency functions of RA multi-unit activity relative to LMAN spikes (also multi-unit) revealed several different types of LMAN-RA coherency functions during both spontaneous (Fig. 3-5) and evoked activity (Fig. 3-6). LMAN-RA coherency functions exhibited either a) two narrow peaks that were well separated in time, b) two narrow peaks that were either not clearly separable and/or where one of the two peaks was not significant ('non-separable/significant'), c) a single peak, or d) no significant peaks. Two peaks were considered well-separated when the difference in their time delays was greater than the sum of their half-widths. The majority of the LMAN-RA multi-unit pairs, 15/40 (37.5%) during spontaneous activity (Fig. 3-5a) and 13/40 (32.5%) during evoked activity (Fig. 3-6a), exhibited two well-separated peaks in their coherency functions. The two-well separated peaks had distinct time delays (Table 3-1): one had a positive time delay, while the other, a negative time delay. This suggests that these two peaks represent different correlations (see following section).

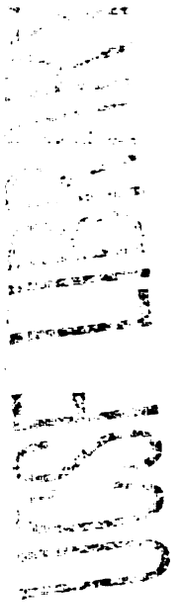

Examination of the LMAN-RA coherency peaks derived from single unit activity showed the same types of coherency functions as were observed for multi-unit activity. During spontaneous activity, 6/22 (27%) LMAN-RA unit pairs exhibited two well separated peaks, 5/22 (23%) pairs exhibited 'non-separable/significant' peaks, 2/22 (9%) pairs exhibited a single peak, and 9/22 (41%) pairs did not show any significant peaks. During evoked activity, 7/22 (32%) pairs exhibited 'non-separable /significant' peaks, and 15/22 (58%) pairs had no significant peaks. As in the multi-unit activity, the two well-separated peaks had distinct time delays, where one had a negative time delay and the other, a positive time delay (Fig. 3-4; Table 3-1). The same criterion for peak separation was applied as in the multi-unit activity data. This indicates that the neuronal interactions between LMAN and RA activity at the multiple and single unit level are similar.

During spontaneous multi-unit activity, 6/40 (15%) LMAN-RA pairs showed 'non-separable/significant' peaks in their coherency functions (Fig. 3-5b), while during evoked

multi-unit activity, 6/40 LMAN-RA pairs exhibited such peaks (Fig. 3-6b). Compared to the two well-separated peaks in multi-unit coherency functions, these 'non-separable/significant' peaks had, on average, a similar positive time delay (spontaneous: 5.55±7.80 msec, n=6; evoked: 8.50±3.95 msec, n=6), and a negative time delay that was shifted closer to zero (spontaneous: -20.94±23.55 msec, n=4; evoked: -9.31±2.85 msec, n=3). This suggests that the two narrow peaks that were well separated in other cases may have overlapped in time, and that this overlap was primarily due to the shift of the negative time delay closer to zero. Also, in cases where one of the two peaks was not significant, it was always the peak with a negative time delay that was not significant. This suggests that in coherency functions with two putative peaks, the peak with a negative time delay is most likely to vary in strength.

In 8/40 (20%) LMAN-RA pairs during spontaneous multi-unit activity (Fig. 3-5c) and 3/40 (7.5%) LMAN-RA pairs during evoked multi-unit activity (Fig. 3-6c), only a single coherency peak was observed. The single peaks were symmetric, which may indicate a single correlation or completely overlapping correlations. Eleven out of 40 (27.5%) LMAN-RA pairs did not exhibit any significant peak during spontaneous multi-unit activity, while 18/40 (45%) LMAN-RA pairs also did not have any significant peaks during evoked multi-unit activity. We will focus initially on the peaks found in LMAN-RA coherency functions with two separable peaks or a single peak because the time delays, widths, peak and overall strengths of these peaks can be well characterized.

Coherency functions with two well-separated peaks. The two well-separated narrow LMAN-RA coherency peaks had distinct time delays. One peak had a positive time delay (LR+ peak), indicating an increase in RA firing probability after a LMAN spike (LMAN->RA), while the other peak had a negative time delay (LR- peak), indicating an increase in RA firing probability before a LMAN spike (RA->LMAN; Fig. 3-5a, 3-6a). The mean time delays of the LR- and LR+ peaks were significantly different from each other during both

spontaneous and evoked activity (Table 3-1; Fig. 3-7a, b). The correlation represented by the LR+ peak is consistent with a direct excitatory connection from LMAN to RA (Perkel et al, 1967; Moore et al, 1970), in agreement with the known direct excitatory projection from LMAN to RA (Okuhata and Saito, 1987; Bottjer et al., 1989; Mooney and Konishi, 1991; Mooney, 1992). The LR- peaks could in theory represent RA firing directly driving LMAN activity, but the time delay is very long for a direct connection, and no such direct connections are known to exist. An alternative is that the correlation represents common excitatory input to both areas, with one post-synaptic area (RA) receiving the pre-synaptic spike earlier than the other area (LMAN: Moore et al, 1970). The most likely source of common input is HVc, because it sends projections directly to RA and indirectly to LMAN, via several intervening nuclei (Figure 3-1a; Mooney and Konishi, 1991; Mooney, 1992). This could result in an increase in RA firing probability before an LMAN spike (Fig. 3-8).

The overall strengths of the correlation represented by the LR- and LR+ peaks, as measured by the area under the LR- and LR+ peaks (*amplitude* × *width*), were similar during both spontaneous (Fig. 3-7g) and evoked activity (Fig. 3-7h; Table 3-1). However, the shapes of the peaks indicated different neural interactions. The LR- peak was significantly wider and lower in peak strength than the LR+ peak during both spontaneous and evoked activity (Fig. 3-7c, d, e, f), indicating correlated activity between LMAN and RA that was relatively weaker and more dispersed in time (Table 3-1; Figure 3-2b, inset). The LR+ peak, on the other hand, exhibited narrow width and high peak strength, representing a brief but strong LMAN and RA correlation (Table 3-1; Figure 3-2b, inset). The difference in peak strength between the two peaks was less during evoked activity due to a significant increase in LR- peak strength during evoked activity ($p<.0001$, Mann-Whitney). Presentation of the BOS resulted in narrower LR- and LR+ widths, although a significant decrease was observed only in the LR+ peaks (Table 3-1; $p<.05$, Mann-Whitney). A serial, indirect connection between two areas would be expected to result in correlations that are weaker and more dispersed in time than correlated activity between areas that are directly

connected (Fetz and Cheney, 1980). The differences in width and peak strengths between LR- and LR+ peaks are thus consistent with the LR- correlation including an indirect connection (namely, HVc to LMAN) and the LR+ correlation, a direct connection (specifically, from LMAN to RA; Fig. 3-8).

Coherency functions with a single peak. The mean time delay of the peaks observed in LMAN-RA functions with a single peak (LR peaks) was not significantly different from zero during both spontaneous and evoked activity (Table 3-2; $p>.73$, One Sample Sign Test). Moreover, the time delay of the LR peaks was different from those of the two well-separated peaks (LR-, LR+ peaks). The mean LR time delay was significantly more positive than the mean time delay of the LR- peaks during both spontaneous ($p<.001$, Mann-Whitney; Fig. 3-7a) and evoked activity ($p<.01$, Mann-Whitney; Fig. 3-7b). The mean time delay of the LR peaks was more negative than the mean LR+ time delay, but this difference was significant only during evoked activity ($p<.05$, Mann-Whitney; Fig. 3-7a, b). Presentation of the BOS did not have any significant effects on the time delay of the LR peaks. The differences in time delay between the LR and the two well-separated peaks suggest that the correlation represented by the LR peak is unlike those represented by the LR- and LR+ peaks, and could represent synchronized firing between LMAN and RA.

There were also differences in width, peak and overall strengths between LR peaks and two well-separated peaks, providing more evidence that the LR peaks are quite distinct from LR- and LR+ peaks. The correlation represented by the LR peak was more dispersed in time than the correlation represented by LR+ peaks, but was similar to that of LR- peaks (Tables 3-1 and 3-2; Fig. 3-7c, d). However, the difference in width between LR and LR+ peaks was significant only during spontaneous activity, primarily because the LR peaks showed a large and significant decrease in width during evoked activity ($p<.05$, Mann-Whitney). The mean peak strength of LR peaks was significantly weaker than that of the LR+ peaks, but was similar to that of the LR- peaks during spontaneous activity (Tables 3-

1, 3-2; Fig. 3-7e). However, the mean overall strength (*amplitude x width*) of the LR peaks was significantly higher than those of the LR- and LR+ peaks during spontaneous activity (Fig. 3-7g), primarily because the LR peaks had a greater mean width than the LR- and LR+ mean widths. During evoked activity, the peak and overall strengths of the LR peaks were not significantly different from those of the LR- and LR+ peaks (Fig. 3-7f, h), although BOS stimulation did not significantly change the peak and overall strengths of the LR peaks.

Coherency functions of single unit LMAN and RA activity. To further assess whether the correlated activity between LMAN and RA at the single unit level is similar to that observed at the multi-unit level, we compared the temporal characteristics and correlation strengths of the two well separated peaks and single peaks from single and multiple unit data. The mean time delays and widths of the two well separated peaks for single unit data (LR-,su and LR+,su peaks) were not significantly different from that of their corresponding coherency peaks from multi-unit data (Table 3-1). However, the mean peak strength of LR+,su peaks and mean overall strength of the LR-,su peaks, both during spontaneous activity, were significantly lower than those of the corresponding multi-unit coherency peaks ($p<.05$, Mann-Whitney; Table 3-1). The single peaks observed in LMAN-RA coherency functions for single unit data (n=2) during spontaneous activity had a mean time delay, width, peak and overall strengths that were not significantly different from those of the single peaks (n=8) obtained from multi-unit data during spontaneous activity (Table 3-2). The data suggest that the correlated activity between LMAN and RA at the single and multiple unit levels has similar temporal characteristics, although the peak and overall strengths are different, as expected from recording the activity of multiple vs. single units.

Topographical alignment of LMAN and RA recording sites. We examined whether the locations of the LMAN and RA recording site pairs with respect to the topography of

LMAN projections to RA correlated with the coherency between LMAN and RA activity. There was no difference in the time delay, widths, peak and overall strengths of coherency peaks between LMAN and RA site pairs that were in matching topographical compartments and pairs located in compartments that were not well matched (see Methods). This was true for LMAN-RA coherency functions that exhibited two well-separated narrow peaks ($p \geq .11$; Kruskal-Wallis Test) and for functions that showed a single peak ($p > .08$, Mann-Whitney Test). Moreover, there was no relationship between the type of coherency functions observed (functions with two well-separated, 'non-separable/significant', single or no peaks), and how well the LMAN and RA compartments matched topographically during both spontaneous and evoked activity ($p > .74$, χ^2 test). This suggests that the topographical organization of LMAN projections to RA does not strictly predict the interaction between LMAN and RA activity.

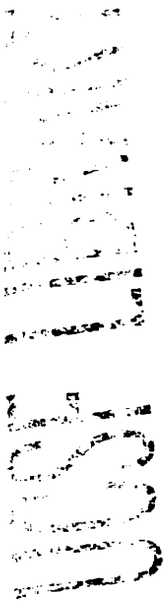

Correlation of Activity between HVc, LMAN and RA

If the LMAN-RA coherency peak with a negative time delay is due to the common input of HVc to LMAN and RA, then the correlated activity between LMAN and RA should reflect the correlation of activity between HVc and LMAN, and HVc and RA (Fig. 3-8). We therefore recorded multi-unit activity from HVc, LMAN and RA auditory neurons simultaneously (n=6 sets of sites, from 3 birds) or in a pair-wise manner, that is, collecting activity from two nuclei at a time from a set of HVc, LMAN and RA sites (n=5 sets, from 1 bird; see Methods) during spontaneous and evoked activity. All the multi-unit sites in HVc preferred the BOS over songs of other zebra finches (CON), as shown by the mean $d'_{BOS-CON}$ of 2.95 ± 1.37 (n=9 sites), and were BOS order selective; for example, the HVc neurons responded more strongly to the BOS presented in forward order than in reverse (REV) (mean $d'_{BOS-REV} = 3.70 \pm 1.48$, n=7 sites). These results are as expected from previous studies (Margoliash and Konishi, 1985; Margoliash, 1986; Theunissen, 1997).

Coherency of LMAN-RA and HVc-LMAN activity. The coherency of LMAN activity relative to HVc spikes was well correlated with the association of LMAN and RA activity. When LMAN-RA coherency functions exhibited two well-separated narrow peaks (n=5 during spontaneous; n=2 during evoked activity), the corresponding HVc-LMAN coherency functions in all but one case showed a significant positive peak with a long positive time delay of 59.01±14.60 msec (n=5) during spontaneous activity, and 22.06 msec (n=1) during evoked activity (HL peaks; Figure 3-9a, b). In the remaining case, a LMAN-RA coherency function with two peaks during evoked activity corresponded to an HVc-LMAN coherency function that exhibited a peak with a similar long positive time delay but did not reach significance. An HVc-LMAN coherency peak with a positive time delay indicates an increase in LMAN firing probability after an HVc spike, which is consistent with an indirect, net excitatory projection from HVc to LMAN.

LMAN-RA coherency functions that exhibited either a single peak (n=3 during spontaneous, n=2 during evoked activity; Fig. 3-9d), or 2 peaks that were either not separable and/or one of the two peaks was not significant (n=1 for spontaneous, n=3 for evoked) corresponded to HVc-LMAN coherency functions that either had no peaks (n=2 for spontaneous, n=1 for evoked) or a positive peak with a much shorter time delay than those of the HL peaks described above (for spontaneous: 5.53±6.73 msec, n=2; for evoked: 3.58±3.16, n=4; Fig. 3-9e). In cases where the LMAN-RA coherency functions did not have any significant peaks (n=4 for spontaneous, n=1 for evoked; Fig. 3-9g), the corresponding HVc-LMAN coherency functions also did not show significant peaks (Fig. 3-9h). The variability of positive time delays of the HVc-LMAN peaks suggest that there may be factors as yet unknown that influence the correlation between HVc and LMAN activity. The data also suggest that the correlated activity between LMAN and RA depends upon the temporal characteristics and existence of correlated activity between HVc and LMAN. Specifically, the component of the LMAN-RA coherency function that may be affected by the correlation of activity between HVc and LMAN is the peak with a negative

time delay since this peak, unlike the peak with a positive time delay, exhibits variable time delay and strength. This idea is consistent with the hypothesis that the LMAN-RA coherency peak with a negative time delay is due to the common input from HVc.

In 4/5 HVc-LMAN pairs that exhibited a peak with a long positive time delay during spontaneous activity, a peak with a short negative time delay was also observed (time delay= -7.33±3.24 msec, n=4; Figure 3-9b). This interaction may indicate modulation of HVc and LMAN activity by a common input or a direct excitatory connection from LMAN to HVc. There are no known forebrain areas that project to both HVc and LMAN, nor has a projection from LMAN to HVc been shown in zebra finches. In canaries, however, a projection from LMAN to HVc has been suggested (Nottebohm et al, 1982).

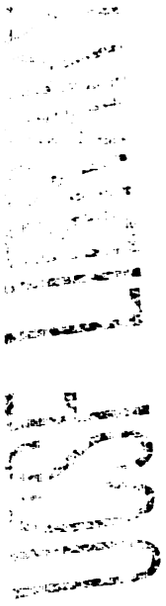

Coherency of LMAN-RA and HVc-RA activity. Unlike the HVc-LMAN coherency, the correlated activity between HVc and RA was consistently strong regardless of the type of LMAN-RA coherency function. In all cases examined, the coherency of RA activity relative to HVc spikes exhibited a tall, positive central narrow peak that was slightly to the right of zero during spontaneous and evoked activity (central peak; Figure 3-9c, f, i; Table 3-3). In one HVc-RA coherency function, the central peak found during evoked activity did not reach significance, although the coherency peak during spontaneous activity from the same site was significant. The central peak indicates an increase in RA firing probability that occurs shortly after an HVc spike, consistent with a direct excitatory connection from HVc to RA. The reliable nature of the HVc-RA correlation suggests that it does not contribute to the variability of the coherency between LMAN and RA activity.

Aside from the central peak, very small positive peaks (side peaks) that flanked the central peak were observed in some HVc-RA coherency functions, both during evoked (n=2/12 pairs) and spontaneous activity (n=6/12 pairs; Figure 3-9c, arrows). The time delays, peak and overall strengths of the side peaks were significantly different from those of the central peaks ($p<.05$, Mann-Whitney; Table 3-3, except for E, side peaks(+) since

n=1). During spontaneous activity, the side peaks appeared to symmetrically flank both sides of the central peak at a 43-49 msec time interval (n=4/12 pairs). We examined the HVc and RA auto-covariance functions and found that only the HVc-RA pairs that showed significant side peaks in the coherency function exhibited corresponding significant peaks in both HVc and RA auto-covariance plots, indicating bursting activity on a similar time scale within HVc and RA (data not shown). Therefore, the side peaks, unlike the central peak, may not reflect a direct interaction between HVc and RA, but instead may represent burst firing in both HVc and RA that is correlated and not completely eliminated by the normalization for the temporal structure of firing within HVc and RA.

Prediction of the time delay of LR- peaks. If the peak with a negative time delay (LR- peak) observed in LMAN-RA coherency functions with two peaks is due to the common input to the two nuclei from HVc, we should be able to predict the time delay of the LR- peak from the time delays of the HVc-LMAN and HVc-RA coherency peaks. We therefore examined the time delays of coherency peaks derived from simultaneously recorded HVc, LMAN and RA activity. The predicted negative time delay of the LMAN-RA coherency peak ($t_{LMAN\text{-}RA(-)}$) should be equal to the difference between the positive time delays of the coherency peaks that represent the interaction of HVc input to RA ($t_{HVc\text{-}RA(+)}$), and HVc input to LMAN ($t_{HVc\text{-}LMAN(+)}$), i.e., $t_{LMAN\text{-}RA(-)} = t_{HVc\text{-}RA(+)} - t_{HVc\text{-}LMAN(+)}$ (Figure 3-9a, b, c). Table 3-4 shows that for each set of HVc, LMAN and RA data, the $t_{LMAN\text{-}RA(-)}$ can indeed be predicted from $t_{HVc\text{-}RA(+)}$ and $t_{HVc\text{-}LMAN(+)}$, within the standard deviation of the mean time delays of each peak. This provides further evidence that the LMAN-RA coherency peak with a negative time delay is most likely due to the common input from HVc to both nuclei.

Contribution of HVc activity to the correlation of activity between LMAN and RA

To directly test whether common input of HVc to LMAN and RA gives rise to the LMAN-RA coherency peak with a negative time delay (LR-), we examined the effect of

disrupting HVc activity on the correlation of RA activity relative to LMAN spikes (LMAN-RA coherency). If the LR- peak is indeed due to HVc, then interrupting the activity of HVc should weaken the strength represented by this peak more than it would the strength of the peak that represents the direct connection from LMAN to RA. We simultaneously recorded multi-unit activity from HVc, LMAN and RA of anesthetized adult zebra finches before and during silencing of HVc activity at and around the recording site using a glutamate receptor antagonist, kynurenate. We silenced HVc activity only when the LMAN-RA coherency function contained two peaks (n=3 cases in 2 birds), one with a negative time delay (LR-) and the other with a positive time delay (LR+). The kynurenate trials included in the analysis were trials collected when the spontaneous firing rate before stimulus presentation was stable (see Methods).

Consistent with inactivation of activity at and around the HVc recording site, the spontaneous firing rate in HVc decreased dramatically by 89% (range: 70-99%). LMAN and RA, both of which receive input from HVc, exhibited a 56% (range: 14-82%) and 16% (range: 13-18%) decrease, respectively, in their spontaneous firing rate during silencing of HVc activity. Similarly, HVc exhibited a 100% (range: 99.7-100%) decrease in it response to song during its inactivation. LMAN showed a 69% decrease (range: 44-86%), and RA a 84% decrease (range: 65-100%) in their response to song during HVc inactivation.

In all three cases examined, the LMAN-RA coherency peaks during HVc inactivation revealed an attenuation in the overall strength between LMAN and RA activity (Figure 3-10a). Moreover, the LR- peak decreased in overall strength by a larger amount than the decrease observed in the LR+ peak (Figure 3-10b). In all three cases, the LR- peaks were not significant by our criterion (see Methods) during disruption of HVc activity, while the LR+ peaks remained significant. This indicates that without normal HVc activity, the LR- peak is not distinguishable from a correlation that occurred by chance, while the LR+ peak is largely independent of HVc activity. These results strongly suggest that the

correlation between LMAN and RA activity represented by the LR- peak is largely due to the shared excitatory input to both nuclei from HVc.

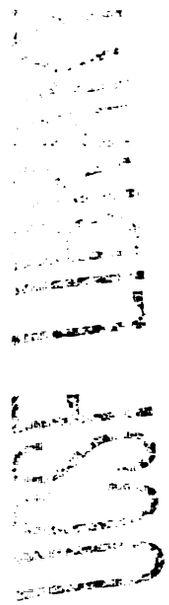

DISCUSSION

The present study illustrates that robust correlated activity can be detected between indirectly, as well as directly, connected nuclei within the song system. This suggests that the functional connectivity within the song system may involve broad divergent and reconvergent connections between song nuclei, and extensive intrinsic connections within each nucleus. The LMAN and RA correlated activity that reflects the direct projection from LMAN to RA was significant in adults, suggesting that the AFP may modulate the activity of the motor pathway even when lesions in the AFP no longer affect normal song production. Moreover, the correlated activity within the AFP is variable, as indicated by the different types of HVc-LMAN coherency functions. The functional connectivity in the song system may thus be physiologically modulated, reflecting the state of the animal's song plasticity or social behavior.

LMAN-RA correlated activity over a long time scale during spontaneous and evoked activity

Cross-covariance analysis of LMAN and RA spontaneous activity revealed correlated activity over a long time scale (hundreds of msec), as indicated by the wide positive peaks. These wide peaks, however, were absent in the coherency functions of LMAN and RA activity. Since the coherency function is equivalent to the cross-covariance function normalized by the auto-covariance of firing within LMAN and RA, this suggests that the wide peaks are related to the temporal structure of firing within LMAN and RA. A similar type of correction for auto-correlation properties of the input activity eliminated the presence of broad peaks in the cross-correlation functions of activity in the auditory cortex (Eggermont and Smith, 1996). The wide peaks may represent global synchronized firing within LMAN and within RA, that is, a general increase in firing probability in LMAN is accompanied by a general increase in firing probability in RA.

The wide peaks observed in the cross-covariance function during spontaneous activity disappeared when the bird's own song (BOS), the optimal stimulus for eliciting a strong response in both LMAN and RA neurons, was presented. The decrease of positively correlated activity by stimulus playback has also been observed in the primary auditory cortex of cats (Frostig et al, 1983) and primary stages of the auditory pathway in songbirds (Janata and Margoliash, 1999). The BOS presentation may change the temporal structure of firing in LMAN and RA in different ways, such that the general increase in activity in these nuclei is no longer correlated. This suggests that stimulus playback results in different patterns of intrinsic activity within LMAN and RA.

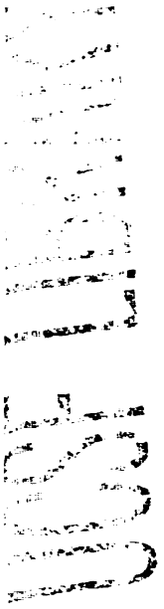

LMAN-RA peaks with positive time delays reflect the direct interaction of LMAN with RA

The LMAN-RA coherency peaks with positive time delays (LR+) observed in functions with two well separated peaks most likely represent the correlation due to the direct excitatory projection from LMAN to RA. The positive time delay indicates an increase in the firing probability of RA that occurs after LMAN spikes. The relatively shorter time delays and narrower widths of the LR+ peaks compared to the peaks with negative time delays (LR-) are also consistent with a correlation that represents the direct connection from LMAN to RA. However, the LR+ peaks are wider and have longer time delays than correlated single unit activity between thalamocortical and cortical neurons (for example: Alonso et al, 1996; Alonso and Martinez, 1998). This may be because neurons recorded in those studies were connected only monosynaptically, while the LMAN and RA neurons in our experiments may be connected both monosynaptically, and polysynaptically via intrinsic connections within RA. Moreover, the connection from LMAN to RA is unusual in being mediated primarily by NMDA receptors (Kubota and Saito, 1991; Mooney and Konishi, 1991; Mooney, 1992; Stark and Perkel, 1999), whose slow kinetics are likely to make the synaptic delay longer.

Rather than a direct input from LMAN to RA, two alternative anatomical circuits could account for the correlation represented by the LR+ peaks. One possibility is that the *LR+* peak is due to common input from HVc to LMAN and RA such that LMAN activity appears to be correlated with the increase in RA firing induced by the HVc activity. If this were the case, the increase in LMAN firing probability relative to HVc spikes should occur before the increase in RA firing probability relative to HVc spikes, to account for the positive time delay of the LR+ peaks. The positive time delay of the LR+ peaks (T_{LR+}) should be equal to the difference between the time delay between HVc and RA activity (T_{HR}) and the time delay between HVc and LMAN activity (T_{HL}), i.e. (T_{HR}) - (T_{HL}) = T_{LR+}. Figure 3-11a shows a scattergram of the predicted and actual time delays of LR+ peaks (shown as cross symbols,+) whose corresponding HVc-LMAN and HVc-RA peaks were known. The predicted LR+ time delays are more negative than the actual LR+ time delays and do not lie on the unity line (predicted = actual time delays). Thus, it is unlikely that LR+ peaks are due to the joint modulation of LMAN and RA activity by HVc.

A second possibility is that LMAN induces an increase in RA firing probability by driving HVc. In a small number of cases (n=4), the coherency function between HVc and LMAN activity showed not only a peak with a positive time delay, but also one with a negative time delay (HL- peaks), indicating that LMAN firing probability increases before an HVc spike. This suggests that an excitatory connection from LMAN to HVc could exist. Thus, LMAN could drive HVc, with HVc then driving RA, as indicated by a variety of evidence including the sharp central peaks in the HVc-RA coherency functions (HR peaks) observed here. However, an anatomical connection from LMAN to HVc has not been shown in zebra finches. Moreover, if LMAN was inducing RA to fire via HVc, one would expect that the width of the resulting LR+ peaks would be as wide as or wider than the sum of the widths of the HL- and HR coherency peaks. As shown in Figure 3-11b, the measured width of the LR+ peaks is narrower than the predicted width of LR+ peaks, indicating that the LR+ peaks are unlikely to be due to LMAN induction of RA activity via HVc. Thus, the

most probable anatomical connection that gives rise to the correlation represented by the LR+ peaks is the direct excitatory projection from LMAN to RA.

The robust interaction observed between LMAN and RA in adult birds, due to the direct LMAN to RA projection, challenges the prevailing hypothesis that LMAN's influence on RA activity is largely abolished as the bird matures. The number of LMAN synapses on RA neurons has been shown to decline by 53 days of age (Herrmann and Arnold, 1991), and previous studies have shown that LMAN lesions in adults do not cause changes in normal song, whereas lesions in juveniles do (Bottjer et al, 1984; Sohrabji et al, 1990; Scharff and Nottebohm, 1991). Our results suggest that, despite the decreased number of LMAN to RA connections, the functional strength of these synapses, and perhaps of the intrinsic connections within RA, must be maintained. Consistent with this idea, studies show that LMAN does indeed play a role in adult singing behavior and plasticity. LMAN is strongly active in singing zebra finches (Hessler and Doupe, 1999), and LMAN is required for any plastic changes in adult song due to late learning, tracheosyringeal nerve section and deafening (Morrison and Nottebohm ,1993; Williams and Mehta, 1999; Brainard and Doupe, 2000).

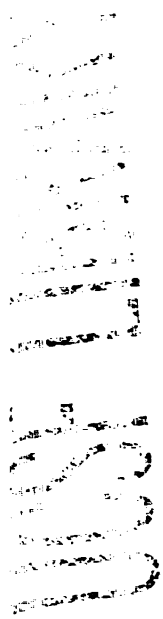

LMAN-RA peaks with negative time delays reflect the correlation due to common input from HVc

The peaks with negative time delays (LR- peaks) in LMAN-RA coherency functions with two well-separated peaks most likely represent the modulation of LMAN and RA activity by the common input of HVc (see Figure 3-8). The relatively longer time delays and greater widths of the LR- peaks compared to those of the LR+ peaks are consistent with a correlation that involves an indirect connection, namely that from HVc to LMAN. Moreover, the time delays of the LR- peaks can be predicted from the time delays of the HVc-RA and HVc-LMAN peaks with positive time delays based on the assumption that the LR- peaks are due to HVc common input (Fig. 3-11a, squares; Table 3-4). Finally, the marked

decrease of the correlation represented by the LR- peaks when HVc activity was disrupted provides direct evidence that strongly supports this interpretation.

An alternative hypothesis is that the LR- peaks are due to a direct excitatory projection from RA to LMAN, but no such anatomical connections have been shown. In addition, the greater width of the LR- peaks would be inconsistent with a direct projection from one nucleus to another. LR- peaks are in fact significantly wider than peaks thought to represent a direct interaction between LMAN and RA (LR+ peaks; Fig. 3-7). Alternatively, the LR- peaks could be due to an indirect projection from RA to LMAN via DLM; however, the projection from RA to DLM is rather weak (Vates et al, 1997). Moreover, the decrease in LR- overall strength due to silencing parts of HVc is inconsistent with this hypothesis. Thus, the common input from HVc to LMAN and RA is the most probable source that gives rise to the correlation represented by LR- peaks.

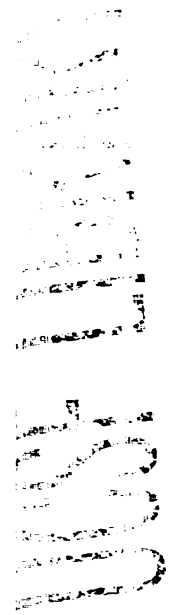

Functional connectivity within the song system

Correlated activity between HVc and LMAN and the component of the LMAN and RA correlation (LR- peaks) that involves these areas are both surprisingly strong in the song system. In many systems, correlations between neurons that are disynaptically connected are difficult to detect (Perkel et al, 1967). Moreover, the strength of correlated activity between indirectly connected neurons is two orders of magnitude weaker than direct connections, and the strength of correlated activity due to a common input involving at least a trisynaptic loop is expected to be negligible (Fetz and Cheney, 1980). This calculation is based on serially connected neurons, with a pre-synaptic neuron making a single excitatory synaptic connection to a post-synaptic neuron at each level. If the functional connectivity of the song system is arranged in this manner, where activity flows in parallel, isolated channels (Figure 3-12a), the probability of detecting correlated activity between indirectly connected neurons would be low. On the other hand, if there are extensive intrinsic connections within each song nucleus such that the within-nucleus activity is synchronized,

and broad divergent and reconvergent connections between song nuclei (Figure 3-12b), then there is a higher chance of detecting correlated activity between indirectly connected neurons. Our data are consistent with the latter model, suggesting that information in the song system is processed through a highly interconnected network of neurons.

Although the two schemes of functional connectivity in Figure 3-12 represent the extremes, there is anatomical and electrophysiological evidence to support the model in Figure 3-12b. Activity in response to the BOS in anesthetized animals appears to be similar and thus perhaps synchronized across large areas of HVc and LMAN (Sutter and Margoliash, 1994; Doupe, 1997). The synchronized activity within HVc may be forwarded widely on to other nuclei because the anatomical projections from HVc to RA and Area X (Figure 3-1a) are not topographically organized (Fortune and Margoliash, 1995; Vates and Nottebohm, 1995; Foster and Bottjer, 1998). Small injections of anterograde tracer into HVc label cells in RA and Area X that are uniformly distributed across each nucleus (Foster and Bottjer, 1998). On the other hand, the projections within the AFP are topographically organized and form a closed loop within the AFP (Luo et al, 1999). The LMAN to RA projections are also topographically organized in broad, overlapping compartments (Johnson and Bottjer, 1995). This should theoretically result in loss of correlated activity when recording in compartments that are not topographically matched. We found, however, that the topographical alignment of the LMAN and RA recording sites did not seem to have an effect on the correlation of their activity. This suggests that extensive intrinsic connections within song nuclei like those observed in LMAN, RA, and HVc (Foster and Bottjer, 1998; Kittelberger and Mooney, 1999; Spiro et al, 1999), act in addition to the broad HVc projections to synchronize the activity within each nucleus of the AFP such that the topographical alignment of recording sites does not matter.

A divergent and reconvergent structure of functional connectivity has been proposed for another nervous system, the cortex -> basal ganglia -> thalamic -> cortex loop in mammals (Graybiel, 1994 and 1998). The similarity in functional connectivity is consistent

with the neurochemical and electrophysiological studies which suggest that the anterior forebrain pathway loop, HVc/LMAN -> Area X -> DLM-> LMAN, is homologous to the cortical-basal ganglia mammalian loop. As in the mammalian basal ganglia, Area X receives robust dopaminergic projections from avian ventral tegmental area and substantia nigra (Lewis et al, 1981; Bottjer, 1993; Bottjer et al; 1989; Soha et al, 1996). Area X sends inhibitory projections to DLM (Luo and Perkel, 1999a and 1999b), similar to the inhibitory efferents of the globus pallidus, the output nucleus of the basal ganglia. The similarity in functional connectivity between the AFP loop and the cortical-basal ganglia loop suggest that both loops may process information in a similar manner.

Variability of neuronal interactions within the AFP

The LMAN-RA coherency functions with 'non-separable/significant' peaks and with a single peak indicate that the neural interaction between LMAN and RA is variable. In these coherency functions, the 'non-separable/significant' peaks may represent cases in which the two usually well-separated peaks have instead overlapped in time, and the single peak cases may indicate a complete overlap. In particular, the overlap or lack of significant peak may be due to the variable time delay and strength of the peak with a negative time delay. Consistent with this idea, in cases of 'non-separable/significant' peaks, the peak with a negative time delay was shifted closer to zero or no longer significant compared to those in functions with two well-separated peaks. Similarly, the single peaks were at intermediate time delays and had greater widths relative to those of the two-well separated peaks, consistent with the idea that single peaks may represent a complete overlap of the two well-separated peaks.

This hypothesis was strengthened by examination of cases in which activity of all three nuclei was recorded. The existence and degree of overlap in time of the actual LMAN-RA coherency peaks was predicted by the time delay and strength of the corresponding HVc-LMAN correlated activity. For example, in cases where the increase in LMAN firing

probability occurred shortly after HVc spikes, the time delay of the HVc-LMAN peak may not be sufficiently long to result in a LMAN-RA peak with a long negative time delay that is clearly separable from the LMAN-RA peak with a positive time delay. Similarly, when HVc and LMAN were not significantly correlated in time, the LMAN-RA peak with a negative time delay was broad and weakly significant or not significant at all. It is possible that in 'non-separable/significant' and single peak cases, the LMAN-RA correlated firing is due to both the direct interaction between LMAN and RA, and near coincident firing of HVc and LMAN. Thus, the correlated activity between LMAN and RA appears to depend critically on the variable neural interaction within the AFP (HVc->LMAN).

Possible modulation of the functional connectivity within the song system

The existence and positive time delays of the HVc-LMAN coherency peaks, which correlated well with the types of LMAN-RA coherency functions, were variable. This suggests that the neural interaction between HVc and LMAN may be physiologically modulated. This modulation is unlikely to be due to variable arousal states of the bird despite evidence that auditory responsiveness of RA neurons depend on the bird's wakefulness (Vicario and Yohay, 1993; Dave and Margoliash, 1998). HVc-RA coherency functions have consistent strength and temporal characteristics regardless of the corresponding type of HVc-LMAN and LMAN-RA coherency functions. The different states of the functional connectivity may reflect changes in the underlying circuitry from HVc to LMAN. In cases where the time delay from HVc to LMAN is long, the activity from HVc may travel through indirect loops, perhaps within Area X, which has complex circuitry. While in other cases, the indirect loops may be shut down, allowing the presynaptic activity to reach LMAN sooner.

A candidate modulatory input which could alter the functional connectivity between HVc and LMAN is dopamine. Dopaminergic projections to HVc, LMAN and Area X originate from the avian ventral tegmental area and substantia nigra (Lewis et al, 1981). In

mammalian basal ganglia, decreasing the dopamine levels is known to increases the synchronization of activity (sub-second time scale) within two areas of the basal ganglia, thus changing the functional connectivity within the basal ganglia (Raz et al, 1996; Bergman et al, 1998). Dopamine receptor activation has also been shown to increase the frequency and regularity of multisecond oscillations in firing rate of neurons in the basal ganglia (Ruskin et al, 1999). A similar mechanism may be occurring in the song system, where dopamine may shape the functional connectivity between HVc and LMAN by altering the intrinsic connectivity within Area X.

The functional connectivity of the song system in awake, behaving birds may be modulated by its behavioral state. Singing related activity of LMAN and Area X in awake zebra finches is modulated by the social context in which the singing is performed. The activity of LMAN and Area X is higher and more bursty in character, and more variable across song renditions when a bird sings by itself (undirected) than when singing is directed to another bird (Hessler and Doupe, 1999a). This raises the possibility that overall activity is more synchronized in one state than the other. Similarly, the induction of an immediate early gene, ZENK, is higher during undirected than directed singing in LMAN, RA and lateral Area X (Jarvis et al, 1998). Thus, changes in the song system that depend on the social context of singing may reflect altered functional connections within the song system.

In summary, the cross-covariance and coherency analysis of activity in LMAN, HVc and RA indicate that correlated activity between indirectly connected nuclei, as well as directly connected nuclei, is robust in the song system. This suggests that the functional connectivity within the song system involves broad divergent and reconvergent connections between song nuclei, and also extensive intrinsic connectivity within song nuclei. The strong correlated activity between LMAN and RA that represents the direct LMAN to RA projection suggests that the AFP plays a role in birdsong behavior even in adults. Moreover, the neural interaction within the AFP is variable, indicating that the functional connectivity

from HVc to LMAN may be physiologically modulated. Altering the dopamine levels in Area X, as well as determining the functional connectivity in awake, behaving birds during directed and undirected singing, may shed light on the different neuronal interactions within the AFP. Lastly, because the song system mediates song learning, determining the functional connectivity of the song system in juveniles undergoing learning may indicate whether neural interactions within the song system are modulated during learning.

Figure 3-1 a) Schematic of the anatomy of the song system. The black nuclei (HVc, RA, nXIIts and respiratory nuclei) make up part of the descending motor pathway for song, while the gray nuclei (Area X, DLM, and LMAN) form the anterior forebrain pathway (AFP). nXIIts is a motor nucleus that controls the muscles of the syrinx, the bird's vocal organ, while the respiratory nuclei control the respiratory muscles. b) Quantification of amplitude, width and time delay of coherency peaks. The coherency function measures the association of neural activity between two areas as a function of time delay relative to the spikes in one area. The actual data, which are peaks from a coherency function of RA activity relative to LMAN spikes, are depicted by the dark blue line, while the green line shows the two Gaussian functions fit to the central portion (-100 to +100 msec) of the data. The $\pm$JN lines indicate the $\pm$3x square root of the Jacknife variance (see Methods) and are used as thresholds to determine significance of the peaks. The amplitude, time delay, and width of the coherency peaks were measured from the Gaussian fits. The width of the peak is measured as the half-width at 61% amplitude height ($amplitude * e^{-1/2}$). The peak strength of the correlation is given by the peak amplitude, while the overall strength is quantified as the area under the curve, calculated as $amplitude * width$. The same fitting procedure is applied to the cross-covariance functions, except that the outside region (all the data except the central region) of the data is also fitted with one Gaussian function (see Figures 3-2a and 3-3a).

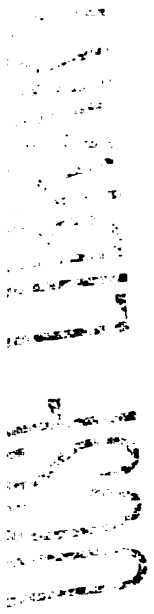

Figure 3-1

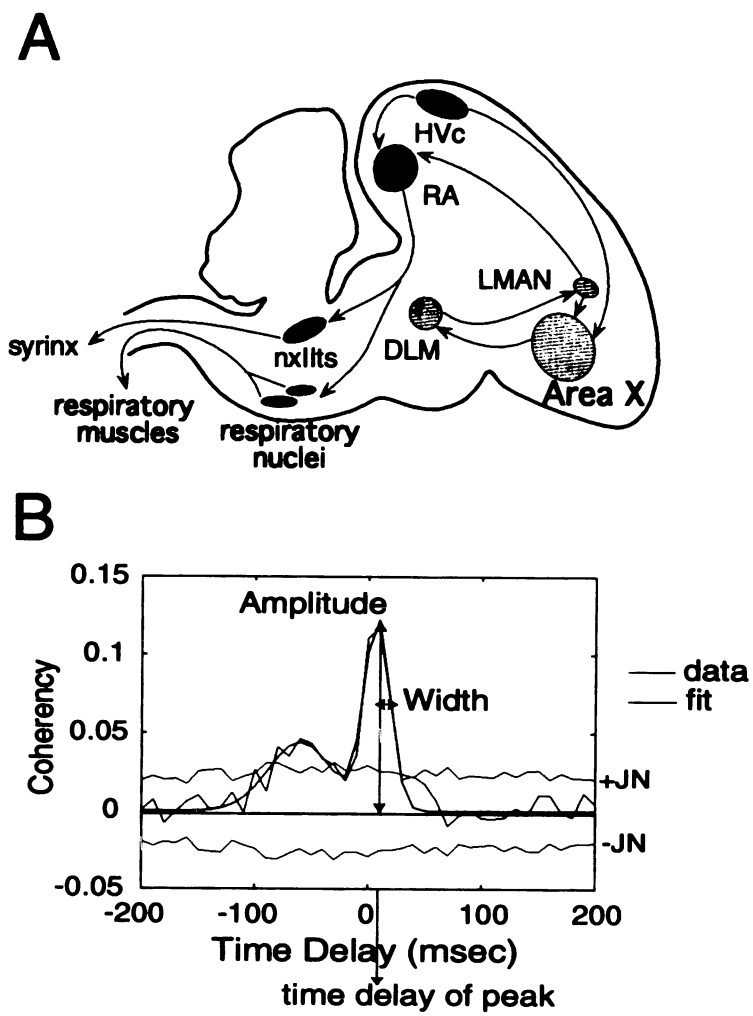
A
HVc
RA
LMAN
DLM
Area X
syrinx
nXIIts
respiratory muscles
respiratory nuclei
B
0.15
0.1
0.05
0
-0.05
Coherency
Amplitude
Width
data
fit
+JN
-JN
-200
-100
0
100
200
Time Delay (msec)
time delay of peak

Figure 3-2 Cross-covariance and coherency functions of RA activity relative to LMAN spikes during spontaneous activity for multiple (2-5 units) unit data. The data are plotted as described in Fig. 3-1b. The cross-covariance and coherency (ordinate) are plotted against the time delay of RA activity relative to a LMAN spike at time delay=0 (abscissa). Thus, changes in RA firing that follow a LMAN spike occur at time delay > 0 (LMAN->RA), while those that precede a LMAN spike occur at time delay < 0 (RA-> LMAN). a) The cross-covariance between multi-unit LMAN and RA spontaneous activity showed positive peaks with two widths: wide and narrow. In this example, the time delays of the two narrow peaks (see inset) are -65.54 and 6.20 msec, and the corresponding widths are 25.68 and 18.21 msec, while the wide peak has a time delay of -28.21 msec and a width of 494.68 msec. b) The coherency between multi-unit LMAN and RA spontaneous activity revealed only narrow positive peaks, illustrated more clearly in the inset. In this example, the coherency function, which was derived from the same LMAN and RA activity as in (a), exhibits two well-separated peaks, one with a negative time delay of -61.59 msec (width=21.27 msec) and the other, a positive time delay of 5.28 msec (width=10.77 msec). No significant wide peaks were detected.

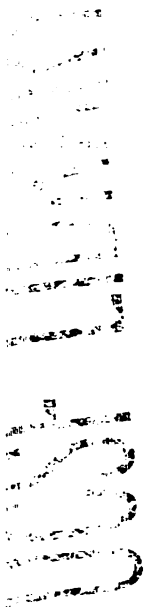

Figure 3-2

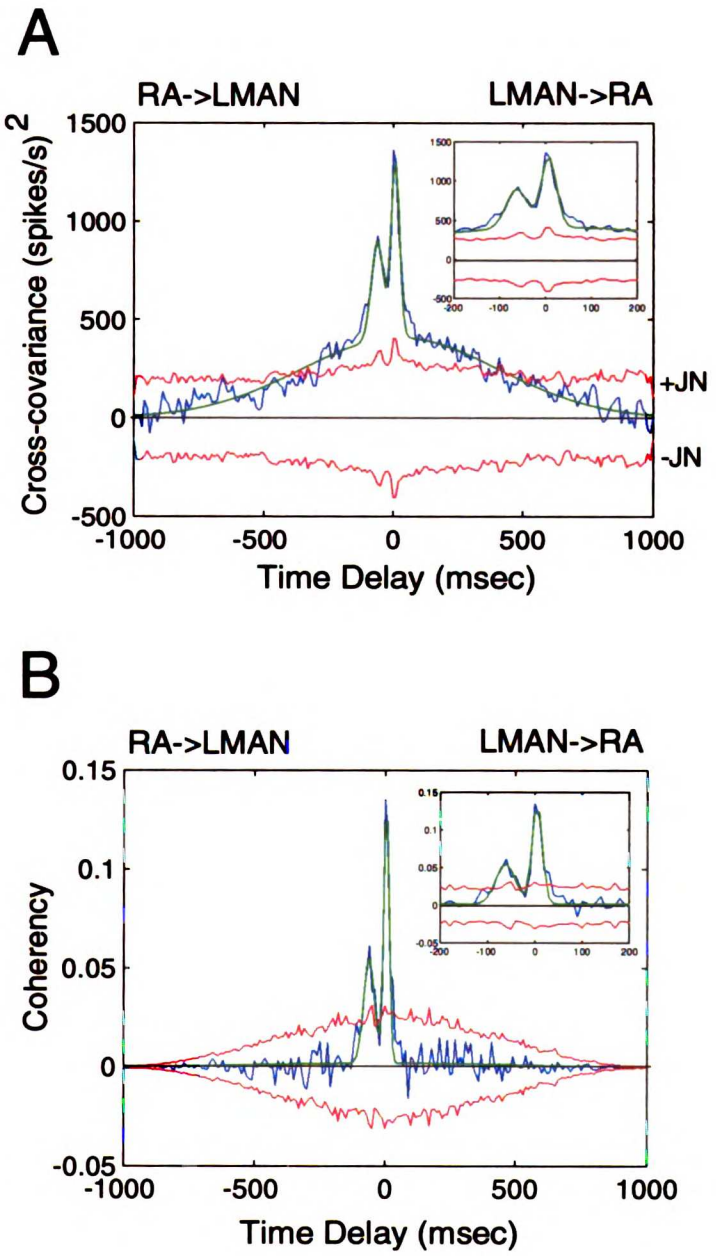

Figure 3-3 Cross-covariance functions of RA activity relative to LMAN spikes during spontaneous and evoked activity. The cross-covariance is plotted as in Fig. 3-1b. a) An example of a cross-covariance function between LMAN and RA multi-unit activity during spontaneous activity that showed a wide peak (width= 204.66 msec, time delay=-34.06 msec, R^2=.92) and two narrow peaks (time delays=-19.20, 6.49 msec and respective widths=10.30, 10.38 msec). b) When a stimulus (BOS) is presented, the cross-covariance function from the same LMAN and RA sites as in (a) no longer has a wide peak (R^2=.07), but has retained a narrow peak (time delays=-2.68 msec, width=23.47 msec). During evoked activity, only 2/40 LMAN-RA site pairs exhibited wide peaks in their cross-covariance functions, and those peaks were not significant.

Figure 3-3

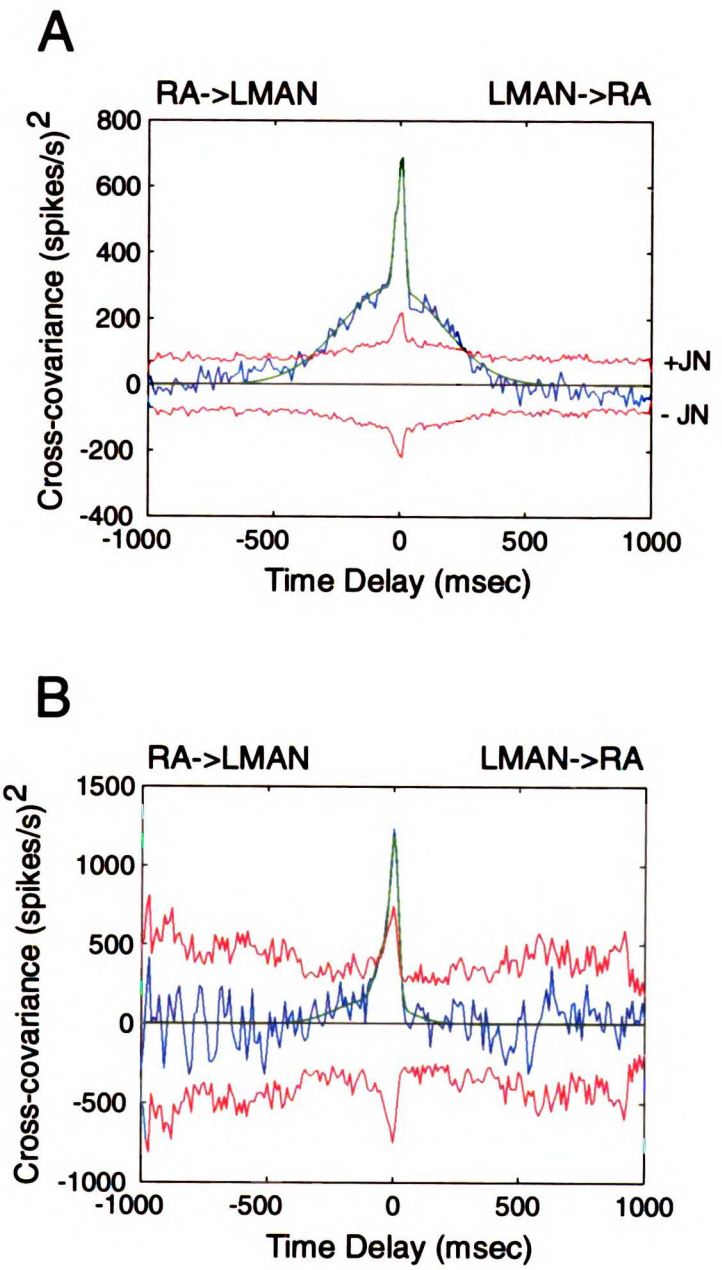
A
RA->LMAN
LMAN->RA
Cross-covariance (spikes/s)2
800
600
400
200
0
-200
-400
-1000
-500
0
500
1000
Time Delay (msec)
+JN
- JN
B
RA->LMAN
LMAN->RA
Cross-covariance (spikes/s)2
1500
1000
500
0
-500
-1000
-1000
-500
0
500
1000
Time Delay (msec)

Figure 3-4 Coherency of RA single unit activity relative to spikes from an LMAN neuron. The coherency between single unit activity in both nuclei also displays two narrow peaks (see inset), with similar time delays and widths (time delay=-41.11 msec, width=39.61 msec and time delay=12.15 msec, width=11.25 msec) to those observed in multi-unit coherency functions.

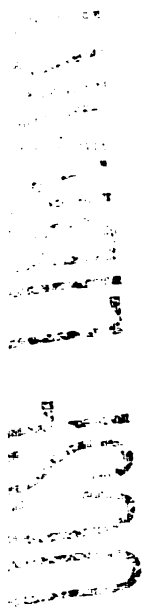

Figure 3-4

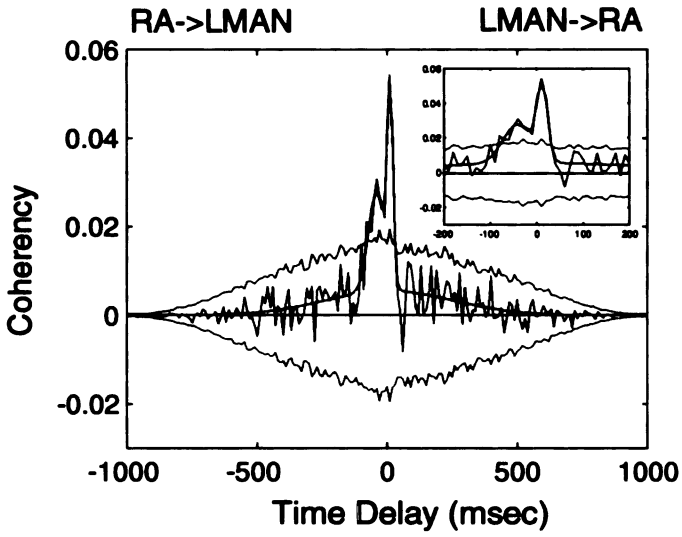
RA->LMAN
LMAN->RA
0.06
0.04
0.02
0
-0.02
Coherency
-1000
-500
0
500
1000
Time Delay (msec)

Figure 3-5. Types of LMAN-RA coherency functions during spontaneous activity. The left column shows individual data, while the right column shows mean data for each type of coherency function. The individual data are presented as in Fig. 3-1b. For the mean data plots, the mean data are represented by the blue curves, and the mean+standard deviation (SD) and mean-SD are represented by the red and green curves, respectively. a) LMAN-RA coherency functions with two separable peaks. The individual data showed peaks with time delays -43.83 and 10.52 msec, and the respective widths were 22.96 and 12.34 msec. b) LMAN-RA coherency functions with two peaks that were either not separable and/or with one of the two peaks that was not significant. The upper panel in the left column is an example where the two peaks were not separable (time delays=-18.39, 10.00 msec and respective widths=57.61, 9.62 msec). The lower panel in the left column is an example where only one of the two peaks was significant (time delay=-2.40 msec and width=25.05 msec). c) LMAN-RA coherency functions with a single peak. The example in the left column shows a peak with time delay=8.49 msec, and width=19.77 msec.

Figure 3-5

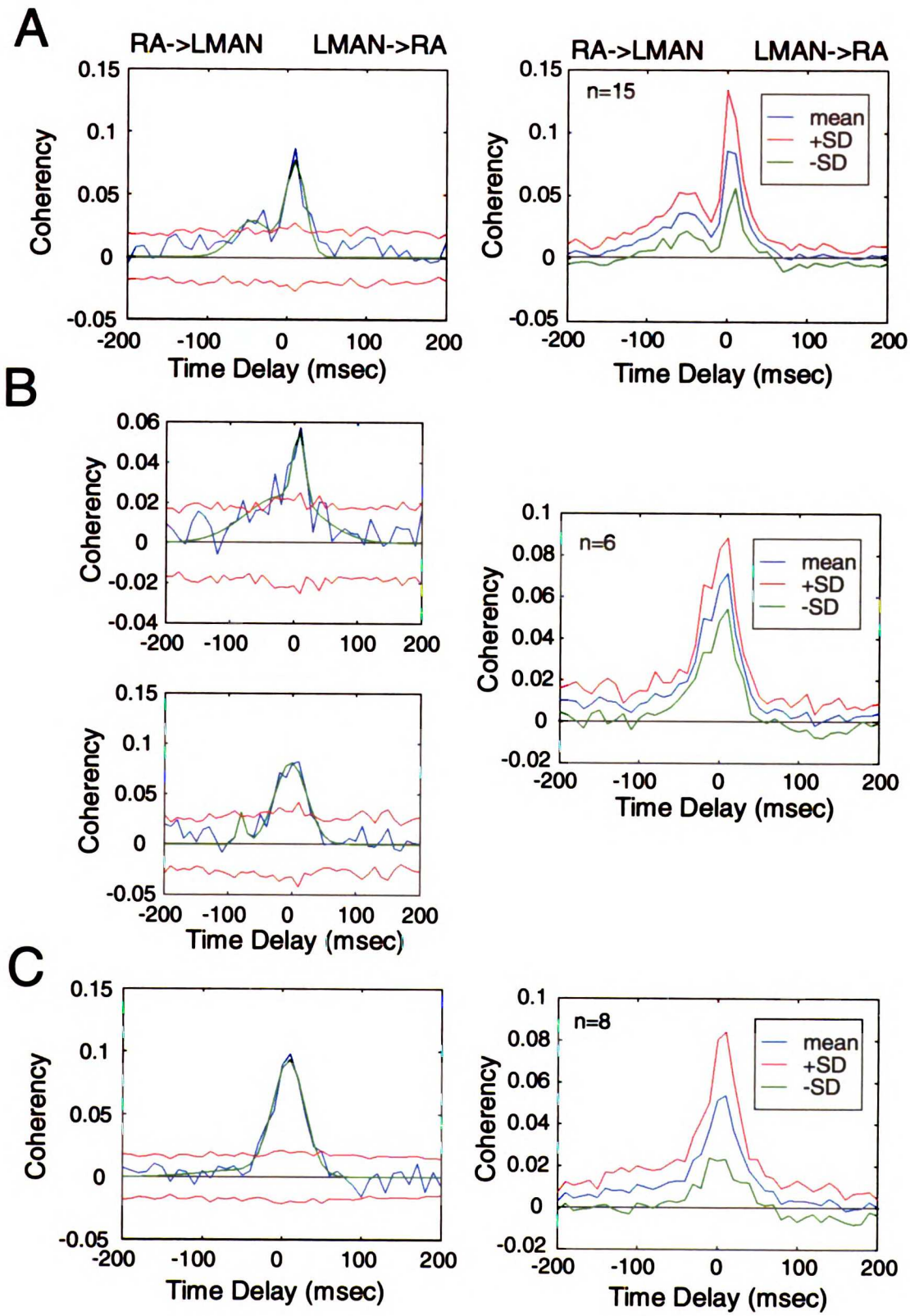
A
RA->LMAN
LMAN->RA
Coherency
Time Delay (msec)
n=15
mean
+SD
-SD
B
n=6
C
n=8

Figure 3-6. Types of LMAN-RA coherency functions during evoked activity. The data are illustrated as in Fig. 3-5. a) LMAN-RA coherency functions with two separable peaks. The individual data example shows two peaks with time delays of -61.92 and 10 msec and respective widths of 23.23 and 6.07 msec. b) LMAN-RA coherency functions with two peaks that were not separable and/or one peak that was not significant. The upper left panel in the left column shows two peaks that were not separable (time delays=-11.75, 10 msec; respective widths=17.72, 9.96 msec). The lower panel in the left column shows two overlapping peaks, where only the peak with a positive time delay was significant (time delay=8.08 msec; width=16.99 msec). The left shoulder (with a negative time delay) of the positive peak represents the non-significant peak. c) LMAN-RA coherency functions with a single peak. The example of individual data shows a peak with time delay of -1.71 msec and width=10.85 msec.

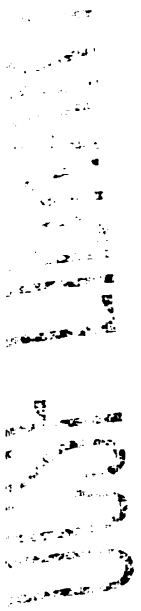

Figure 3-6

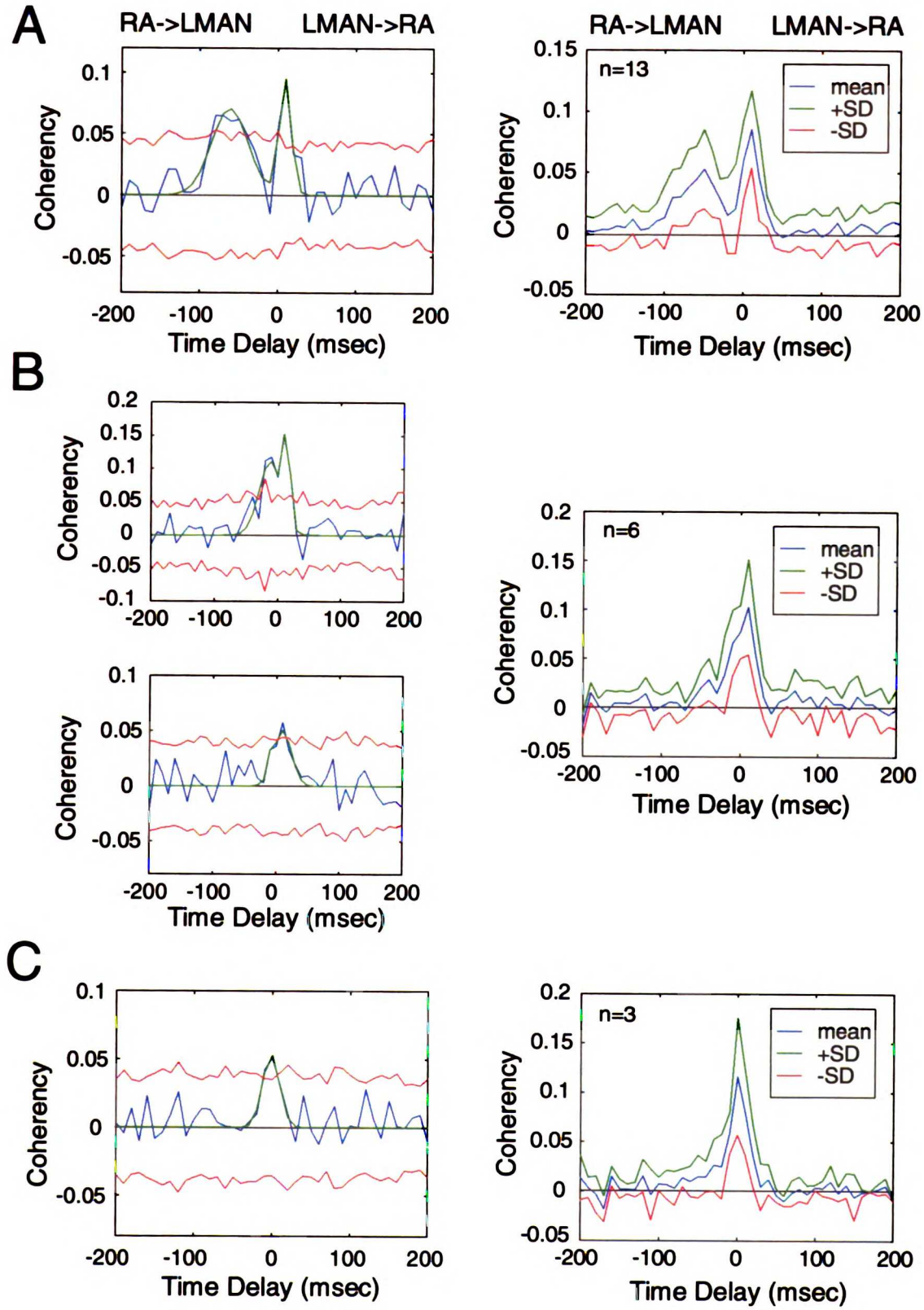

Figure 3-7. Quantification of LMAN-RA coherency peaks from functions with two well separated peaks or a single peak. Individual data points (circles) are plotted, as well as the means (diamonds) and standard deviation (error bars) for each peak category. LR- and LR+ are peaks with negative and positive time delays, respectively, that were observed in LMAN-RA (hence, the abbreviation LR) coherency functions with two separable peaks, while LR represents peaks found in LMAN-coherency functions with a single peak. a) Time delays of the LR-, LR+ and LR peaks during spontaneous activity and b) evoked activity. c) Widths of the peaks during spontaneous and d) evoked activity. e) Peak strengths represented by the peaks during spontaneous and f) evoked activity. g) Overall strengths represented by the peaks during spontaneous and h) evoked activity. *p<.05, **p<.01, ***p<.001, Wilcoxon Signed Rank Test. #p<.05, ##p<.01, ###p<.001, Mann-Whitney.

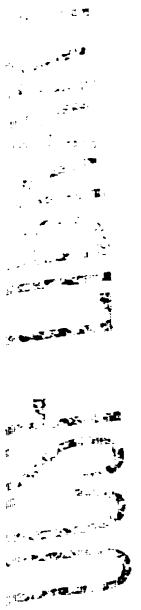

Figure 3-7

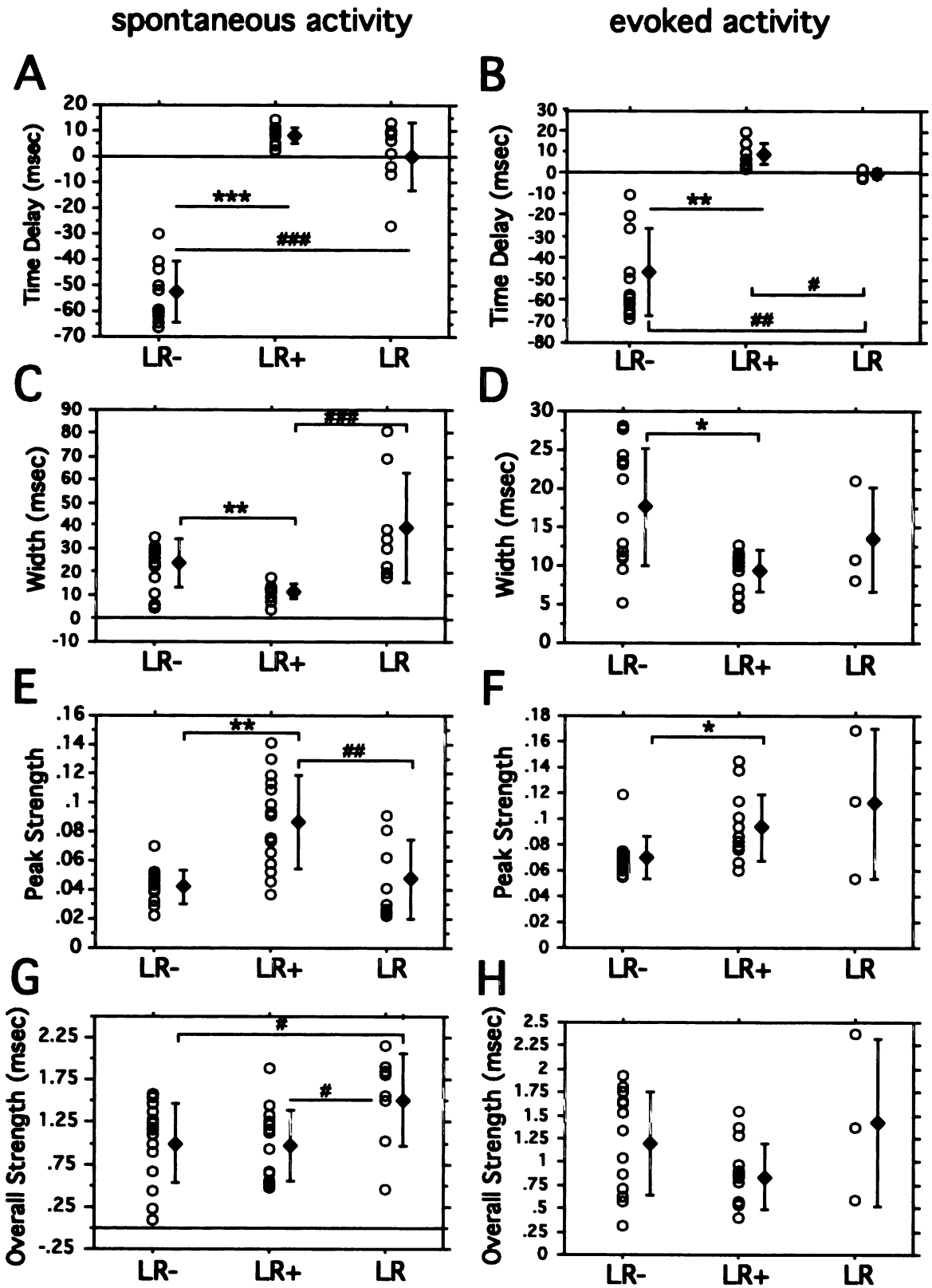
spontaneous activity
evoked activity
A
B
C
D
E
F
G
H
Time Delay (msec)
Width (msec)
Peak Strength
Overall Strength (msec)
LR-
LR+
LR
***
###
**
#
##
*

Figure 3-8 Diagrams of the song system and of simultaneous activity between HVc, LMAN and RA. a) HVc projects directly to RA, and indirectly to LMAN via two nuclei in the anterior forebrain pathway. LMAN, in turn, sends direct projections to RA. b) The cartoon illustrates the likely temporal relationship of activity between HVc, LMAN and RA. When HVc fires, it elicits reliable responses in RA at a short time delay, while responses in LMAN are less reliable, although detectable (see Figure 3-9b), and appear at a longer time delay. Thus, the LMAN spikes in response to HVc pre-synaptic spikes are delayed relative to the HVc-driven RA spikes. When LMAN fires, it then elicits another response in RA, also with a short time delay. Hence, the anatomical connections are consistent with the presence of two narrow peaks in the cross-covariance and coherency between LMAN and RA activity. Note that the presence of the peak with a negative time delay depends critically on the correlated activity between HVc and LMAN.

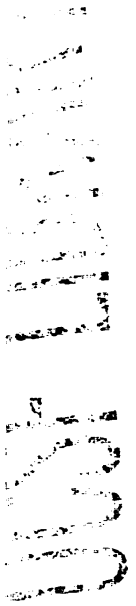

Figure 3-8

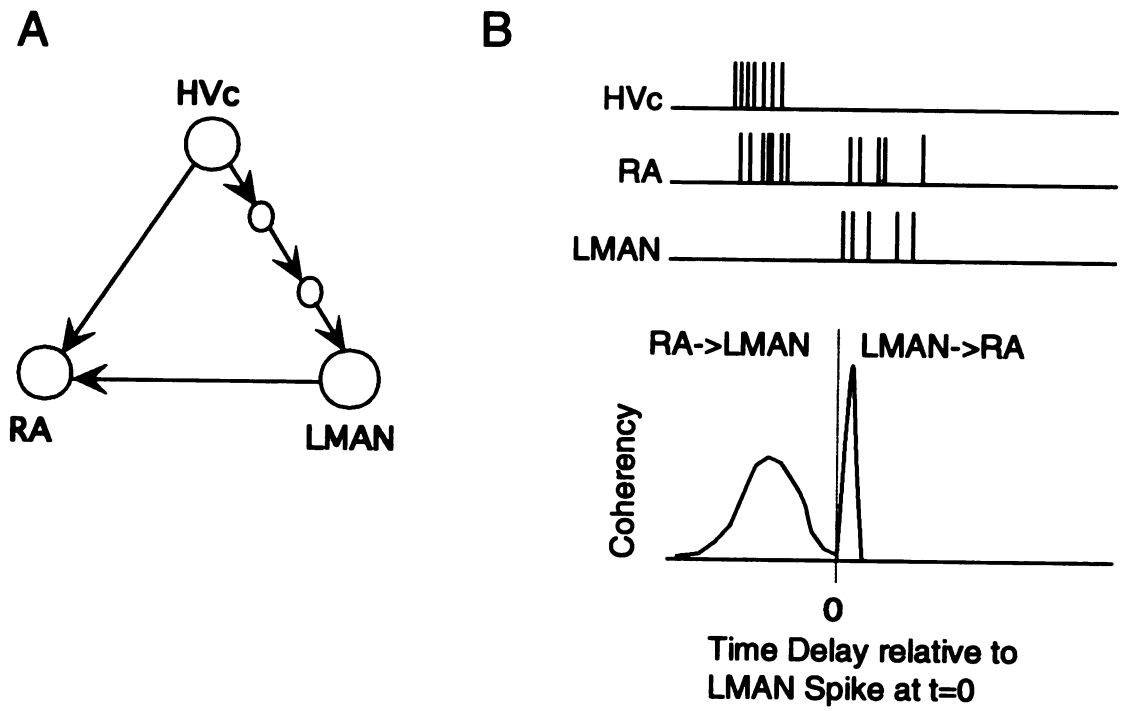
A
HVc
RA
LMAN
B
HVc
RA
LMAN
RA->LMAN
LMAN->RA
Coherency
0
Time Delay relative to
LMAN Spike at t=0

Figure 3-9 Coherency between LMAN-RA, HVc-LMAN and HVc-RA spontaneous activity. Each row shows corresponding coherency functions obtained from the same LMAN, RA and HVc sites. The first and third rows show coherency functions derived from simultaneously recorded HVc, LMAN and RA multi-unit activity, while the second row is derived from pair-wise recording of nuclei. Conventions are as in Fig. 3-1b. a) Coherency function of spontaneous RA activity relative to LMAN spikes (at time delay=0) with two well-separated peaks with time delays of -64.37 and 5.00 msec. b) The corresponding coherency function of spontaneous LMAN activity relative to HVc spikes at time delay = 0; thus, LMAN firing follows HVc spikes at time delays > 0 (HVc->LMAN), and precedes HVc spikes at time delays < 0 (LMAN->HVc). This function shows two significant positive peaks, one with a long positive time delay (67.26 msec), and the other with a short negative time delay (-5.00 msec). c) The corresponding coherency function of spontaneous RA activity relative to HVc spikes at time delay = 0; RA activity follows HVc spikes at time delays > 0 (HVc->RA), and precedes HVc spikes at time delays < 0 (RA-> HVc). The HVc-RA coherency function reveals a tall, narrow central peak that is slightly displaced to the right of zero (time delay=5.00 msec). Side peaks (arrows) flank the central peak, with time delays of -40.00 and 50.00 msec. d) LMAN-RA coherency function during spontaneous activity with a single peak with time delay=8.49 msec. e) The corresponding HVc-LMAN coherency function during spontaneous activity with a single peak (time delay=0.77). f) The corresponding HVc-RA coherency function during spontaneous activity with a tall, narrow peak at time delay=5.00 msec. g) LMAN-RA coherency function during evoked activity with no significant peaks. h) The corresponding HVc-LMAN coherency function during evoked activity also shows no peaks. i) The corresponding HVc-RA coherency function during evoked activity shows a tall narrow peak at time delay=3.20 msec.

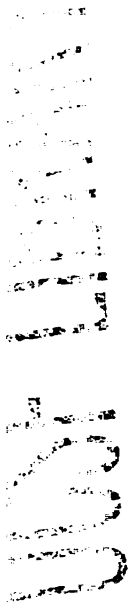

Figure 3-9

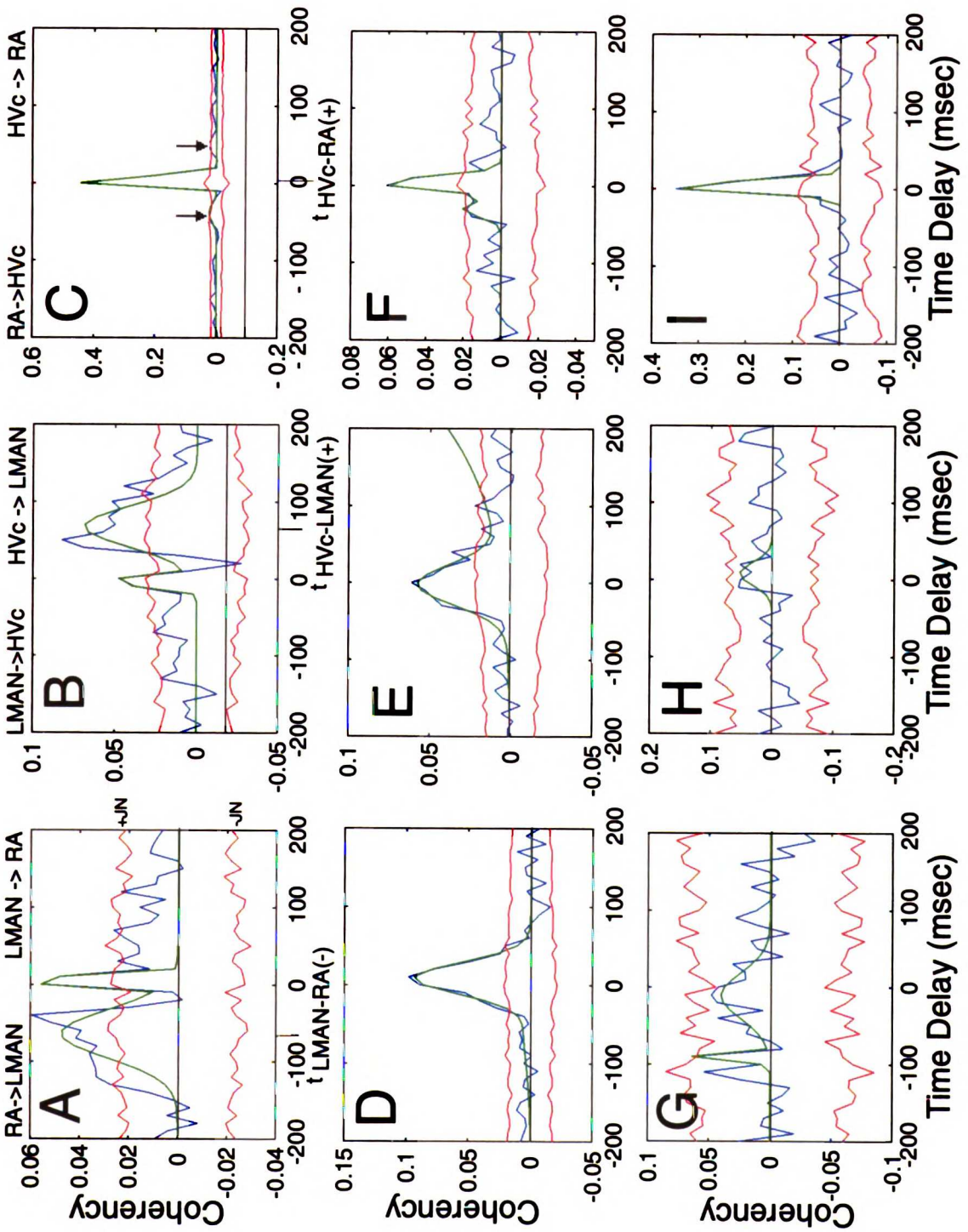

Figure 3-10 Effect of disrupting HVc activity on the coherency of LMAN and RA activity. a) The coherency between LMAN and RA before (pre-kynurenate: blue line), and during (kynurenate: green line) silencing of HVc activity by pressure injection of kynurenate, a glutamate receptor antagonist, into HVc. The overall strength of the narrow peaks decreased when HVc activity was silenced (overall strength for LR- : pre-=1.47 and kynurenate= 0.17; for LR+: pre-= 0.49 and kynurenate=0.32). Note that the kynurenate LR- peak is no longer significant by our criterion (below the JN level), while the LR+ peak remained significant. b) The percent overall strength of the kynurenate peaks that persisted after kynurenate infusion into HVc. After disrupting HVc activity, none of the LR- peaks were significant by our criterion, and the mean overall strength was only 50% (error bars represent standard error, SE=23%) of the overall strength represented by the pre-kynurenate LR- peak, while the LR+ peaks remained significant and retained, on average, 95% (SE=28%) of their pre-kynurenate LR+ overall strength.

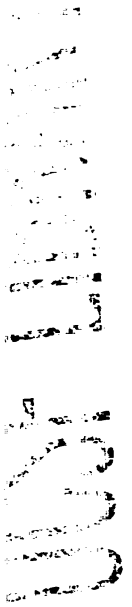

Figure 3-10

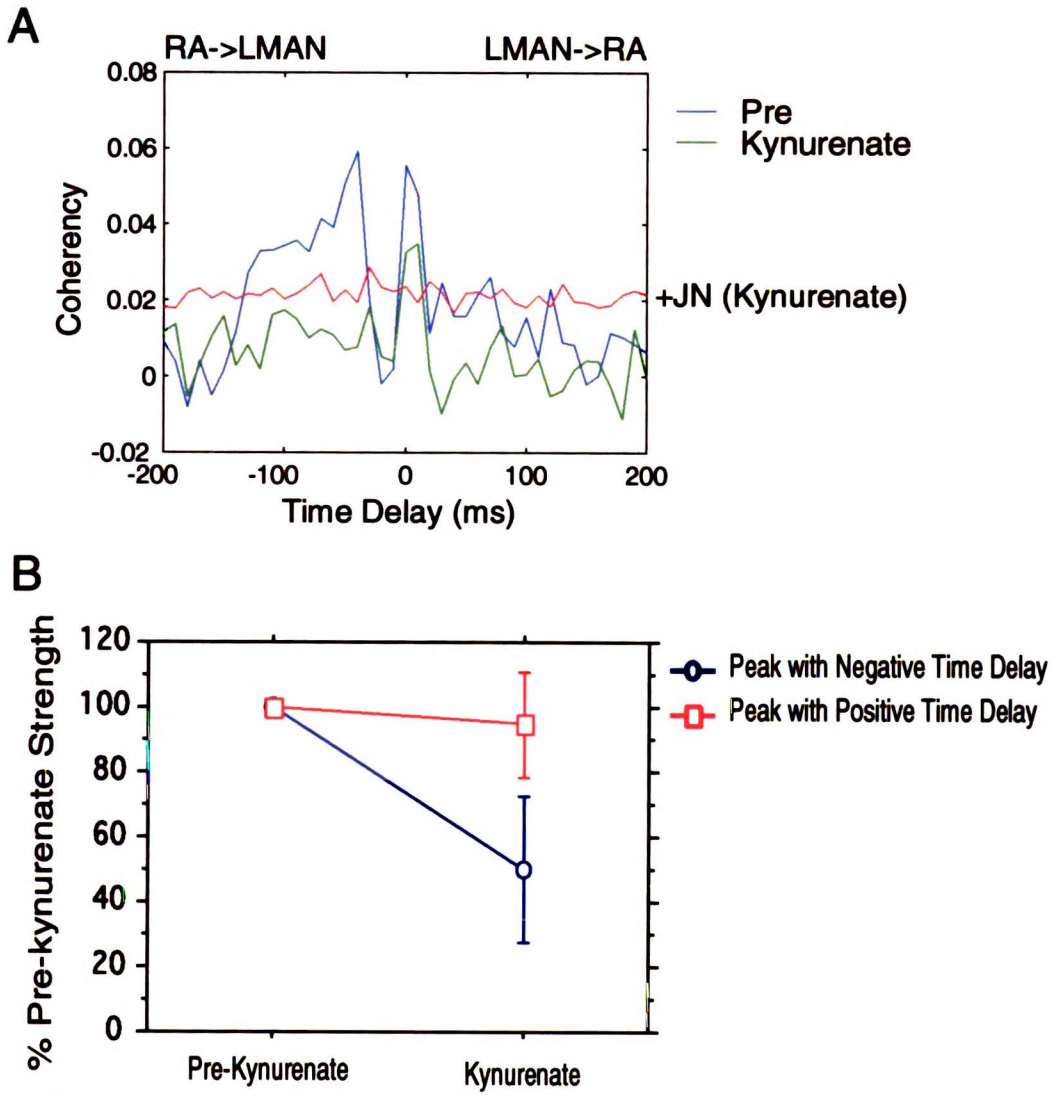

Figure 3-11. Predicted Time Delays and Widths of LMAN-RA Coherency Peaks. a) Scatterplot of the measured and predicted time delays of LMAN-RA coherency peaks from experiments where activity was recorded in LMAN, RA and HVc. The predicted time delay is determined by the difference in time delays of the HVc-RA and the HVc-LMAN peaks. The diagonal line represents the unity line, where predicted = measured time delays. Squares (□) and plus (+) symbols represent the peak with negative and positive time delays, respectively, in LMAN-RA coherency functions with two well-separated peaks. b) Scatterplot of the measured and predicted widths of LR+ peaks from LMAN-RA coherency functions that had corresponding HVc-LMAN coherency functions with a peak with a short negative time delay (HL- peaks). The predicted width, calculated as the sum of the widths of the HL- and HVc-RA coherency peaks, is always larger then the actual LR+ peak width. The diagonal line represents the unity line.

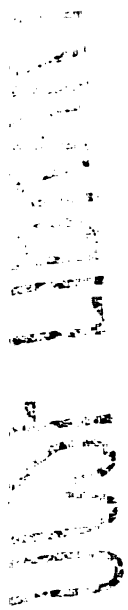

Figure 3-11

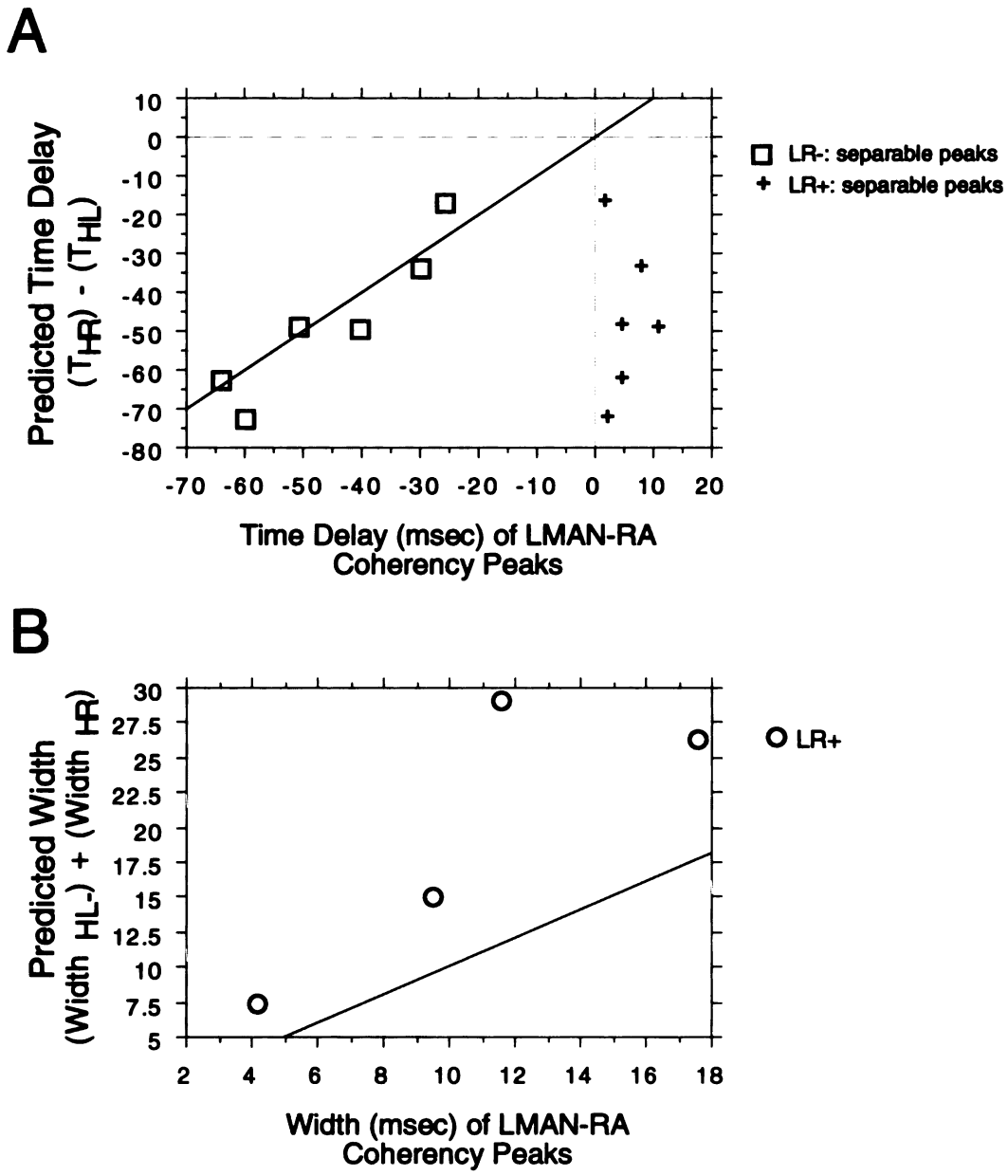
A
Predicted Time Delay
(T_HR) - (T_HL)
10
0
-10
-20
-30
-40
-50
-60
-70
-80
-70 -60 -50 -40 -30 -20 -10 0 10 20
Time Delay (msec) of LMAN-RA
Coherency Peaks
LR-: separable peaks
LR+: separable peaks
B
Predicted Width
(Width HL-) + (Width HR)
30
27.5
25
22.5
20
17.5
15
12.5
10
7.5
5
2 4 6 8 10 12 14 16 18
Width (msec) of LMAN-RA
Coherency Peaks
LR+

Figure 3-12. Two models of functional connectivity of the song system. In both models, each row denotes sites within a nucleus. The model in (a) illustrates functional connectivity that is organized in a parallel manner. The panel on the upper right represents the low probability of obtaining significant correlation of activity between sites 1 and 2. The model shown in (b) involves extensive convergence and divergence of connections between nuclei, and also short and long-range intrinsic connections within each nucleus. The probability of detecting significant correlation between the activity of sites 1 and 2, as illustrated on the lower right panel, would be higher than in (a).

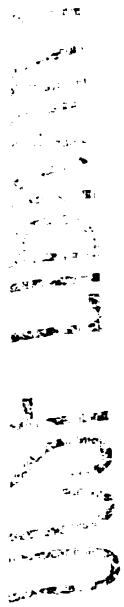

Figure 3-12

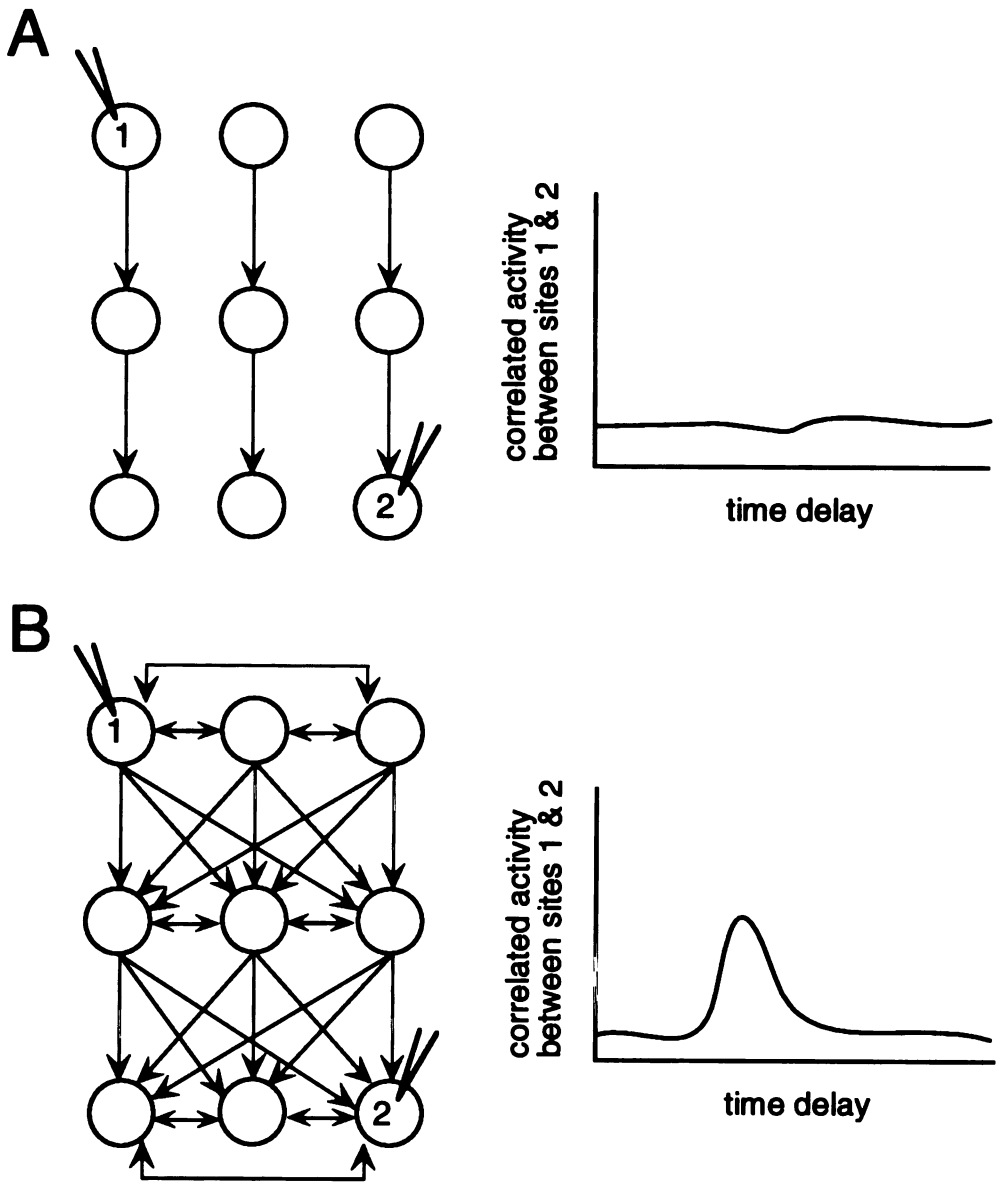
A
1
2
correlated activity between sites 1 & 2
time delay
B
1
2
correlated activity between sites 1 & 2
time delay

Table 3-1. LMAN-RA coherency functions with two well-separated peaks from multiple and single unit activity

Property	S,LR-,mu (15)	S,LR-,su (6)	S,LR+,mu (15)	S,LR+,su (6)	E,LR-,mu (13)	E ,LR+,mu (13)
Time Delay (msec)	-52.60±11.75[a]	-47.78±10.09	8.21±3.20[a]	10.22±2.59	-46.92±20.57[b]	8.75±4.84[b]
Width (msec)	23.98±10.25[c]	18.99±13.32	11.78±3.33[c,j]	15.03±7.47	17.41±7.63[d]	9.22±2.69[d,j]
PeakStrength	.042±.012[e,i]	.033±.009	.087±.032[e,g]	.044±.004[g]	.070±.016[f,i]	.093±.026[f]
Overall Strength (msec)	1.02±0.47[h]	0.55±0.33[h]	0.99±0.42	0.64±0.27	1.21±0.55	0.86±.36

Numbers are means ± standard deviation. S = spontaneous activity, E = Evoked activity; LR- = peak with negative delay, LR+ = peak with positive delay; su = single unit, mu = multi-unit activity.

Significant differences are: (*p<.05, **p<.01, ***p<.001, Wilcoxon Signed Rank Test; #p<.05, ##p<.01, ###p<.0001, Mann-Whitney)

a) LR- < LR+: S,mu time delay ***

b) LR- < LR+: E,mu, time delay **

c) LR- > LR+: S,mu width **

d) LR- > LR+: E,mu width *

e) LR- < LR+: S, mu peak strength **

f) LR- < LR+: E,mu peak strength *

g) mu > su: S,LR+ peak strength ##

h) mu > su: S,LR- overall strength #

i) E > S: LR-,mu peak strength ###

j) S > E: LR+,mu width [#]

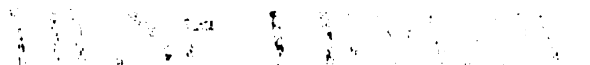

Table 3-2. LMAN-RA coherency functions with a single peak.

Property	MU, Spontaneous Activity (n=8)	SU, Spontaneous Activi ty (n=2)	MU, Evoked Activity (n=3)
Time Delay (msec)	0.15±12.97[a]	1.43±6.30	-0.39±2.23[b,c]
Width (msec)	39.22±23.38[d]	28.39+4.23	13.30±6.77
Peak Strength	.047±.027[e]	.036+.001	.112±.058
Overall Strength (msec)	1.53±.55[f,g]	1.02+.13	1.44±0.90

Numbers are means ± SD. MU = multi-unit activity, and SU = single unit activity

Significant differences between LR (single peaks from LMAN-RA coherency functions), LR- and LR+ peaks (see Table 3-1) during spontaneous (S) and evoked mulit-unit activity (E) are: ($^{\#}p<.05$, $^{\#\#}p<.01$, $^{\#\#\#}p<.001$, Mann-Whitney)

a) LR > LR-: S, time delay $^{\#\#\#}$

b) LR > LR-: E, time delay $^{\#\#}$

c) LR < LR+: E, time delay $^{\#}$

d) LR > LR+: S, width $^{\#\#\#}$

e) LR < LR+: S, peak strength $^{\#\#}$

f) LR > LR-: S, overall strength $^{\#}$

g) LR > LR+: S, overall strength $^{\#}$

Table 3-3. Peaks from HVc-RA Coherency Functions

Property	S, side peaks(-) (n=7)	S, central peaks (n=12)	S, side peaks(+) (n=4)	E, side peaks(-) (n=2)	E, central peaks (n=11)	E, side peaks(+) (n=1)
Time Delay (msec)	-40.71±10.20	4.39±2.30	58.75±14.36	-15.00±7.07	5.04±2.34	50.00
Width (msec)	10.91±4.79	8.20±2.63	9.95±2.27	10.85±4.88	7.01±2.21	4.80
Peak Strength (msec)	.035±.010	.203±.118	.034±.015	-.040±.002	.206±.112	.052
Overall Strength (msec)	0.36±.16	1.50±0.63	0.33±.11	-0.44±.21	1.35±0.73	0.25

Numbers are means ± standard deviation. 'S' indicates spontaneous activity, while 'E' indicates evoked activity. 'side peaks(-)' and 'side peaks(+)' indicate side peaks with negative and positive time delays, respectively.

Table 3-4. Prediction of LMAN-RA negative time delays from HVc-LMAN and HVc-RA peak time delays obtained from simultaneous recordings of HVc, LMAN and RA activity.

site	$t_{Hvc-RA(+)}$	$t_{Hvc-LMAN(+)}$	$t_{Hvc-RA(+)} - t_{HVc-LMAN(+)}$ predicted	$t_{LMAN-RA(-)}$ experimental
a58.s1,S	1	50	-49	-51
a75.s2,S	5	67	-62	-64
a75.s6,S	5	54	-49	-41
a80.s4,S	7	80	-73	-60
±SD	±2	±21		±14

Numbers are time delays, and SD = standard deviations for all observed time delays during spontaneous activity for type of peak. 'S' = spontaneous activity.

Chapter 4:

Developmental Changes in Timing and Strength of the Correlated Activity Between Anterior Forebrain and Motor Pathway Nuclei of the Song System

ABSTRACT

The anterior forebrain pathway (AFP) in songbirds may mediate the auditory feedback that is crucial for song learning, thereby guiding the plasticity in the motor pathway for song. Very little is known, however, about how the AFP modulates the activity of the motor pathway during song learning in an intact animal. Understanding the development of neural interactions between the AFP and the motor pathway may help elucidate the neural process by which the AFP mediates song learning. We therefore recorded simultaneously from the output nucleus of the AFP (LMAN), and its target nucleus in the motor pathway (RA), in juveniles undergoing song learning. In some cases, we also recorded the activity in nucleus HVc, the afferent source of input to both the AFP and RA. We then compared LMAN, RA, and HVc correlated activity in juveniles to those observed in adults that have completed song learning.

As in the adults, cross-covariance and coherency analysis in juveniles revealed that the activity of song nuclei that are indirectly, as well as directly connected, was strongly correlated. This suggests that the functional connectivity between song nuclei in juveniles includes broad divergence and re-convergence of connections between song nuclei, as well as robust intrinsic connectivity within song nuclei, and that this is already established before song learning is completed. Correlated activity between LMAN and RA, and between HVc and LMAN, varied in the same manner as in the adults, suggesting that, as in adults, the functional connectivity in juveniles is physiologically modulated. However, we found significant differences between juveniles and adults in the timing, strength and frequency of correlated activity between LMAN and RA, and in the timing of correlated activity between HVc and RA. This indicates that fine tuning of the functional connectivity occurs as song learning is completed. These developmental changes in functional connections in the song system may have important implications for the neural processes that underlie song learning.

INTRODUCTION

Vocal learning in songbirds occurs in two discrete phases, both of which depend critically on hearing. During the first phase, called the sensory phase, a juvenile bird listens and memorizes a tutor song (Fig. 4-1a). This is followed by the sensorimotor phase, during which the juvenile bird initially produces variable songs, called plastic songs, which it gradually matches to the memorized tutor song using auditory feedback of its own vocalizations (Konishi, 1965a; Immelmann, 1969; Price, 1979). The anterior forebrain pathway (AFP) of songbirds is required for song learning, suggesting that it may mediate the auditory feedback that is crucial for normal song learning (Bottjer, 1984; Sohrabji et al, 1990; Scharff and Nottebohm, 1991). Consistent with this idea, the neurons in the AFP exhibit auditory responsiveness whose selectivity for the bird's own song gradually emerges during song learning (Doupe and Konishi, 1991; Doupe, 1997; Solis and Doupe, 1997).

The AFP is part of a specialized circuit of nuclei unique to songbirds, known as the song system (Fig. 4-1b). The output nucleus of the AFP, the lateral magnocellular nucleus of the anterior neostriatum (LMAN), projects to another circuit of the song system, called the motor pathway, which is essential throughout the bird's life for song production (Nottebohm et al, 1976; Simpson and Vicario, 1990). Specifically, LMAN sends direct excitatory projections to a forebrain nucleus of the motor pathway, the robust nucleus of the archistriatum (RA). RA innervates brainstem nuclei that control the bird's vocal and respiratory musculature, and therefore controls the motor expression of song (Nottebohm et al, 1976; Vicario, 1993; Wild, 1993). Both the AFP and RA receive input from HVc (abbreviation used as a proper name), a forebrain nucleus that is also part of the motor pathway. Thus, these two functionally distinct circuits, the AFP and the motor pathway, diverge at the level of HVc and re-converge in a feed-forward manner at the level of RA. Neurons in RA receive synapses from both HVc and LMAN (Canady et al, 1988;

Herrmann and Arnold, 1991; Mooney and Konishi, 1991; Mooney, 1992), and are thus a candidate site for plasticity in the song system during song learning.

Very little is known, however, about how the AFP influences RA activity in intact animals, especially during song learning. Understanding the neural interactions between the AFP and the motor pathway during song learning may help elucidate the process by which the AFP mediates song learning. In adults who have completed learning, the neural interaction between LMAN and RA indicates that in most cases, it consists of two components: one that reflects the direct projection from LMAN to RA, and another which is most likely due to the common input of HVc, and thus reflects the correlation of activity within the song system (see Chapter 3). It is therefore of great interest to determine whether the LMAN-RA neural interactions in juveniles also consist of similar components. If so, then the functional connectivity of the song system is already established during song learning. However, if the correlated activity between LMAN and RA in juveniles are vastly different from that of adults, then gross changes in neural interactions within the song system may occur as a result of song learning. In the case where the basic functional connectivity is already established, fine tuning of the functional connectivity of the song system may still occur, much like experience-dependent changes in other neural circuits (for reviews: Singer, 1995; Shatz, 1990; Katz and Shatz, 1996; Kossut, 1998; Rauschecker, 1999). Changes in the strength and temporal characteristics of the correlated activity between LMAN and RA may also give insight into the dynamics of the functional connectivity of the song system during song learning.

We therefore investigated the development of neural interactions between LMAN, RA and HVc in the song system of zebra finches. We recorded simultaneously from LMAN, RA and/or HVc, collecting both spontaneous and song evoked activity, in anesthetized male juveniles during song learning, but after the time of large scale developmental changes in the anatomy of the song system (51 days of age). We then compared the data from these juveniles with those of adult male zebra finches (data reported

in Chapter 3). Cross-covariance and coherency analysis of simultaneously recorded activity revealed that the types of correlated activity between song nuclei remained largely unchanged between the juveniles of this age and adults. This suggests that the functional connectivity within the song system is already established during song learning. The variability of the neural interaction between song nuclei observed in juveniles was similar to that observed in adults, suggesting that the functional connectivity of the song system in juveniles is physiologically modulated in the same manner as in adults. However, we observed significant changes in frequency, strength and temporal characteristics of the correlated activity between LMAN and RA, and of that between HVc and RA. This indicates that during song learning, fine tuning of the functional connectivity occurs that does not parallel large-scale anatomical changes. Thus, these functional changes in the neural interaction between song nuclei may reflect synaptic and cellular changes that have implications for the neural processes that underlie song learning.

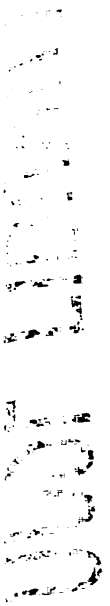

MATERIALS and METHODS

Animals and Song Recording. Data were collected from juvenile male zebra finches of 51±1 days old (mean±SD; range, 45-53d; n=15 birds). At this age, the juvenile birds were near the end of their sensory phase and in the middle of their sensorimotor learning (Fig 4-1a). Birds were housed as described in chapter 3 (adult experiments). Songs of juveniles sung 0-5 days before the experiment, and songs of their tutors (defined as in chapter 3) were recorded as described in chapter 3. At this stage of sensorimotor learning, juveniles sang plastic songs. Plastic songs were recorded on tapes, then digitized and scanned in a SPARC IPX computer using a song editing program. The plastic song that was most frequently sung, if any, was chosen as an experimental stimulus. Two to three other versions of the bird's own plastic songs (BOS), containing song elements not represented in the frequently sung version of the BOS, were also chosen as experimental stimuli. If a frequently sung plastic song was not identifiable, 3-4 plastic songs were chosen as experimental stimuli such that most, if not all, of the song elements sung were represented in the stimulus set. Songs were digitized and stored in a SPARC IPX computer.

Surgery. In the same manner as described in chapter 3, juvenile birds were prepared for electrophysiology experiments at least two days before the experiment.

Auditory Stimuli and Presentation. The stimulus set consisted of the same stimuli enumerated in chapter 3, with the following exceptions: 1) the bird's own song was replaced by 3-4 selected versions of the BOS, 2) songs of other 45-55d old juvenile zebra finches were added to the stimulus set, and 3) brothers' songs were from brothers of the same age range. The auditory stimuli were presented in the same manner as described in the adult experiments (chapter 3).

Electrophysiology. We recorded simultaneously from LMAN and RA of juvenile zebra finches (Figure 4-1b). In some experiments, we recorded neuronal activity of juvenile HVc, LMAN, and RA (one electrode in each nucleus) in a pair-wise manner as described in the adult experiments. Electrophysiology experiments and histological reconstruction of the location of recording sites were performed as described in chapter 3.

Data Analysis. Data analysis was performed on neuronal activity recorded from pairs of sites that were both auditory to at least one stimulus type, and confirmed to be located in the corresponding nucleus. Auditory responsiveness was defined as in chapter 3.

To assess how well correlated the activity of two nuclei were, we calculated the cross-covariance and coherency functions. The cross-covariance, coherency and estimates of the standard error of the cross-covariance and coherency functions were calculated as outlined in chapter 3. Both functions were calculated for data collected during a 2 second period of spontaneous activity immediately before stimulus onset, and during stimulus presentation of BOS versions that elicited auditory responses (evoked activity). The data for spontaneous activity included all trials, regardless of the stimulus presented in each trial. As described in chapter 3, the cross-covariance and coherency functions were fit with three Gaussian functions, and the following parameters were measured: peak strength, overall strength, width, and time delay of the peaks (Fig. 4-1c). The same criteria for significance and goodness of fit (R^2 value and visual inspection) were applied as in the adult data. The R^2 values of the Gaussian fit of the wide peaks in the coherency functions of RA activity relative to LMAN spikes (LMAN-RA coherency) were very low (mean+SD = 0.25$\pm$0.20; range, 0-.66), and were thus not considered to be significant. Hence, as in the adult data, LMAN-RA coherency functions were fit with two Gaussian functions. LMAN-RA coherency functions with one peak were re-fit with one Gaussian function. Note that the juvenile cross-covariance and coherency data were analyzed in exactly the same manner as the adult data.

To describe the selectivity of auditory responses for each neuronal site, we compared responses to two stimulus types using d' values as described in chapter 3. In assessing the song selectivity for the BOS, we calculated d' values between responses to BOS versions that elicited auditory responses and other song stimulus types. The BOS order selectivity was evaluated by comparing responses to the version of BOS whose temporal order was manipulated and the same BOS version presented in normal temporal order (see Methods, Chapter 3).

Topographical alignment of LMAN and RA recording sites. We evaluated the topographical alignment of the pairs of LMAN and RA recording sites as described in chapter 3.

RESULTS

Song and order selectivity of juvenile LMAN and RA neurons

We recorded simultaneously from auditory multi-unit sites (2-5 units) in LMAN and RA of juvenile male zebra finches that had undergone most of their sensory learning and were in the middle of their sensorimotor phase of learning (n=15 birds; range, 45-53 days of age; Fig. 4-1a). The song selectivity of the responses was measured using a metric d': a d' value >0.5 or < -0.5 was defined to indicate that the site was selective while a d' value -0.5< d' >0.5 indicated that the site was not selective (see Methods). The mean d' value for bird's own plastic songs (BOS) relative to tutor song (TUT) response ($d'_{BOS-TUT}$) of all LMAN sites was 0.87±0.68 (± standard deviation; n=25), while the mean d' value for BOS response relative to the response to songs of other adult zebra finches (conspecific songs, CON; $d'_{BOS-CON}$) was 1.03±0.62 (n=27). Most of the LMAN multi-unit sites were selective for the BOS over the tutor song ($d'_{BOS-TUT}$>0.5; 16/25 sites) and conspecific songs ($d'_{BOS-CON}$>0.5; 21/27 sites; Fig. 4-2a). Nine out of 25 (36%) LMAN sites were auditory but did not show any preference for the BOS vs. tutor songs (-0.5< $d'_{BOS-TUT}$ >0.5), and 6/27 (22%) LMAN sites responded equivalently to the BOS and conspecific songs (-0.5< $d'_{BOS-CON}$ >0.5). The heterogeneity of LMAN selectivity in young birds has been shown in previous studies (Solis and Doupe, 1997). The mean $d'_{BOS-TUT}$ of RA multi-unit sites was 0.86±0.86 (n=25) and the mean $d'_{BOS-CON}$ was 0.90±0.96 (n=27). The majority of the RA multi-unit sites were selective (d' >0.5) for the BOS over the tutor song (n=16/25) and conspecific songs (n=16/27; Fig. 4-2b). Two out of 25 (8%) RA sites preferred the tutor song over the BOS, while 7/25 (28%) did not show any preference for the BOS vs. tutor song. Ten out of 27 (37%) of the RA sites were not selective for the BOS over conspecific songs, and 1/27 (4%) preferred conspecific songs over tutor songs.

We examined the BOS order selectivity of the LMAN and RA multi-unit sites from juveniles by comparing responses to the normal BOS and BOS with altered temporal order. The temporal order was changed in two ways: reverse song (REV), where the entire song

(including the song syllables) was reversed, and reverse order (RO), in which the local order of each song syllable was kept intact but the global order of the syllables was reversed (see Methods). The mean $d'_{BOS-REV}$ of all LMAN sites was 0.96±0.64 (n=28), and of all RA sites, 0.94±0.72 (n=26). The majority of individual LMAN (23/28: 82%) and RA (20/26: 77%) sites exhibited BOS order selectivity, preferring the BOS in forward order over fully reversed songs (Fig. 4-2c, d). The rest of the LMAN sites either had no preference for BOS vs. reverse song (4/28: 14%) or preferred the reverse song over the BOS (1/28: 4%). For RA sites, 6/26 (23%) were non-selective, responding equally to the BOS and reverse song. The $d'_{BOS-REV}$ values indicate that most LMAN and RA neurons are sensitive to the temporal order of the BOS.

A large number of the LMAN and RA sites, however, did not exhibit any preference for the BOS vs. the less dramatically altered reverse order song. The mean d'_{BOS-RO} of all LMAN sites was 0.34±0.58 (n=23), and of all RA sites was 0.33±0.66 (n=24). Twelve out of 23 (52%) of the LMAN sites and 15/24 (62.5%) of the RA sites responded equally to the BOS and the BOS presented in reverse order (Fig. 4-2c, d). Only nine out of 23 (39%) LMAN sites had $d'_{BOS-RO} > 0.5$, indicating selectivity for the BOS over reverse order BOS, and 2/23 (9%) preferred the reverse order BOS over the BOS. For RA sites, only 8/24 (33%) sites were selective for the BOS in forward over reverse order, while 1/24 (4%) responded more strongly to the reverse order BOS than the normal BOS. This indicates that neither the majority of individual LMAN and RA sites nor LMAN and RA as a whole were sensitive to the global order of song elements. A more detailed analysis of the song and order selectivity of LMAN and RA sites, including changes during development, will be presented in the next chapter.

Correlated activity between juvenile LMAN and RA

Correlated activity over a long time scale. To measure the correlation of activity between LMAN and RA, we calculated the cross-covariance and coherency functions of RA activity

relative to LMAN spike times (at time delay = 0) during spontaneous activity for all trials, and during presentation of versions of BOS that elicited an auditory response in both LMAN and RA (evoked activity). We recorded activity from 33 pairs of LMAN and RA multi-unit sites (n=15 birds). Correlation of LMAN and RA activity that resulted from time locked responses to events that occurred identically across trials (typically the stimulus) were removed by subtracting the shuffled cross-correlation (Perkel et al, 1967; Aertsen et al, 1989; see Methods). The LMAN-RA cross-covariance (Fig. 4-3a) and coherency (Fig. 4-3b) functions exhibited positive peaks that were significant by our criterion (see Methods) during spontaneous and evoked activity. This indicates that in juveniles, LMAN and RA activity were significantly correlated in the positive direction. That is, when LMAN activity increased, so did the activity in RA. In the cross-covariance calculations, 23/33 (70%) pairs of LMAN-RA sites exhibited at least one significant positive peak during spontaneous activity, while during evoked activity, 22/33 (67%) pairs showed at least one significant peak. Similarly, the coherency functions showed that the activity of 27/33 (82%) of the LMAN-RA pairs of sites were correlated during spontaneous activity, showing at least one significant peak in their coherency function, while during evoked activity, the activity of 23/33 (70%) LMAN-RA pairs were significantly correlated.

We fitted the data with Gaussian functions and measured the following (see Methods): a) time delay of the peak relative to LMAN spikes at time delay = 0, b) width, measured as the half-width at 61% height ($\frac{1}{\sqrt{e}} * amplitude$), c) peak strength, which is equivalent to the amplitude of the peak, and d) overall strength, quantified as the area under the peak (*amplitude x width*). The cross-covariance functions revealed correlated activity between LMAN and RA over short and long time scales, as indicated by the overlapping narrow and wide peaks in the cross-covariance plots (Fig. 4-3a, b), while coherency functions showed correlated activity over a short time scale only (narrow peaks; Fig. 4-3c, d). We analyzed the peaks that were significant by our criterion (see Methods). In the

cross-covariance functions, the mean width of the narrow peaks was 23.59±12.25 msec (n=27/33 site pairs) during spontaneous activity, and 16.73±8.61 msec (n=18/33 site pairs) during evoked activity. The narrow peaks observed in the LMAN-RA coherency functions are presented in detail in the next section. The wide peaks in the cross-covariance functions had a mean width of 286.81±83.64 msec (n=17/33 site pairs) during spontaneous activity, which was significantly smaller than the mean width observed during evoked activity (464.91±126.24 msec, n=15/33; $p<.001$, Mann-Whitney). The time delays of the wide peaks, -14.83±41.62 msec for spontaneous activity and 5.22+114.57 msec during evoked activity, were not significantly different from zero ($p>0.3$, One Sample Sign Test).

The Gaussian function fit of coherency functions yielded very low goodness of fit values (R^2) for wide peaks, where a value of $R^2 > 0.7$ was considered a good fit. The mean R^2 value was 0.35+0.21 (n=33) for spontaneous activity and 0.14+0.11 (n=33) for evoked activity, indicating the lack of wide peaks in the LMAN-RA coherency functions. Since the coherency function is equivalent to the cross-covariance function normalized by the auto-correlation of firing within LMAN and RA, the wide peaks that were eliminated by this normalization are thus primarily due to the temporal structure of firing within LMAN and RA. The wide peaks in the cross-covariance function may therefore be interpreted as synchronized firing between LMAN and RA over a long time scale, arising mainly from the intrinsic pattern of firing within LMAN and RA. Because the coherency function provides a normalized estimate of the correlation between LMAN and RA activity, from here on we will focus on the results derived from the coherency analysis.

Coherency of LMAN and RA activity over a short time scale. Coherency functions of RA activity relative to LMAN spike time (at time delay = 0) revealed different types of functions: functions with a) 2 well separated narrow peaks, b) 2 narrow peaks that were either not separable and/or with one of the two peaks not significant ('non-separable/significant' peaks), c) a single narrow peak, and d) no significant peaks. Figure 4-

4 shows individual and group data of each type of function (except for functions with no peaks) during spontaneous activity, and Figure 4-5 shows coherency functions obtained during evoked activity. Table 4-1 shows the percentage of LMAN-RA pairs that exhibited each type of function during spontaneous and evoked activity, and compares these percentages to those obtained in adults. Two peaks were considered well separated in time if the difference between their time delays was greater than the sum of their widths. The two well-separated peaks may indicate two isolated correlations in time, one before the LMAN spike (negative time delay) and the other after the LMAN spike (positive time delay; Table 4-2; Fig. 4-4a, Fig. 4-5a).

In most cases that showed 'non-separable/significant' peaks, the peak observed was asymmetric with a shallow slope on the left side (negative time delays) and a steep slope on the right side (positive time delays; Fig. 4-4b and 4-5b). This suggests that in these cases, the correlations represented in other cases by the two well-separated peaks may have overlapped in time. In particular, as in adults, the peak with a negative time delay appeared to be the most labile and variable in timing and strength compared to the relatively stable peak with a positive time delay. In 'non-separable/significant' peaks, the peak with the negative time delay was shifted closer to zero compared to the approximately 50 - 60 msec negative time delay of this peak when there were two well separated peaks (Table 4-2; spontaneous -28.39$\pm$21.42 msec, n=5; evoked -27.67$\pm$22.75 msec, n=8). In most cases where there was only one significant peak, it was the peak with a negative time delay that was not significant (spontaneous, 4/4; evoked, 4/7).

The peak with a positive time delay (evoked activity: 0.93$\pm$13.13 msec, n=9) also exhibited some variability in a small number of cases during evoked activity, although in most cases (n=6/9) these peaks exhibited similar time delays (8.32$\pm$7.24 msec) and widths (9.65$\pm$3.89 msec) as those of the peak with a positive time delay in cases with two-well separated peaks (Table 4-2). In 3/9 cases, the time delays of the significant peak were shifted to the left of zero (-13.83$\pm$8.28 msec). However, this was accompanied by a large

increase in width (26.08±13.76 msec) compared to that of the positive time delay peak in two well separated peaks (Table 4-2), raising the possibility that an almost completely overlapping peak with a negative time delay shifted the positive time delay peak to the left of zero. Also, in 3/7 cases during evoked activity in which only one peak was significant, the peak with a positive time delay was not significant, indicating a slight variability in its strength.

Finally, some coherency functions showed single peaks that were symmetric, which may indicate a single correlation, or perhaps 2 (or more) completely overlapping correlations (Fig. 4-4c, 4-5c). Further analysis will focus primarily on functions with 2 well separated peaks and those with a single peak because the time delays and widths of these peaks that can be well characterized.

Coherency functions with 2-well separated peaks. As observed in the adults, the time delays of the two well separated narrow peaks were distinct: one had a negative time delay (LR- peak; Table 4-2), indicating an increase in RA firing probability preceding an LMAN spike (RA ->LMAN), and the other, a positive time delay (LR+ peak; Table 4-2), indicating an increase in RA firing probability after an LMAN spike (LMAN -> RA). The time delays of LR- and LR+ were significantly different from each other during both spontaneous (Fig. 4-6a) and evoked activity ($p<.05$, Wilcoxon Signed Rank Test; Fig. 4-6b). The correlation represented by the LR+ peaks is consistent with an excitatory interaction between LMAN and RA (Perkel et al, 1967; Moore et al, 1970), and the relatively short time delay implies a direct connection from LMAN to RA. This is consistent with the direct excitatory projection from LMAN to RA (Bottjer et al, 1989; Mooney and Konishi, 1991; Mooney, 1992). Also, BOS presentation significantly decreased the time delay of the LR+ peaks ($p<.01$, Mann-Whitney). The LR- peaks, on the other hand, imply an excitatory interaction from RA to LMAN. However, there are no known projections from RA to LMAN. An alternative

interpretation is that this correlation is due to a common input to LMAN and RA from HVc (see Chapter 3). Experiments in the adults strongly support this hypothesis (see Chapter 3).

The LR- peaks were wider than the LR+ peaks, but this difference was significant only during evoked activity ($p<.05$, Wilcoxon Signed Rank Test; Fig. 4-6d; Table 4-2). The greater width of the LR- peaks indicates that the correlation is more dispersed in time and is consistent with correlated activity between indirectly connected areas (Fetz and Cheney, 1980). The narrow width of the LR+ peaks, on the other hand, indicates a brief and tight correlation between LMAN and RA, consistent with a direct projection from LMAN to RA. During spontaneous activity, the difference between the LR- and LR+ widths (Fig. 4-6c) was not significant largely because of a significant increase in the width ($p<.01$, Mann-Whitney) and variability of the LR+ peaks during spontaneous activity compared to during evoked activity. The data indicate that during presentation of the BOS, the correlation represented by the LR+ peaks becomes less dispersed in time (narrower), making it distinguishable from the wide LR- peaks.

The peak strengths of the correlation depicted by the LR- and LR+ peaks were similar (Table 4-2; Fig. 4-6e, f). In contrast to the LR- peak, the LR+ peak strength was significantly affected by stimulus playback. The LR+ peaks had higher peak strength during evoked than during spontaneous activity ($p<.05$, Mann-Whitney). The increase in peak strength was, however, less dramatic than the decrease in width of the LR+ peak during BOS presentation (see above), such that the overall strength (*amplitude x width*) of the LR+ peak decreased during evoked activity. Thus, it was only during evoked activity that the overall strength of the correlation in the LR+ peaks was significantly lower than that of the LR- peaks (Table 4-2; $p<.05$, Wilcoxon Signed Rank Test; Fig. 4-6g, h). The data indicate that the maximum coherency of LMAN and RA activity represented by the LR- and LR+ peaks is the same, but because the time course of correlation (width) represented by the LR- peaks is longer than that of the LR+ peaks, the strength considered over all time delays is higher in LR- peaks.

Coherency functions with a single peak. To determine whether single LMAN-RA (LR peaks) are different from those that occur in pairs (LR- and LR+ peaks), we compared their time delays, widths, peak and overall strengths (Table 4-2). The mean time delays of the LR peak during spontaneous and evoked activity were significantly greater than the mean LR- peak time delay, and significantly less than LR+ peak time delay (Fig. 4-6a, b; Table 4-2; $p<.05$, Mann-Whitney). Moreover, the mean time delays of the LR peaks were not significantly different from zero ($p>.45$, One Sample Sign Test). The differences in time delay between LR, LR- and LR+ peaks suggest that the correlation represented by the LR peaks is different from those of the LR- and LR+ peaks, and may reflect synchronized firing between LMAN and RA or completely overlapping peaks.

In general, the LR peaks were very different from the LR+ peaks in width, peak and overall strengths. The correlation depicted by the LR peaks was more dispersed in time than the correlation represented by LR+ peaks during spontaneous and evoked activity (Table 4-2; $p<.01$, Mann-Whitney; Fig. 4-6c, d). During evoked activity, the LR peak had a significantly higher mean peak strength than the LR+ peak (Table 4-2, $p<.05$, Mann-Whitney), but was not significantly different from the LR+ peak during spontaneous activity (Table 4-2, Fig. 4-6e, f). The total strength over all time delays (overall strength, *amplitude x width*) of the LR peaks during spontaneous and evoked activity was significantly higher than those of the LR+ peaks ($p<.01$, Mann-Whitney; Table 4-2, Fig. 4-6g, h).

In contrast, the LR peaks was resembled the LR- peaks in some ways, particularly during evoked activity. For example, during evoked activity, the LR peaks had widths similar to those of the LR- peaks, but during spontaneous activity, the mean width of the LR peak was significantly wider than the LR- peaks (Table 4-2; $p<.05$, Mann-Whitney; Fig. 4-6c, d). The mean peak strength of the LR peaks was not significantly different from the peak strengths of the LR- peaks during both evoked and spontaneous activity (Table 4-2, Fig. 4-

6e, f). The LR mean overall strength was similar to that of the LR- peak during evoked activity, but significantly larger than the LR- peaks during spontaneous activity (Table 4-2, $p<.05$, Mann-Whitney). Thus, similar to the LR- peaks, the correlation depicted by the LR peak may also involve correlated activity between indirectly connected areas. However, because of the slight differences between LR and LR- peaks, the LR peaks may also include correlations that are not represented by the LR- peak.

Topographical alignment of the LMAN and RA recording sites. We examined whether the anatomical locations of the pairs of LMAN and RA recording sites correlated in any way with the time delay, width, peak and overall strengths of coherency between LMAN and RA activity. LMAN projections to RA are topographically organized into compartments by the time birds are 45-55 days of age and the organization of projections is the same as in adults (Johnson and Bottjer, 1995; Iyengar and Bottjer, 1999). The alignment of the LMAN and RA recording pairs were rated according to the topographical projection of LMAN to RA (see Methods). We found that the alignment of the pairs of LMAN and RA recording sites did not predict whether correlations would be of the two-well separated, 'non-separable/significant', single or no peaks type (spontaneous: $p=.22$, evoked: $p=.63$, χ^2 test). Moreover, topographical alignment did not have a significant effect on the strength and temporal characteristics of the correlated activity between LMAN and RA during spontaneous and evoked activity, neither for the peaks that occurred in pairs (LR- and LR+ peaks; $p>.06$, Kruskal Wallis Test) nor for peaks that occurred in isolation, (LR peaks; $p>.10$, Kruskal Wallis Test). This indicates that other factors, such as intrinsic connectivity within each nucleus, may play a role in shaping the correlation of activity between LMAN and RA.

Correlated activity between HVc, LMAN and RA

Coherency functions of HVc and LMAN activity. The coherency function of LMAN activity relative to HVc spikes (n=6 pairs from 3 birds) exhibited positive significant peaks, indicating that HVc and LMAN activity are strongly correlated even though the two nuclei are indirectly connected via two intervening nuclei (Fig. 4-1b). HVc-LMAN coherency functions during spontaneous and evoked activity showed either a) 2 well-separated significant peaks, one with a short negative time delay (HL- peak) and the other a long positive time delay (HL+ peak; Fig. 4-7b; n=3), b) one significant coherency peak with a short positive time delay (HL peak; Fig. 4-7e; n=2), or c) no significant peaks at all (Fig. 4-7h; n=7). The mean time delays of the HL- and HL+ peaks during spontaneous activity were -3.89 msec and 63.64 msec (n=1), respectively, and during evoked activity, -4.27$\pm$1.03 msec and 50.83$\pm$13.92 msec (n=2), respectively. The single HL peaks had shorter time delays than the HL+ peaks: during spontaneous and evoked activity, the time delays of the HL peaks were 34.06 msec (n=1) and 31.66 msec (n=1), respectively. The positive time delays of the HL and HL+ peaks indicate an increase in LMAN firing probability following an HVc spike, which is consistent with a net excitatory interaction from HVc to LMAN (Perkel et al, 1967; Moore et al, 1970). On the other hand, the short negative time delay of the HL- peaks indicates an increase in LMAN firing probability that precedes HVc spikes, and is consistent with either a direct excitatory projection from LMAN to HVc or modulation of both HVc and LMAN activity by a common input source. However, there are no known anatomical projections that support either possibility, although a projection from LMAN to HVc has been suggested in canaries (Nottebohm et al, 1986).

Coherency of RA activity relative to HVc spikes. All HVc-RA coherency functions (from n=5 pairs of sites from 3 birds) exhibited a tall, narrow positive peak that was slightly displaced to the right of zero (HR peak) during both spontaneous and evoked activity, indicating that HVc and RA activity are strongly correlated in the positive direction (Fig. 4-7c, f, i). The mean time delay, width, peak and overall strength of the HR peaks during

spontaneous and evoked activity are shown in Table 4-3. The short positive time delays of the HR peaks indicate an increase in RA firing probability that occurs immediately after HVc spikes. The high overall strength and narrow width of the HR coherency peaks suggest that the correlation between HVc and RA activity is robust and tightly associated in time. The correlation depicted by the HR peak is consistent with the direct excitatory projection from HVc to RA (Perkel et al, 1967; Moore et al, 1970).

HVc-LMAN, HVc-RA and LMAN-RA coherency functions. To further understand the neural interaction between LMAN and RA activity, we compared the correlations between a pair of LMAN and RA sites with the correlated activity between the same LMAN site and an HVc site, and with the correlated activity between the same RA and HVc sites (n=5 sets of sites from 3 birds). We placed electrodes in all three sites and recorded the simultaneous activity of any two sites (in different nuclei, i.e. LMAN-RA , HVc-LMAN, and HVc-RA pairs), one after the other (see Methods).

We found that the types of LMAN-RA and HVc-LMAN coherency functions were correlated with each other, whereas the HVc-RA function exhibited the same type of coherency function regardless of the LMAN-RA coherency function type. In cases where the LMAN-RA coherency function exhibited two well separated peaks, the corresponding HVc-LMAN coherency function had 2 peaks, one with a short negative time delay (HL-) and the other, a long positive time delay (HL+; during spontaneous activity, n=1; evoked activity, n=1; Fig. 4-7a, b). When a LMAN-RA coherency function exhibited either a single peak (n=2, spontaneous activity), or 'non-separable/significant' peaks (n=1, spontaneous; n=1, evoked activity; Fig. 4-7d), the corresponding HVc-LMAN coherency function had either one peak, which had shorter time delays than the HL+ peaks (see above; HL peak; n=1 for spontaneous, n=1 for evoked activity; Fig. 4-7e) or no significant peaks (n=2, during spontaneous activity). This is consistent with the observation that the LMAN-RA coherency peak with a negative time delay, which is most likely due to the common input of

HVc to LMAN and RA, was the peak that was variable in timing and strength when peaks were 'non-separable/significant'. When the LMAN-RA coherency function did not exhibit any significant correlations, the corresponding HVc-LMAN coherency function also did not show any significant peaks (n=1 during spontaneous activity, and n=3 during evoked activity; Fig. 4-7g, h). In contrast, all of LMAN-RA coherency functions had corresponding HVc-RA coherency functions that exhibited one narrow peak (n=5 for spontaneous and n=5 for evoked activity; Fig. 4-7c, f, i). The correspondence between the HVc-LMAN and LMAN-RA coherency functions suggest that the correlation of LMAN-RA activity, specifically the separation in time of the LMAN-RA coherency peaks, is affected by the temporal characteristics of HVc-LMAN coherency peaks. In contrast, the consistency of the HVc-RA coherency functions suggest that the correlation between HVc and RA activity does not contribute to the variability of the LMAN-RA coherency functions.

Developmental changes in the correlated activity between LMAN and RA

Wide peaks in LMAN-RA cross-covariance functions. The frequency of wide peaks was significantly higher in juveniles than adults (see Chapter 3) during both spontaneous ($p<.05$, χ^2 test) and evoked activity ($p<.0001$, χ^2 test) . The presence of a wide peak was based on how well the data points at time delays less than -100 msec and greater than +100 msec were fit by a Gaussian function (see Methods). An R^2 value > 0.7 indicated the presence of a wide peak. Twenty six out of 33 (79%) of the LMAN-RA multi-unit pairs of sites in juveniles (Fig. 4-3a) exhibited wide peaks during spontaneous activity, while in adults, only 20/40 (50%) pairs showed wide peaks (Fig. 4-8). During evoked activity, 20/33 (61%) of the juvenile LMAN-RA pairs had wide peaks in their cross-covariance functions, while in adults only 2/40 (5%) LMAN-RA pairs exhibited wide peaks; however, neither wide peak in the adults was significant by our criterion (see Methods). Moreover, the effect of stimulus playback on wide peaks was only apparent with increasing age: in juveniles, the frequency of a wide peaks was similar during spontaneous and evoked activity ($p>.10$, χ^2 test), while

in adults, wide peaks were significantly more frequent during spontaneous than evoked activity ($p<.0001$, χ^2 test).

We considered wide peaks that were significant by our criterion for comparison between juveniles and adults. The wide peaks from adult LMAN-RA cross-covariance functions for evoked activity were not significant; hence, we only compared significant wide peaks observed during spontaneous activity. The time delays and widths of the wide peaks were not significantly different between juveniles and adults ($p>.16$, Mann-Whitney). The wide peaks from juvenile LMAN-RA cross-covariance functions had a mean time delay of -14.83$\pm$41.62 msec and width of 286.81$\pm$83.64 msec (n=17). For adult cross-covariance functions, the mean time delay and width were -41.99$\pm$69.55 msec and 353.16$\pm$135.46 msec (n=15), respectively. The data indicate that the temporal characteristics of the LMAN-RA correlation over a long time scale do not change after 50 days of age, but the tendency for this correlation to exist and its sensitivity to stimulus playback changed markedly.

Mean of all LMAN-RA coherency functions. To describe the developmental changes of the LMAN-RA coherency functions, we compared the adult and juvenile data in two ways. We first calculated the mean coherency of all functions with at least one significant peak in juveniles and adults, during both spontaneous and evoked activity, and analyzed the properties of these means. We did this because, although there were several types of LMAN-RA correlations with at least one significant peak in our data (two well separated peaks, 'non-separable/significant' peaks, a single peak), these types may well represent a continuous distribution of data points. By calculating the mean of all these types, we did not exclude any data nor make any potentially artificial separations between correlation types. Second, we analyzed the properties of all individual correlations in juveniles and adults that fall into coherency function types in which the time delay and width of the peaks can be well characterized. These function types are those with two well-separated peaks, or a single peak. We then compared the mean properties of these two types between juveniles and

adults, as well as those of the mean coherency of all correlation types. We describe first the mean of coherency functions of all correlations, followed by a description of how the population of coherency types varied between juveniles and adults. Finally, we compare the properties of the coherency functions with two well separated peaks between juveniles and adults, and also those of functions with a single peak between juveniles and adults.

We fitted each mean coherency function with two Gaussian functions, as we did for the individual data (Fig. 4-9). Despite inclusion of data including functions with a single peak, the mean were well fit ($R^2 > .97$) with two Gaussian functions, resembling the data from coherency functions with two peaks. During spontaneous activity, the mean peak with a positive time delay ($LR+_{mean}$) exhibited differences in timing and strength between juveniles and adults, while the mean peak with a negative time delay ($LR-_{mean}$) showed slight developmental changes (Fig. 4-9a). The time delay of the $LR+_{mean}$ coherency peak was longer in juveniles (9.98 msec, n=27) than adults (6.56 msec, n=29; 34% decrease), and the width of the $LR+_{mean}$ peak was larger in juveniles (14.67 msec) than in adults (9.77 msec; 33% decrease). These changes were accompanied by a large increase in peak strength (.026 in juveniles to .057 in adults; 119% increase), and an increase in the overall strength (0.39 msec in juveniles to 0.56 msec in adults; 44% increase) represented by the $LR+_{mean}$ peak.

In contrast to the $LR+_{mean}$ peak, the $LR-_{mean}$ peak during spontaneous activity showed only slight developmental changes in timing and strength. The time delay of the $LR-_{mean}$ peak in juveniles (-30.61 msec) was very similar to that in the adults (-28.22 msec; 8% increase), and the widths of the $LR-_{mean}$ in juveniles (59.86 msec) and adults (58.34 msec) were comparable (3% decrease). The peak strength represented by the $LR-_{mean}$ peak in juveniles (.027) was the same as that in adults (.027; 0% change), while the overall strength decreased only slightly by 4% from juveniles (1.62 msec) to adults (1.56 msec).

During evoked activity, both $LR+_{mean}$ and $LR-_{mean}$ peaks changed in timing and strength as song learning was completed (Fig. 4-9b). The time delay of the $LR+_{mean}$ during evoked activity was shorter in juveniles (5.82 msec, n=23) than in adults (7.86 msec, n=22;

35% increase), while the width in juveniles (12.50 msec) was slightly greater than that in adults (10.96 msec; 12% decrease). The strength of the $LR+_{mean}$ increased substantially from juveniles to adulthood. The peak strength almost doubled (83%) from juveniles (.046) to adults (.084), while the overall strength increased from 0.57 msec in juveniles to 0.93 msec in adults (63% increase). For the $LR-_{mean}$ peak, the time delay was more negative in the adults (-50.72 msec) than in juveniles (-43.31 msec; 15% change). The width of the $LR-_{mean}$ peak was wider in juveniles (44.65 msec) than in adults (30.57 msec, 32% decrease). The peak strength represented by the $LR-_{mean}$ peak was similar between juveniles (.037) and adults (.034; 8% decrease), while the overall strength decreased by 37% during development (juveniles, 1.65 msec; adults, 1.04 msec). Thus, on average, the direct LMAN-RA correlated activity during both spontaneous and evoked activity ($LR+_{mean}$) showed more dramatic changes in timing and strength during development than the LMAN-RA correlation due to the common input from HVc ($LR-_{mean}$). These results proved to be similar to those obtained from the analysis of coherency functions with two well separated peaks (see below).

Frequency of types of LMAN-RA coherency functions. The types of LMAN-RA coherency functions observed in juveniles were the same as those observed in adults (see Chapter 3). The percentages of LMAN-RA multi-unit pairs that exhibited each type of LMAN-RA coherency function in juveniles and adults are shown in Table 4-1. The frequency of each type of LMAN-RA coherency function was not significantly different between juveniles and adults for data from spontaneous activity ($p=.41$, χ^2 test) and evoked activity ($p=.13$, χ^2 test). This suggests that the types of neuronal interaction between LMAN and RA do not change between 50 days of age and adulthood.

LMAN-RA Coherency functions with 2 well separated peaks. The temporal characteristics of the LR+ peaks (peaks with positive time delays) changed with age, but this was evident only during spontaneous activity (Fig. 4-10). The mean time delay of the LR+ peaks during

spontaneous activity in adults was significantly smaller than that of juveniles ($p<.01$, Mann-Whitney; Fig. 4-11a; Table 4-2). The LR+ peaks derived from spontaneous activity were also significantly narrower in adults than those in juveniles ($p<.05$, Mann-Whitney; Fig. 4-11c; Table 4-2). These changes are similar to those obtained from the mean of all coherency functions, although the evoked $LR+_{mean}$ peak showed a slight developmental change in time delay, which may well be within the variability of the individual evoked LR+ peak data. The changes in the spontaneous LR+ peak suggest that, as the brain matures, the increase in RA firing probability following an LMAN spike during spontaneous activity occurs sooner, and the direct interaction from LMAN to RA becomes more tightly correlated in time. The lack of similar developmental changes during evoked activity (Fig. 4-11b, d) may be attributed to the effect of stimulus playback on LR+ correlations in juvenile birds. That is, during evoked activity, the time delay and width of the LR+ peaks of juveniles becomes significantly smaller than those during spontaneous activity, and more similar to those in adults ($p<.01$, Mann-Whitney; Table 4-2).

The peak and overall strength of the LR+ peaks exhibited an increase with age (Figure 4-10). These changes are strikingly similar to those observed in the mean data. During both spontaneous and evoked activity, the adults showed a significantly higher mean LR+ peak strength than the juveniles ($p<.01$, Mann-Whitney; Fig. 4-12a, b; Table 4-2). The mean overall strength of the LR+ peak, which is the total coherency over all time delays, was higher in adults than in juveniles; however, this difference was significant only during evoked activity ($p<.05$, Mann-Whitney; Fig. 4-12c, d; Table 4-2). These data indicate that the strength of coherency due to the direct projection from LMAN to RA at the peak time delay and over all time delays increases as the bird reaches adulthood.

The mean time delay and width of the LR- peaks during spontaneous and evoked activity in juveniles were not significantly different from those of adults (Fig. 4-10; Table 4-2). Nevertheless, there were some trends. These trends are similar to those observed in the mean of all coherency functions, except for the slight changes in time delay of the $LR-_{mean}$

peak, which may be within the variability of the individual LR- peak data. The time delay of the LR- peaks in juveniles had a tendency to be more negative (i.e. longer) than those of adults (Fig. 4-11a, b). During evoked activity, the LR- peaks had a tendency to be wider in juveniles than in adults (Fig. 4-11d). During spontaneous activity, however, the mean width of the LR- peaks was similar between juveniles and adults (Fig. 4-11c). This suggests that the temporal characteristics of the correlation represented by the LR- peaks, which is likely due to the common input of HVc to LMAN and RA, do not change between 50 days of age and adulthood.

Similarly, the peak and overall strength of the correlation represented by LR- peaks did not significantly change as the brain matured (Figure 4-10; Table 4-2). The distribution and mean of peak strengths of the LR- peaks are shown in Figure 4-12a and b. This lack of developmental change in peak strength was also observed in the overall mean data. The LR- peaks had a tendency to have a higher mean overall strength in juveniles than in adults during both spontaneous and evoked activity (Fig. 4-12c, d); however, the differences were not significant. This tendency was also observed in the overall mean data. These data suggest that the strength of the correlation due to the common input of HVc to LMAN and RA, measured both at the peak time delay (peak strength) and over all time delays (overall strength), remains largely unchanged from 50 days of age to adulthood. In general, the changes in timing and strength of the LR+ and LR- peaks resembled those changes observed in the means of all coherency function types, suggesting that analysis of the functions with two well separated peaks as a group did not introduce a bias into the results.

LMAN-RA Coherency functions with a single peak. The peak and overall strength of the correlation represented by the single LMAN-RA coherency peaks (LR peaks) did not significantly change during development, although the juveniles had a tendency to have higher overall strengths than the adults (Fig. 4-13c, d; Table 4-2). Similarly, the temporal characteristics of the LR peaks did not change significantly with age, except for one feature

during evoked activity (Fig. 4-13a, b; Table 4-2): the mean width of the LR- peaks during evoked activity was significantly higher in juveniles than in adults ($p<.05$, Mann-Whitney; Fig. 4-13b; Table 4-2). The data suggest that LR peaks, which may represent merged LR+ and LR- peaks that resulted from the altered timing of the LR- peaks, remains largely unchanged as the brain matures.

HVc-LMAN coherency functions. The types of coherency functions of LMAN activity relative to HVc spikes observed in the juveniles (described earlier) were similar to those found in adults (see Chapter 3), indicating that the types of neuronal interaction between HVc and LMAN activity remain the same as the brain develops. However, because of the low number of cases of each type studied in juveniles, we were unable to draw meaningful conclusions from the direct comparison of juvenile and adult HVc-LMAN coherency functions. Figure 4-14 shows the distribution of the time delays, widths, peak and overall strengths of the HVc-LMAN coherency functions in juveniles and adults.

The correspondence between types of HVc-LMAN and LMAN-RA coherency functions found in juveniles (described earlier; see Fig. 4-7) was similar to that observed in adults (see Chapter 3, Fig. 3-9). This suggests that the apparent effect of the correlation between HVc and LMAN activity on the LMAN-RA coherency does not change as the bird reaches adulthood

Coherency of RA activity relative to HVc spikes. In both juveniles and adults (see Chapter 3), the coherency of RA activity relative to HVc spikes exhibited a tall, narrow peak that was displaced to the right of zero (HR peak, Fig. 4-7c, f, i; 'central peak', Chapter 3, Fig. 3-9), indicating that the excitatory interaction from HVc to RA found in adulthood is present at 50 days of age. However, the HVc-RA coherency functions from juveniles did not show the small peaks that were observed in the adults. In adults, these small peaks flanked the central peak on one or both sides. The small side peaks are thought to represent correlated activity

between HVc and RA that is due to intrinsic burst firing within HVc and RA (see Chapter 3). The lack of side peaks in HVc-RA coherency functions may indicate there is no or negligible correlated burst firing between HVc and RA in juveniles.

The HVc-RA coherency peaks exhibited changes in their temporal characteristics between 50 days of age and adulthood; however, there were no significant changes in peak and overall strength as the brain matured (Figure 4-15d, e; Table 4-3). In juveniles, the HR peaks had longer time delays and narrower widths than the central peaks in adults. The mean time delays in juveniles were significantly longer than those of adults during both spontaneous and evoked activity (Fig. 4-15a, b; $p<.05$, Mann-Whitney). The mean widths of the central peak in juveniles were narrower than those in adults. However, this difference was significant only during evoked activity ($p<.05$, Mann-Whitney; Fig. 4-15c). Thus, the data suggest that as the bird reaches adulthood, the direct interaction from HVc to RA has a shorter mean time delay but also becomes more dispersed in time (at least during evoked activity), perhaps reflecting increased polysynaptic correlations within RA (or HVc), while the peak and overall strength of this interaction remain largely unchanged.

DISCUSSION

The goal of this study was to describe the correlated activity between nuclei in the song system of juveniles undergoing song learning, and to compare this to the correlation of activity observed in adults that have completed song learning (Chapter 3). We found that the types of neural interaction between song nuclei were similar between adults and juveniles. As in adults, correlations due to shared inputs and those between indirectly connected areas were robust, as was correlated activity between directly connected areas. This suggests that the basic functional connectivity of the song system is already established before song learning is completed. The variability of LMAN-RA correlated activity reflects the different types of HVc-LMAN correlated activity in the same manner as in the adults. This suggests that the functional connectivity of the song system in juveniles also has variable states, similar to those observed in adults. However, we also observed significant changes in the timing, strength, sensitivity to stimulus playback and existence of correlated activity between LMAN and RA, and changes in the timing of correlated activity between HVc and RA. Because the song system is the most likely neural substrate for song learning, these developmental changes may play a role in the neural processes that underlie song learning.

LMAN-RA correlated activity with a long time scale is observed more frequently in juveniles

LMAN and RA activity in juveniles was correlated over a long time scale (hundreds of msec), similar to the correlations observed in adults. As in the adult brain, correlations in juveniles over a long time scale were observed only in cross-covariance functions and not in coherency functions. Coherency functions provide estimates of correlated activity between two nuclei that are normalized for the auto-correlation of firing within each nucleus, whereas cross-covariance functions do not (Rosenberg et al, 1989; see Methods). This loss of wide peaks after normalization suggests that these wide peaks reflect the correlated increase in firing probability in LMAN that occurs when LMAN neurons spike, and in RA when RA

neurons fire an action potential. Moreover, the average time delay of the wide peaks was not significantly different from zero, suggesting that the wide peaks represent broad synchronization of intrinsic firing between LMAN and RA.

The frequency of wide peaks in LMAN-RA cross-covariance functions was significantly higher in juveniles than adults, suggesting that global synchronized activity between LMAN and RA could play a role in the development of the song system. In particular, the frequency of wide peaks was strikingly higher in juveniles than adults during playback of the bird's own songs (BOS); adult LMAN-RA coherency functions did not exhibit any significant wide peaks during evoked activity. The data suggest that the pattern of intrinsic activity within LMAN and RA is more similar in juveniles than adults, and that BOS presentation does not disrupt this similarity between nuclei in juveniles as it does in adults. The juvenile patterns of LMAN and RA activity, however, may have changed to some extent in response to BOS presentation, as indicated by the significant increase in width of the wide peaks during evoked activity. Spontaneous or evoked correlated activity in developing nervous systems is thought to guide the formation and modification of neural connections (for reviews see: Shatz, 1990; Katz and Shatz, 1996; Wong, 1999; Feller, 1999). Thus, the high degree of similarity in intrinsic activity between LMAN and RA in juveniles may ensure that both nuclei form similar patterns of intrinsic connections that reflect song learning, especially during auditory experience of their own songs.

LMAN-RA correlated activity reflecting the direct LMAN to RA projection changes in timing and strength during song learning

The types of correlated LMAN-RA activity over short time scales (approximately 10-35 msec; narrow peaks) were also similar to those observed in adults, indicating that the basic neural interactions between LMAN and RA do not change from 50 days of age to adulthood. LMAN-RA coherency functions exhibited either two well-separated peaks, two peaks that were either not clearly separable and/or where one of the two peaks was not

significant, a single peak, or no significant peaks. As in the adults, the two well-separated peaks had distinct time delays: a positive and a negative time delay. The peak with a negative time delay (LR-) most likely represents a correlation that is due to the common input of HVc to LMAN and RA, with the HVc presynaptic input reaching RA before LMAN. The peak with a positive time delay (LR+) most likely represents correlations due to the direct connection from LMAN to RA. As was observed in the adults, the relatively greater width and longer time delay of the LR- peaks compared to those of the LR+ peaks are consistent with LR- peaks representing a correlation that involves indirectly connected nuclei, while LR+ peaks represent correlated activity between directly connected nuclei (Fetz and Cheney, 1980). Moreover, experiments in adults further support this hypothesis: disruption of HVc activity resulted in severe attenuation in overall strength of the LR- peak, but only a slight decrease in the overall strength of the LR+ peak (see Chapter 3).

No significant changes were observed in the LR- peaks from 50 days of age to adulthood, but significant changes in the timing and strength of the LR+ peaks were observed over the same period. This indicates that the correlated activity due to the common input of HVc to LMAN and RA remains largely unchanged by this assay during song learning, while the correlated activity due to the direct LMAN to RA projection changes as song learning is completed. Compared to adults, the direct LMAN-RA correlated activity in juveniles exhibited a significantly larger time delay, and more variability in time delays of the increase in RA activity following LMAN spikes. The slow temporal characteristics of the correlated activity between LMAN and RA in juveniles may play a role in the plasticity of the song during song learning. We also observed a significant rise in peak strength of the LR+ peaks, suggesting that in adults, LMAN can induce a response in RA at a specific time delay in a more reliable manner than in juveniles. Thus, during song learning, there is a strengthening of the direct neural interaction between LMAN and RA, and an overall shortening and tightening of its time delay.

One factor that could contribute to both the decrease in jitter and time delay as birds mature is the shortening of the NMDA receptor-mediated excitatory post-synaptic currents (NMDA-R EPSCs) of the LMAN synapses in RA during development (White et al, 1999; Stark and Perkel, 1999; Livingston et al, 2000). The LMAN synapses in RA are almost exclusively mediated by NMDA receptors. The faster decay of the NDMA-R EPSCs would reduce the time window for temporal summation of the post-synaptic currents, thereby decreasing the time delay and tightening the correlation of the LR+ peaks. A similar developmental change appears to occur in the intrinsic synapses within LMAN (Boettiger, unpublished observations), where a large portion of the intrinsic EPSCs are also mediated by NMDA receptors (Boettiger and Doupe, 1998).

The increase in reliability of inducing a spike in RA due to LMAN input may result from changes in synaptic efficacy of the LMAN synapses in RA. In addition, changes in RA might affect the probability of inducing a post-synaptic response in RA neurons; for instance, altered excitability or inputs could place the RA neurons closer to the threshold for firing. This may be less likely since we did not observe any significant developmental changes in peak and overall strengths of the correlated activity between HVc and RA (see below). It is possible, however, that the hypothesized altered excitability of RA neurons is due to subthreshold HVc input. The LMAN input then induces a response in RA more reliably in adults than in juveniles, without significant developmental changes in the strength of the HVc-RA functional connection as measured by spiking (suprathreshold) activity. Ultimately, to address this issue, it may be informative to stimulate HVc, and measure the responsiveness of RA neurons to subsequent LMAN stimulation.

The observed changes in correlated activity reflecting the direct projection from LMAN to RA from 50 days of age to adulthood might in principle be due to anatomical changes that also occur during the same period. However, few such changes have been observed during the developmental period examined in this study. In particular, the volume of the LMAN nucleus in zebra finches does not change significantly from 50 days of age to

adulthood (Korsia and Bottjer, 1989), and the number of LMAN projection neurons does not significantly change with age (Nordeen et al, 1992). The volume of RA decreases only slightly from approximately 50 days of age to adulthood (Konishi and Akutagawa, 1985; Herrmann and Arnold, 1991), and the number of RA neurons does not significantly change during development (Konishi and Akutagawa, 1985). Most importantly, the number of LMAN and HVc synapses in RA does not significantly decrease from 53 days of age to adulthood (Herrmann and Arnold, 1991). On the other hand, the decline in intrinsic connections within RA from 45-50 days of age to adulthood (Herrmann and Arnold, 1991; Kittelberger and Mooney, 1999) could contribute to the shortening and tightening of temporal characteristics of the direct LMAN-RA correlated activity. The lack of gross anatomical changes in the LMAN projection to RA, at least by the analyses to date, suggest that the changes in the LMAN-RA functional connectivity is at the level of the synapse, and/or within RA intrinsic connectivity.

The apparent loss of LMAN function in adults

Although LMAN has been thought to be unnecessary for song behavior when the bird has completed learning (Bottjer et al, 1984; Sohrabji et al, 1990; Scharff and Nottebohm, 1991; Nordeen and Nordeen, 1993), data from this study indicate that the LMAN-RA correlated activity due to the direct projection from LMAN to RA becomes more robust during development. However, normal LMAN activity is not required for adult song maintenance, since LMAN lesions do not affect adult song production. In adults, the HVc synapses in RA may be strong and stable, such that elimination of the LMAN input does not affect the motor expression of song. It is clear, however, that the synapses in the motor pathway are modifiable in adults, since gradual changes in crystallized song result from deafening, altered auditory feedback, tracheosyringeal nerve section or late learning (Williams and McKibben, 1992; Nordeen and Nordeen, 1992; Morrison and Nottebohm, 1993; Williams and Mehta, 1999; Brainard and Doupe, 2000; Woolley and Rubel, 1999;

Leonardo and Konishi, 1999). In these cases, it is evident that LMAN activity is necessary for changes in adult song (Morrison and Nottebohm, 1993; Williams and Mehta, 1999; Brainard and Doupe, 2000). Thus, LMAN activity is required throughout life for vocal plasticity, consistent with the significant direct LMAN-RA correlated activity observed here in juveniles and adults. However, the vocal plasticity in juveniles and adults occur at different rates: plastic song in juveniles changes rapidly during learning, while the deterioration of crystallized song does not happen immediately after manipulation of the auditory feedback, and occurs gradually over a long period of time (Nordeen and Nordeen, 1992; Brainard and Doupe, 2000; Leonardo and Konishi, 2000; Lombardino and Nottebohm, 2000). It is possible that the strong and tight correlation of LMAN and RA activity observed in adults sets a higher threshold for changes in song to occur, while the slow and broad temporal characteristics of the LMAN-RA direct correlation in juveniles provide a neural substrate allowing vocal plasticity to occur more quickly.

Auditory stimulation mirrors developmental changes in LMAN-RA correlated activity

Auditory experience of the bird's own song in juveniles may facilitate the observed developmental changes in the functional connectivity from LMAN to RA. The changes in strength, width and time delay of LR+ peaks that occur as birds mature were also observed acutely when the bird's own song was played to juvenile birds. That is, the peak strength of the LR+ peaks in juveniles was significantly higher, and the width and time delays significantly lower during evoked than spontaneous activity. The strong similarity in the acute changes in LR+ peaks during stimulus playback in juveniles to the long-term developmental changes suggests that during evoked activity, the direct correlated activity between LMAN and RA in juveniles is very adult-like. Consistent with this, there is a lack of developmental change in time delay and width of the LR+ correlation during evoked activity in juveniles. One possible explanation for this is that during evoked activity, the

direct LMAN-RA correlated activity in juveniles involves synapses that are already mature. However, these synapses were still stronger in adults, as indicated by the increase in peak and overall strengths of the LR+ peak during evoked activity. Alternatively, since the correlations described here measure both mono- and polysynaptic contributions to connectivity, the stimulus may differentially recruit connections that sharpen and shorten the overall timing of correlated activity. Whatever the mechanism, the moment to moment changes in LR+ correlated activity between spontaneous and evoked activity in juveniles are strikingly similar to the changes exhibited by the LR+ peak as song learning is completed. This may be coincidental, but it could also indicate that the short-term mechanistic changes in the LMAN-RA functional connectivity, presumably induced by auditory experience of the BOS, are involved in the long-term developmental changes in the direct LMAN-RA correlated activity.

Developmental changes in timing of HVc-RA correlated activity

The coherency functions of RA activity relative to HVc spikes both in juveniles and adults exhibit a tall narrow peak (HR peak) that is slightly displaced to the right of zero. This indicates that the tight correlation between HVc and RA activity is already established before adulthood. The HR peak exhibited changes in timing, but not in strength, from 50 days of age to adulthood. The time delay of these peaks was significantly shorter in adults than in juveniles during both spontaneous and evoked activity. This may be due to the significant decrease in the relative contribution of the NMDA receptor-mediated excitatory post-synaptic currents (EPSCs) to HVc synapses in RA between juvenile ages (40-60 days of age) and adulthood (Stark and Perkel, 1999). Also, the width of the HR peaks became significantly larger in adults than in juveniles during evoked activity. This may reflect an increase in strength and/or number of intrinsic connections in either or both HVc and RA of adults, effectively increasing the jitter in time delays (represented by the width of the peak) between the increase in RA activity and HVc spikes. Consistent with the increased intrinsic

connectivity in adults is the emergence of correlated burst firing (represented by side peaks) between HVc and RA in adults, which was absent in juveniles. Fine tuning of the tight correlation between HVc and RA activity is thus observed as the bird completes song learning, and may result from developmental changes in the temporal dynamics of HVc-RA interaction at the receptor level, and in intrinsic connections in either or both HVc and RA.

The changes in the temporal characteristics of the correlated activity between HVc and RA from 50 days of age to adulthood can not be accounted for by the known anatomical changes in HVc and RA during the same period. The number of HVc synapses in RA does not change from 53 days of age to adulthood (Herrmann and Arnold, 1991), consistent with the lack of change in strength of the HR peaks, but inconsistent with the observed increase in variability (width of HR peaks) of time delays in adults. Moreover, the number of RA projecting neurons added in HVc is higher in juveniles than adults (Nordeen and Nordeen, 1988), implying that the strength and jitter of time delays of HR peaks would decrease as the bird completed song learning; however, this is different from what we observed. Similarly, RA at approximately 45-50 days of age has the most intrinsic interconnections compared to RA at 20 days of age and in adulthood (Herrmann and Arnold, 1991; Kittelberger and Mooney, 1999). However, this is inconsistent with the significantly smaller jitter in time delays of HR peaks in juveniles than adults. Thus, the discrepancy between anatomical changes and changes in neural interaction between HVc and RA indicate that these changes are functional rather than structural changes. Moreover, as discussed above, these changes may be occurring at the level of synapses, i.e. they may represent changes in strength of the synapses involved in intrinsic connectivity.

Functional connectivity of the song system during development

The significant correlation of activity between indirectly connected nuclei that is due to common input in the song system of juveniles strongly suggests that, as in the adults, there is an extensive divergence and re-convergence of connections between nuclei, and

robust intrinsic connectivity within some nuclei (Fig. 4-15a). The locations of pairs of LMAN-RA recording sites relative to the topographical projections from LMAN to RA do not seem to have an effect on the strengths and temporal characteristics of the LMAN-RA correlated activity. This suggests that the intrinsic connectivity within LMAN and RA allows activity within each nucleus to be strongly correlated so that the anatomical location is not a primary factor in shaping the correlation between LMAN and RA activity. The broad divergent and re-convergent connectivity between song nuclei would further enable the correlation of activity of song nuclei across the entire circuit. This suggests that, as in the adults, information within the song system of juveniles is processed by a highly interconnected network of neurons.

As in adults, the functional connectivity of the song system in juveniles appears to have different states, as evinced by the different types of LMAN-RA coherency functions. These LMAN-RA coherency function types corresponded well with the different types of HVc-LMAN coherency functions, in the same manner as observed in adults. As was observed in the adults, the variable state of the functional connectivity in juveniles seems unlikely to be due to the overall arousal state of the animal since all HVc-RA coherency functions consistently exhibited a tall narrow peak regardless of the type of corresponding LMAN-RA and HVc-LMAN coherency functions. Moreover, all the sites included in the analysis responded to auditory stimuli. This suggests that to some extent, the data were sampled from birds at relatively the same level of arousal, since auditory responsiveness in RA and HVc have been shown to be sensitive to the bird's wakefulness (Vicario and Yohay, 1993; Dave et al, 1998). The separation and significance of the two LMAN-RA coherency peaks, which is mostly due to the variability in strength and time delay of the peak with a negative time delay, seems to depend on the timing and strength of HVc-LMAN correlated activity. This is consistent with the idea that the peak with a negative time delay is due to the common input of HVc to LMAN and RA. Thus, the state of the functional connectivity may

depend on the neural interactions within the anterior forebrain pathway (from HVc to LMAN).

In summary, the functional connectivity of the song system in juveniles, as in adults, involves broad divergence and re-convergence of connections between nuclei, and extensive intrinsic connections within song nuclei. This suggests that the basic structure of the functional connectivity is already established at 50 days of age. However, developmental changes in the neural interaction between LMAN and RA, and HVc and RA indicate fine tuning of the functional connectivity as song learning is completed. The changes in correlated activity between LMAN and RA, which are mirrored by stimulus playback of the bird's own song in juveniles, are likely neural substrates for song learning. It remains to be demonstrated whether disrupted correlated activity between LMAN and RA will interrupt song learning, and whether the functional connectivity of the song system will be abnormal in birds that did not learn their songs properly.

Figure 4-1. a) Time line of song learning in zebra finches. b) Schematic of the anatomy of the song system. HVc, RA, nXIIts and respiratory nuclei, shown in black, make up part of the descending motor pathway for song, while Area X, DLM, and LMAN, shown as open symbols, form the anterior forebrain pathway (AFP). c) Quantification of amplitude, width and time delay of coherency peaks. The actual data, which are peaks from a coherency function of RA activity relative to LMAN spikes, are shown in blue, while the fit of the central portion (-100 to +100 msec) of the data with two Gaussian functions is shown by the green curve. The ±JN curves (in red) indicate the ±3X the square root of the Jacknife variance (see Methods), which provide thresholds for significance of a peak. The amplitude, time delay, and width of the coherency peaks were measured from the Gaussian function fit. The width of the peak is measured as the half-width at 61% amplitude height ($amplitude * e^{-1/2}$). The peak strength is equivalent to the *amplitude*, while the overall strength of the correlation is quantified as the area under the curve, calculated as $amplitude * width$. The same fitting procedure was applied to the cross-covariance functions. In addition, the outside region (all the data except the central region) of the cross-covariance function was fit with one Gaussian function.

Figure 4-1

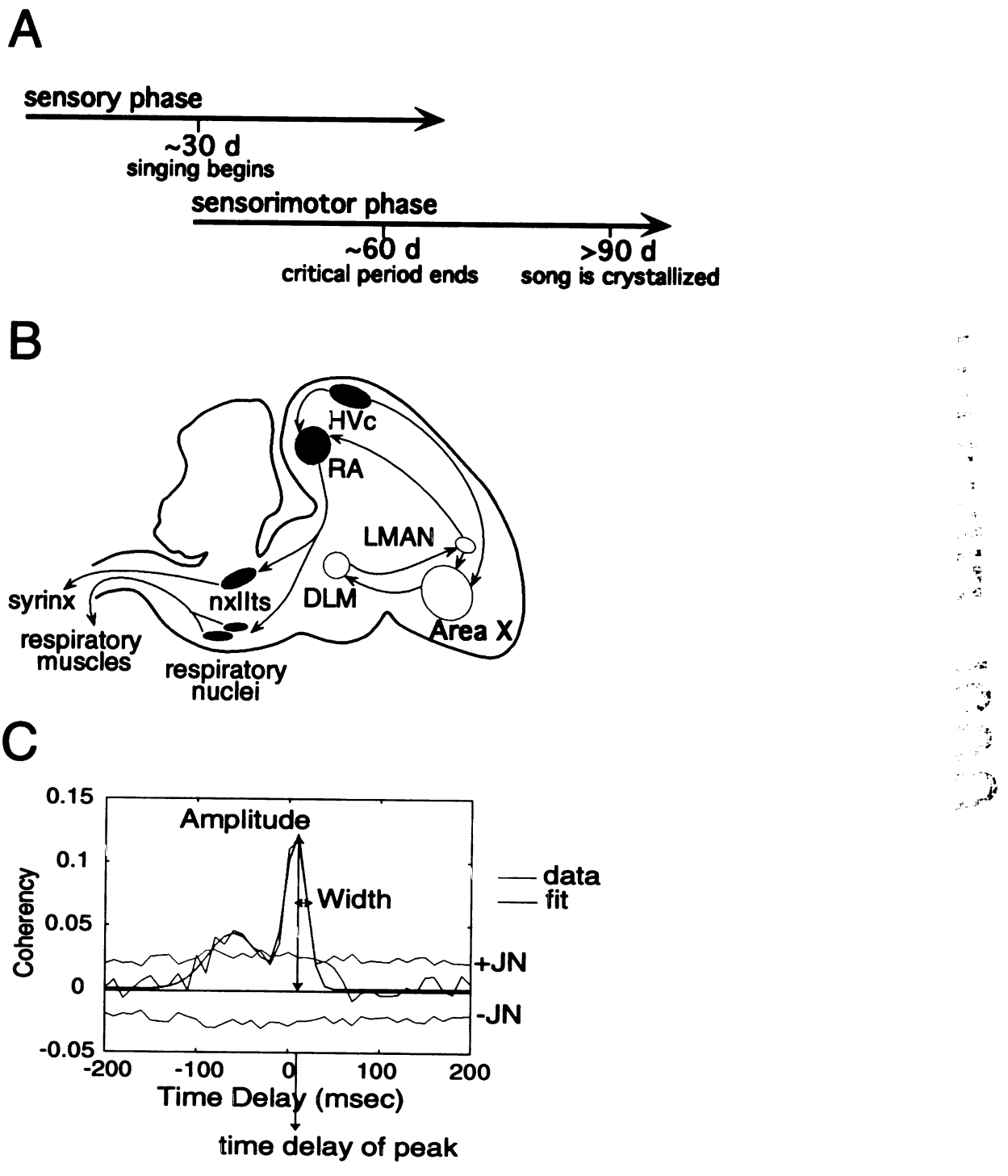
A
sensory phase
~30 d
singing begins
sensorimotor phase
~60 d
critical period ends
>90 d
song is crystallized
B
HVc
RA
LMAN
DLM
nXIIts
syrinx
respiratory muscles
respiratory nuclei
Area X
C
Amplitude
Width
data
fit
+JN
-JN
Coherency
0.15
0.1
0.05
0
-0.05
-200
-100
0
100
200
Time Delay (msec)
time delay of peak

Figure 4-2. Song and order selectivity of *juvenile* LMAN and RA clusters of neurons. In all graphs, the sites with -0.5<d'<+0.5 values (within the $\pm$0.5 boundaries) were considered non-selective for either stimulus. a) The cumulative distribution plot of $d'_{BOS-TUT}$ (circles, n=25 sites) and $d'_{BOS-CONS}$ (squares, n=27 sites) values for LMAN sites. b) The cumulative distribution plot of $d'_{BOS-TUT}$ (circles, n=25) and $d'_{BOS-CONS}$ (squares, n=27) values for RA sites. c) The cumulative probability distribution of $d'_{BOS-REV}$ (circles, n=28) and d'_{BOS-RO} (squares, n=23) for LMAN sites. d) The cumulative probability distribution of $d'_{BOS-REV}$ (circles, n=26) and d'_{BOS-RO} (squares, n=24) for RA sites.

Figure 4-2

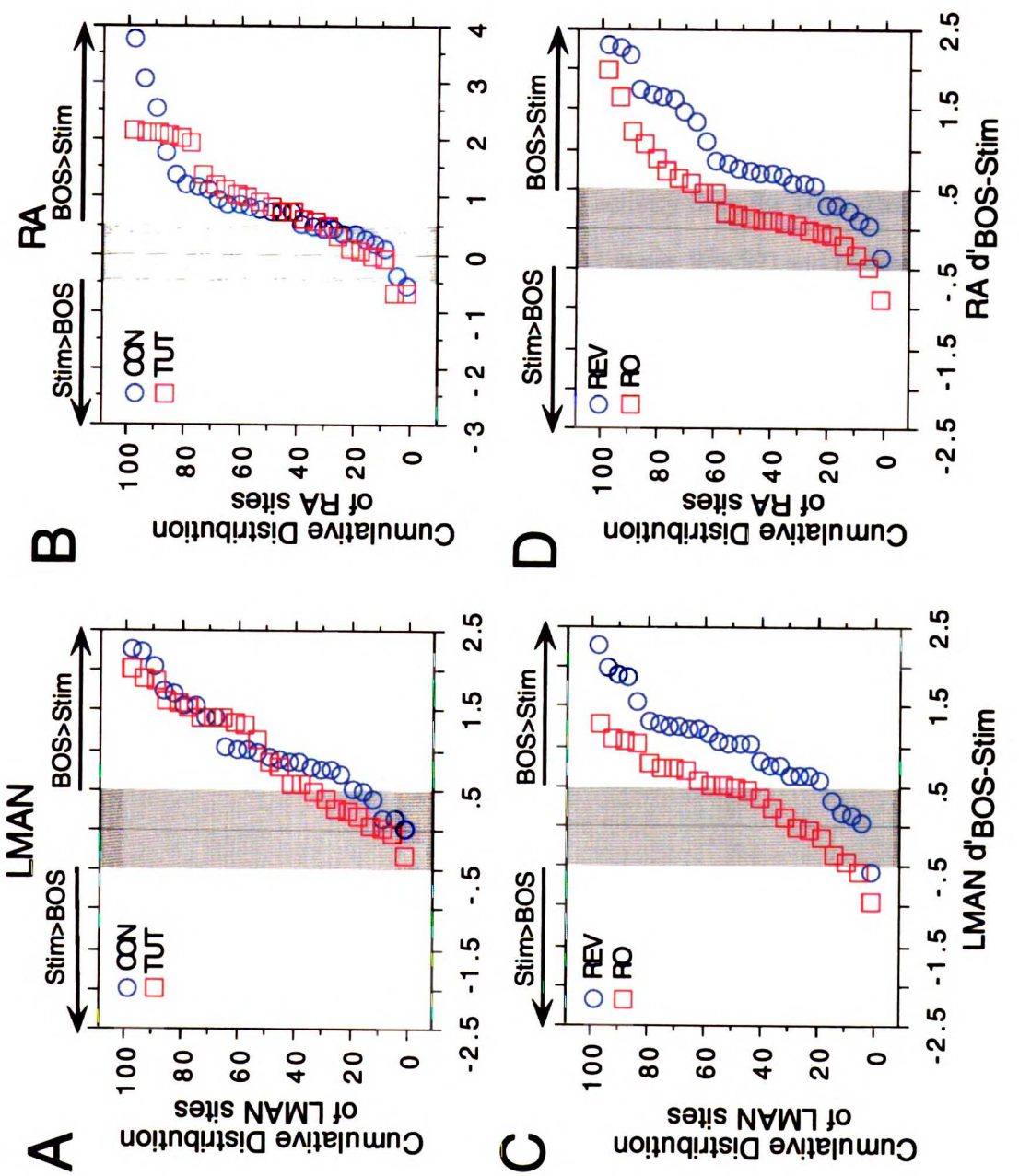
A
LMAN
Stim>BOS
BOS>Stim
CON
TUT
Cumulative Distribution of LMAN sites
-2.5 -1.5 -.5 .5 1.5 2.5
B
RA
Stim>BOS
BOS>Stim
CON
TUT
Cumulative Distribution of RA sites
-3 -2 -1 0 1 2 3 4
C
Stim>BOS
BOS>Stim
REV
RO
Cumulative Distribution of LMAN sites
LMAN d'BOS-Stim
D
Stim>BOS
BOS>Stim
REV
RO
Cumulative Distribution of RA sites
RA d'BOS-Stim

Figure 4-3. Cross-covariance and coherency functions of RA activity relative to LMAN spikes in *juveniles*. The abscissa is the time delay relative to LMAN spikes at time delay = 0. Thus, RA activity follows LMAN spikes for time delays >0 (LMAN -> RA), and RA activity precedes LMAN spikes at time delays < 0 (RA -> LMAN). The data are illustrated as in Fig. 4-1c. a) An example of a LMAN-RA cross-covariance function in juveniles during spontaneous activity that exhibited a significant wide peak (time delay=-15.30 msec, width=344.47 msec, goodness of fit R^2=.96). The narrow peaks were not significant. b) The LMAN-RA cross-covariance function during evoked activity from the same sites as in (a) exhibited wide (time delay=47.23 msec, width=605.11 msec, R^2=.87) and narrow peaks (time delays: -60.44 and 10 msec, and widths: 27.40 and 8.25 msec). Note that in both (a) and (b), the narrow peaks overlapped with the wide peaks c) An example of a LMAN-RA coherency function in juveniles during spontaneous activity that exhibited only narrow peaks (wide peak, R^2=.53). The narrow peaks had time delays of -79.30 and 5.81 msec, and corresponding widths of 34.55 and 45.93 msec. d) LMAN-RA coherency function during evoked activity from the same LMAN and RA sites as in (c) also showed only narrow peaks (wide peak, R^2=.19). The narrow peaks had time delays of -60.46 and 10.00 msec, and corresponding widths of 29.22 and 7.49 msec.

Figure 4-3

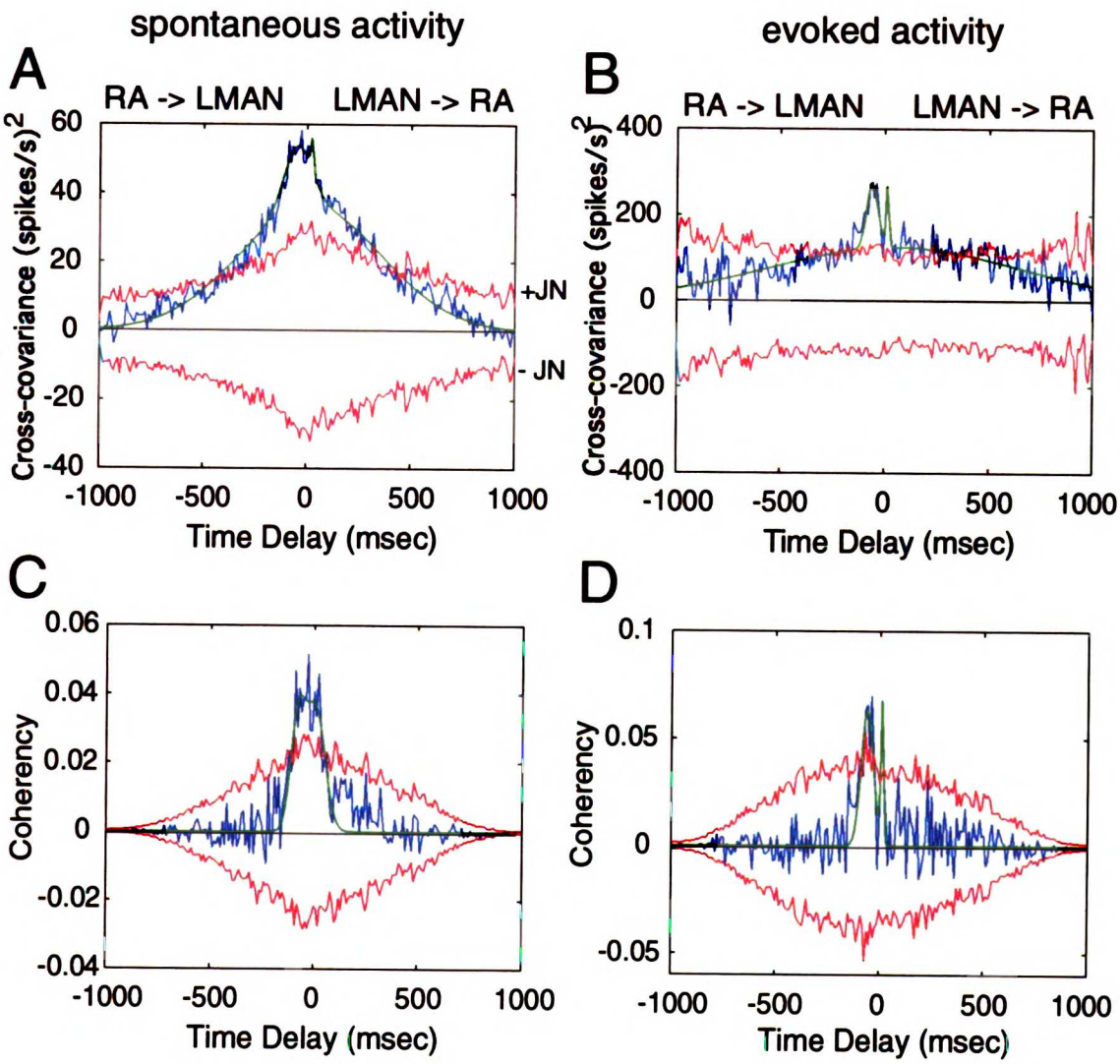

Figure 4-4. Types of coherency functions of RA activity relative to LMAN spikes observed in *juveniles* during spontaneous activity. LMAN spikes occurred at time delay = 0. The panels in the left column are examples of individual data of each type, while the panels on the right column are group data. The individual data are represented as in Fig. 4-1c. For the group data, the mean is represented by the blue curve, while the mean + standard deviation (SD) and mean-SD are represented by the red curve and green curves, respectively. a) LMAN-RA coherency functions with two well-separated peaks. The individual data peak shown had time delays of -55.96 and 12.68 msec, and corresponding widths of 26.35 and 13.01 msec. b) LMAN-RA coherency functions with 2 peaks that are not separable (left column, upper panel) and/or one of the two peaks was not significant. The upper panel on the left is an example where the two peaks were not well-separated. The peaks had time delays of -49.69 and 2.26 msec, and corresponding widths of 75.11 and 14.76 msec. The lower panel on the left is an example of a LMAN-RA coherency function with two peaks where one peak was not significant. The significant peak had a time delay of 4.91 msec and a width of 15.36 msec. The group data in (b) include both types of coherency functions. c) LMAN-RA coherency functions with a single peak. The individual data peak shown had a time delay of 14.36 msec and width of 23.35 msec.

Figure 4-4

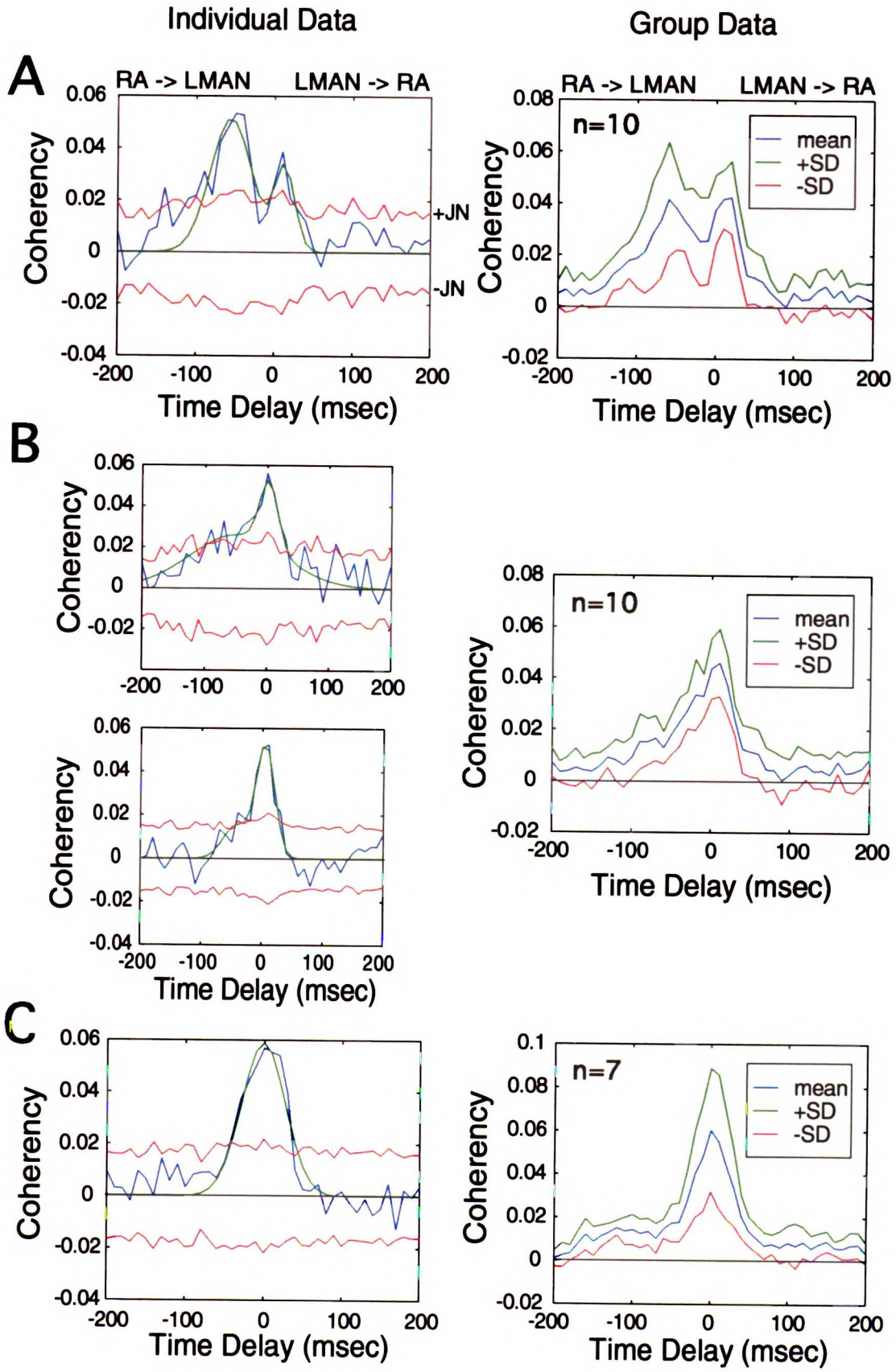
Individual Data
Group Data
A
RA -> LMAN
LMAN -> RA
Coherency
+JN
-JN
Time Delay (msec)
n=10
mean
+SD
-SD
B
C
n=7

Figure 4-5. Types of coherency functions of RA activity relative to LMAN spikes observed in *juveniles* during evoked activity. The data are presented as in Fig. 4-4. a) LMAN-RA coherency functions with two well-separated peaks. The individual data peaks had time delays of -67.91 and 5.00 msec, and corresponding widths of 21.04 and 8.09 msec. b) LMAN-RA coherency functions with 2 peaks that were either not well-separated and/or one of the two peaks was not significant. The upper panel in the left column shows peaks that had time delays of -15.15 and 8.59 msec, and corresponding widths of 10.60 and 18.08 msec. The lower panel on the right shows 2 peaks, but only one peak is significant (time delay=10.00 msec, width=8.43 msec). c) LMAN-RA coherency functions with a single peak. The individual data show a single peak with a time delay of 7.66 msec and a width of 21.00 msec.

Figure 4-5

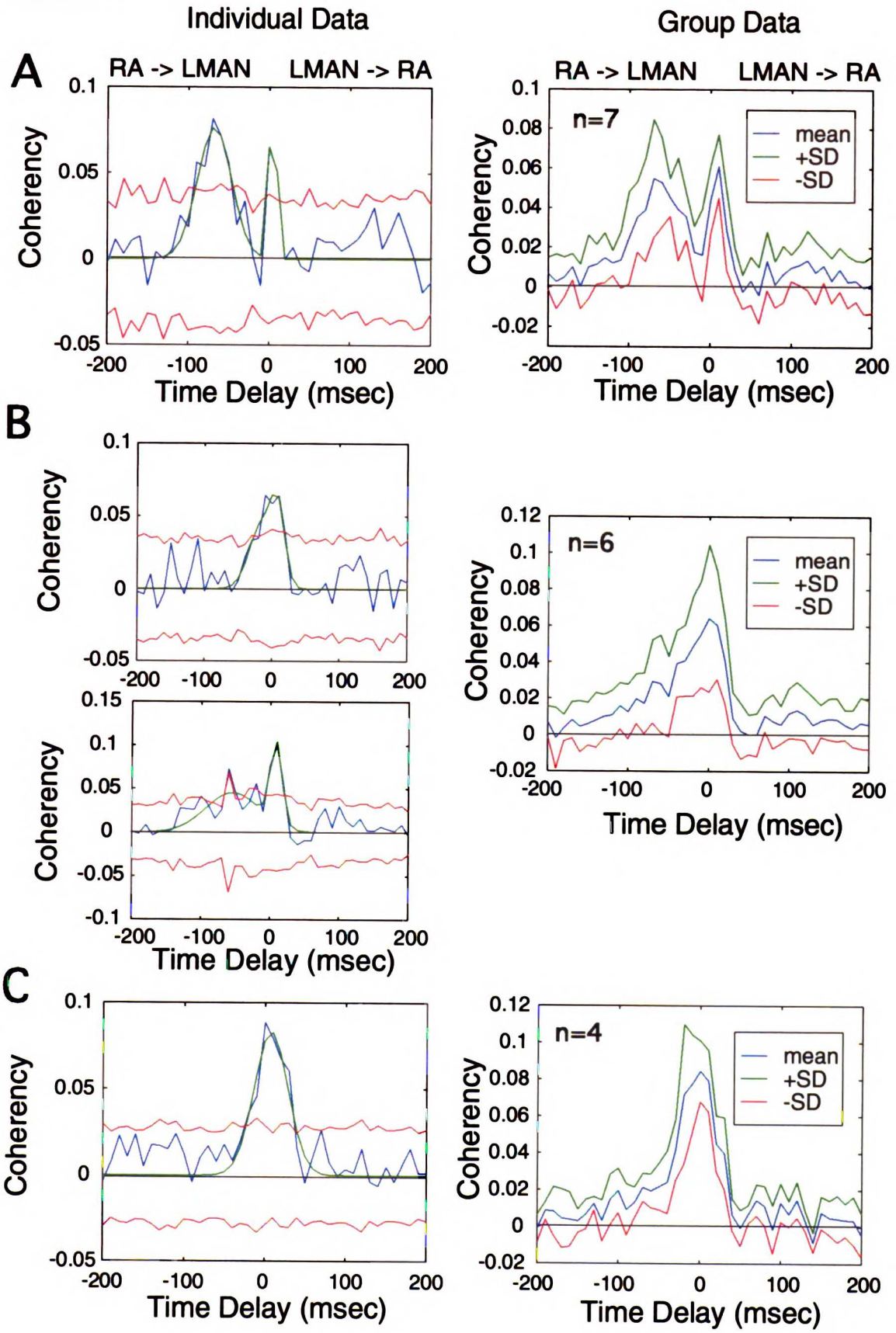
Individual Data
Group Data
A
RA -> LMAN
LMAN -> RA
Coherency
Time Delay (msec)
n=7
mean
+SD
-SD
B
n=6
C
n=4

Figure 4-6. Comparisons between the two well-separated LMAN-RA coherency peaks and the single LMAN-RA coherency peak in *juveniles*. The left column represents data during spontaneous activity, while the right column shows data collected during evoked activity. The following parameters of the two peaks were compared: a) time delay, b) width, c) peak strength and d) overall strength. Individual data points (circles) for each category of peaks are plotted, as well as the mean (black diamond) and standard deviations (error bars) for each category. The peak categories are LR- and LR+: peaks with negative and positive time delays, respectively, observed in LMAN-RA coherency functions with two separable peaks, and LR peaks: single LMAN-RA coherency peaks. The mean$\pm$SD values are given in Table 4-2. *$p<.05$, **$p<.01$, Wilcoxon Signed Rank Test. $^{\#}p<.05$, $^{\#\#}p<.01$, $^{\#\#\#}p<.001$, Mann-Whitney.

Figure 4-6

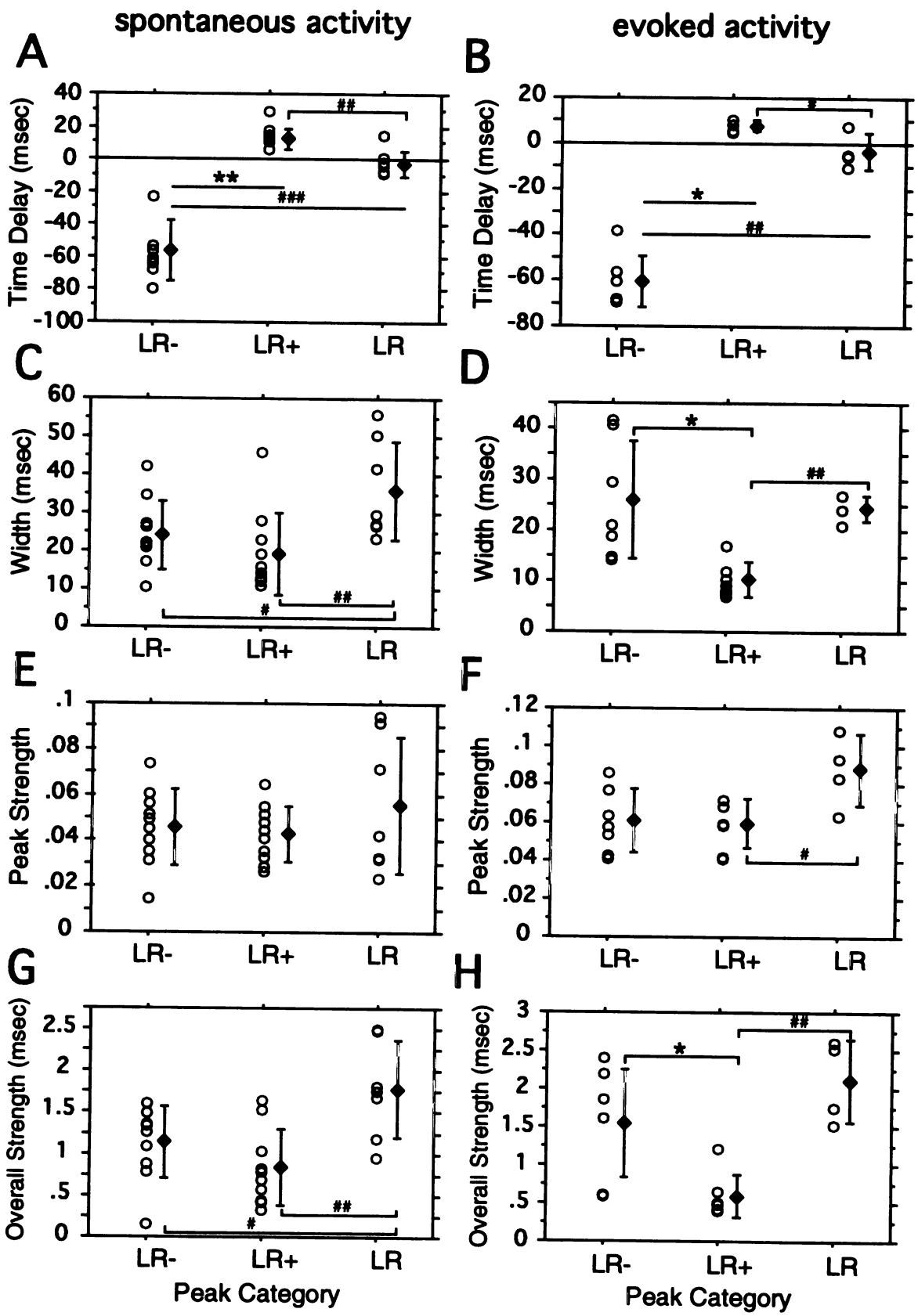
spontaneous activity
evoked activity
A
B
C
D
E
F
G
H
Time Delay (msec)
Width (msec)
Peak Strength
Overall Strength (msec)
LR-
LR+
LR
Peak Category
**
###
##
*
#

Figure 4-7. Coherency between LMAN & RA (left column), HVc & LMAN (middle column) and HVc & RA (right column) activity in *juveniles*. Each row shows corresponding coherency functions derived from the same LMAN, HVc and RA sites. The data are presented as in Fig. 4-1c. a) Coherency function of evoked RA activity relative to LMAN spikes (at time delay = 0) with two separable peaks, LR- (time delay = -69.77 msec) and LR+ (time delay = 10.00 msec). b) Coherency function of evoked LMAN activity relative to HVc spikes at time delay = 0; thus, LMAN firing follows HVc spikes at time delays > 0, and precedes HVc spikes at time delays < 0. This HVc-LMAN coherency function has two peaks, HL- (time delay = -5.00 msec) and HL + (time delay = 60.68 msec). c) Coherency function of evoked RA activity relative to HVc spikes at time delay = 0; RA activity follows HVc spikes at time delays > 0, and preceded HVc spikes at time delays < 0. This HVc-RA coherency function exhibits a central peak with time delay = 10.00 msec. d) LMAN-RA coherency function during evoked activity with 2 non-separable peaks, where one of the two peaks is not significant. The non-significant peak is represented by an overlapping broad peak with a time delay of 25.16 msec, and the time delay of the significant peak is -15.94 msec. e) HVc-LMAN coherency function with one peak during evoked activity (time delay = 31.66). f) HVc-RA coherency function with a central peak at time delay = 8.47 msec during evoked activity. g) LMAN-RA coherency function with no significant peaks during spontaneous activity. h) HVc-LMAN coherency function with no significant peaks during spontaneous activity. i) HVc-RA coherency function with a central peak at time delay = 10.00 msec during spontaneous activity.

Figure 4-7

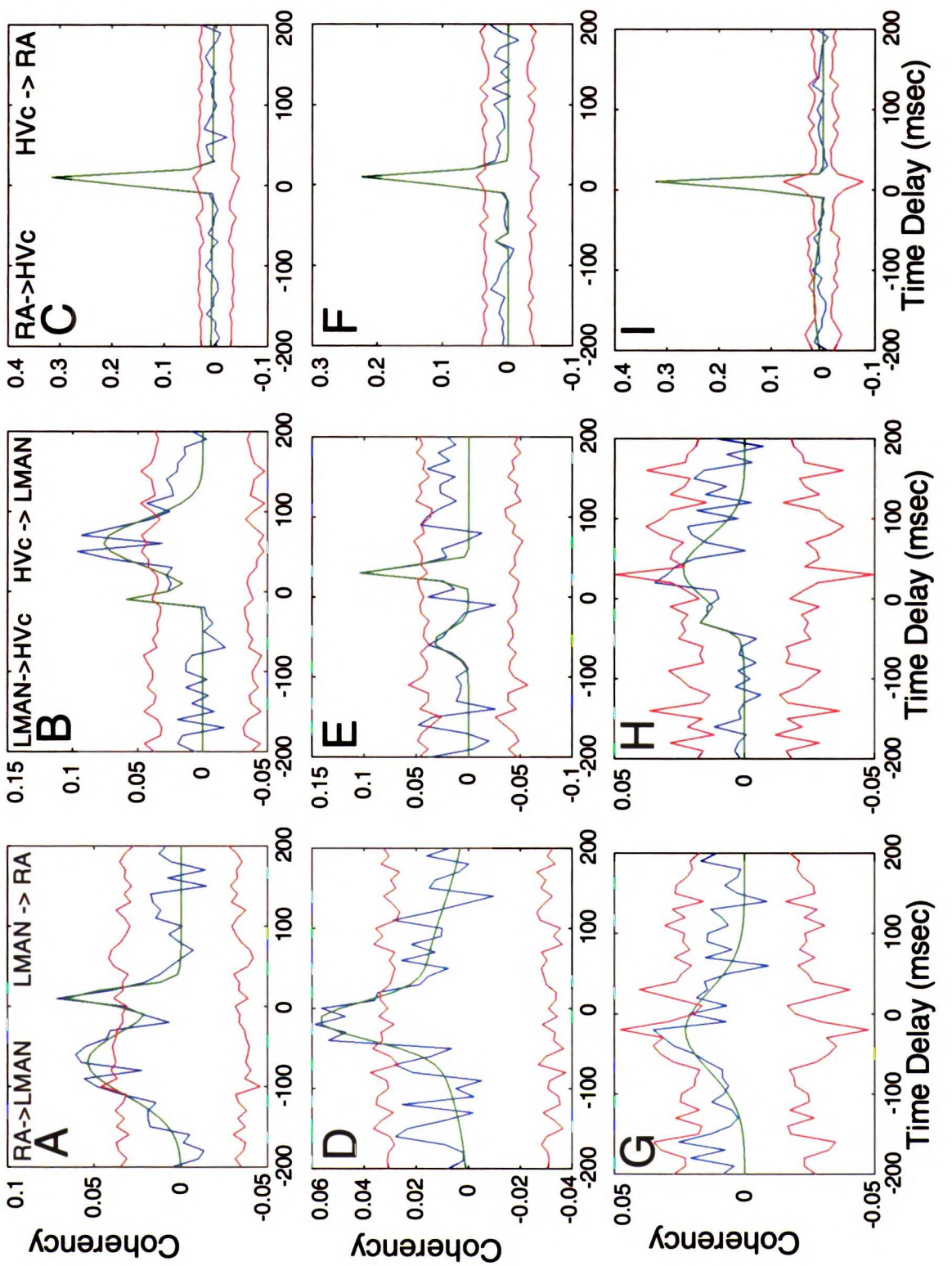
A
RA->LMAN
LMAN -> RA
B
LMAN->HVc
HVc -> LMAN
C
RA->HVc
HVc -> RA
D
E
F
G
H
I
Coherency
Time Delay (msec)

Figure 4-8. LMAN-RA cross-covariance function in *adults*. The data are plotted as in Fig. 4-1c. a) An example of a LMAN-RA cross-covariance function in adults during spontaneous activity that exhibited a wide peak (time delay=-60.23 msec, width=278.42 msec, R^2=0.91). The tall narrow peak has a time delay of 3.04 msec and a width of 4.47 msec. b) An example of a LMAN-RA cross-covariance function during evoked activity from the same LMAN and RA sites as in (a). The cross-covariance function does not exhibit a wide peak (R^2=.19), but shows one significant narrow peak (time delay=0.10 msec and width=8.18 msec).

Figure 4-8

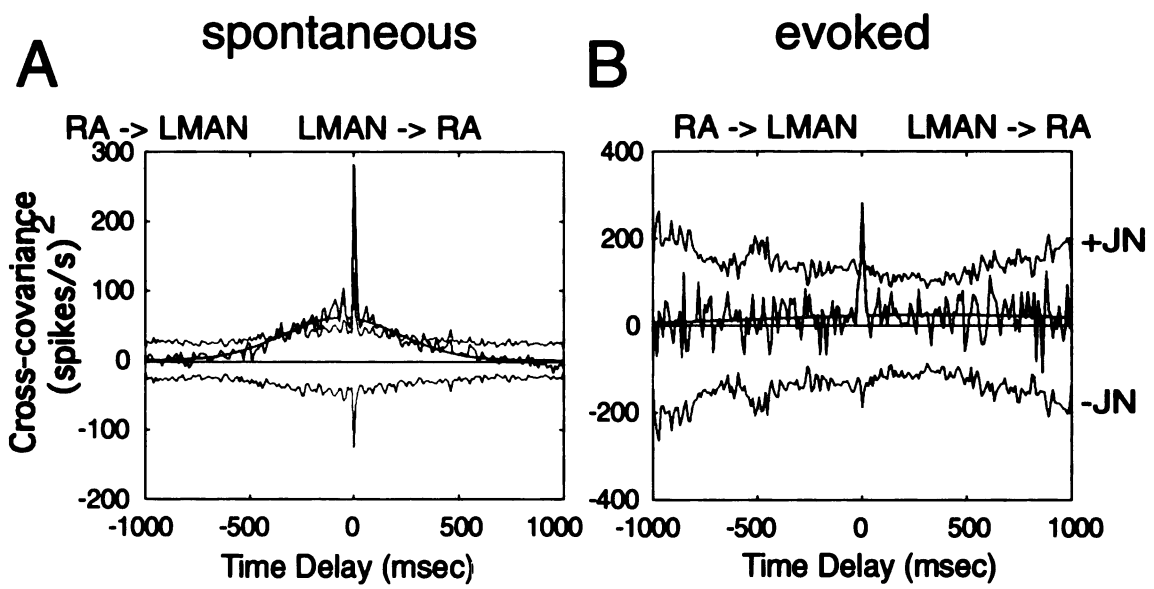
A
spontaneous
RA -> LMAN
LMAN -> RA
Cross-covariance (spikes/s)
300
200
100
0
-100
-200
-1000
-500
0
500
1000
Time Delay (msec)
B
evoked
RA -> LMAN
LMAN -> RA
400
200
0
-200
-400
+JN
-JN
-1000
-500
0
500
1000
Time Delay (msec)

Figure 4-9. Mean of all types of LMAN-RA coherency functions with at least one significant peak in *juveniles* and *adults*. a) The mean LMAN-RA coherency during spontaneous activity (juveniles, n=27; adults, n=29), and b) during evoked activity (juveniles, n=23; adults, n=22), plotted as a function of the time delay relative to LMAN spikes (at time delay = 0). The thick line represents the mean in *juveniles* (J), and the thin line represents the mean in *adults* (A).

Figure 4-9

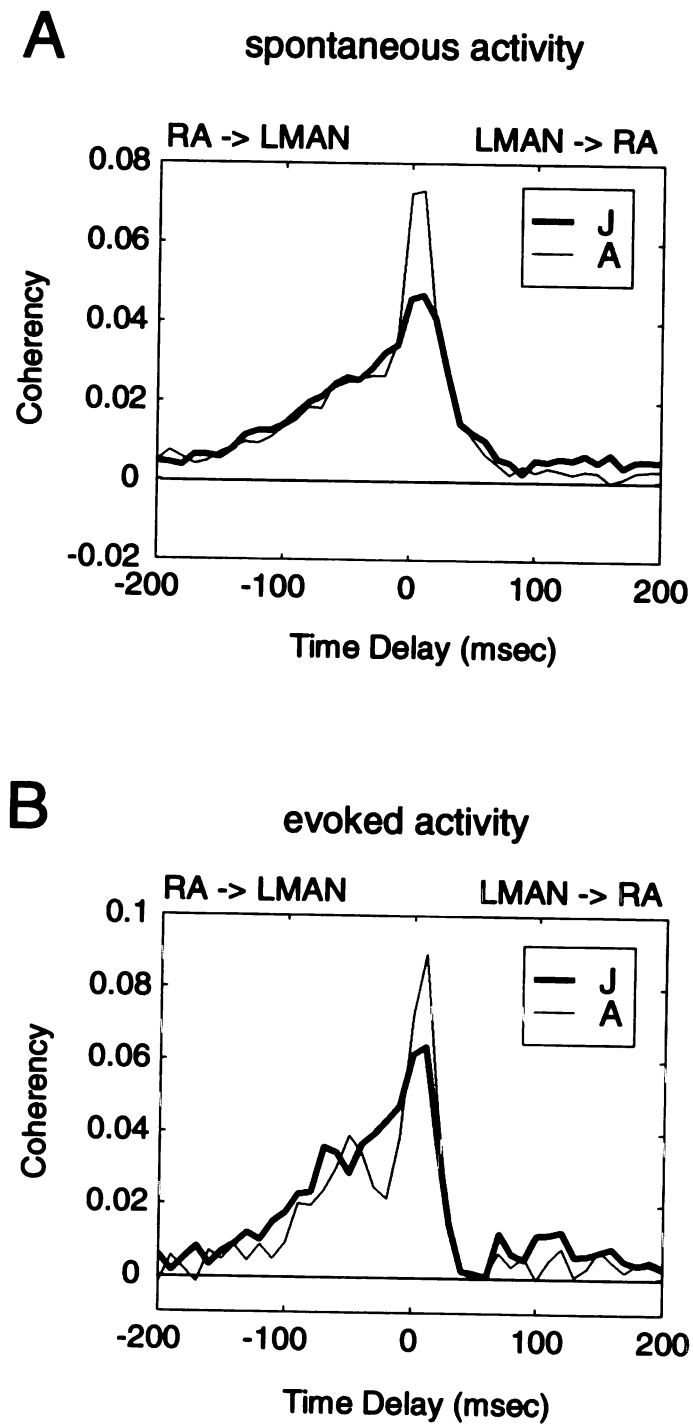
A
spontaneous activity
RA -> LMAN
LMAN -> RA
J
A
Coherency
0.08
0.06
0.04
0.02
0
-0.02
-200
-100
0
100
200
Time Delay (msec)
B
evoked activity
RA -> LMAN
LMAN -> RA
J
A
Coherency
0.1
0.08
0.06
0.04
0.02
0
-200
-100
0
100
200
Time Delay (msec)

Figure 4-10. LMAN-RA coherency functions with 2 well-separated peaks in *juveniles* and *adults*. The data are illustrated as in Fig. 4-1c. a) LMAN-RA coherency function of a LMAN-RA recording site pair from *juveniles* during spontaneous activity (time delays=-68.11, 12.24 msec; respective widths=21.89, 11.02 msec), and b) evoked activity (time delays=-69.30, 10 msec; corresponding widths=18.75, 6.73 msec). c) LMAN-RA coherency function from *adult* LMAN-RA sites during spontaneous activity (time delays=-60.69, 8.10 msec; respective widths=29.62, 11.25 msec), and d) evoked activity (time delays=-61.92, 10.00 msec; respective widths=23.23, 6.07 msec). e) The mean of all LMAN-RA coherency functions with two well-separated peaks during spontaneous activity, in *juveniles* (J, thick line; n=10) and *adults* (A, thin line; n=15). f) The mean of all LMAN-RA coherency functions with two well-separated peaks during evoked activity, in *juveniles* (J, thick line; n=7) and in*adults* (A, thin line; n=13).

Figure 4-10

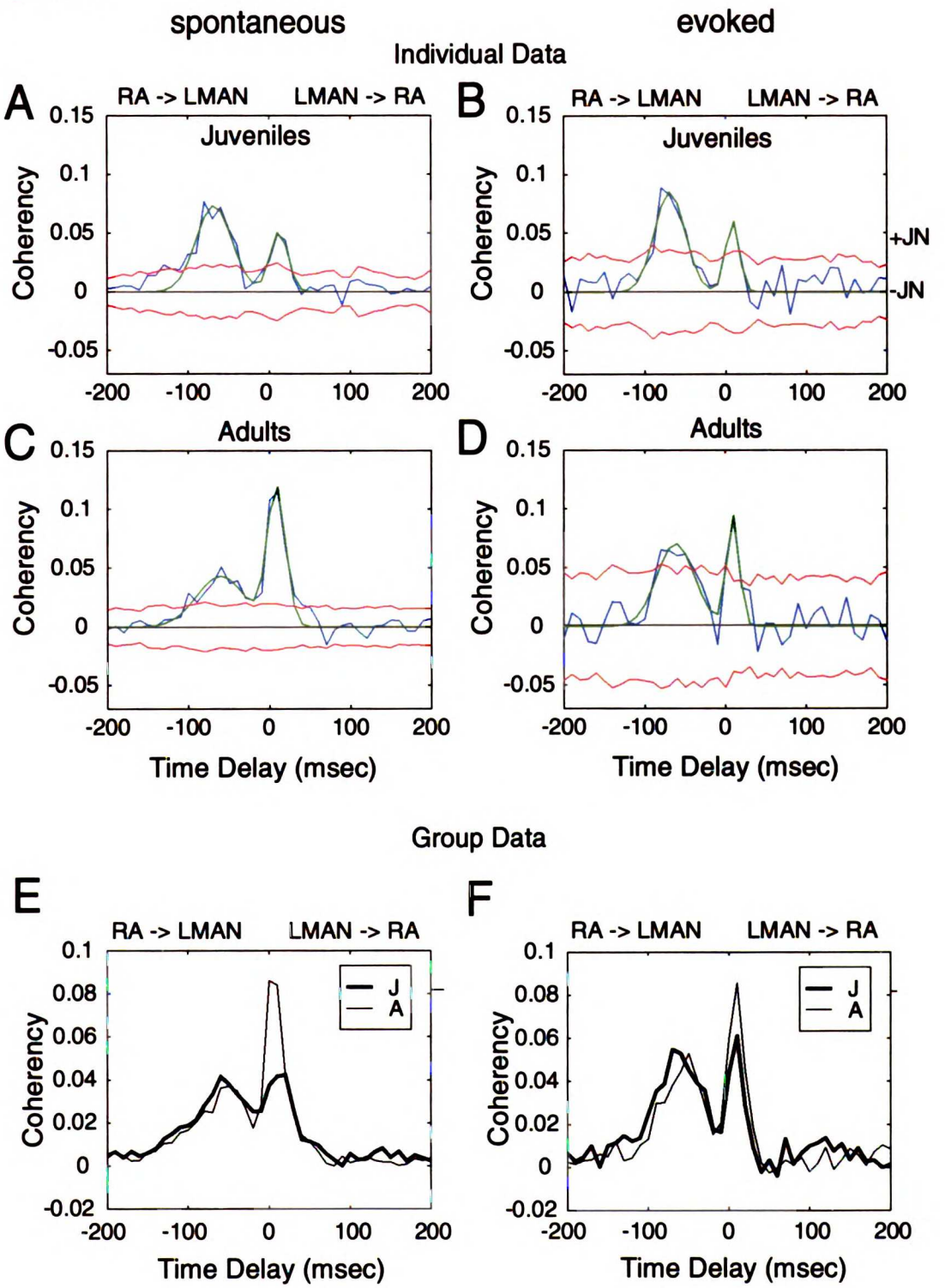
spontaneous
evoked
Individual Data
A
RA -> LMAN
LMAN -> RA
Juveniles
B
RA -> LMAN
LMAN -> RA
Juveniles
+JN
-JN
C
Adults
D
Adults
Coherency
0.15
0.1
0.05
0
-0.05
-200
-100
0
100
200
Time Delay (msec)
Group Data
E
RA -> LMAN
LMAN -> RA
J
A
F
RA -> LMAN
LMAN -> RA
J
A
Coherency
0.1
0.08
0.06
0.04
0.02
0
-0.02
Time Delay (msec)

Figure 4-11. Comparison of time delays and widths of the two well-separated LMAN-RA coherency peaks between *juveniles* and *adults*. a) Distribution of time delays in juveniles (gray bars) and in adults (open bars) during spontaneous and b) evoked activity. Black arrows indicate mean time delays for juveniles (see Table 4-2) and open arrows indicate the mean time delays for adults (see Table 4-3). Note that the -65 to -70 bin in the spontaneous activity plot and the -55 to -60 bin in the evoked activity plot represent complete overlaps of the juvenile and adult distributions. c) Widths of the two well separated peaks obtained during spontaneous and d) evoked activity from juveniles (circles) and adults (squares) plotted by category with the mean (black diamonds) and standard deviation (error bars) for each category . The peak categories are: J,LR- = peaks with negative time delays (LR-) from juveniles (J), A,LR- = peaks with negative time delays from adults (A), J,LR+ = peaks with positive time delays (LR+) from juveniles, and A,LR+= peaks with positive time delays from adults. *p<.05, **p<.01, Wilcoxon Signed Rank Test.

Figure 4-11

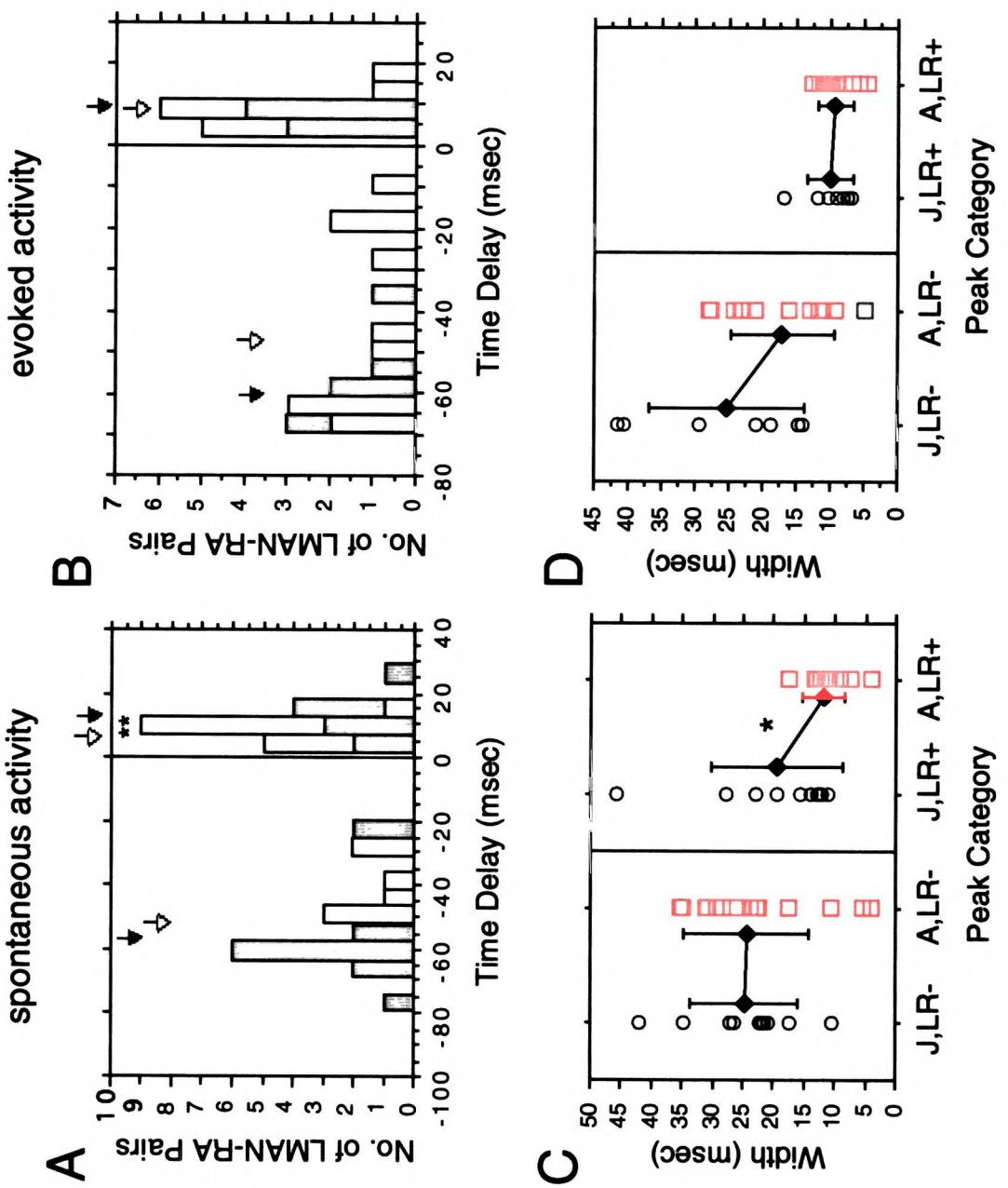
A
spontaneous activity
No. of LMAN-RA Pairs
Time Delay (msec)
B
evoked activity
No. of LMAN-RA Pairs
Time Delay (msec)
C
Width (msec)
J,LR-
A,LR-
J,LR+
A,LR+
Peak Category
D
Width (msec)
J,LR-
A,LR-
J,LR+
A,LR+
Peak Category

Figure 4-12. Comparison of peak and overall strengths of the two well-separated LMAN-RA coherency peaks between *juveniles* and *adults*. a) Peak strength during spontaneous activity and b) evoked activity from juveniles (circles) and adults (squares) are plotted by categories with the mean (black diamonds) and standard deviation (error bars) for each category (see Tables 4-2 and 4-3). The peak categories are as in Figure 4-10. c) Overall strength during spontaneous and d) evoked activity. The overall strength is plotted as in (a) and (b), and the peak categories are as in Figure4-10. *$p<.05$, **$p<.01$, Wilcoxon Signed Rank Test.

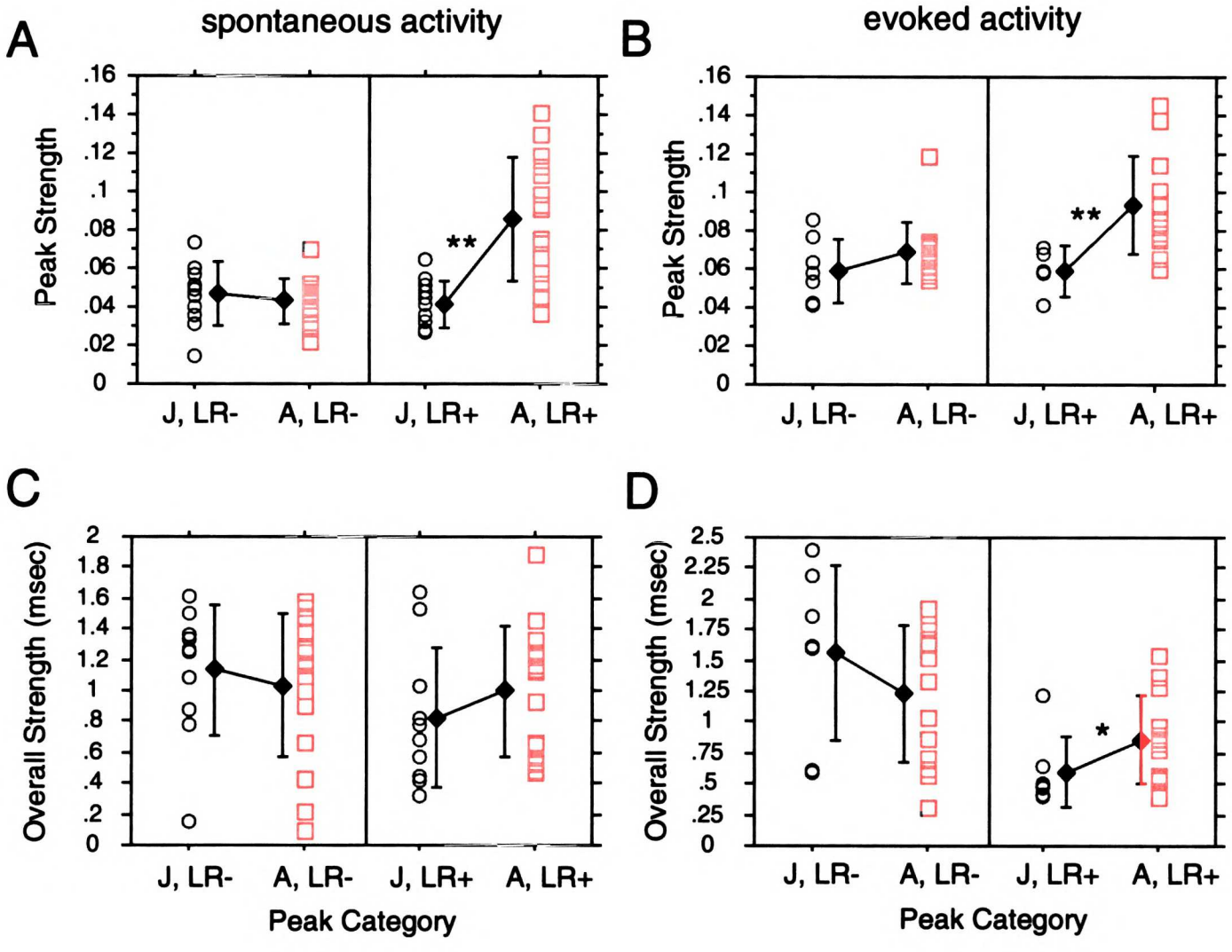
A
spontaneous activity
B
evoked activity
Peak Strength
.16
.14
.12
.1
.08
.06
.04
.02
0
**
J, LR-
A, LR-
J, LR+
A, LR+
C
D
Overall Strength (msec)
2
1.8
1.6
1.4
1.2
1
.8
.6
.4
.2
0
2.5
2.25
2
1.75
1.5
1.25
1
.75
.5
.25
*
Peak Category

Figure 4-12

Figure 4-13. LMAN-RA coherency functions with single peaks from *juveniles* and *adults*. The a) time delay, b) width, c) peak strength and d) overall strength of the LMAN-RA single coherency peaks are plotted by peak category, with the mean (black diamonds) and standard deviation (error bars) for each peak category (see Tables 4-2 and 4-3). The peak categories are: J,S, which are peaks obtained during spontaneous (S) activity in juveniles (J); A,S are peaks obtained during spontaneous activity in adults (A); J,E are peaks obtained during evoked (E) activity in juveniles; and A,E are peaks during evoked activity in adults. *p<.05, Mann-Whitney.

Figure 4-13

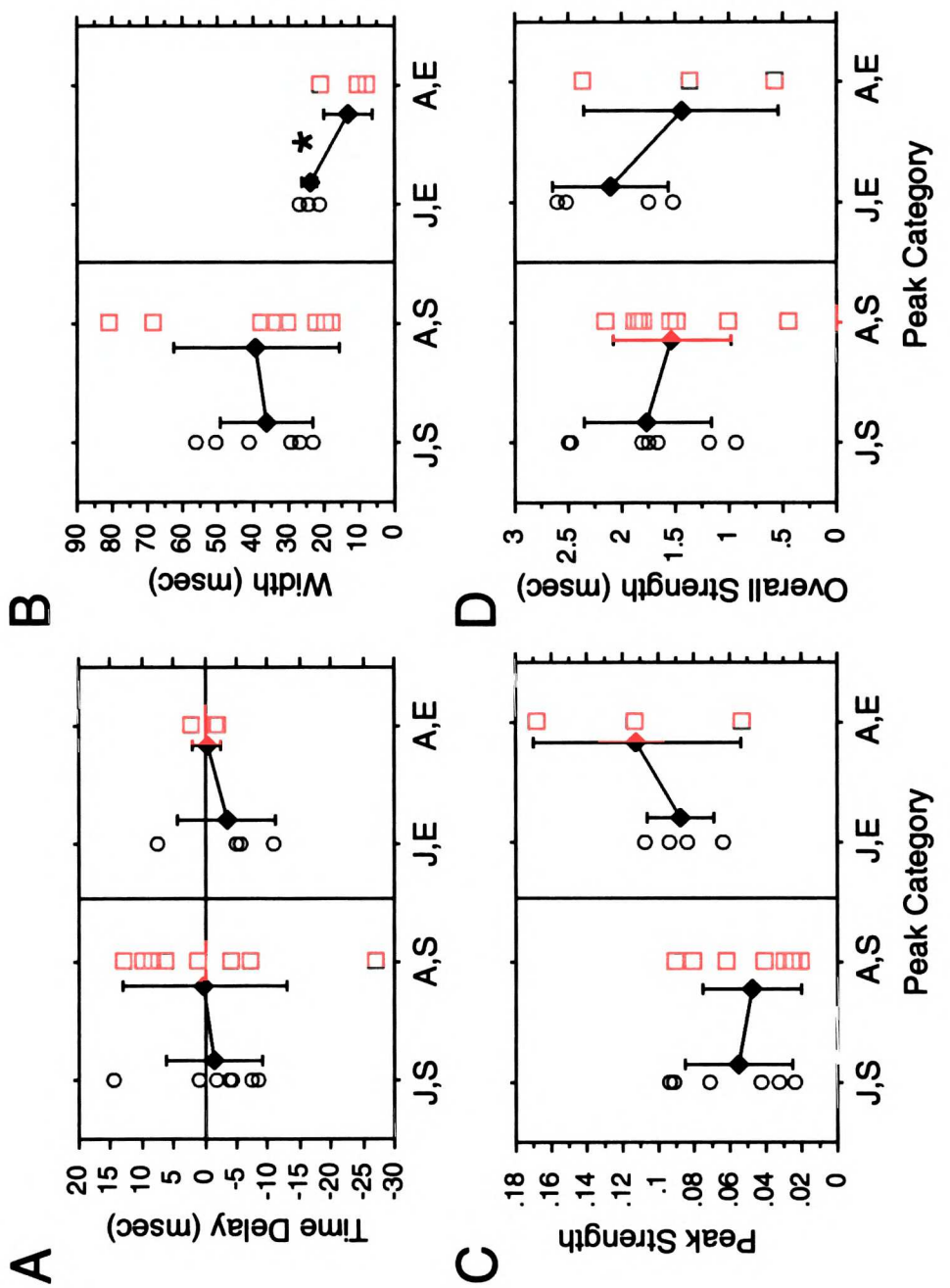
A
Time Delay (msec)
20
15
10
5
0
-5
-10
-15
-20
-25
-30
B
Width (msec)
90
80
70
60
50
40
30
20
10
0
*
C
Peak Strength
.18
.16
.14
.12
.1
.08
.06
.04
.02
0
D
Overall Strength (msec)
3
2.5
2
1.5
1
.5
0
J,S
A,S
J,E
A,E
Peak Category

Figure 4-14. HVc-LMAN coherency functions in *juveniles* and *adults*. The data from HVc-LMAN peaks of coherency functions that exhibited two peaks are shown in squares, while the data from HVc-LMAN peaks of coherency functions that showed a single peak are represented by the circles. The left half of each panel are data obtained during spontaneous activity, while the right half are data from evoked activity. The a) time delay, b) width, c) peak strength, and d) overall strength of HVc-LMAN coherency peaks are plotted for each peak category. The peak categories are: J,HL- are peaks with negative time delays (HL-) from juveniles (J); A,HL- are peaks with negative time delays from adults (A); J,HL+ are peaks with positive time delays (HL+) from juveniles; and A,HL+ are peaks with positive time delays from adults.

Figure 4-14

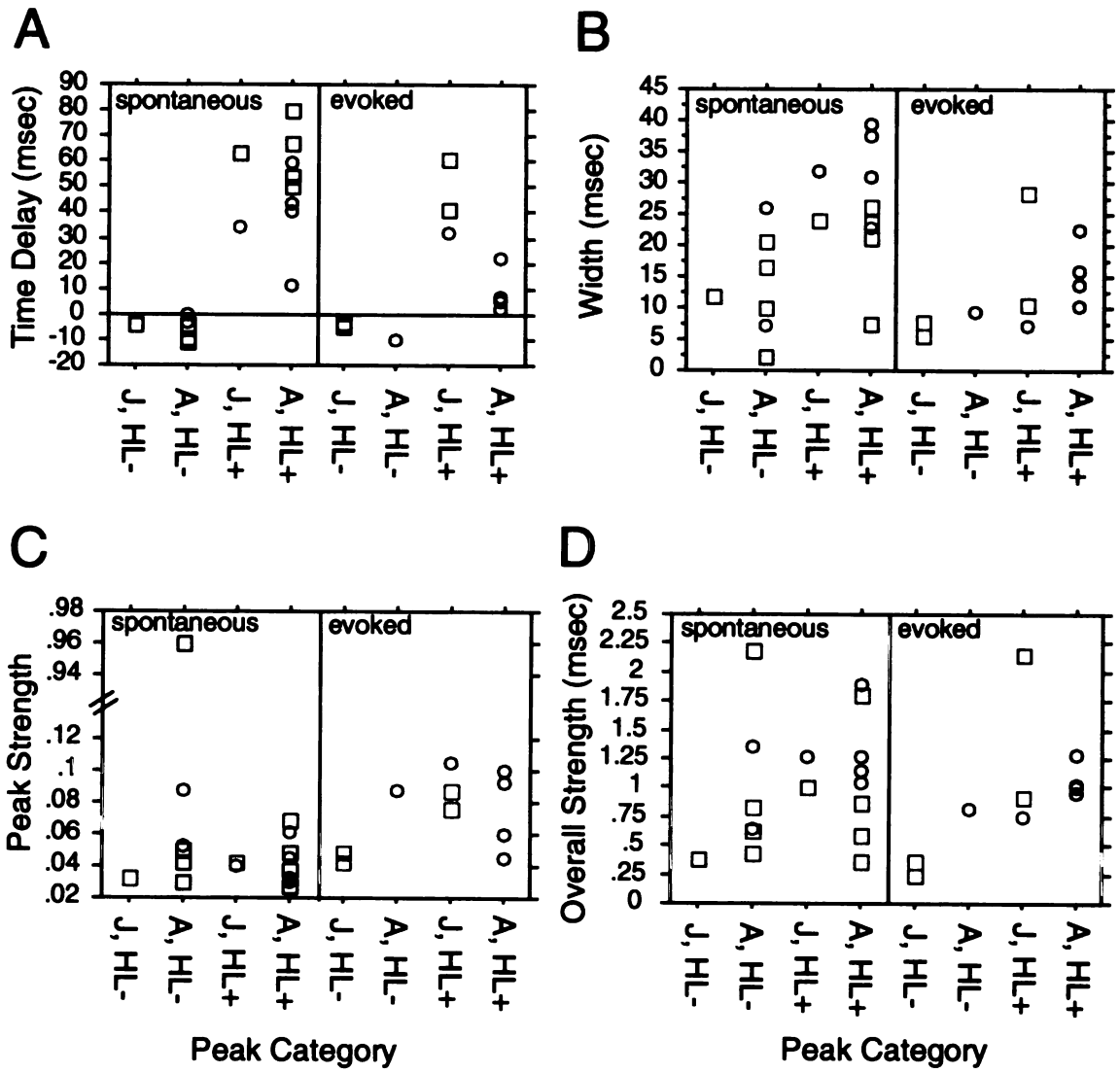
A
B
C
D
spontaneous
evoked
Time Delay (msec)
Width (msec)
Peak Strength
Overall Strength (msec)
J, HL-
A, HL-
J, HL+
A, HL+
Peak Category

Figure 4-15. Comparison of central peaks from *juvenile* and *adult* HVc-RA coherency functions. a) Distribution of time delays of central peaks from juveniles (gray bars) and adults (open bars) during spontaneous and b) evoked activity. Black arrows indicate mean time delays from juveniles (spontaneous: 8.54±2.21 msec; evoked: 8.69±2.17 msec), and open arrows indicate means from adults (spontaneous: 4.34±2.47 msec; evoked: 5.04±2.34 msec). The c) width, d) peak strength , and e) overall strength of the central peaks are plotted by peak categories with the mean (black diamonds) and standard deviation (error bars) for each category. The peak categories are as in Figure 4-12 (J = juveniles, A = adults, S = spontaneous activity, E = evoked activity). *$p<.05$, **$p<.01$, Mann-Whitney.

Figure 4-15

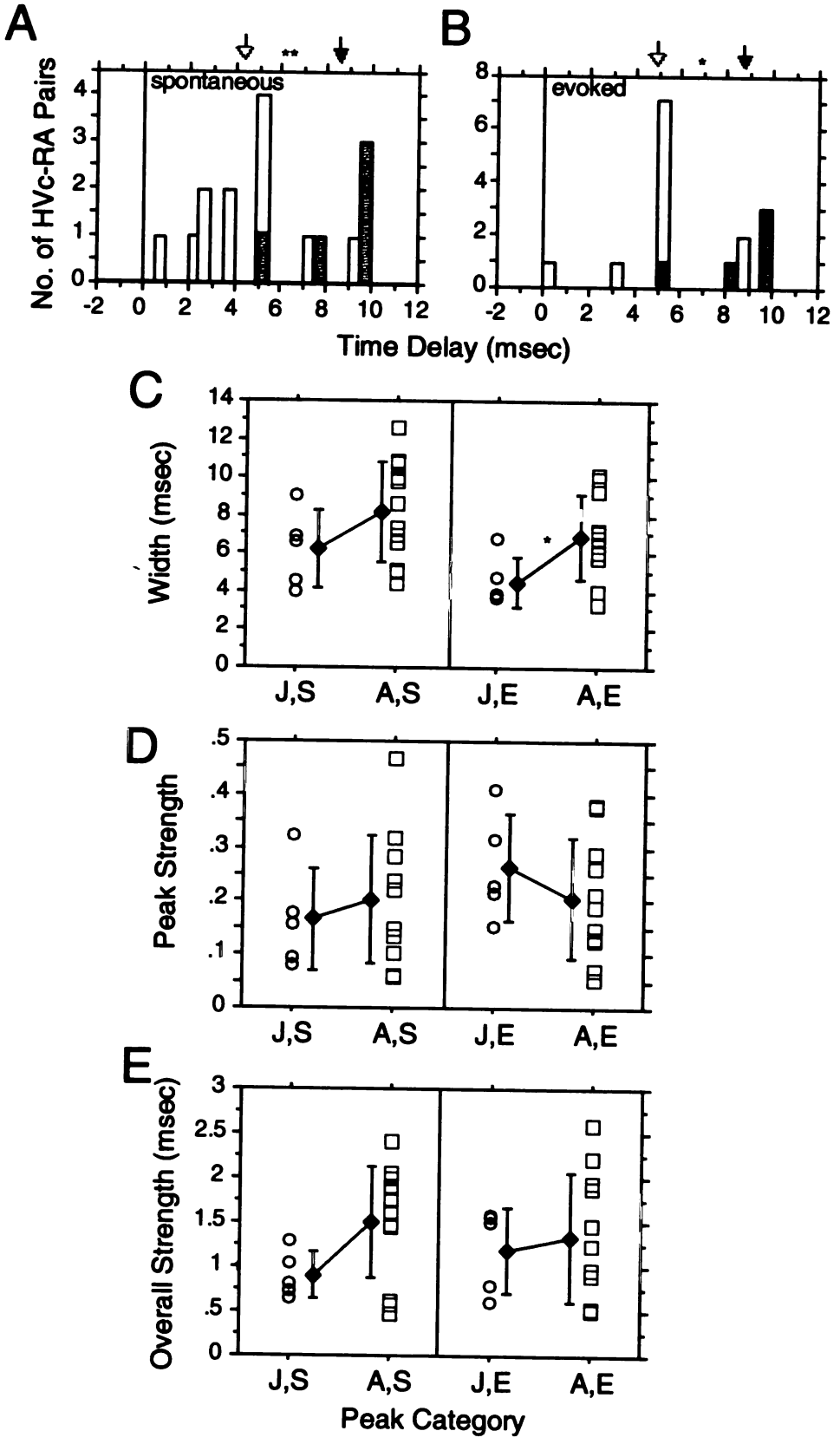
A
B
spontaneous
evoked
No. of HVc-RA Pairs
Time Delay (msec)
C
Width (msec)
D
Peak Strength
E
Overall Strength (msec)
J,S
A,S
J,E
A,E
Peak Category

Table 4-1. Percent of total LMAN-RA pairs for each type of LMAN-RA coherency function

Type LMAN-RA Coherency Function	Juveniles; Spontaneous Activity	Adults; Spontaneous Activity	Juveniles; Evoked Activity	Adults; Evoked Activity
2 well-separated narrow peaks	30% (10/33)	37.5% (15/40)	21% (7/33)	32.5% (13/40)
2 narrow peaks: not well separated and/or one is not significant	30% (10/33)	15% (6/40)	36% (12/33)	15% (6/40)
one narrow peak	21% (7/33)	20% (8/40)	12% (4/33)	7.5% (3/40)
no peaks	19% (6/33)	27.5% (11/40)	31% (10/33)	45% (18/40)

Table 4-2. Juveniles and Adults: LMAN-RA coherency peaks from coherency functions with two well-separated peaks or a single peak

	S,LR-	S,LR+	E,LR-	E,LR+	S,LR	E,LR
Juveniles (45-53 d)	(n=10)	(n=10)	(n=7)	(n=7)	(n=7)	(n=4)
Time Delay (msec)	-55.12±18.27 [a]	13.50±6.47 [a,e,h]	-60.28±11.11 [b]	7.71±2.43 [b,e]	-1.51±7.73	-3.49±7.89
Width (msec)	24.43±8.83	19.47±10.75 [f,i]	25.70±11.61 [c]	10.06±3.51 [c,f]	36.38±12.98	24.04±2.42 [m]
Peak Strength	.046±.016	.043±.012 [g,j]	.060±.017	.059±.013 [g,k]	.055±.030	.087±.019
Overall Strength (msec)	1.12±0.43	0.82±0.45	1.55±0.71[d]	0.59±0.29[d,l]	1.76±0.59	2.10±0.54
Adults (>120 d)	(n=15)	(n=15)	(n=13)	(n=13)	(n=8)	(n=3)
Time Delay (msec)	-52.60±11.75	8.21±3.20 [h]	-46.92±20.57	8.75±4.84	0.15±12.97	-0.39±2.23
Width (msec)	23.98±10.25	11.78±3.33 [i]	17.41±7.63	9.22±2.69	39.22±23.38	13.30±6.77 [m]
Peak Strength	.042±.012	.087±.032 [j]	.070±.016	.093±.026 [k]	.047±.027	.112±.058
Overall Strength (msec)	1.02±0.47	0.99±0.42	1.21±0.55	0.86±.36 [l]	1.53±0.55	1.44±.90

Numbers are means ± standard deviation (SD). S, Spontaneous activity; E, Evoked activity; LR-, peaks with negative time delays and LR+, peaks with positive time delays from LMAN-RA coherency functions with 2 well-separated peaks; LR, peaks from LMAN-RA coherency functions with a single peak. For all statistical comparisons: *p<.05, **p<.01

Significant differences between LR- and LR+ peaks in *juveniles* (Wilcoxon Signed Rank Test):

a) S,LR- < S,LR+ time delay**

b) E,LR- < E,LR+ time delay*

c) E,LR- > E,LR+ width*

d) E,LR- > E,LR+ overall strength*

Significant differences between spontaneous and evoked activity in *juveniles* (Mann-Whitney):

e) S,LR+ > E,LR+ time delay**

f) S,LR+ > E,LR+ width**

g) S,LR+ < E,LR+ peak strength*

Significant differences between juveniles and adults (Mann-Whitney):

h) juveniles > adults, S,LR+ time delay**

i) juveniles > adults, S,LR+ width*

j) juveniles < adults, S, LR+ peak strength**

k) juveniles < adults, E,LR+ peak strength**

l) juveniles < adults, E,LR+ overall strength*

m) juveniles > adults, E,LR width*

Table 4-3. HVc-RA central coherency peaks from juveniles and adults.

Coherency Function	Juveniles; Spontaneous Activity (n=5)	Adults; Spontaneous Activity (n=12)	Juveniles; Evoked Activity (n=5)	Adults; Evoked Activity (n=11)
Time Delay (msec)	8.54±2.21[a]	4.34±2.47[a]	8.69±2.17[b]	5.04±2.34[b]
Width (msec)	6.23±2.01	8.34±2.34	4.61±1.31[c]	7.01±2.21[c]
Peak Strength	.166±.096	.200±.120	.265±.100	.206±.112
Overall Strength (msec)	0.90±0.26	1.49±0.62	1.21±0.47	1.35±0.73

Numbers are means ± standard deviation.

The following were significant differences between juveniles and adults during spontaneous (S) and evoked (E) activity (Mann-Whitney: *p<.05, **p<.01):

a) juveniles > adults; S, time delay**

b) juveniles > adults; E, time delay*

c) juvenile < adults; E, width*

Chapter 5:

Song and Order Selectivity of RA Neurons: Developmental Changes and Comparison with LMAN Selectivity

ABSTRACT

Birdsong is a complex learned behavior that requires normal auditory feedback and experience for song learning and maintenance. Consistent with the behavior, neurons that respond to auditory stimuli are prevalent in brain structures that mediate birdsong behavior. These brain structures are organized into two pathways: the motor pathway for song production, and the anterior forebrain pathway (AFP), which is required for song learning and vocal plasticity in adults. The AFP has been thought to provide auditory feedback-based signals via its output nucleus, LMAN, which may guide neural plasticity in the motor pathway. However, very little is known about how the AFP interacts with the motor pathway in an intact animal. In chapters 3 and 4, we showed that the activity between LMAN and its target motor pathway nucleus, RA, is strongly correlated. We also showed that the activity between RA and HVc, the source of afferents for both the AFP and RA, is also robustly correlated. However, it is unclear whether these functional connections are involved in biasing the auditory responses in RA. Comparing the auditory responses in RA, LMAN and HVc may shed light on how these nuclei interact, and on how auditory selectivity relates to birdsong behavior at different stages of learning.

To compare the auditory responses of LMAN and RA, we recorded simultaneously in both nuclei, from juveniles in the middle of song learning (50 days of age) and from adults that had completed song learning. When possible, we also recorded auditory-evoked activity in HVc. In juveniles, RA responses were selective for the bird's own song (BOS), and sensitive to the temporal order of the BOS. This RA selectivity was increased by adulthood, suggesting that BOS selectivity in RA may play a role in song learning. In both juveniles and adults, the selectivity of RA responses was similar in some ways to that of LMAN, and in other ways to that of HVc. This indicates that both LMAN and HVc may influence the activity in RA during song learning, and even when song learning is completed. However, there were also slight differences between LMAN, RA and HVc

INTRODUCTION

Songbirds, like humans, depend critically on normal auditory experience early in life to learn their vocalizations. Song learning begins with the sensory phase, during which the bird listens to and memorizes the tutor song. This is followed by the sensorimotor phase, in which the bird begins to sing. It eventually matches its rambling songs (called plastic songs) to the memorized copy of the tutor song (Immelmann, 1969; Price, 1979). Songbirds that are not exposed to or can not hear a tutor song during the sensory phase of song learning do not produce normal songs (Eales, 1985; Morrison and Nottebohm, 1993). Similarly, normal auditory feedback of the bird's vocalizations during the sensorimotor phase is critical for normal song learning (Konishi, 1965; Price, 1979). Even in adulthood, when the bird has completed song learning and now produces a stable "crystallized" song, normal hearing is still necessary to maintain the crystallized song (Nordeen and Nordeen, 1992; Williams and McKibben, 1992; Woolley and Rubel, 1999; Brainard and Doupe, 2000; Loenardo and Konishi, 2000; Lombardino and Nottebohm, 2000).

A specialized set of nuclei unique to songbirds, known as the song system, mediates song learning and production. One pathway in the song system, a descending motor pathway, is required throughout the bird's life for normal song production (Nottebohm et al, 1976; Simpson and Vicario, 1990). It includes HVc (abbreviation used as a proper name), the robust nucleus of the archistriatum (RA), respiratory nuclei in the brainstem, and the tracheosyringeal portion of the hypoglossal nucleus (nXIIts). Another pathway in the song system, the anterior forebrain pathway (AFP), indirectly connects HVc and RA via three nuclei that make up the AFP: Area X, the medial portion of the dorsolateral nucleus of the thalamus (DLM), and the lateral portion of magnocellular nucleus of the anterior neostriatum (LMAN). The AFP is necessary during song learning, but is not required for normal song production in adults (Bottjer et al, 1984; Sohrabji et al, 1990; Scharff and Nottebohm, 1991; Nordeen and Nordeen, 1993). Recent studies show that in adults, however, LMAN is essential for vocal plasticity. The changes in adult crystallized song that

result from alteration or removal of auditory feedback are largely prevented by lesions in LMAN (Williams and Mehta, 1999; Brainard and Doupe, 2000).

Neurons in the song system respond to acoustic presentation of song (Margoliash, 1983, 1986; Williams and Nottebohm, 1985; Doupe and Konishi, 1991; Vicario and Yohay, 1992; Theunissen and Doupe, 1998), and because auditory experience is required for song learning and maintenance, these responses may be involved in the neural mechanisms that underlie birdsong behavior. The auditory responses in the AFP are of particular interest because of its role during song learning. The AFP has been hypothesized to mediate the auditory feedback that is crucial for song learning (Nordeen and Nordeen, 1992; Doupe, 1993). In particular, LMAN, the output nucleus of the AFP, may send evaluation signals that guide the vocal plasticity in the motor pathway during song learning and maintenance (Brainard and Doupe, 2000). Consistent with this hypothesis, neurons in LMAN are selective for the bird's own song (BOS) in adults and this selectivity emerges during development (Doupe, 1997; Solis and Doupe, 1997).

RA is a candidate site where neural changes during song learning and maintenance may occur. RA neurons not only receive LMAN input but also receive excitatory synapses from HVc (Williams, 1989; Kubota and Saito, 1991; Mooney and Konishi, 1991; Mooney, 1992), providing a site where LMAN and HVc afferents may interact to influence the song output during song learning and maintenance. RA and HVc neurons in adults are also selective for the BOS (Margoliash, 1986; Doupe and Konishi, 1991; Vicario and Yohay, 1993; Theunissen and Doupe, 1998; Mooney, 2000); however, little is known about how much LMAN and HVc contribute to the degree of selectivity in RA. Although RA neurons require HVc activity, and not LMAN, for auditory responsiveness in adults (Doupe and Konishi, 1991; Vicario and Yohay, 1993), LMAN activity still sends signals to RA that affect vocal plasticity in adults (Williams and Mehta, 1999; Brainard and Doupe, 2000). Indeed, LMAN and RA activity is strongly correlated in adults (Chapter 3). Moreover, it is unknown whether RA auditory responses are selective during song learning, and whether

one afferent input dominates in biasing the auditory response properties of RA during song learning. We therefore undertook to study the auditory response properties of RA in juveniles in the middle of song learning, and in adults when song learning is completed, and compared these properties to those of LMAN, and, when available, to those of HVc.

In this chapter, we used in vivo extracellular recordings of the activity of small clusters of units to measure the simultaneous responses of RA, LMAN, and in some cases, HVc, to stimulus playback. The data presented here are from the same neurons described in Chapters 3 and 4. We found that at around 51 days of age, which is near the end of sensory learning and in the middle of sensorimotor learning, RA neurons were selective for the BOS (at this time, plastic songs) over other song types, and were also sensitive to the temporal order of the BOS. There was an increase in BOS and BOS order selectivity in RA as the bird reached adulthood. In both juveniles and adults, RA exhibited auditory response characteristics observed in both LMAN and HVc. There were, however, slight differences in their auditory responses, which revealed different mechanisms by which selectivity of auditory responses may be shaped.

MATERIALS and METHODS

Animals and Song recording. The male juvenile and adult zebra finches used for these experiments were the same animals used for the experiments described in Chapters 3 (adults) and 4 (juveniles). The juveniles were of 51 days old (mean; range, 45-53d; n=15 birds), and the adults were >120 days old (n=15 birds). They were raised as described in chapters 3 and 4. Songs were also recorded as described in Chapters 3 and 4.

Surgery. The surgical procedure applied in preparation for electrophysiology experiments is as described in chapter 3.

Electrophysiology. The stimulus set included the bird's own song (BOS), its tutor song, brothers' songs, adult and juvenile conspecific songs, songs of other species (heterospecific songs: songs of white-crowned sparrows), a broad-band white noise (100 or 300 msec duration), and 300 msec pure tone bursts (1, 2, 3, or 4 kHz). In juveniles, the BOS were plastic songs, and 3-4 versions of the BOS were chosen to provide a roughly complete representation of all syllables sung 0-5 days before the experiment. Also, for the juvenile experiments, the juvenile and brothers' songs were from age-matched birds (45-55 days old). The stimulus set also included versions of the BOS where the entire BOS was reversed in time (reverse BOS), and where only the temporal sequence of the BOS syllables was reversed in time (reverse order BOS). The presentation of auditory stimuli, electrophysiology experiments and histological reconstruction of recording sites are illustrated in chapters 3 and 4.

Data analysis. Multi-unit activity from neuronal sites that exhibited auditory responses and were used for the cross-covariance and coherency analysis (Chapters 3 and 4) were analyzed for this chapter. A neuronal site was defined as auditory when it exhibited a significant increase ($p<.05$, paired students t-test) in firing rate in response to any type of auditory stimulus relative to the spontaneous firing rate during a two second period

immediately before stimulus presentation. The difference in the firing rate during stimulus presentation and during the designated spontaneous activity is the response strength (RS) of a neuronal site.

To quantify the selectivity of a neuronal site for stimulus A over stimulus B, two values were calculated: the d' value and the selectivity index. The d' value is a measure from psychophysics (Green and Swets, 1966; Theunissen and Doupe, 1998) that quantifies the discriminability between two stimuli, and is calculated as:

$$d'_{A-B} = \frac{2(\overline{RS}_A - \overline{RS}_B)}{\sqrt{\sigma_A^2 + \sigma_B^2}}$$

where $\overline{RS}_A$ and $\overline{RS}_B$ are the mean response strengths to stimulus A and B, respectively, and $\sigma^2{}_A$ and $\sigma^2{}_B$ are the variance of $\overline{RS}_A$ and $\overline{RS}_B$, respectively (see also Chapter 3). Thus, the d' measure takes into account not only the difference in RS, but also the variability (measured as the standard deviation, SD) of the responses. It also has the advantage of being less sensitive to the size of the sample, since it considers the SD value instead of the standard error. Neuronal sites with $d'_{A-B}>0.5$ are defined to be selective for stimulus A over B, and those with $d'_{A-B}<-0.5$ selective for stimulus B over A. Sites with $-0.5<d'_{A-B}<0.5$ values are considered not to show a preference between stimuli A and B.

The d' value, however, does not reflect the relative magnitude of the responses. Thus, we calculated the selectivity index (SI):

$$SI = \frac{\overline{RS}_A}{\overline{RS}_A + \overline{RS}_B}$$

Neuronal sites with SI values close to 1 prefer stimulus A over B, while those close to 0 prefer stimulus B over A. Sites with SI values near 0.5 do not show a preference for either stimulus. The SI values, however, become non-linear when negative RS (i.e. inhibitory responses) are involved. All negative RS were therefore set to zero, and so the SI values range from 0 to 1.0. Due to this adjustment, the SI does not represent differences in selectivity between stimuli that did not evoke a response and those that elicited an inhibitory

RESULTS

Song and order selectivity of RA at 50 days of age

We recorded the activity of multiple units (2-5 units; n=27 sites) in RA of male juvenile zebra finches (n=13 birds) at the average age of 51 days (range: 45-53 days). Juvenile birds at this age are near the end of their sensory learning, but in the middle of their sensorimotor phase (Fig. 5-1a). We analyzed RA sites that exhibited an auditory response to at least one stimulus type; that is, the firing rate during stimulus presentation was significantly higher than the spontaneous firing rate during a two second period immediately preceding stimulus presentation ($p<.05$, paired t-test between firing rates during stimulus presentation and spontaneous activity of each trial). To quantify the strength of response to each stimulus type, we calculated the response strength (RS), defined as the difference between the firing rates during stimulus presentation and during spontaneous activity.

Figure 5-2 a-c shows responses by a small cluster of RA neurons (2-5 units) to the BOS, tutor song and adult conspecific song. RA multi-unit sites responded, on average, more strongly to the bird's own song (BOS) than to any other song stimulus (Fig. 5-2d; $p<.001$, tutor song, n=25; $p<.0001$ songs of adult zebra finches, n=26; $p<.01$, brothers' songs, n=17; $p<.001$, songs of juvenile zebra finches, n=27; $p<.001$, songs of other species, n=18; paired student's t-test between BOS and song stimulus at each RA site). The average response strength (RS) to each song stimulus, normalized by the response strength to the BOS, was less than one, indicating that RA's response to other songs is only a fraction of its response to the BOS (Fig. 5-2e).

The stronger response to the BOS was also reflected in the d' measure of selectivity (see Methods). Multiple-unit sites in RA, on average, preferred the BOS over the tutor (TUT) song, with a mean $d'_{BOS-TUT}$ value of $0.86\pm.86$ (n=25; Fig. 5-2f). Similarly, RA neurons preferred the BOS over songs of adult zebra finches (aCON), with a mean of $d'_{BOS-aCON}$ of $0.95\pm.93$ (n=26; Fig. 5-2f), songs of age-matched brothers (BRO; mean $d'_{BOS-BRO}$ =

0.64±.68, n=17), songs of age-matched juvenile zebra finches (jCON; mean $d'_{BOS-jCON}$ = 0.80±.85, n=27) and songs of other species (HET; mean $d'_{BOS-HET}$ = 1.63±.83, n=18). Table 5-1 shows the percentage of selective RA sites for each type of stimulus comparison examined.

RA neurons at 50 days were sensitive to the temporal order of the BOS. BOS presented in normal order elicited a stronger response (Fig. 5-3a) than the BOS presented in reverse (REV; Fig. 5-3b), in which the order of song elements (syllables) and the syllables themselves were reversed in time (Fig. 5-3d, e; $p<.001$, paired student's t-test, n=23). The mean $d'_{BOS-REV}$ of 0.93±.75 (n=23) also indicates that, on average, RA neurons preferred the BOS presented in forward temporal order over the reversed BOS (Fig. 5-3f). However, when only the order of syllables was reversed in time, leaving the local order of each syllable intact (reverse order, RO; Fig. 5-3c; Solis and Doupe, 1997; Doupe, 1997), RA neurons responded almost as strongly to the BOS reverse order as to the BOS (Fig. 5-3d, e): the RS to the BOS and reverse order BOS were not significantly different from each other ($p=.10$, paired student's t-test, n=25). RA neurons also did not show any preference for the BOS over reverse order BOS as indicated by the mean d'_{BOS-RO} of 0.35±.65 (n=25; Fig. 5-3f). This suggests that although neurons in RA were sensitive to the local temporal order of the BOS, they were relatively insensitive to the global temporal order of BOS syllables.

Juvenile RA responses to BOS, tutor song and simple acoustic stimuli

By the age of 50 days, juvenile zebra finches already have considerable experience of listening to their tutor song, and their own plastic songs. This presents an opportunity to determine which auditory experience shaped the selectivity of RA neurons at this age. RA sites exhibited selectivity for the BOS over tutor song, or for the tutor song over BOS (Fig. 5-4a). However, the majority of the RA multi-unit sites were selective for the bird's own song (BOS) over the tutor song (n=17/25), while only 2/25 sites preferred the tutor song

over the BOS ($d'_{BOS-TUT} < -0.5$). Six out of 25 RA sites did not show any preference for either BOS or tutor song ($-0.5 < d'_{BOS-TUT} < 0.5$). This suggests that RA may contain information on both the BOS and tutor song, with individual neurons that reflect either type, or both types of auditory experience.

It is possible that the RA sites that were not selective for either the BOS or the tutor song ($-0.5 < d'_{BOS-TUT} < 0.5$) were simply non-selective neurons. However, these sites exhibited other types of selectivity. Some RA sites that did not exhibit a preference for the BOS vs. tutor song (Fig. 5-4b, in the gray region) showed a slight preference for the BOS over adult conspecific songs ($d'_{BOS-aCON} > 0.5$; Fig. 5-4b, open circles) and/or for the tutor song over adult conspecific songs ($d'_{TUT-aCON} > 0.5$; Fig. 5-4b, filled circles). Similarly, some of these sites also exhibited song order selectivity. Some of the RA sites that were not selective for either BOS or tutor song (Fig. 5-4c, in the gray region) responded more strongly to the BOS in normal order than to reversed BOS ($d'_{BOS-REV} > 0.5$; Fig. 5-4c, open circles) and/or to reverse order BOS ($d'_{BOS-RO} > 0.5$; Fig. 5-4c, filled circles).

Despite the strong selectivity for the BOS exhibited by the RA sites, neurons in RA did not strongly prefer the BOS over a broad-band white noise burst (100 or 300 msec duration), which is a relatively simpler acoustic stimulus. Figure 5-5 a and c show the responses of an RA site (the same site as in Fig. 5-2) to the BOS and a broad-band white noise burst. Approximately half of the RA sites exhibited onset responses to white noise bursts, and in all cases these responses were sustained during the duration of the stimulus (for example, Fig. 5-5c). The average RA response strength (RS) to the broad-band white noise burst was similar to the BOS RS (Fig. 5-5d, e): the RS to the BOS was not significantly different from the RS to the broad-band white noise ($n=21$, $p > .09$, paired student's t-test). The d' measure of selectivity indicated that RA neurons did not have a preference for the BOS vs. broad-band white noise (WN; mean $d'_{BOS-WN} = 0.49+1.28$, $n=21$; Fig. 5-5f). However, the same RA sites slightly preferred the BOS over another simple acoustic stimulus, pure tone bursts (300 msec duration; 1 to 4 kHz; Fig. 5-5b). RA

neurons were, on average, slightly selective for the BOS over pure tones (TONE; mean $d'_{BOS-TONE}$ = 0.59+1.15, n=15; Fig. 5-5f). The RS to the pure tone bursts of RA neurons, however, were not significantly different from their respective BOS RS (n=16; p >.11, paired student's t-test; Fig. 5-5d, e).

Comparison of RA and LMAN responses at 50 days of age

It is possible that some of RA's auditory response characteristics simply reflect those of its afferent inputs. In particular, we were interested in any similarities between RA auditory responses and those of LMAN, a source of RA's afferents that has been shown to be necessary for song learning. Thus, while recording RA activity, we recorded simultaneously from LMAN (n=28 sites) of the same juveniles (n=13), allowing us to describe LMAN responses at 50 days of age and to compare these responses to those of RA neurons. As in RA, we collected activity of small clusters of units (2-5) in LMAN during spontaneous and stimulus presentation. On the whole, the auditory responses of LMAN and RA neurons at 50 days of age were very similar, except for their responses to simple acoustic stimuli. RA exhibited stronger responses to simple auditory stimuli than LMAN; in fact, these responses were excitatory while those of LMAN were inhibitory. This also illustrates another difference between RA and LMAN auditory responses at 50 days of age.

We analyzed LMAN sites that exhibited an auditory response to at least one stimulus type (see above). As in RA at approximately 50 days of age, LMAN neurons of the same birds responded more strongly to the bird's own song than to other song stimuli. On average, the ratios of RS to songs relative to the BOS RS in LMAN were less than one for each song type (Fig. 5-6a). This indicates that the magnitude of response to each song was only a fraction of the response to the BOS. Moreover, the RS to the BOS was significantly higher than the RS to other song types (Fig. 5-6b; p<.0001, TUT, n=27; p<.0001, aCON, n=27; p<.01, BRO, n=14; p<.01, jCON, n=28; p<.0001, HET, n=18;

paired student's t-test). The d' measure for selectivity also reflected the stronger response to BOS over any other song type (mean d'> 0.5; Fig. 5-6c). Table 5-1 shows the percentage of LMAN sites that were selective in each stimulus comparison examined. This indicates that, on average, LMAN neurons, like RA neurons, preferred the BOS over any other song. As in RA, LMAN neurons that did not exhibit a preference for BOS vs. tutor song were not simply non-selective sites since the same sites also exhibited selectivity for the BOS or tutor song over adult conspecific song, and/or BOS order selectivity (data not shown).

Similar to RA, LMAN neurons were sensitive to the overall temporal order of the BOS, and largely insensitive to slight changes in the temporal order of the song, such as reversing the order of syllables in the BOS. LMAN neurons responded more strongly to the BOS in forward order, than when both the syllables and the order of the syllables were reversed in time (REV; Fig. 5-7a, b; $p<.001$, paired student's t-test, n=24). However, LMAN neurons responded equally to the BOS and to the version of BOS in which only the order of the syllables was reversed in time (reverse order, RO; Fig. 5-7a, b; $p=.13$, paired student's t-test, n=23). The mean $d'_{BOS-REV}$ of $0.93\pm.63$ indicates that LMAN neurons prefer the BOS in normal temporal order over the reversed BOS, whereas the mean d'_{BOS-RO} of $0.38\pm.56$ shows that the same LMAN neurons do not discriminate well between the BOS and the BOS in reverse order (Fig. 5-7c).

RA and LMAN neurons differed, however, in their RS to simple acoustic stimuli. In RA neurons, the RS to a broad-band white noise burst (100 or 300 msec duration) and pure tone bursts (300 msec duration; 1 - 4 kHz) were indistinguishable from the RS to the BOS (see above; Fig. 5-5). In contrast, LMAN neurons responded poorly to broad-band white noise and pure tone bursts, relative to the RS to the BOS (Fig. 5-8a). The RS to the BOS in LMAN was significantly higher than the RS to a broad-band white noise burst (WN; $p<.0001$, paired student's t-test, n=25; Fig. 5-8b) and pure tone bursts (TONE; $p<.0001$, paired student's t-test, n=17; Fig. 5-8b). These were also reflected in the mean d' measure for selectivity: the mean d'_{BOS-WN} of $1.30\pm.77$ and the mean $d'_{BOS-TONE}$ of $1.14\pm.69$ indicate

the strong preference of LMAN neurons for the BOS over broad-band white noise and pure tones, respectively (Fig. 5-8c). This suggests that LMAN is better than RA at discriminating between BOS and simple acoustic stimuli.

The broad-band white noise burst responses of LMAN and RA neurons were in fact fundamentally different. In LMAN, 5/25 (20%) sites that were presented with a white noise burst exhibited significant inhibitory responses ($p<.05$, paired student's t-test between stimulus evoked and spontaneous firing rate), while none of the sites in RA (0/21) exhibited significant inhibitory responses to white noise bursts (Fig. 5-9a, b). A small number of RA neurons, however, are capable of responding in an inhibitory manner. In RA, 3/27 sites (11%) exhibited significant inhibitory responses to song stimuli such as heterospecific, juvenile conspecific and adult conspecific songs (Table 5-2). A similar fraction of LMAN sites (3/28) also responded in an inhibitory manner to the same song stimulus types (Table 5-2). The inhibitory responses in RA to song stimuli indicate that although RA neurons can be inhibited, they are not inhibited in response to white noise bursts. Indeed, in many cases, RA neurons were excited by white noise bursts. This is true despite the observation that neurons in LMAN, which sends direct projections to RA, were not excited by white noise bursts and, in fact, in some cases were inhibited during white noise burst presentation. The lack of inhibitory responses to white noise bursts in RA may be due to modulation of its activity by HVc, which sends direct excitatory projections to RA. Of the small number of HVc sites from which we recorded simultaneously with RA or LMAN sites (n=7 sites; n=4 birds), only one of the HVc sites was significantly inhibited in response to adult conspecific songs (Table 5-2). Moreover, HVc responses to white noise bursts were all significant excitatory responses (n=5/5; Fig. 5-9c), and most of the responses to song stimulus types were also significant excitatory responses.

Comparison of RA and LMAN selectivity at 50 days of age

To determine the similarity between LMAN and RA auditory response selectivity, we directly compared the selectivity of simultaneously recorded RA and LMAN auditory responses, as measured by the d' value and the selectivity index (SI; see Methods). Because the LMAN and RA activity was simultaneously recorded from the same bird, we were able to perform a paired comparison of the mean d' and SI values of each nucleus within each bird. The d' value takes into account both the difference in magnitude of RS between the two stimuli being compared and the variability of these responses, while the SI only reflects the relative magnitude of the responses.

The d' measure of selectivity indicated that the preference for the BOS over tutor (n=11), adult conspecific (n=13), brothers' (n=8) and juvenile conspecific songs (n=13) was similar in juvenile LMAN and RA (Fig. 5-10a; $p>0.24$, paired student's t-test). LMAN, however, had higher SI values than RA for the same song comparisons (Fig. 5-10b). The SI values for BOS-tutor song comparison and for BOS-adult conspecific song comparison were significantly higher in LMAN than RA ($p<.01$, paired student's t-test). This suggests that based on RS alone, LMAN has higher selectivity for the BOS over tutor or adult conspecific songs than RA. However, the variability must be higher in LMAN than in RA because the d' values of the two nuclei were not significantly different. Similarly, the d' measure showed that RA was significantly better at discriminating between BOS and heterospecific songs ($p<.01$, paired student's t-test, n=10), although the corresponding SI values for LMAN and RA were similar. This indicates that the difference between LMAN and RA $d'_{BOS-HET}$ may be due to higher variability of responses in LMAN than in RA, and not necessarily due to difference between the RS to BOS and heterospecific songs. Based on the d' measure of selectivity, LMAN and RA have similar selectivity for the BOS vs. other zebra finch songs; however, RA is more selective than LMAN for the BOS over songs of other species.

The BOS order selectivity of LMAN was not significantly different from that of RA when measured using d', since LMAN and RA had similar $d'_{BOS-REV}$ and d'_{BOS-RO} values

(Fig. 5-10c). The LMAN responses, however, must be more variable than those in RA, since the SI measure of selectivity for BOS-reverse BOS (n=13), and BOS-reverse order BOS (n=13) comparisons were higher in LMAN than in RA (Fig. 5-10d). The difference between the mean SI values for BOS-reverse BOS comparison was significant ($p<.05$, paired student's t-test), indicating that the LMAN BOS RS relative to reversed BOS is significantly higher than that of RA. Thus, by the SI measure of selectivity, LMAN is more sensitive to the temporal order of the BOS than RA, although the d' values indicate similar BOS order selectivity between LMAN and RA.

LMAN had higher d' and SI values than RA for both the BOS vs. broad-band white noise burst (n=12) and BOS vs. tones (n=8) comparisons (Fig. 5-10a, b). The differences in both d' and SI values were significant for the BOS vs. broad-band white noise burst comparison ($p<.05$, paired student's t-test). The differences in SI suggests the RS to BOS relative to RS to simple acoustic stimuli were much higher in LMAN than in RA at 50 days of age. Consistent with this, LMAN neurons can respond in an inhibitory manner to broad-band white noise bursts, while RA neurons do not (see above). Moreover, the d' values indicate that LMAN responded more strongly to the BOS over simple acoustic stimuli than RA. Thus, LMAN is more sensitive to song-like vs. simple acoustic stimuli than RA, and significant inhibitory responses to white noise bursts in LMAN may help to shape this selectivity.

We also compared the tutor song selectivity of LMAN and RA (Table 5-1; Fig. 5-11a, b). Although neurons in both nuclei were non-selective for tutor vs. songs of other zebra finches ($-0.5 < d'_{TUT-aCON}, d'_{TUT-BRO}, d'_{TUT-jCON} < 0.5$), LMAN had a significantly higher mean d' value for tutor vs. adults conspecific songs than RA ($p<.05$, paired student's t-test, n=12). RA, on the other hand, preferred the tutor song over heterospecific songs (mean $d'_{TUT-HET} = 0.63+1.13$, n=9) more strongly than LMAN (mean $d'_{TUT-HET} = 0.31+.76$, n=9), although this difference was not significant. Thus, LMAN at 50 days old is slightly more sensitive than RA to the tutor song relative to songs of adult zebra finches, although in

each nucleus, the responses to tutor and adult conspecific songs were much less than the response to BOS.

Selectivity of juvenile and adult RA

To assess any developmental changes in auditory response selectivity of RA, we compared the selectivity of juvenile RA and adult RA. We recorded multi-unit RA activity of adults (the same data reported in Chapter 3), and analyzed the data from sites that were auditory to at least one stimulus type ($p<.05$, paired student's t-test between stimulus and spontaneous firing rate).

An overall increase in song and order selectivity for the BOS was observed in adult RA neuronal responses (Fig. 5-12a). The d' values for BOS vs. other stimulus types were higher in adults than in juveniles, and these differences were significant for the following d' values: BOS vs. adult conspecific songs, brothers' songs, reversed BOS and reverse order BOS ($p<.01$, unpaired student's t-test). For many of these stimuli, such as those mentioned above, the increase in selectivity appears to be due not only to increase in RS to the BOS, but also to greatly decreased responses to the non-BOS stimulus types (data not shown). This is evident in the response to adult conspecific songs and reversed BOS, which drop below spontaneous activity (Fig. 5-12b, c, d, e). For the other non-BOS stimuli, a comparison of unnormalized RS between adults and juveniles (data not shown) suggests that the RS to non-BOS stimuli decreases during development. However, this comparison of firing rates can only be suggestive because it compares the activity of small clusters of units across birds. Curiously, the normalized RS to tutor song (Fig. 5-12b, c) does not change significantly during development. This suggests that some responsiveness to the tutor song remains, consistent with the slight but not significant increase in $d'_{BOS-TUT}$ from juvenile ages to adulthood. The significant increase in d'_{BOS-RO} indicates that adult RA neurons are now sensitive to the reversal of the global temporal order of syllables. Thus,

adult RA neurons are more selective for the BOS, and its normal temporal order, than juvenile RA neurons.

We examined the tutor selectivity of juvenile and adult RA neurons. We found that RA neurons in adults became better at discriminating between the tutor song and songs of other adult zebra finches. On average, adult RA neurons preferred the tutor song over adult conspecific songs (mean $d'_{TUT-aCON} = 0.67 \pm .94$, n=26) whereas juvenile RA neurons did not (mean $d'_{TUT-aCON} = 0.01 \pm 1.22$, n=25); the difference between adult and juvenile $d'_{TUT-aCON}$ was significant ($p<.05$, unpaired student's t-test; Fig. 5-13a). The data indicate that RA neurons become more strongly responsive to the tutor song relative to adult conspecific songs as the bird completes song learning. The tutor RS - adult conspecific RS comparison involves a large portion of sites (25/25 or 100% in juveniles, and 15/26 or 58% in adults) that exhibited a significant RS to the tutor and/or adult conspecific songs (Fig. 5-13a, red symbols). This indicates that we are not simply comparing responses that are close to the spontaneous firing rate. Rather, these small responses to non-preferred stimuli may be relevant to downstream neurons.

A comparison of responses to the tutor and brothers' songs revealed that both juvenile and adult RA neurons did not, on average, show any strong preference for tutor vs. brothers' songs. The mean $d'_{TUT-BRO}$ values were not significantly different between juveniles and adults (Fig. 5-13b; n=16 for juveniles, n=14 for adults). However, the distribution of $d'_{TUT-BRO}$ values in adults was quite different from the distribution in juveniles. In adults, 12/14 (86%) RA sites had $d'_{TUT-BRO}$ values that were between -0.5 and 0.5, while in juveniles, only 6/16 (37%) had $d'_{TUT-BRO}$ values in the same range (Fig. 5-13b). The rest of the RA sites in juveniles strongly preferred either the tutor song (n=5/16) or the brothers' songs (n=5/16). This indicates that in juveniles, there is a heterogeneous distribution of tutor vs. brothers' songs selectivity, and this heterogeneity disappears in adulthood, where most of the RA neurons do not exhibit a strong preference for tutor vs. brothers' songs. The adult data, however, are difficult to interpret, since many of the sites

examined did not show a significant auditory response to either stimulus type (Fig. 5-13b). All of the sites in juveniles, on the other hand, exhibited a significant response to one or both song stimulus types (Fig-5-13b, red symbols). The heterogeneity of the tutor vs. brothers' songs selectivity in juveniles may reflect the acoustic properties of the songs at this age. That is, the wide range of $d'_{TUT-BRO}$ in juveniles may indicate that brothers' songs are more variable in juveniles, and either resemble the tutor song, or do not resemble it much at all, giving rise to several response types. By adulthood, however, the brothers' songs may stabilize, perhaps with a good degree of similarity between tutor and brothers' songs. This could then account for the poor ability of adult RA neurons to discriminate between the two types of songs. Acoustic analysis of the songs, and comparison of the acoustic properties of these songs to the selectivity data would be informative with respect to the results outlined above.

Adult RA neurons exhibited more inhibitory responses than juvenile RA neurons, although the number of sites exhibiting significant inhibitory responses between juveniles and adults were not significantly different (Table 5-2). In adults, 6/28 (21%) sites exhibited significant inhibitory responses, while in juveniles, it was only 3/27 (11%). In both juveniles and adults, the significant inhibitory responses were only to song stimulus types. RA neurons in adults did not exhibit any significant inhibitory responses to broad-band white noise bursts. Moreover, as in juveniles, the RS to the BOS in adult RA were not significantly different from the RS to broad-band white noise ($p>.20$, paired student's t-test, $n=26$). Thus, RA exhibited a slight increase in its capacity to respond in an inhibitory manner that was stimulus specific.

Comparison of adult RA, LMAN and HVc selectivity

To determine the similarity between RA auditory response selectivity and that of its afferent nuclei, LMAN and HVc, in adult zebra finches, we recorded the activity of two or three nuclei from the same bird simultaneously. The RS of adult RA neurons to songs other

than the BOS were only a fraction of the RS to the BOS, similar to what is observed in adult LMAN neurons (Fig. 5-14a, b). This was unlike HVc, whose RS to tutor song was close to its BOS RS (Fig. 5-14c). In response to adult conspecific songs, both RA and LMAN neurons exhibited inhibitory responses on average, while HVc neurons responded in an excitatory manner to the same stimulus (Fig. 5-14a, b, c). RA, however was more similar to HVc in its response to broad-band white noise bursts: in LMAN, the RS to BOS was significantly higher than the RS to broad-band white noise burst ($p<.0001$, paired student's t-test, n=27), while in HVc and RA, the RS to BOS was similar to the RS to broad-band white noise burst. Also, RA exhibited an excitatory mean response to reverse order BOS, similar to HVc and different from LMAN, which exhibited inhibitory responses to reverse order BOS (Fig. 5-14d, e, f). These data suggest that neurons in adult RA share some auditory response characteristics with LMAN, and other characteristics with HVc neurons.

The fraction of sites that exhibited significant inhibitory responses ($p<.05$, paired student's t-test between stimulus evoked and spontaneous firing rate) in LMAN, RA and HVc was significantly different between nuclei ($p<.0001$, χ^2 test). LMAN in adults had the largest fraction of sites with significant inhibitory responses, compared to RA and HVc (Table 5-2). Eighteen / 29 (62%) sites in LMAN exhibited significant inhibitory responses, while in RA it was only 6/28 (21%). HVc sites did not exhibit any significant inhibitory responses at all (n=0/13 sites, 0%). However, 8/26 (31%) LMAN sites that were tested for white noise burst response were significantly inhibited, while none of the RA sites were significantly inhibited. All of the significant inhibitory responses in RA were to song stimuli (Table 5-2). Thus, RA is similar to LMAN in its capacity to respond in an inhibitory manner, although not to the same extent as LMAN.

The d' measure of selectivity showed that the ability of adult RA neurons to discriminate between songs is similar to that of LMAN and HVc, but also revealed differences in selectivity between the three nuclei. RA, HVc and LMAN exhibited the same degree of d' selectivity for the BOS over tutor and adult conspecific songs (Fig. 5-15a). The

SI values, however, indicate that LMAN and RA have larger differential responses to BOS vs. another song than HVc (Fig. 5-15b). Indeed, LMAN's SI for BOS vs. adult conspecific songs comparison was significantly higher than that of HVc ($p<.05$, paired student's t-test of mean SI of each nucleus from each bird, n=6). Based on the d' values, LMAN preferred the BOS over broad-band white noise bursts more strongly than RA and HVc ($p<.05$, paired student's t-test of mean d' for each nucleus from each bird; n=6 for comparison with HVc; n=13 for RA). These were also reflected in the SI values ($p<.05$, paired student's t-test). RA, however, was more selective for the BOS over broad-band white noise bursts ($d'_{BOS-WN} = 0.88\pm1.1$, n=13) than HVc ($d'_{BOS-WN} = 0.16\pm1.39$, n=6), although these d' values were not significantly different. As for order selectivity, RA exhibited a significantly higher d' value for BOS vs. reverse BOS than LMAN ($p<.01$, paired student's t-test, n=6), although the RA and LMAN SI values for BOS vs. reverse BOS were similar. The data indicate that RA auditory response selectivity in adults is not exactly the same as that of LMAN or HVc.

DISCUSSION

In this chapter, we describe the selectivity of RA auditory responses in approximately 50 day old juveniles, and compare the RA selectivity to that of LMAN in the same birds. RA auditory responses and selectivity in juveniles shared some characteristics with LMAN, and other characteristics with HVc. By one measure of selectivity (d'), LMAN and RA in juveniles exhibited similar song and BOS order selectivity. However, by another measure of selectivity (SI), which does not take the variability of responses into account, juvenile LMAN had higher BOS selectivity than RA. In either measure of selectivity, LMAN neurons showed a stronger preference for the BOS over simple acoustic stimuli. LMAN neurons displayed inhibitory responses to white noise bursts, while RA neurons did not. The responses of RA neurons to simple acoustic stimuli resembled those of HVc, since neurons in both nuclei were likely to respond in an excitatory manner to these stimuli. During development, RA neuronal responses became more selective for the BOS, and more sensitive to the temporal sequence of the BOS syllables. This suggests that BOS selectivity is influenced by experience of the BOS, and could thus play a role in song learning. These changes in selectivity were accompanied by a significant decrease in the normalized response to some stimuli in adults, and a slight increase in the proportion of RA sites that exhibited stimulus-specific inhibitory responses. As in juveniles, RA in adults shared some response and selectivity properties with LMAN, and other properties with HVc. The data from this study raise the possibility that, in juveniles and adults, RA auditory response characteristics may be influenced by both LMAN and HVc activity. The data also suggest that both inhibitory mechanisms and the variability of responses to a stimulus are involved in enhancing the selectivity of auditory responses.

Selectivity of RA neurons at 50 days

The data here suggest that at 50 days old, RA neurons are able to distinguish between the BOS and other songs, with a strong preference for the BOS. However, RA

neurons can not discriminate well between BOS and a version of the BOS where the order of syllables has been reversed. This is similar to what was observed in LMAN neurons at 60 days old (Solis and Doupe, 1997), and is consistent with the result that zebra finches appear to memorize first the syllables of the tutor song, and then the sequence of these syllables (Immelmann, 1969).

Selective auditory responses may play a role in song learning, because song learning depends crucially on normal auditory experience and feedback, and selective auditory responses are exhibited by neurons in structures that mediate song learning (Margoliash and Konishi, 1985; Margoliash, 1986; Doupe and Konishi, 1991; Volman, 1993; Vicario and Yohay, 1993; Maekawa and Uno, 1996; Theunissen and Doupe, 1998). As shown in this study, neurons in LMAN and RA of juveniles near the end of sensory learning, and in the middle of sensorimotor learning (50 days of age), exhibit BOS and BOS order selectivity. It is unclear, however, what role, if any, selective auditory responses may play in song learning. These selective responses could provide information on the state of vocal learning, which would be useful for a system that compares the vocal output to the memorized copy of the tutor song. The BOS selectivity may act as a filter that determines which auditory input will be used for the comparison signal (Solis et al, 2000). Selective auditory responses may also be involved in song recognition and discrimination processes, since LMAN and HVc have been shown to be required for these behavioral processes (Brenowitz, 1991; Scharff et al, 1998; Burt et al, 2000; Gentner et al, 2000).

The examination of BOS vs. tutor song selectivity is a first step towards determining which auditory experience, the BOS or the tutor song, shapes the selectivity of RA neurons. Although the majority of RA sites were selective for the BOS over tutor song, approximately 10% of the sites were selective for tutor song over BOS. Moreover, another 25% of the RA sites responded equally to both BOS and tutor song. These neurons with equal BOS and tutor responses did not simply involve non-selective sites, since some of these sites showed other types of selectivity, such as BOS or tutor song vs. adult

conspecific song selectivity, or BOS order selectivity. The sites that did not show a preference for BOS vs. tutor song may reflect experience of both the BOS and tutor song. Thus, the selectivity for BOS vs. tutor song may be heterogeneous at this age. The degree of similarity of BOS to tutor song is crucial to interpreting the BOS-tutor song selectivity. When these stimuli are acoustically similar, as they frequently are, they may elicit similar responses regardless of which experience shaped the selectivity of RA neurons. It would therefore be informative to examine the RA responses in birds where the similarity between tutor song and BOS has been experimentally decreased.

Both individually and as a population, RA neurons were surprisingly poor in discriminating between BOS and broad-band white noise bursts. This suggests that despite their high degree of selectivity for the BOS, RA neurons do not distinguish well between song-like sounds and relatively brief and simpler acoustic stimuli that are presented outside of a song-like context. It would be of interest to determine whether RA neurons at this age would also respond to white noise presented in a song-like manner, such as a sequence of white noise bursts with amplitude modulation similar to that of the BOS (Margoliash, 1992).

RA becomes more selective for the BOS and BOS order in adults

A comparison of RA selectivity in juveniles with that of adults indicates that the selectivity for the BOS significantly increases between 50 days of age and adulthood. Moreover, RA neurons become sensitive to the global order of BOS syllables in adulthood, consistent with behavioral experiments that show that the sequence of syllables appears to be acquired later during song learning (Immelmann, 1969). The larger degree of selectivity for the BOS in adults suggests that the auditory feedback of the BOS during sensorimotor learning may have shaped the selectivity of the RA responses. A caveat is that BOS selectivity does not necessarily reflect experience of the bird's own voice. That is, the bird might have inaccurately memorized the tutor song, but then produce a good motor copy of

the poorly memorized tutor song. If so, the BOS would be a better stimulus than the tutor song for driving neurons that nonetheless represented the bird's memory of the tutor song. One way to resolve this issue is to cause birds to sing an abnormal BOS. In our experiments, we examined BOS selectivity only in birds that had normal song learning. However, studies of LMAN in 60 day old birds whose song had been manipulated to be abnormal, and thus very different from the tutor song, indicate that the auditory experience of this abnormal BOS contributes to shaping the selectivity of LMAN neurons (Solis and Doupe, 1999). It seems likely that, in RA as well, the bird's own vocalizations contribute to the selectivity of RA neurons, although this remains to be determined.

RA auditory responses share characteristics with those in LMAN, and also in HVc

A hierarchy of selective responses, where downstream areas exhibit a higher degree of selectivity, has been shown for other systems (for reviews, see Langner, 1992; Vidyasagar et al, 1996; Sompolinsky and Shapley, 1997; Covey and Casseday, 1999; Knudsen, 1999; Mori et al, 1999;). In the song system, the anterior forebrain pathway (Area X -> DLM -> LMAN) has been shown to exhibit slightly increasing selectivity for the BOS (Doupe, 1997). A within-bird comparison of RA and LMAN selectivity revealed that the degree of LMAN selectivity at 50 days old is not exactly reflected by the RA neurons at this age, although LMAN and RA selectivity had many similarities. By the d' measure of selectivity, which takes into account the difference between stimuli RS and the variability of responses, LMAN and RA had similar BOS and BOS order selectivity. However, the SI measure of selectivity, which considers only the relative magnitude of stimuli RS, indicated that LMAN was more selective for the BOS than RA. Moreover, by both measures, LMAN responded more strongly to the BOS vs. a broad-band white noise burst than did RA, indicating that LMAN is more sensitive to the BOS than RA. If BOS selectivity is important for the progression of song learning from 50 days of age onwards, then LMAN would be well suited to guide song learning. Consistent with this hypothesis, LMAN has been

thought to participate in guiding song learning based on auditory experience and feedback (Nordeen and Nordeen, 1992; Doupe, 1991).

The lack of selectivity for BOS over white noise bursts in RA at 50 days and adulthood may be due to the HVc input to RA. Although our sample was small, our studies of 50 day HVc in the same birds indicate that HVc neurons exhibited strong significant excitatory responses to white noise bursts, in contrast to the inhibitory responses in LMAN to the same stimulus. One caveat with respect to the HVc data is that we collected activity from small clusters of units, potentially averaging the activity of three different types of HVc neurons: interneurons, RA- and Area X-projecting neurons. The RA and Area X-projecting neurons of HVc may differ in their selectivity during song learning, with the RA-projecting neurons exhibiting selectivity that is consistent with RA selectivity, and that of the Area X-projecting neurons consistent with LMAN selectivity. Recent evidence shows that in adult zebra finches, RA- and Area X- projecting neurons have different subthreshold BOS vs. reverse BOS selectivity, but similar mean firing rate d' selectivity (Mooney, 2000).

Some of the data in this study suggest that during development, RA response and selectivity properties become more similar to those of LMAN than HVc. For example, the SI values for BOS-tutor song and BOS-adult conspecific song comparisons in RA became similar to those of LMAN and different from those of HVc as song learning was completed. The d' measure of selectivity, however, did not reflect these results. As discussed further below, it is not really clear which measure of selectivity is more appropriate to describe the auditory response selectivity of neurons in the song system. The fraction of sites exhibiting inhibitory responses also indicated that RA's responses became more LMAN-like than HVc-like. The fraction of inhibited sites in RA slightly increased from 50 days of age to adulthood, in parallel to the significant increase in the fraction of inhibited sites in LMAN. This is quite different from adult HVc responses, which did not include significant inhibitory responses. However, as in juveniles, adult RA neurons still did not respond in an inhibitory manner to white-noise bursts, which is similar to the responses

exhibited by adult HVc neurons. The caveat concerning our HVc data also applies here: our HVc data may involve averaging the responses of different types of HVc neurons, although all types had similar BOS vs. reverse BOS d' selectivity (based on firing rates) (Mooney, 2000). A careful analysis of the d' and SI selectivity of the different types of HVc neurons would therefore be of interest.

The shared selectivity properties of RA with LMAN, and of other properties with HVc, at 50 days of age and adulthood raises the possibility that the auditory response selectivity of RA neurons are influenced by both LMAN and HVc activity. This is consistent with the presence of both LMAN and HVc synapses in RA at 50 days of age and adulthood (Herrmann and Arnold, 1991), and the strong positive correlated activity between LMAN and RA, and between HVc and RA at both ages (Chapters 3 and 4). It is unclear, however, what each afferent nucleus contributes to the auditory responsiveness and selectivity of RA neurons, and whether these two synapses in the same RA neuron interact in a non-linear fashion. Doupe and Konishi (1991) showed that in adults, RA auditory responses to BOS are dependent on HVc, and do not appear to require LMAN activity. However, this study did not assess the selectivity of RA neurons in the absence of LMAN activity. Based on the experiments described in this chapter, the degree of song and order selectivity in RA was not exactly the same as that of HVc, suggesting that LMAN may influence the responses in RA in adults. It is possible that HVc primarily endows RA with auditory responsiveness in adults, but that LMAN also affects RA selectivity in a more subtle way, perhaps biasing RA's subthreshold selectivity properties. Determining the suprathreshold and subthreshold selectivity of RA neurons through intracellular recordings, while silencing one of the inputs so that either is the only known input present in RA, would help elucidate the contribution of each nucleus in shaping the responses and selectivity in RA.

Selectivity of responses may be shaped by inhibition and variability of responses

The increase in RA selectivity during development was accompanied by a significant decrease in response strength to non-BOS stimulus types. It is possible that an increase in the response to the BOS also contributed to the increase in d' selectivity, as observed in the emergence of selectivity of LMAN neurons (Solis and Doupe, 1997); however, this was difficult to assess in this study, since the RA activity was recorded from small clusters of neurons rather than single units. A slightly larger fraction of adult RA sites responded in an inhibitory manner to non-BOS song types than in juvenile RA. This indicates that one mechanism by which selectivity of auditory responses is shaped during development is an enhancement of inhibitory responses to non-preferred stimuli. In HVc, inhibitory mechanisms have been implicated in shaping the temporal sensitivity of HVc neurons (Lewicki and Konishi, 1995; Lewicki, 1996; Mooney, 2000). Similarly, in vivo intracellular recordings in adult LMAN have showed that the local inhibitory circuitry in LMAN is required for the expression of the BOS-reverse BOS selectivity, although the extrinsic afferents of LMAN were also selective (Rosen and Mooney, 2000). The local inhibitory circuitry in RA of adults may also have the same effect on RA selectivity, and this effect may emerge during song learning since there was a slight increase in the percent of RA sites that exhibited inhibitory responses during development.

An alternative mechanism that may underlie the slight developmental increase in percentage of RA sites that exhibited significant inhibitory responses is modulation of the responses by the LMAN input. During song learning, LMAN and RA had a similar fraction of inhibited sites in response to song stimuli; in adulthood, LMAN exhibited the largest proportion of sites that showed inhibitory responses. Adult LMAN neurons show either no response or inhibitory responses to some non-preferred song stimulus types. HVc in adults, on the other hand, did not exhibit a significant decrease in firing rate in response to non-preferred stimuli, and, in fact, exhibited significant excitatory responses to most stimuli. If both the HVc and LMAN inputs are necessary to shape RA neuronal responses, then decreased responses to the non-preferred stimulus in RA, relative to HVc responses, may

emerge as a result of decreased LMAN input to excitatory neurons in RA. This could enhance the selectivity of RA responses as song learning is completed.

RA inhibitory responses could also result from modulation of the balance of excitation and inhibition in RA by both LMAN and HVc. Both LMAN and HVc input may contribute to inhibitory responses in RA, since LMAN and HVc neurons synapse onto RA inhibitory interneurons, as well as onto RA projection neurons (Sakaguchi et al, 1987; Mooney, 1992; Spiro et al, 1999; Kittelberger and Mooney, 1999). Moreover, more complex interactions between LMAN and HVc, such as long-term depression of HVc input when paired with a silent LMAN input in RA, could be involved in the development of responses in RA that no longer resemble HVc inputs. It would therefore be informative to determine the selectivity of RA in cases when LMAN is the only known input to RA, or when LMAN is manipulated to eliminate its inhibitory response to non-preferred stimuli.

In most song comparisons, LMAN exhibited higher SI values than RA in juveniles, and than HVc in adults. However, for these same comparisons, the d' values were similar between LMAN, RA and HVc. Which of these measures best reflects selectivity as it is used by neurons in the song system? Because d' values also take into account the variability of responses, the consistency of the neurons' responses to a particular stimulus affects their preference for one stimulus over another as assessed by this measure. In LMAN and Area X, there is an inverse relationship between d' values and response variability of single neurons during song development (Solis, 1999 doctoral thesis). The variability of auditory responses is important if downstream neurons do not average their afferent activity (see Solis and Doupe, 1997). In this case, the d' measure of selectivity may be the best measure of selectivity. The variability of responses across neurons may be less important to downstream neurons, however, if these neurons receive many convergent inputs. As discussed in chapter 3, the functional connectivity in the song system may involve broad divergent and re-convergent connections between song nuclei. This implies that a downstream neuron may have numerous afferents from different upstream neurons, and

average out the variability of the activity from the individual neurons. Thus, the selectivity index may be the best measure of selectivity for downstream neurons. However, if the variability of responses between neurons is correlated, then the variability will not be averaged out even when downstream neurons receive convergent inputs. If RA neurons receive non-correlated convergent input from LMAN neurons, then one would expect that the variability of RA responses to be lower than that of LMAN. This predicts higher d' values in RA than in LMAN, if both LMAN and RA neurons have similar relative stimuli RS, as measured by SI values. In adults, however, LMAN and RA had similar SI and d' values for song comparisons, raising the possibility that the variability of LMAN inputs is not averaged out by adult RA neurons. In juveniles, LMAN and RA also had similar d' values for most comparisons; however, juvenile RA had lower SI values than LMAN, perhaps reflecting its HVc inputs. This suggests that, in juveniles, RA neurons average out the input variability from LMAN neurons. Overall, it is not entirely clear what the consequences of the variability of responses in LMAN neurons are for the selectivity of the RA downstream neurons. A study of the variability of responses of simultaneously recorded single-units in LMAN or HVc, and RA, and of the selectivity of these units, would help determine the relationship between the selectivity of downstream neurons to the variability of responses in upstream neurons.

In summary, RA neurons near the end of sensory learning, and in the middle of sensorimotor learning exhibit BOS and BOS order selectivity, which increases as the bird reaches adulthood. This suggests that the selectivity for the BOS in RA may play a role in song learning. The selectivity of RA in juveniles is similar to that of juvenile LMAN, but also exhibits auditory response characteristics found in juvenile HVc. Similarly, RA neurons in adults also share auditory response characteristics with LMAN, and other characteristics with HVc. This suggests that RA responses and selectivity in juveniles and adults are influenced by both LMAN and HVc activity. Determining if this is indeed the

case, and how LMAN and HVc input interact within an RA neuron to influence its auditory responsiveness, would help elucidate the emergence of selectivity of responses in RA. The underlying mechanisms of these interactions may be involved in how song learning is guided in the pre-motor nucleus that controls the motor expression of song. Finally, the data in this study suggest that both inhibitory mechanisms and the consistency of auditory response patterns contribute to the selectivity of responses in the song system.

Figure 5-1 a) Time line of song learning in zebra finches. b) Schematic of the song system. HVc (abbreviation used here as proper name), the robust nucleus of the archistriatum (RA), the tracheosyringeal portion of the hypoglossal nucleus (nXIIts), and respiratory nuclei, shown in black, make up part of the descending motor pathway for song. The nuclei Area X, the medial portion of the dorsolateral nucleus of the thalamus (DLM), and the lateral portion of magnocellular nucleus of the anterior neostriatum (LMAN), shown as open symbols, form the anterior forebrain pathway (AFP). The AFP indirectly connects HVc and RA, and is required during song learning.

Figure 5-1

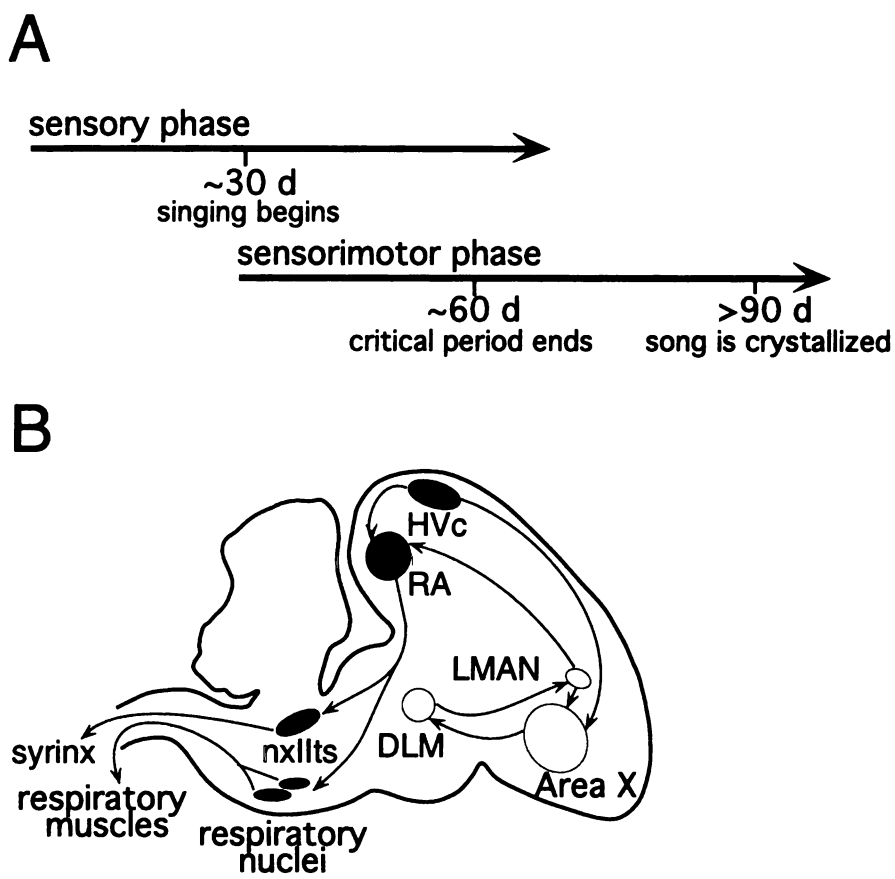
A
sensory phase
~30 d
singing begins
sensorimotor phase
~60 d
critical period ends
>90 d
song is crystallized
B
HVc
RA
LMAN
nXIIts
DLM
Area X
syrinx
respiratory muscles
respiratory nuclei

Figure 5-2 Song selectivity of RA neurons at 50 days of age a) The response to the BOS of a small cluster of units in RA, while b) is the response to the bird's tutor song (TUT), and c) is the response to an adult conspecific song (aCON) of the same RA site. Below the peri-stimulus time histogram are the sonogram representation of the song (frequency vs. time plot, with high energy represented by the darkness of the sonogram), and the oscillogram (amplitude waveform) of the song stimulus. d) The mean RS to BOS of each RA site is plotted against its mean RS to tutor song (open circles, n=25), and adult conspecific song (filled circles, n=26). The diagonal line represents the unity line, where the RS to the BOS and tutor or adult conspecific songs are equal. e) The mean RS to song stimuli, expressed as a fraction of the typical maximal response, the BOS RS. Thus, values near one indicate that, on average, the RS is as high as the BOS RS. The song stimuli include age-matched brothers' songs (BRO), juvenile conspecific songs (jCON) and heterospecific songs (HET). The numbers in parentheses indicate the number or sites for each mean %BOS RS. Error bars indicate standard error (SE). f) The cumulative distribution of $d'_{BOS-TUT}$ (open circles, n=25) and $d'_{BOS-aCON}$ (filled circles, n=26) values from RA sites. The open and filled arrows indicate the mean $d'_{BOS-TUT}$ and $d'_{BOS-aCON}$, respectively. The gray shaded area represents the region that is considered non-selective ($-0.5 < d' < 0.5$).

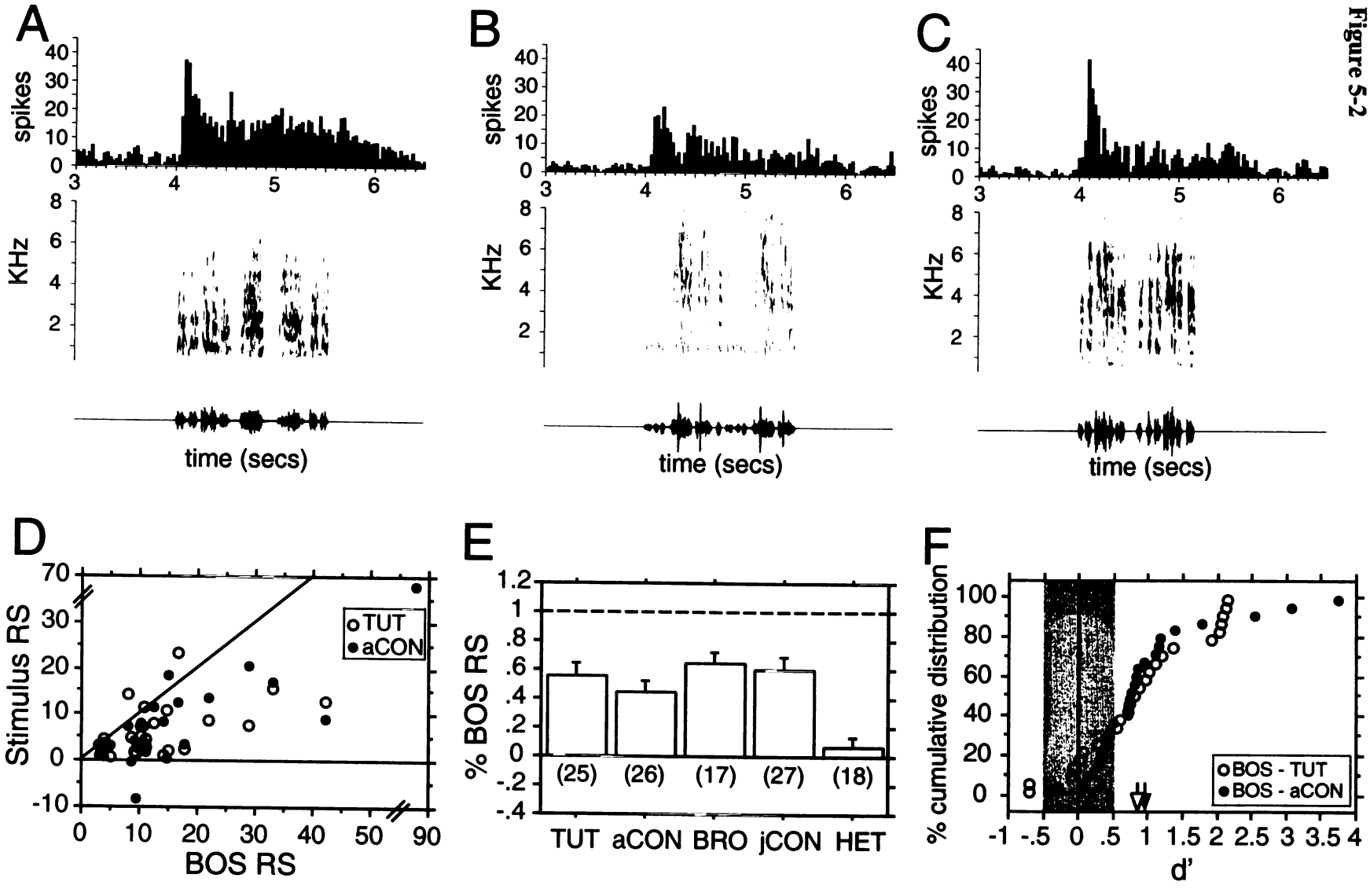
A
B
C
spikes
KHz
time (secs)
D
E
F
Stimulus RS
BOS RS
TUT
aCON
% BOS RS
(25) (26) (17) (27) (18)
TUT aCON BRO jCON HET
% cumulative distribution
d'
BOS - TUT
BOS - aCON

Figure 5-2

Figure 5-3 BOS order selectivity of juvenile RA neurons a) The response to the BOS of an RA site (same as in Fig. 5-2), and to b) the BOS in reverse (REV) and c) the BOS in reverse order (RO). The song stimuli are represented as in Figure 5-2. d) The mean RS to the BOS of each RA site is plotted against its response to the BOS in reverse (open circles, n=23), and the BOS in reverse order (filled circles, n=25). The diagonal represents equal RS to the BOS and BOS reverse or BOS reverse order. e) The mean RS to BOS reverse and BOS reverse order expressed as a fraction of the BOS RS. The number in parentheses is the number of RA sites for each mean, and error bars indicate the SE. f) The cumulative distribution of $d'_{BOS-REV}$ (open circles, n=23) and d'_{BOS-RO} (filled circles, n=25) from RA sites. The open and filled arrows indicate the mean $d'_{BOS-REV}$ and d'_{BOS-RO}, respectively. Gray shading represents what is considered to be the non-selective region ($-0.5 < d' < 0.5$).

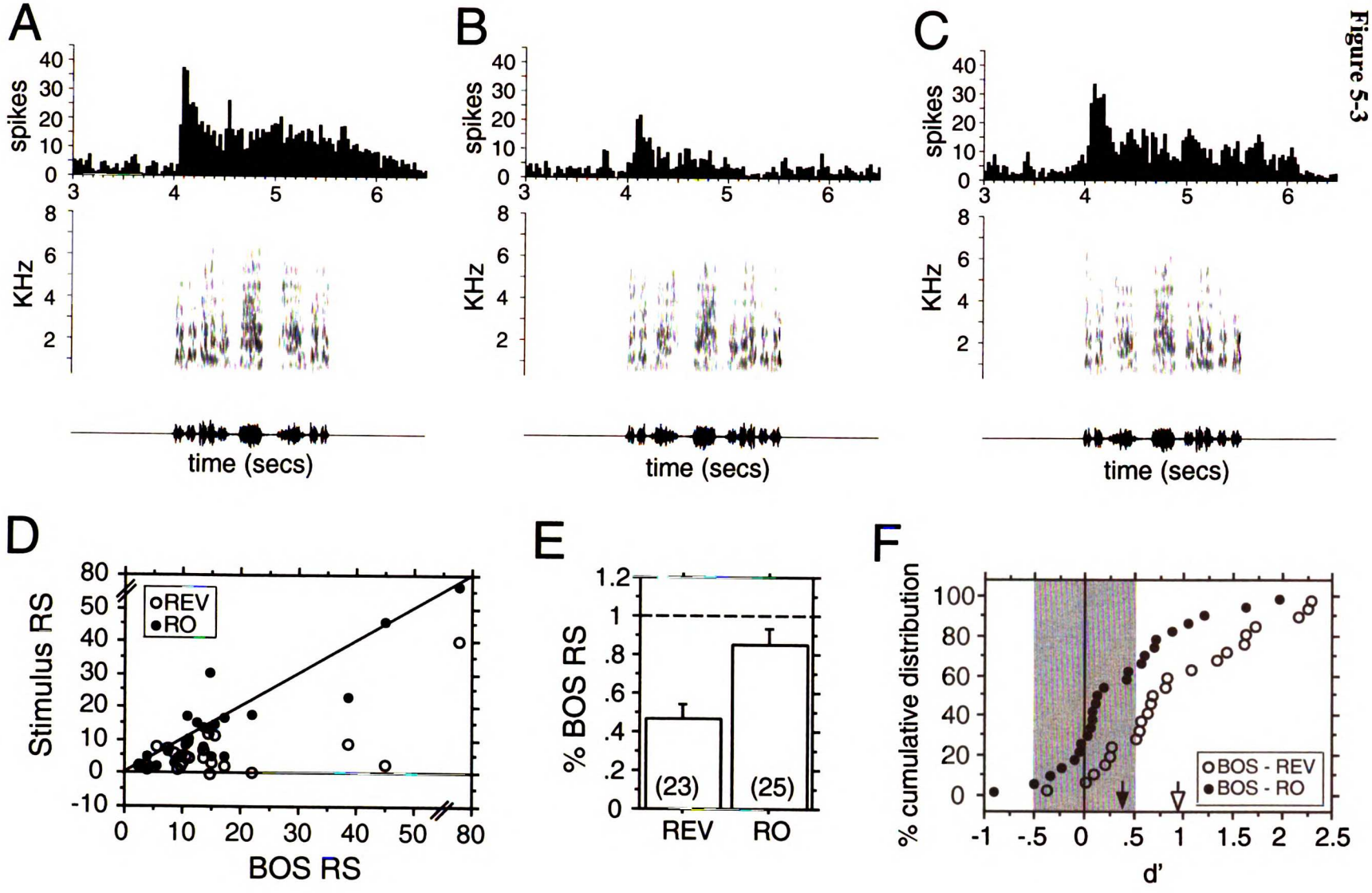
A
B
C
spikes
KHz
time (secs)
D
Stimulus RS
BOS RS
REV
RO
E
% BOS RS
(23)
(25)
REV
RO
F
% cumulative distribution
d'
BOS - REV
BOS - RO

Figure 5-3

Figure 5-4 RA sites that do not show any preference for BOS vs. tutor song are not necessarily non-selective sites. a) The cumulative distribution of $d'_{BOS-TUT}$ values from 25 RA sites, with the gray area indicating sites that are considered non-selective. The mean $d'_{BOS-TUT}$ is indicated by the arrow. b) The $d'_{BOS-TUT}$ of each RA site is plotted against its $d'_{BOS-aCON}$ (open circles, n=25) and $d'_{TUT-aCON}$ (filled circles, n=25). The gray area ($-0.5 < d'_{BOS-TUT} < 0.5$) includes sites that are non-selective for BOS vs. tutor, while the horizontal rectangular box ($-0.5 < d' < 0.5$) includes sites that are non-selective for BOS vs. aCON, or Tutor vs. aCON. c) The $d'_{BOS-TUT}$ of each RA site is plotted against its $d'_{BOS-REV}$ (open circles, n=22) and d'_{BOS-RO} (filled circles, n=24). As in (b), the gray area indicates the region considered to be non-selective for BOS vs. tutor song, and while the horizontal rectangular box is the region considered non-selective for BOS vs. REV, or BOS vs. RO.

Figure 5-4

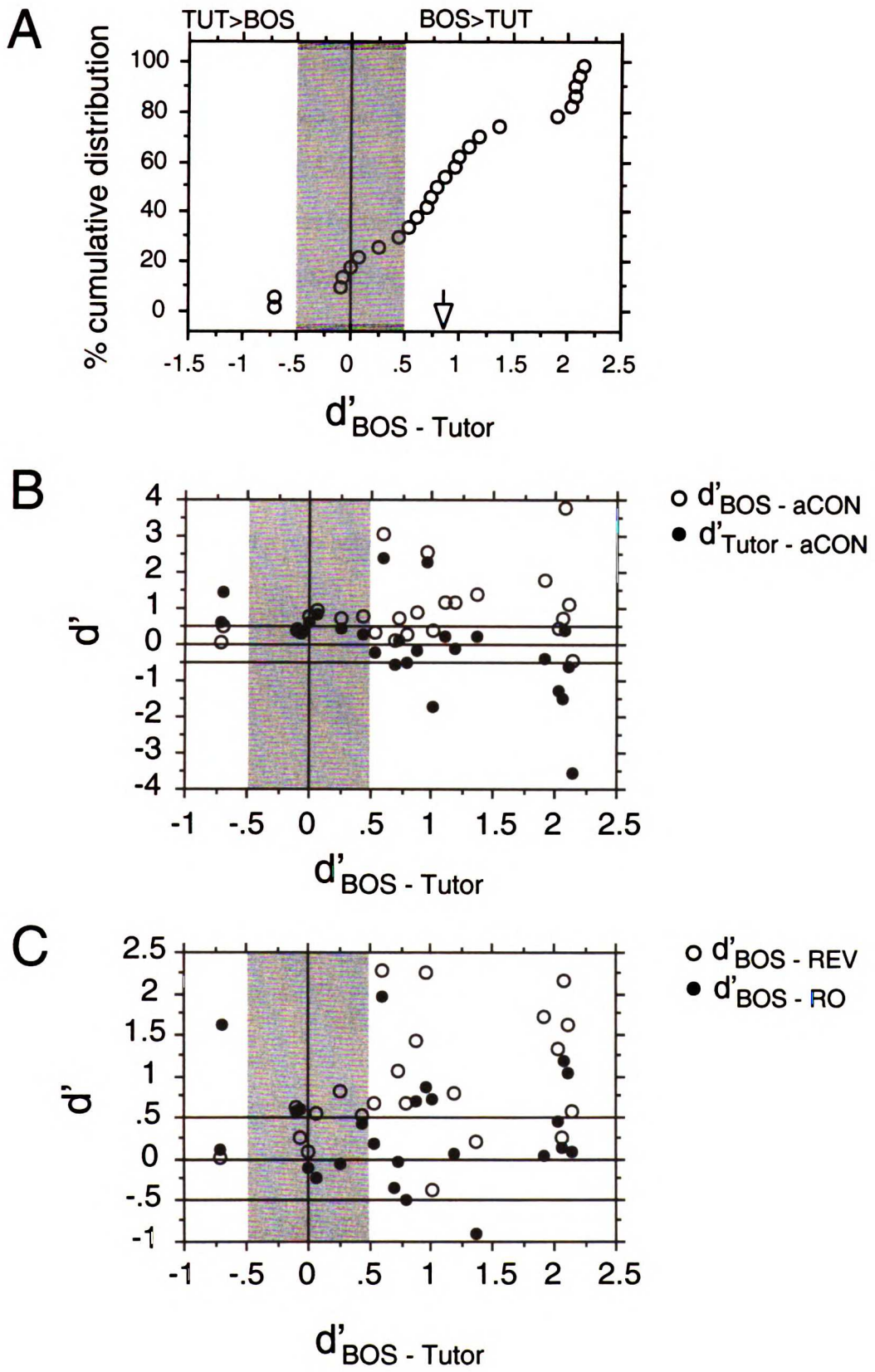
A
TUT>BOS
BOS>TUT
% cumulative distribution
100
80
60
40
20
0
-1.5
-1
-.5
0
.5
1
1.5
2
2.5
d'BOS - Tutor
B
d'
4
3
2
1
0
-1
-2
-3
-4
-1
-.5
0
.5
1
1.5
2
2.5
d'BOS - Tutor
d'BOS - aCON
d'Tutor - aCON
C
d'
2.5
2
1.5
1
.5
0
-.5
-1
-1
-.5
0
.5
1
1.5
2
2.5
d'BOS - Tutor
d'BOS - REV
d'BOS - RO

Figure 5-5 Responses to BOS and simple acoustic stimuli of RA neurons in juveniles a) The response to the BOS of an RA site (same as in Fig. 5-2 and 5-3), and the response to b) a pure tone burst (TONE; 300 msec duration; 1 - 4 kHz), and c) a broad-band white noise burst (WN; 100 or 300 msec duration) of the same RA site. The stimuli are represented as described in Fig. 5-2. d) The mean RS to the BOS of each RA site is plotted against its mean RS to pure tones (open circles, n=15), and to WN (filled circles, n=21). The diagonal line represents equal RS to the BOS and TONE RS or WN RS. e) The mean RS to TONE and WN expressed as a fraction of the BOS RS; error bars indicate SE. The number in parentheses indicates number of RA sites for each mean. f) The cumulative distribution of $d'_{BOS-TONE}$ (open circles, n=15) and d'_{BOS-WN} (filled circles, n=21) from RA sites. The open and filled arrows indicate the mean $d'_{BOS-TONE}$ and d'_{BOS-WN}, respectively. The gray area is considered a non-selective region ($-0.5 < d' < 0.5$).

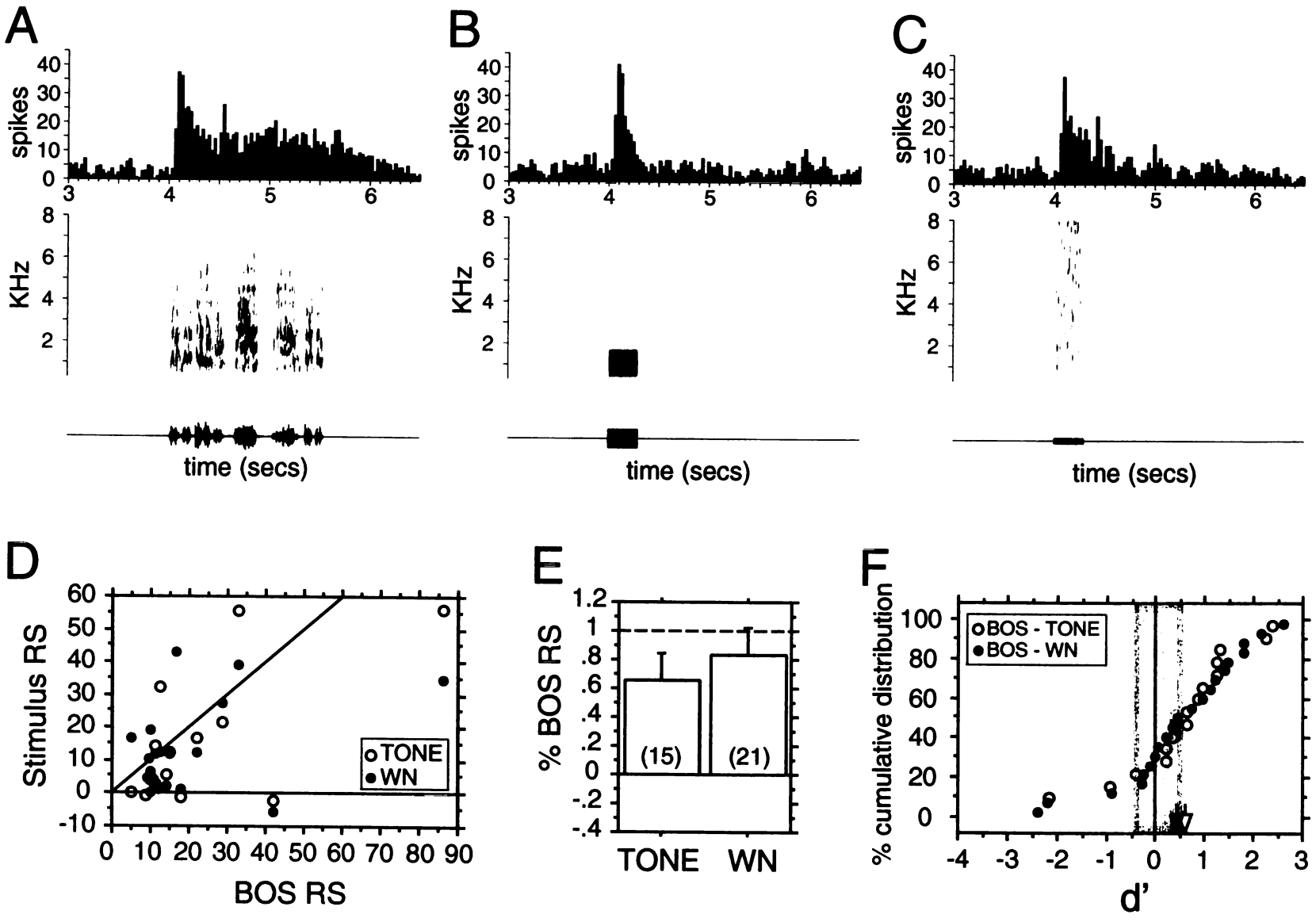
A
B
C
spikes
KHz
time (secs)
D
E
F
Stimulus RS
BOS RS
TONE
WN
% BOS RS
(15)
(21)
% cumulative distribution
BOS - TONE
BOS - WN
d'

Figure 5-5

Figure 5-6 Song selectivity of LMAN neurons at 50 days a) The mean RS to various song types of LMAN sites expressed as a fraction of the BOS RS. The song types are as follows: tutor song (TUT), adult conspecific songs (aCON), brothers' songs (BRO), juvenile conspecific songs (jCON), and heterospecific songs (HET). Numbers in parentheses indicate the number of LMAN sites; error bars indicate SE. b) The mean RS to the BOS of each LMAN site is plotted against its mean RS to the tutor song (open circles, n=27), and mean RS to the adult conspecific songs (filled circles, n=27). The diagonal line represents equal mean RS to the BOS and to the TUT or aCON. c) The cumulative distribution of the $d'_{BOS-TUT}$ (open circles, n=27) and $d'_{BOS-aCON}$ (filled circles, n=27) values from LMAN sites. The open and filled arrows represent the mean $d'_{BOS-TUT}$ and $d'_{BOS-aCON}$, respectively. The gray area includes sites that are considered non-selective ($-0.5 < d' < 0.5$).

Figure 5-6

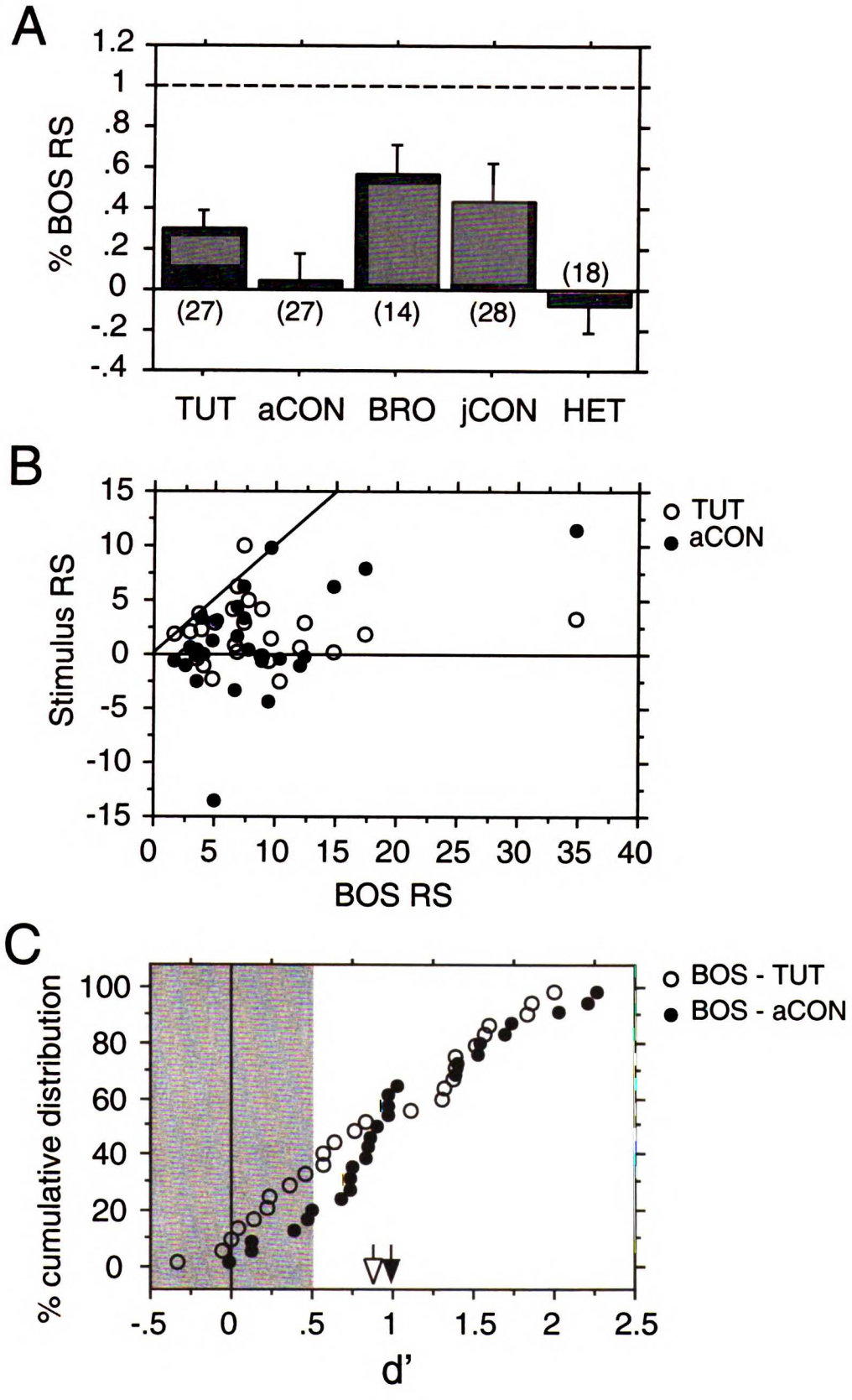
A
1.2
1
.8
.6
.4
.2
0
-.2
-.4
% BOS RS
(27)
(27)
(14)
(28)
(18)
TUT
aCON
BRO
jCON
HET
B
15
10
5
0
-5
-10
-15
Stimulus RS
0
5
10
15
20
25
30
35
40
BOS RS
TUT
aCON
C
100
80
60
40
20
0
% cumulative distribution
-.5
0
.5
1
1.5
2
2.5
d'
BOS - TUT
BOS - aCON

Figure 5-7 BOS order selectivity of LMAN neurons in juveniles a) The fraction of BOS RS that represents the mean RS to the BOS in reverse (REV) and to the mean BOS in reverse order (RO). Number of LMAN sites for each mean is indicated by the number in parentheses. Error bars indicate SE. b) The mean RS to the BOS and the BOS in reverse (open circles, n=24) or reverse order (filled circles, n=23) for each LMAN site are plotted against each other. The diagonal represents the unity line, where BOS RS = stimulus RS. c) The cumulative distribution of $d'_{BOS-REV}$ (open circles, n=24) and d'_{BOS-RO} (filled circles, n=23) values from LMAN sites. Arrows indicate the mean $d'_{BOS-REV}$ (open arrow) and mean d'_{BOS-RO} (filled arrow). The gray area indicates the region considered non-selective for BOS vs. REV, and BOS vs. RO.

Figure 5-7

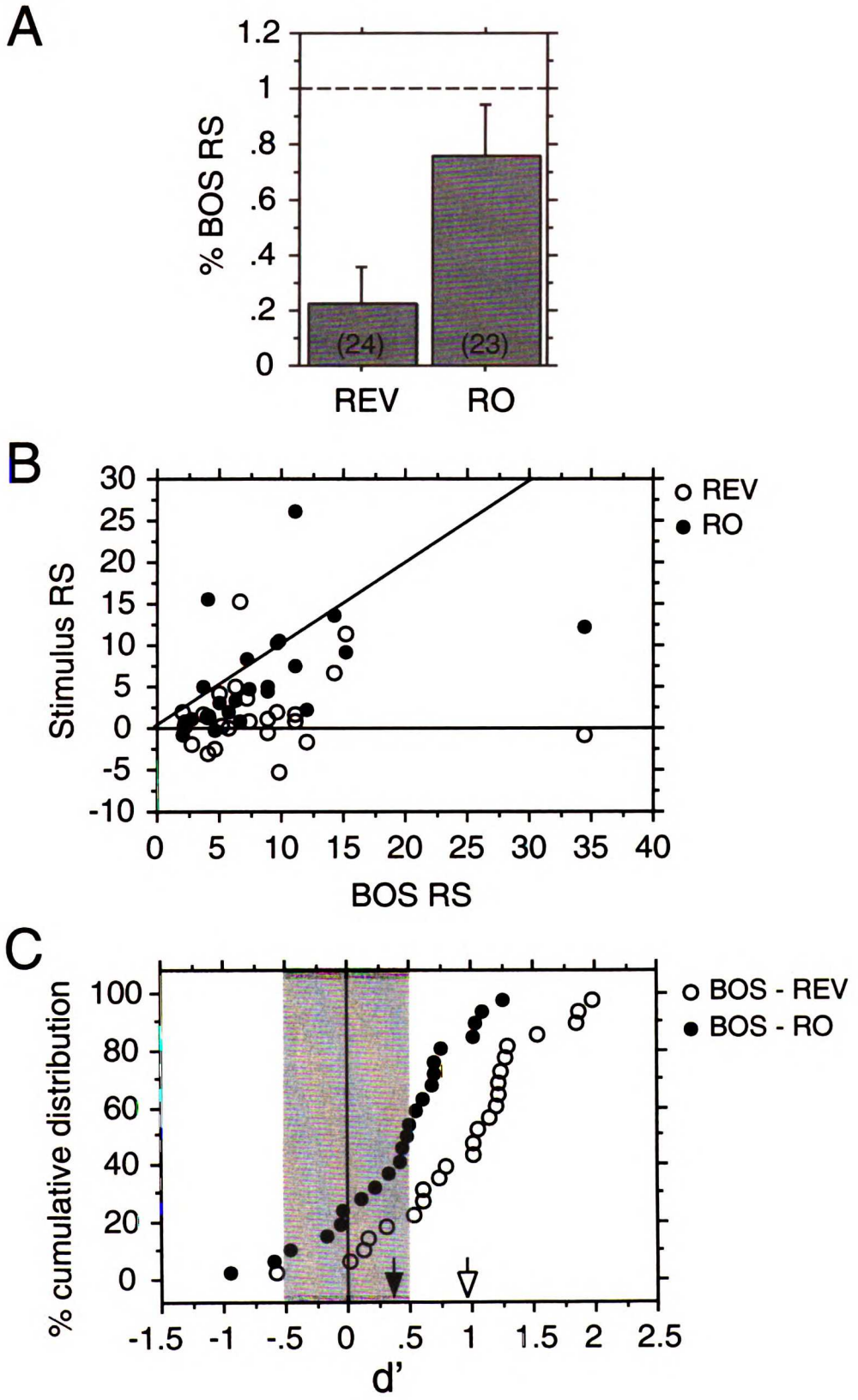
A
1.2
1
.8
.6
.4
.2
0
% BOS RS
(24)
(23)
REV
RO
B
30
25
20
15
10
5
0
-5
-10
Stimulus RS
0
5
10
15
20
25
30
35
40
BOS RS
REV
RO
C
100
80
60
40
20
0
% cumulative distribution
-1.5
-1
-.5
0
.5
1
1.5
2
2.5
d'
BOS - REV
BOS - RO

Figure 5-8 Selectivity for BOS vs. simple acoustic stimuli of LMAN in juveniles a) The mean RS to pure tone bursts (TONE; 1-4 kHz) and a broad-band white noise burst (WN; 100 or 300 msec duration) expressed as a fraction of the BOS RS. Numbers in parenthesis are numbers of LMAN sites, and error bars indicate SE. b) The mean RS to BOS of each LMAN site is plotted against its mean RS to TONE (open circles, n=17), and to WN (filled circles, n=25). The diagonal line represents the unity line, where the RS to BOS are equal to the mean TONE RS or WN RS. c) The cumulative distribution of $d'_{BOS-TONE}$ (open circles, n=17; mean = open arrow) and d'_{BOS-WN} (filled circles, n=25; mean = filled arrow) values from LMAN sites. The gray shading indicates the region considered as non-selective ($-0.5 < d' < 0.5$).

Figure 5-8

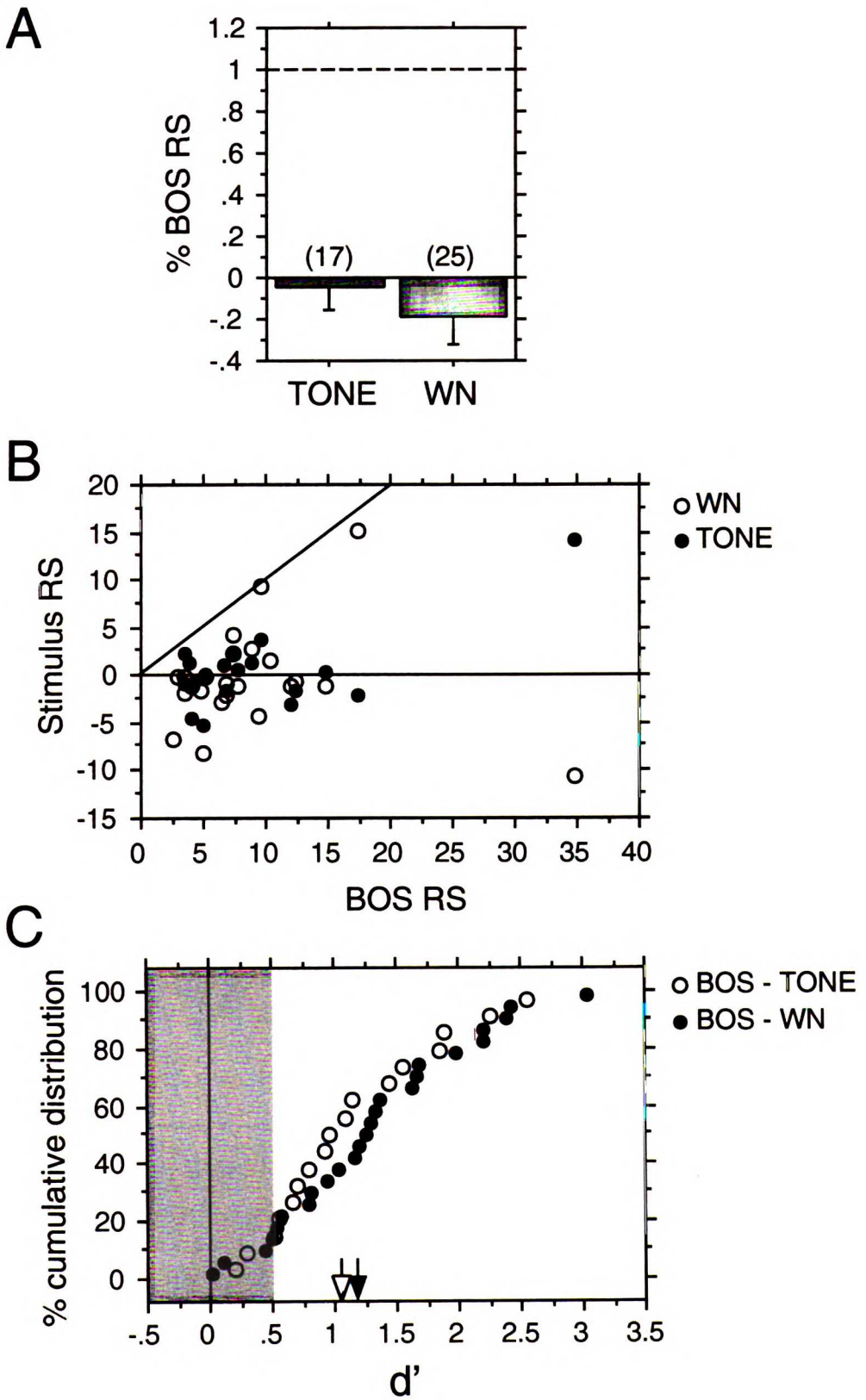
A
1.2
1
.8
.6
.4
.2
0
-.2
-.4
% BOS RS
(17)
(25)
TONE
WN
B
20
15
10
5
0
-5
-10
-15
Stimulus RS
0
5
10
15
20
25
30
35
40
BOS RS
WN
TONE
C
100
80
60
40
20
0
% cumulative distribution
-.5
0
.5
1
1.5
2
2.5
3
3.5
d'
BOS - TONE
BOS - WN

Figure 5-9 Distribution of response strength to simple acoustic stimuli of RA, LMAN and HVc neurons in juveniles a) The distribution of RS, expressed as a fraction of the BOS RS at each site, to pure tone (TONE; 1-4 KHz, 300 msec duration) and broad-band white noise bursts (WN; 100 or 300 msec duration) in juvenile RA, b) in juvenile LMAN, and c) in juvenile HVc neurons. Each box plot shows five horizontal lines that indicate the 10th, 25th, 50th, 75th, and 90th percentiles of the % BOS RS response strength to each song type. Circles represent % BOS RS response strength that are below or above the 10th and 90th percentiles, respectively.

Figure 5-9

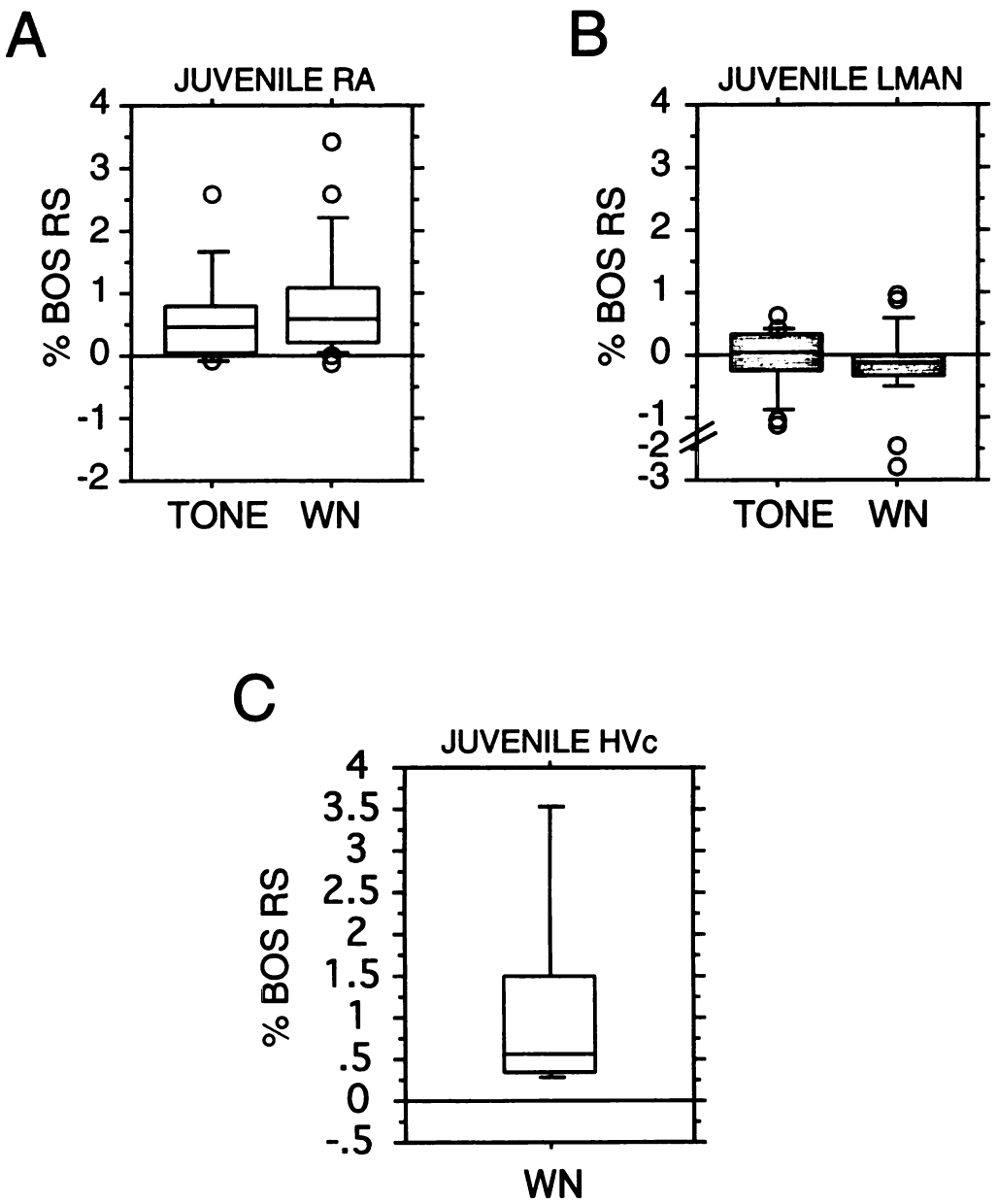
A
JUVENILE RA
% BOS RS
4
3
2
1
0
-1
-2
TONE
WN
B
JUVENILE LMAN
% BOS RS
4
3
2
1
0
-1
-2
-3
TONE
WN
C
JUVENILE HVc
% BOS RS
4
3.5
3
2.5
2
1.5
1
.5
0
-.5
WN

Figure 5-10 Comparison of selectivity of RA and LMAN responses in juveniles a) The mean d' values and b) the mean selectivity indices of each nucleus from each bird for all the stimuli comparisons examined. Filled circles are data from nucleus RA, while open circles are data from LMAN. c) The mean d' values and d) the mean selectivity indices of RA (filled circles) and LMAN (open circles) from each bird for BOS order selectivity comparisons. In the d' plots, means > 0.5 indicate preference for the BOS, while in the SI plots, means > 0.67 indicate that the response strength to the BOS was at least twice as much as the response to the other stimulus. Error bars indicate standard error. The numbers in parentheses indicate the number of RA (first number) and LMAN (second number) nuclei included in calculating the mean. *p<.05, **p<.01, paired student's t-test between RA and LMAN of each bird.

Figure 5-10

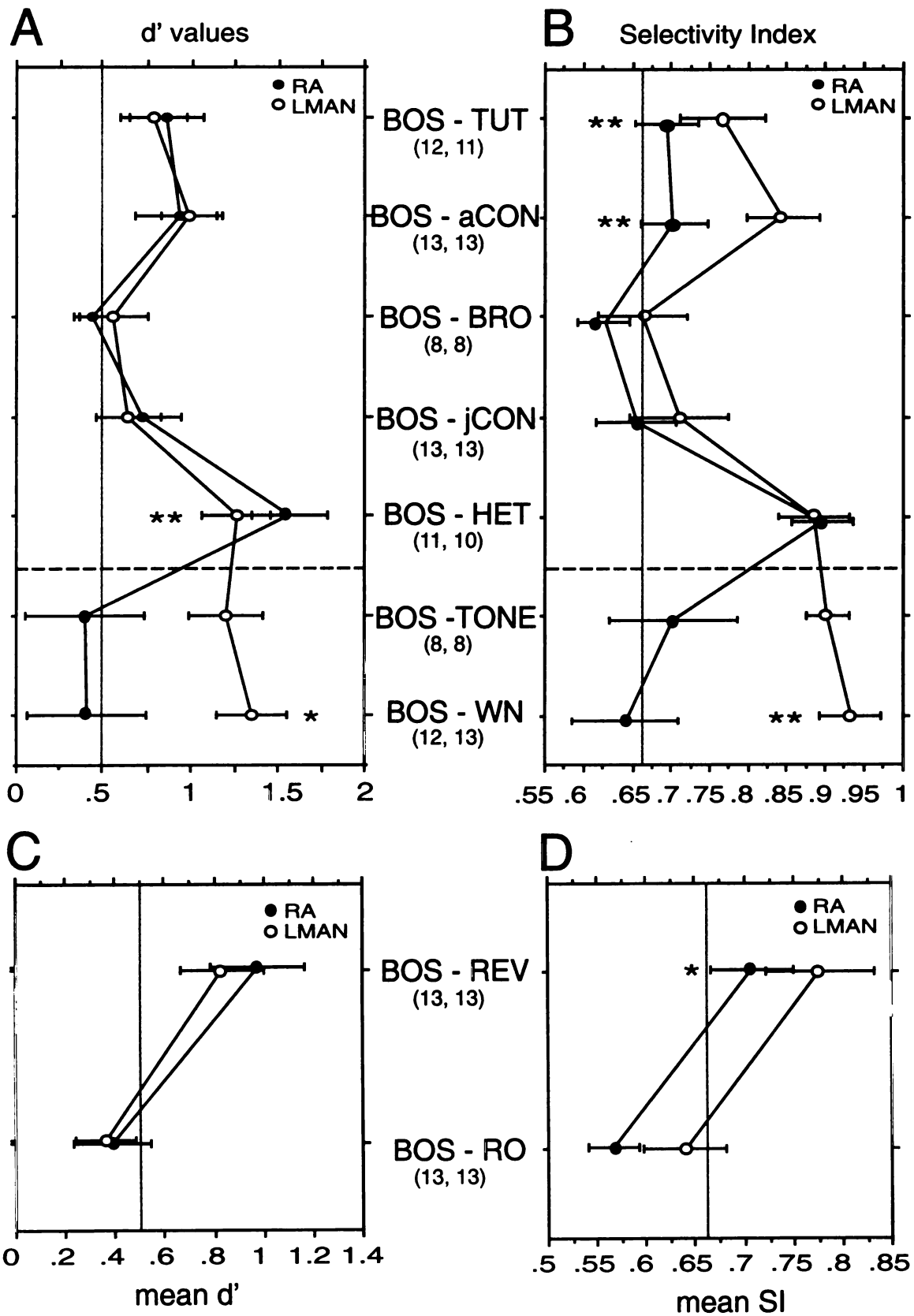
A
d' values
B
Selectivity Index
RA
LMAN
BOS - TUT
(12, 11)
BOS - aCON
(13, 13)
BOS - BRO
(8, 8)
BOS - jCON
(13, 13)
BOS - HET
(11, 10)
BOS -TONE
(8, 8)
BOS - WN
(12, 13)
**
**
**
*
**
0 .5 1 1.5 2
.55 .6 .65 .7 .75 .8 .85 .9 .95 1
C
D
BOS - REV
(13, 13)
BOS - RO
(13, 13)
*
0 .2 .4 .6 .8 1 1.2 1.4
mean d'
.5 .55 .6 .65 .7 .75 .8 .85
mean SI

Figure 5-11 Comparison of tutor song selectivity of RA and LMAN responses in juveniles a) The mean d' values and b) the mean selectivity indices of RA (filled circles) and LMAN (open circles) from each bird for tutor song comparisons. A mean d' value > 0.5 indicates preference for the tutor song vs. other stimulus type, while a mean SI value > 0.67 indicates a tutor song response strength that is at least 2X that of the RS to the other stimulus type. Error bars indicate standard error, and numbers in parentheses indicate the number of nuclei for each mean d' or SI. *p<.05, paired student's t-test between RA and LMAN of each bird

Figure 5-11

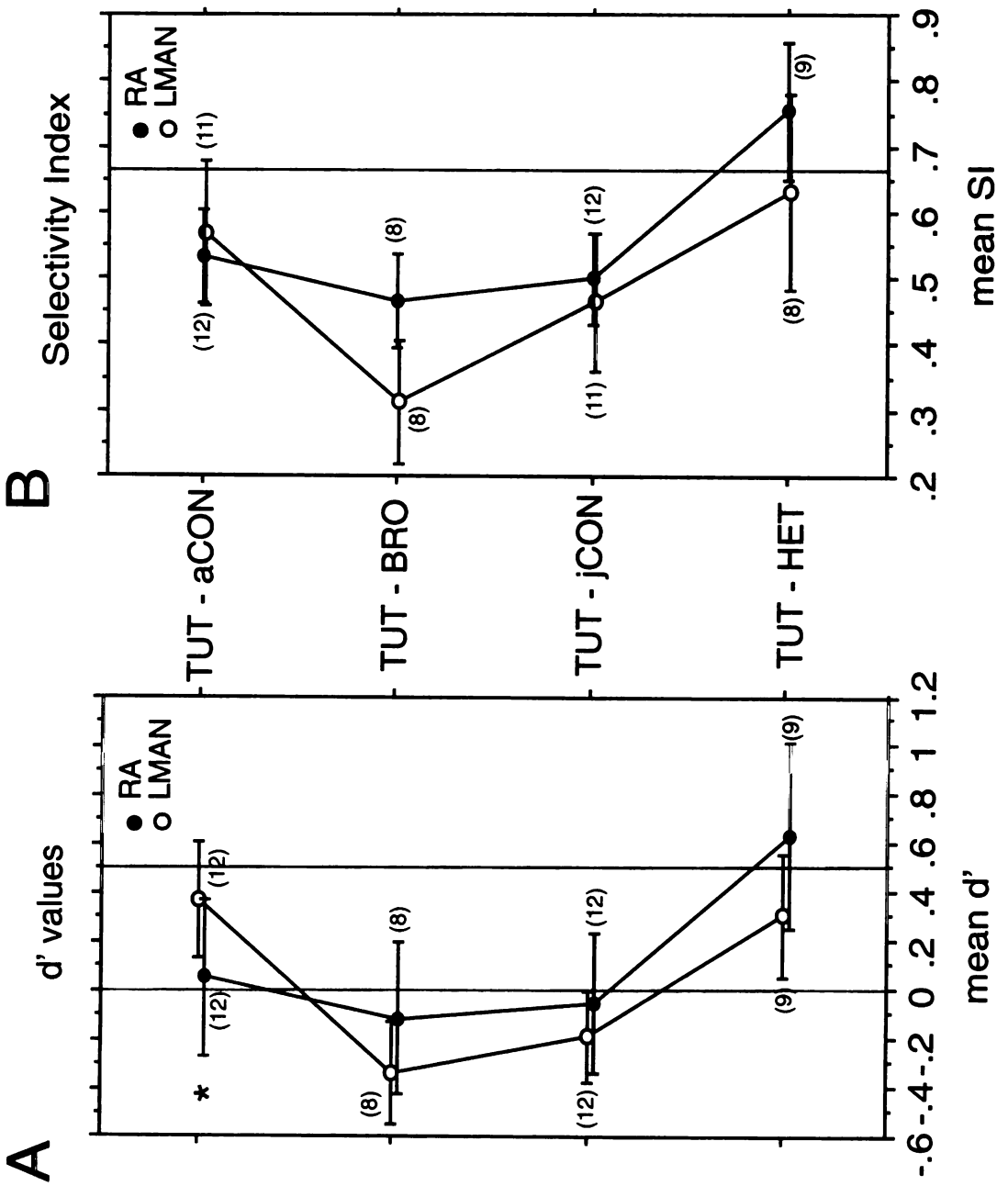
A
d' values
● RA
o LMAN
mean d'
-.6 -.4 -.2 0 .2 .4 .6 .8 1 1.2
TUT - aCON
TUT - BRO
TUT - jCON
TUT - HET
*
(12)
(12)
(8)
(8)
(12)
(12)
(9)
(9)
B
Selectivity Index
● RA
o LMAN
mean SI
.2 .3 .4 .5 .6 .7 .8 .9
(12)
(11)
(8)
(8)
(11)
(12)
(8)
(9)

Figure 5-12 Selectivity and responses of RA in juveniles and adults a) Mean d' values for all stimulus type comparisons of all RA sites in juveniles (circles) and adults (squares). b) Mean RS, normalized by the BOS RS at each site, to different song types and broad-band white noise of RA sites in juveniles and c) in adults. d) Mean RS, expressed as a fraction of the BOS RS, to BOS in reverse and reverse order of RA sites in juveniles and e) in adults. Numbers in parentheses in b-e are number of RA sites; error bars indicate SE in all plots. *p<.001, **p<.0001, unpaired t-test between juveniles and adults

Figure 5-12

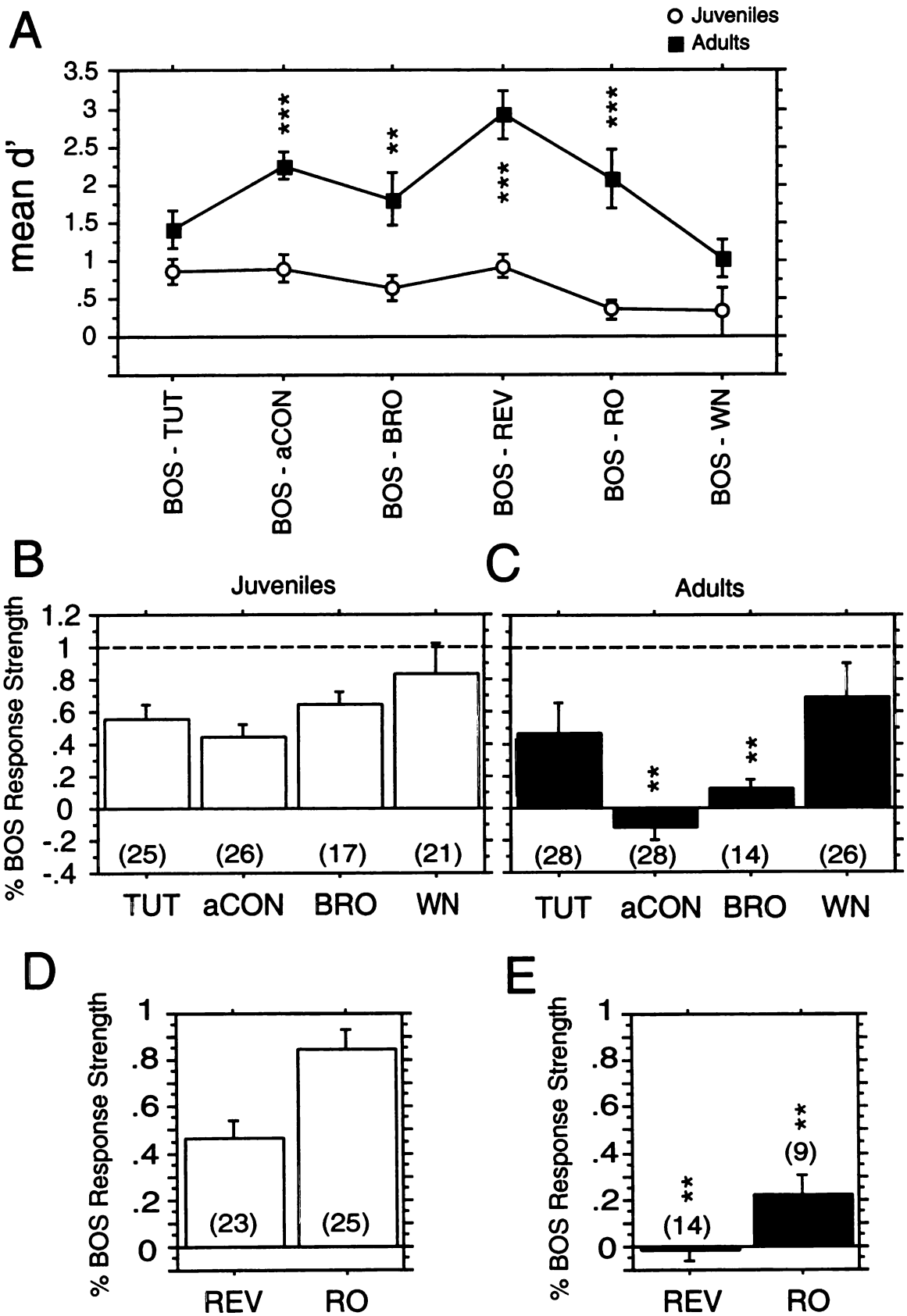
A
Juveniles
Adults
mean d'
3.5
3
2.5
2
1.5
1
.5
0
***
**
***
***
BOS - TUT
BOS - aCON
BOS - BRO
BOS - REV
BOS - RO
BOS - WN
B
Juveniles
% BOS Response Strength
1.2
1
.8
.6
.4
.2
0
-.2
-.4
(25)
(26)
(17)
(21)
TUT
aCON
BRO
WN
C
Adults
**
**
**
(28)
(28)
(14)
(26)
TUT
aCON
BRO
WN
D
% BOS Response Strength
1
.8
.6
.4
.2
0
(23)
(25)
REV
RO
E
% BOS Response Strength
1
.8
.6
.4
.2
0
**
**
(14)
(9)
REV
RO

Figure 5-13 Comparison of tutor selectivity of RA responses in juveniles and adults a) The cumulative distribution of $d'_{TUT-aCON}$ values from RA sites in juveniles (open squares, n=26) and adults (filled squares, n=28). The open and filled arrows indicate the mean $d'_{TUT-aCON}$ in juveniles and adults, respectively. b) The cumulative distribution of $d'_{TUT-BRO}$ values from RA sites in juveniles (open squares; mean = open arrow, n=17) and adults (filled squares; mean = filled arrow, n=14). In both plots, the red symbols indicate that for that site, the response to at least one of the stimuli being compared is significant ($p<0.5$, paired t-test between firing rate in response to the stimulus and spontaneous firing rate of each trial). In (a) and (b), the gray area represents the region considered to be non-selective ($-0.5 < d' < 0.5$).

Figure 5-13

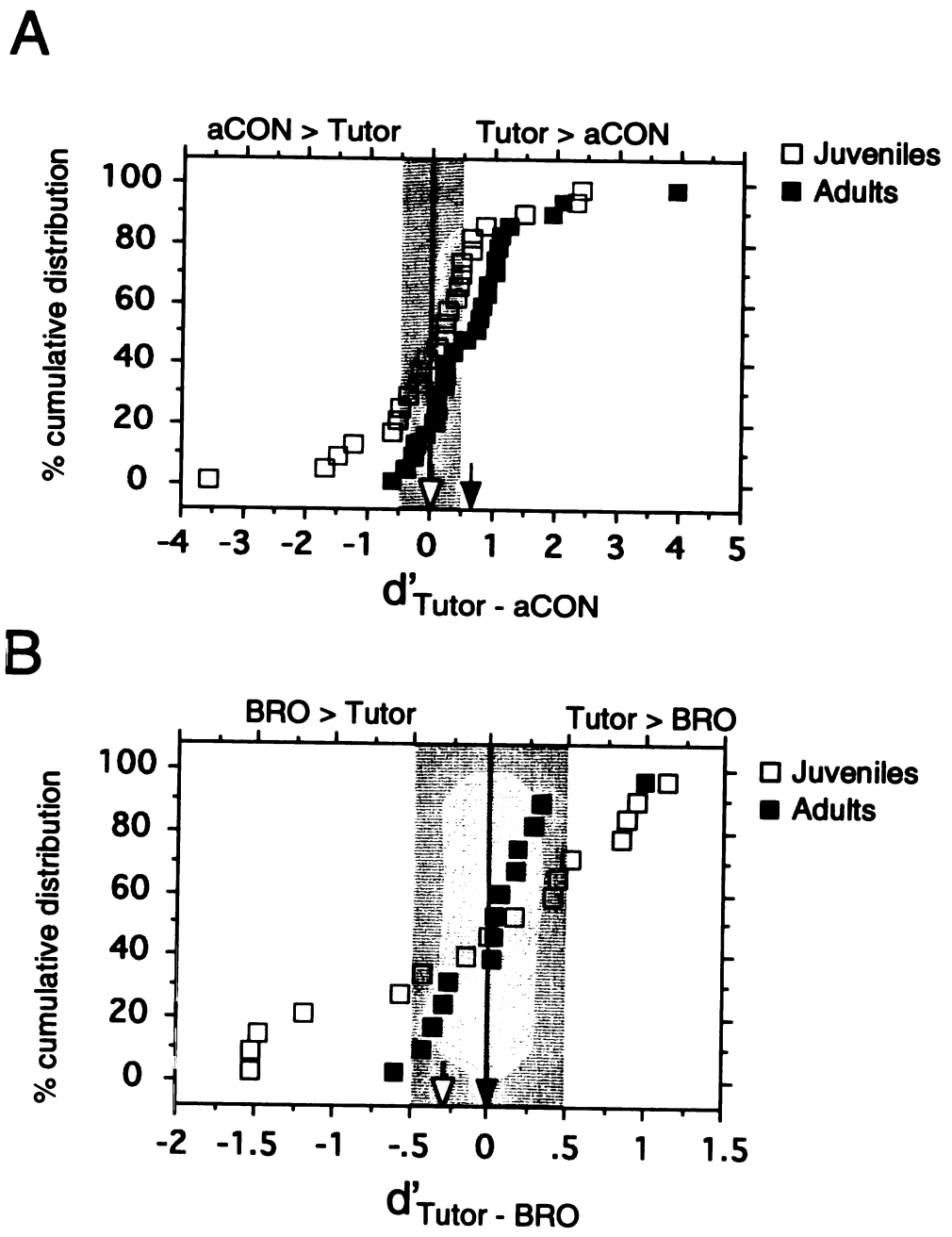
A
aCON > Tutor
Tutor > aCON
Juveniles
Adults
% cumulative distribution
100
80
60
40
20
0
-4 -3 -2 -1 0 1 2 3 4 5
d'Tutor - aCON
B
BRO > Tutor
Tutor > BRO
Juveniles
Adults
% cumulative distribution
100
80
60
40
20
0
-2 -1.5 -1 -.5 0 .5 1 1.5
d'Tutor - BRO

Figure 5-14 Comparison of normalized RS in adult LMAN, RA and HVc a) The mean RS to different song stimuli and broad-band white noise, normalized by the typical maximum response at each site (BOS RS), in adult LMAN, b) RA, and c) HVc. d) The mean RS to BOS in reverse (REV) and reverse order (RO), expressed as a fraction of the BOS RS in adult LMAN, e) RA, and f) HVc. Error bars indicate SE, and numbers in parentheses are the number of sites in each nucleus.

Figure 5-14

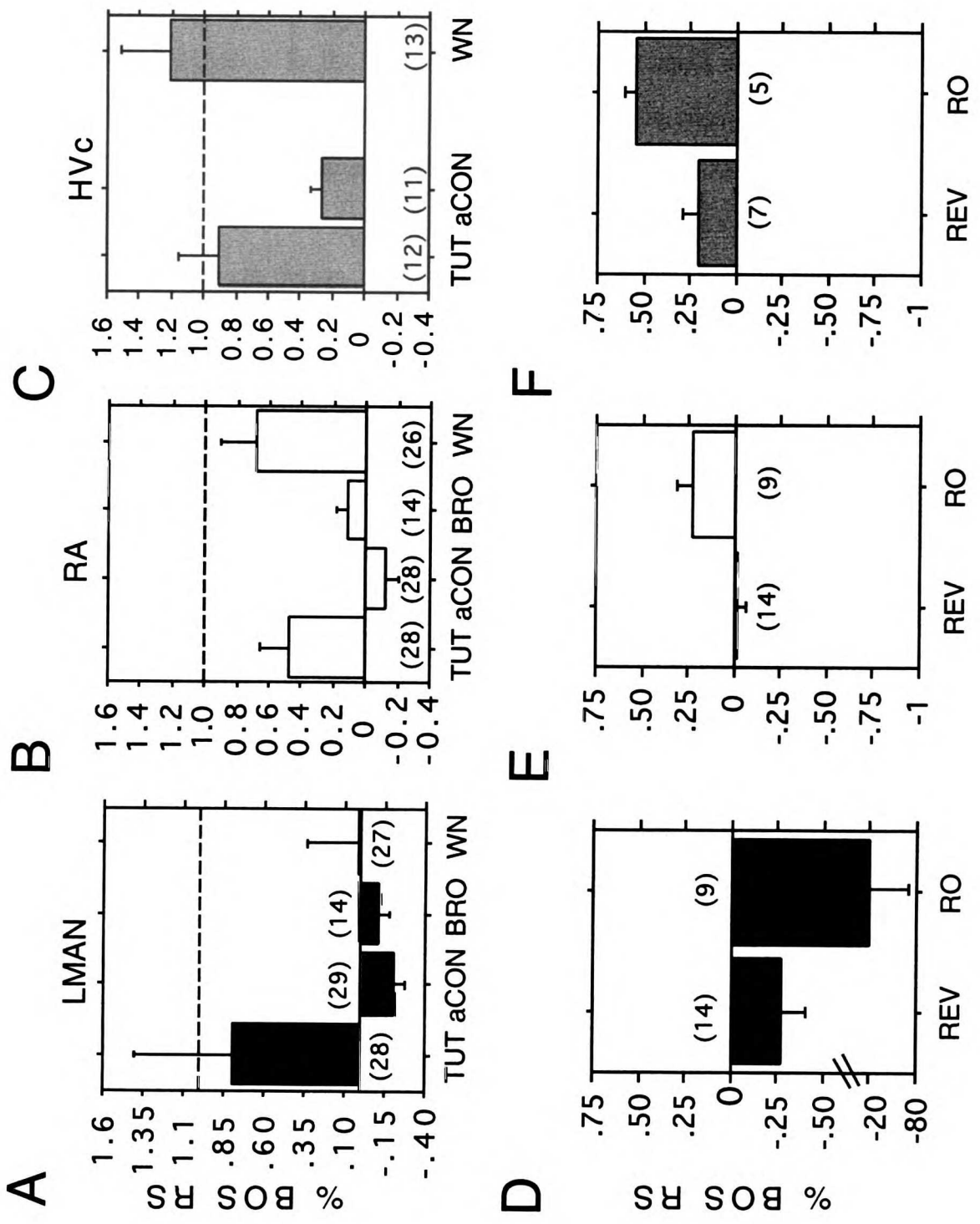
A
LMAN
B
RA
C
HVc
D
E
F
% BOS RS
TUT aCON BRO WN
REV RO
(28) (29) (14) (27)
(28) (28) (14) (26)
(12) (11) (13)
(14) (9)
(14) (9)
(7) (5)

Figure 5-15 Comparison of selectivity between RA, LMAN and HVc responses in adults a) The mean d' values and b) selectivity indices (SI) of RA (square), LMAN (filled circle), and HVc (open circle) from each bird, for each stimulus type comparison examined. A mean d' > 0.5 indicates preference for the BOS over the other stimulus type, while an SI mean > 0.67 indicates a BOS RS that is twice as much as the RS to the other stimulus type. Numbers in parenthesis indicate the number of RA, LMAN and HVc nuclei (in that order) involved in calculating the mean d' and SI, except for the BOS - REV comparison. In the BOS - REV comparison, the top row pertains to number of nuclei for the mean d' values, while the bottom row is for the mean SI values. Error bars indicate SE. *p<.05, **p<.01, paired student's t-test between means of the nuclei indicated in the comparison

Figure 5-15

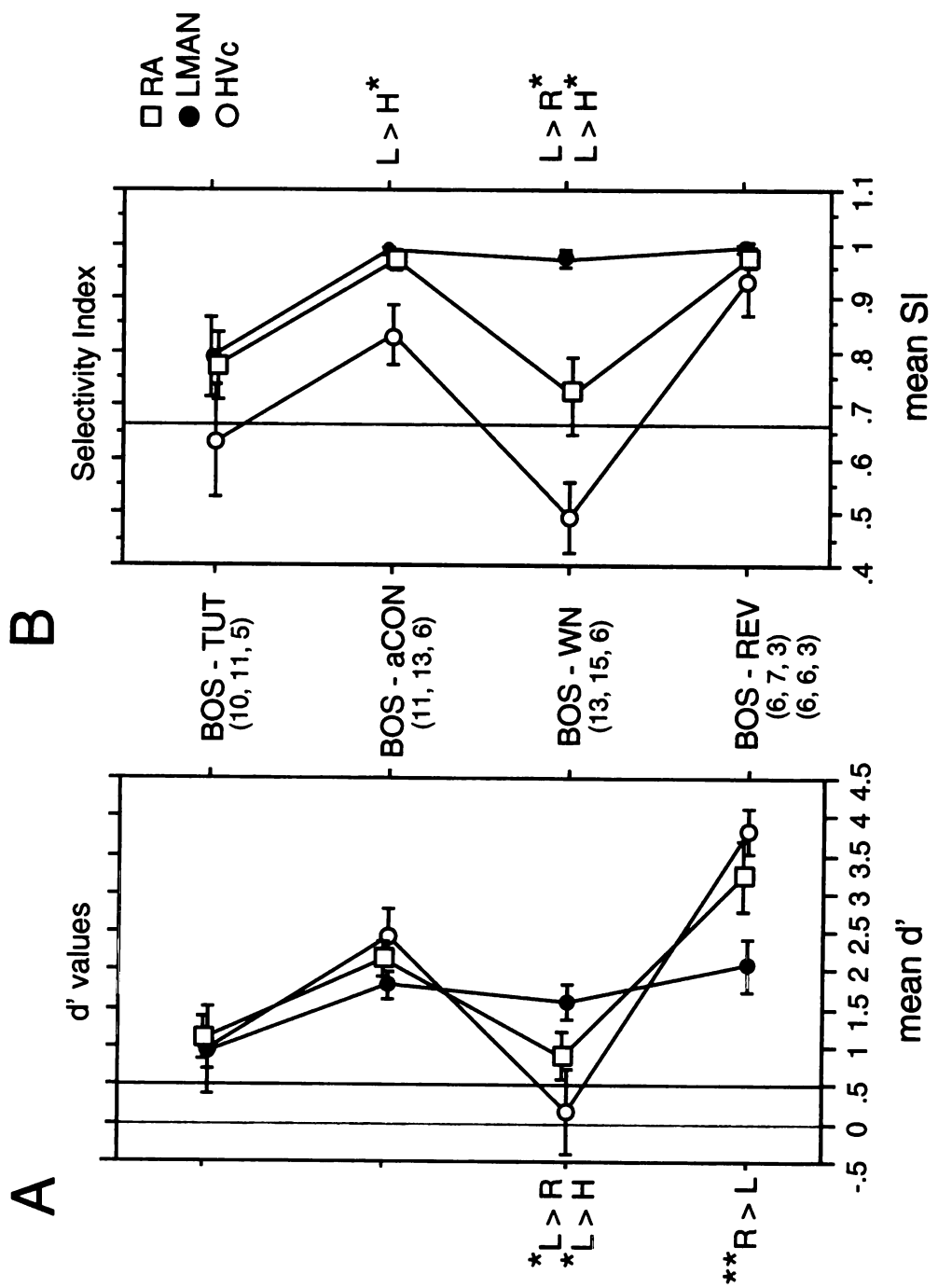
A
B
d' values
mean d'
-.5 0 .5 1 1.5 2 2.5 3 3.5 4 4.5
Selectivity Index
mean SI
.4 .5 .6 .7 .8 .9 1 1.1
RA
LMAN
HVc
BOS - TUT (10, 11, 5)
BOS - aCON (11, 13, 6)
BOS - WN (13, 15, 6)
BOS - REV (6, 7, 3) (6, 6, 3)
L > H*
L > R* L > H
*L > R
*L > H
**R > L

Table 5-1. Song and order selective sites in LMAN, RA and HVc (d'>.5).

Selectivity	JUVENILES		ADULTS		
	LMAN	RA	LMAN	RA	HVc
BOS > Tutor	17/26(65%)	17/25(68%)	20/28(71%)	24/28(86%)	6/12(50%)
BOS > aCon	21/27(78%)	17/26(65%)	29/29(100%)	28/28(100%)	11/11(100%)
BOS > Brother	8/14(57%)	9/17(53%)	13/14(93%)	12/14(86%)	
BOS > jCon	19/28(68%)	16/27(59%)			
BOS > Het	16/18(89%)	17/18(94%)			
BOS > WN	22/25(88%)	10/21(48%)	24/27(89%)	16/26(62%)	6/12(50%)
BOS > Rev	19/24(79%)	17/23(74%)	13/14(93%)	14/14(100%)	7/7(100%)
BOS > RO	10/23(43%)	9/25(36%)	8/9(89%)	9/9(100%)	5/5(100%)
Tutor > BOS	0/26(0%)	2/25(8%)	1/28(4%)	2/28(7%)	2/12(17%)
Tutor > aCON	8/26(31%)	6/25(24%)	10/25(40%)	14/26(54%)	5/9(56%)
Tutor > Brother	2/13(15%)	5/16(31%)	1/14(7%)	1/14(7%)	
Tutor > WN	13/23(57%)	4/19(21%)	9/18(50%)	2/14(14%)	3/11(27%)

BOS = bird's own song

aCon = adult conspecific songs

jCon = juvenile (age-matched) conspecific songs

Het = heterospecific songs

WN = broad-band white noise burst (100 or 300 msec duration)

Rev = reverse BOS

RO = BOS in reverse order

Table 5-2. Fraction of neuronal sites that exhibtied significant inhibitory responses in juvenile and adult LMAN, RA and HVc.

STIMULUS	JUVENILES			ADULTS		
	LMAN	RA	HVc	LMAN	RA	HVc
White Noise Burst	5/25 (20%)	0/21	0/7	8/27 (30%)	0/26	0/13
Tutor	0/27	0/25	0/7	3/28 (11%)	2/28 (7%)	0/12
Adult Conspecific	1/27 (4%)	1/26 (4%)	1/7 (14%)	9/29 (31%)	3/28 (11%)	0/11
Juvenile Conspecific	1/28 (4%)	1/27 (4%)	0/6			
Heterospecific	1/18 (6%)	3/18 (17%)	0/4			
BOS.reverse	0/24	0/23	0/6	1/14 (7%)	1/14 (7%)	0/7
Total number of sites:	6/28 (21%)	3/27 (11%)	1/7 (14%)	18/29 (62%)	6/28 (21%)	0/13

BOS = bird's own song

Chapter 6:

Future Directions

Fos induction in the song system

The induction of an immediate early gene (IEG) product, such as Fos, has been used as a marker for activity in neural systems, although there is not always a correspondence between neuronal activity and immediate early gene expression (see discussion in Chapter 2). An advantage of using Fos induction as a marker for activity is that it allows one to survey the entire brain. Thus, one can compare different brain areas in the same behavioral state. For example, in Chapter 2, we showed that at least two specific populations of neurons in the motor pathway of the song system are active during the motor act of singing: the RA-projecting neurons in HVc, and RA neurons. However, one disadvantage of Fos induction is its low temporal resolution, since the assay for Fos induction is conducted post-mortem. For example, it is unclear when the Fos induction occurred during the singing behavior, and for how long the Fos protein remained induced. It would therefore be useful to determine the level of Fos expression at different time points during, and after singing. However, because Fos induction is highly correlated with the amount of time spent singing, this experiment would require a consistent behavior from all subjects. This type of experiment might also reveal other songbird brain areas that express singing induced Fos that were not observed in the experiments described in Chapter 2, since we focused only on one time frame.

Because Fos is a transcription factor, its expression indicates the transduction of neuronal activity to changes in the neuron's genetic composition. With the advent of cDNA array technology, the experiment of determining which genes are regulated by singing-induced FOS expression has become plausible. Fos (complexed with another transcription factor, Jun) binds to a specific DNA sequence, the AP-1 site (Sheng and Greenberg, 1990). Thus, genes that are regulated by this site, and whose levels of expression correlate well with an increase in Fos expression during singing, are those genes that are most likely regulated by the singing-induced Fos. The identity of these genes might reveal the role of Fos induction during singing, and moreover, would indicate some of the neuronal consequences

of singing in adults. A caveat is that the expression of these genes may not be all or nothing, that is, only expressed during singing or non-singing. Thus, levels of expression of the genes will have to be carefully quantified to assess any significant changes in gene expression that are tightly correlated singing. Singing-induced Fos induction might be involved in the maintenance of adult crystallized song. Hence, genes that are necessary in maintaining the strength and structural integrity of synapses in RA that are involved in the motor expression of the learned song may prove to be regulated by the singing-induced Fos expression.

Despite observations that Area X and LMAN, two nuclei in the anterior forebrain pathway, are active during singing (Hessler and Doupe, 1999a; b), Fos induction was not observed in either nucleus in the experiments described in Chapter 2. This serves as a reminder that Fos induction does not necessarily result from all types of neural activity. The lack of Fos induction observed in these two nuclei during singing in adults has several possible causes. One possibility is that the time course of Fos expression in these nuclei might be different from HVc and RA, as discussed above. A second possibility is that singing in adults may not produce the specific pattern of activity in the AFP required to induce Fos expression. For instance, burst stimulation of the limbic forebrain has been shown to induce Fos expression, whereas non-burst stimulation does not (Chergui et al, 1996). Direct recordings of the activity in LMAN and Area X in awake singing birds have shown that this activity varies in its pattern of firing, based on the social context of singing. That is, when birds sing alone, producing so called undirected song, the activity in LMAN and Area X is higher, exhibits more bursts, and is more variable across song renditions than when birds are singing towards another bird (directed singing) (Hessler and Doupe, 1999a). A large percent of the singing in the experiments in Chapter 2 was directed singing. Thus, the lower and less bursty activity during directed singing may not have resulted in Fos expression in LMAN and Area X. Another IEG, Zenk, has been shown to be more strongly expressed in the song system in undirected vs. directed singing (Jarvis et al, 1998). The

same might be true for Fos, or it may be that Fos has a higher threshold for induction or a more rapid adaptation in response to neuronal activity, as has been observed in other systems (Cole et al, 1989; Sheng and Greenberg, 1990).

Recent studies have shown that LMAN activity is required for vocal plasticity in adults. Adult zebra finches that are deafened, or that receive altered auditory feedback, eventually produce degraded songs (Nordeen and Nordeen, 1992; Williams and McKibben, 1992; Brainard and Doupe, 2000; Leonardo and Konishi, 2000; Lombardino and Nottebohm, 2000). An intact LMAN is required for these changes in adult crystallized song to occur (Williams and Mehta, 1999; Brainard and Doupe, 2000). It is possible that the pattern of activity in LMAN of adult birds whose songs are degraded is different from that in adult birds with normal songs. In the experiments in Chapter 2, only 2/10 of the deaf birds studied produced degraded songs. In the future, it will be important to determine whether singing-induced Fos expression occurs in LMAN in adult birds with deteriorating songs. Moreover, this experiment would also identify other brain structures that are active during singing of degraded songs, suggesting that these structures are involved in song maintenance in adults.

Activation of IEGs and factors upstream of these genes, such as cAMP response element binding protein (CREB), have been observed to be necessary during learning and developmental plasticity (Kaang et al, 1993; Bourtchuladze et al, 1994; Yin et al, 1994; for reviews, see Robertson, 1991; Kaczmarek, 1992; 1993; Carew, 1996). Because the AFP is necessary during song learning, Fos induction might be present in the AFP of juveniles undergoing song learning. The transcription factor, cAMP response element binding protein (CREB), which regulates the expression of Fos, has been shown to be present in Area-X projecting neurons of HVc and Area X neurons (Sakaguchi et al, 1999). In adult zebra finches, CREB was activated in response to conspecific song only in the HVc neurons (Sakaguchi et al, 1999). However, in juveniles undergoing song learning, CREB was activated during passive song presentation in Area X neurons as well as HVc neurons

(Sakaguchi, personal communication). Fos expression might therefore also be induced in the AFP during passive presentation of song in birds still learning to sing. In addition, Fos expression in juveniles during tutor song presentation might identify other brain structures that are active during sensory learning. One such area, the caudal part of the neostriatum (NCM), has been shown to express Zenk and Fos protein during tutor song presentation in adults (Bolhuis et al, 2000). Moreover, in this study, the levels of Zenk and Fos expression in NCM correlated well with the fraction of song elements copied from the tutor song. However, these experiments were conducted in adults, and studies in juveniles undergoing song learning may reveal more or different brain structures. It is also possible that Fos is induced in the juvenile AFP during singing, or during both tutor song presentation and singing. For example, the IEG Zenk is induced in AFP neurons during singing in juvenile birds (Jin and Clayton, 1997).

Computational models of the functional connectivity in the song system

Activity between indirectly connected areas in the song system is strongly correlated, as shown by significant peaks in the HVc-LMAN coherency functions, and the LMAN-RA peak that is due to the common input of HVc to LMAN and RA. This has led to the hypothesis that the functional connectivity within the song system involves broad divergent and reconvergent connections between nuclei, and extensive intrinsic connections within some song nuclei. The latter idea is supported by the observation that the strength and timing of the correlated activity between LMAN and RA did not correlate with how well the locations of the LMAN and RA recording sites matched topographically. A computational model of the AFP (from HVc to LMAN) could be constructed to determine what degree of synaptic connectivity between and within nuclei is required to obtain correlated activity between indirectly connected nuclei. The model would contain at least three levels of neuronal populations: HVc neurons, a set of neurons to represent the connections between HVc and LMAN ('intermediate neurons'), and LMAN neurons (see Fig. 3-12). These three

populations will be functionally connected via broad divergent and reconvergent connections in the following manner: HVc -> intermediate neurons, intermediate neurons ->LMAN. Each population of neurons will also have extensive intrinsic connections, which will initially be all excitatory, although it may be necessary to add inhibitory connections. Initially, all the connections will have the same synaptic weight, where each pre-synaptic input has the same probability of eliciting a response in the post-synaptic neurons. Activity will be injected into the HVc level of neurons, and its propagation will be observed. The goal would be to determine whether the activity between HVc and LMAN neurons in the model is significantly correlated. The model can also be used to determine the smallest number of divergent and reconvergent connections, and intrinsic connections, that are sufficient to produce the observed correlated activity between indirectly connected areas. To 'remove' a functional connection, its synaptic weight can be set to zero. It is also possible that the broad divergent and reconvergent connections alone are sufficient to produce correlated activity between indirectly connected areas in the song system. To test this, the intrinsic connections within neuronal populations in the computational model can be removed, to determine if they are necessary for indirect correlated activity.

The direct LMAN-RA correlated activity can also be modeled computationally to provide hypotheses about possible neural mechanisms that may underlie the observed developmental changes in the direct LMAN-RA correlated activity. From 50 days of age to adulthood, the direct LMAN-RA correlation during spontaneous activity increased in peak strength, and showed a decrease in time delay, and jitter in time delays (width of the peak). As discussed in Chapter 4, one factor that may contribute to the change in timing is the developmental decrease in NMDA receptor kinetics in LMAN synapses in RA, which has been demonstrated by White et al (1999), and Stark and Perkel (1999). LMAN synapses in RA are almost exclusively mediated by NMDA receptors (Mooney and Konishi, 1991; Mooney, 1992). A computational model with two levels of neuronal populations, LMAN and RA, can be constructed, with divergent and reconvergent connections from LMAN to

RA, and also extensive intrinsic connections within each population. The temporal dynamics of the LMAN synapses in RA will be initially set with longer time constants, and then shortened to mimic the developmental changes in NMDA receptor kinetics. The time constants at each age will be taken from measurements made in slice experiments (White et al, 1999; Stark and Perkel, 1999). It will be of interest to determine whether a decrease in the temporal dynamics of the NMDA receptors would be sufficient to also decrease the temporal characteristics of the direct LMAN-RA correlated activity.

Another factor that may contribute to the developmental changes in LMAN-RA correlated activity is changes in the intrinsic connectivity within LMAN and RA. A large portion of the LMAN intrinsic connectivity is mediated by NMDA receptors (Boettiger and Doupe, 1997), and the NMDA receptor kinetics in these synapses may also decrease during development (Boettiger, unpublished observations). This can be incorporated into the model above, by setting the time constant of the LMAN intrinsic synapses at smaller values to mimic the developmental change. The intrinsic connectivity within RA declines from approximately 50 days of age to adulthood (Herrmann and Arnold, 1991; Kittelberger and Mooney, 1999). A more extensive intrinsic connectivity in juveniles may result in a longer time delay between LMAN and RA activity, and more variability in time delays. Using the model mentioned above, the decline in intrinsic connections can be modeled by setting a portion of the intrinsic synaptic weights to zero (number based on anatomical studies by Kittelberger and Mooney, 1999). These computations will help elucidate whether developmental changes in the intrinsic connectivity within LMAN and/or RA could result in the decrease in the temporal characteristics of the direct LMAN-RA correlated activity observed between 50 days of age and adulthood.

Modulation of correlated activity within the song system

The correlation of activity between LMAN and RA was variable, exhibiting either two well-separated peaks, two peaks that were not well separated and/or where one was not

significant, a single broad peak, or no peaks at all. The variability of LMAN-RA correlated activity corresponded well with the different types of HVc-LMAN correlated activity that was observed, suggesting that the variability of correlated activity within the song system may lie within the AFP (HVc to LMAN). One possible source of variability in the correlated activity in the song system is the varying levels of arousal in anesthetized animals (personal observations). For example, not all sites encountered in LMAN and RA respond to the bird's own song, remain auditory throughout the entire recording session, or have stable spontaneous activity. To minimize the contribution of arousal states to variability of correlated activity, we included only pairs of LMAN-RA sites that were auditory and had stable responses and spontaneous firing rates in the cross-covariance and coherency analysis. However, the variability in the types of correlations was observed despite applying these criteria to determine which data to include in the analysis. This suggests that other factors may be involved.

One of these factors may be extrinsic modulation of the correlated activity within the AFP. A candidate source of modulation is the strong dopaminergic projection from brainstem areas to HVc, LMAN and Area X (Lewis et al, 1981). The AFP is homologous to the cortico-basal ganglia loop in mammals, and in the mammalian basal ganglia, dopamine has been shown to modulate the degree of synchronization within the striatum and globus pallidus. Dopamine depletion resulted in an increase in synchronized activity (in the millisecond time scale) within the globus pallidus and within the striatum, and dopamine agonists increased the regularity of multi-second oscillations in the basal ganglia (Raz et al, 1996; Bergman et al, 1998, Ruskin et al, 1999). The effect of dopamine depletion using 1-methyl-2-phenyl-1,2,3,6-tetrahydropyridine (MPTP), or dopamine receptor activation using agonists such as apomorphine, on the correlated activity between HVc and LMAN, and the synchronization of activity within HVc, LMAN and Area X, would shed light on whether dopamine can modulate the correlated activity within the song system.

It is also unknown whether the correlation of activity in the song system of awake animals would be similar to that observed in the anesthetized animals. Auditory responsiveness in RA (Vicario and Yohay, 1993; Dave et al, 1998) and HVc (Schmidt and Konishi, 1998) depend on whether the bird is awake or asleep, indicating that the activity in the song system is modulated by the bird's state of wakefulness. It would thus be of interest to determine the correlated activity in the song system of awake animals, especially during singing and passive presentation of auditory stimuli. Singing-related activity in the AFP is modulated by the social context of singing in a way that suggests that neurons may fire in a more correlated manner during directed singing (Hessler and Doupe, 1999a). Thus, determining whether the social context of singing alters correlated activity in the awake behaving bird would help elucidate how the functional connectivity of the song system may be modulated in awake, behaving birds.

Interactions between the AFP and the motor pathway

The overall strength of the direct LMAN-RA correlated activity slightly decreased when the activity in HVc was interrupted using a glutamate receptor antagonist (see Fig. 3-10). This suggested that HVc activity can influence the direct correlated activity between LMAN and RA. This may reflect interactions between the LMAN and HVc afferents in RA neurons; for instance, an RA neuron may fire an action potential more readily when it is simultaneously, or nearly simultaneously activated by both LMAN and HVc afferents. Evidence for a linear interaction between subthreshold synaptic responses in RA neurons to LMAN and HVc stimulation has been observed in brain slice experiments (Mooney, 1992). However, interactions between suprathreshold responses or spikes induced by these nuclei might be non-linear. In the visual system, non-linear enhancement of the geniculate response occurs when it is stimulated by two nearly simultaneous spikes from the same ganglion cell axon (Usrey et al, 1998). Moreover, the amount of information extracted increases when the timing of precisely correlated spikes in the lateral geniculate nucleus is

considered (Dan et al, 1998). Thus, it would be informative to determine whether precisely correlated firing between HVc and LMAN has non-linear effects on the responsiveness of RA to either stimulus. One way to determine if there is an interaction between LMAN and HVc afferents in RA is to examine the direct LMAN-RA correlated activity when only LMAN spikes that occurred almost simultaneously with an HVc spike are considered. Similarly, the HVc-RA correlated activity can also be examined, using HVc spikes that occurred very close in time to an LMAN spike. This correlated activity can then be compared to that when all the spikes, or only the non-synchronous spikes are considered. Simultaneous recording of HVc, RA and LMAN activity, and filtering of spike trains according to whether a spike occurred nearly simultaneously with the reference spikes would be required.

A direct way of measuring whether there is a non-linear interaction, such as paired-pulse facilitation or paired-spike enhancement, in the LMAN and/or HVc afferents in RA, is to stimulate one or both pathways in vivo. If RA responsiveness is enhanced after paired stimulation of the HVc and LMAN pathways relative to the sum of responses when each pathway is stimulated alone, this could be evidence that the afferents interact in a non-linear fashion to increase the post-synaptic response strength. It would also be important to determine the specific temporal relationship of stimulation in both pathways. For instance, it may be necessary for LMAN activation of RA to precede HVc-induced spikes in RA in order for responses in RA to be enhanced. In addition, long-term changes in the responsiveness of RA neurons to one or both afferents may occur after tetanic stimulation of one, or both pathways. This type of plasticity may underlie the developmental increase in peak strength of the direct LMAN-RA correlated activity.

Disrupting HVc activity may have affected the spontaneous activity in LMAN and RA, thereby affecting the correlated activity between both nuclei during spontaneous activity. It is possible that silencing a portion of HVc resulted in desynchronization of activity across a large area, if not all, of HVc. This may be translated downstream as

desynchronized activity, or as a change in the pattern of intrinsic activity within LMAN. It would thus be of interest to determine the effect of disruption of HVc activity on the correlation of activity within LMAN, and also within RA, and whether any disruption correlates with the observed decrease in strength of correlated activity between LMAN and RA when HVc activity is interrupted. The slight decrease in LMAN-RA correlation strength may be a transient effect, and normal patterns of activity may gradually return, since partial unilateral lesions of HVc have very little effect on the motor expression of song in adult zebra finches (Brainard, personal observations). A longitudinal study of LMAN-RA correlated activity, and correlated activity within LMAN and within RA, during pre- and post- disruption of HVc activity over a longer time period would determine whether recovery of correlated activity would occur.

To further address whether HVc activity affects the direct LMAN to RA correlated activity, it would be informative to interrupt the HVc to RA interaction, leaving the HVc to LMAN pathway intact. This manipulation would not disrupt the LMAN spontaneous activity, nor the correlation of activity within LMAN, whereas directly disrupting HVc inevitably affects LMAN activity. This could be achieved by damaging or transiently inactivating the HVc-RA fiber tract. In this case, if the LMAN-RA direct correlation is compromised relative to the correlations observed when HVc to RA transmission is present, this would clearly indicate that there is an interaction between the two afferents in RA. To determine whether HVc input affects the direct LMAN to RA correlated activity via the AFP, a lesion in the AFP, such as in Area X, would interrupt the HVc-LMAN pathway but would leave the LMAN-RA and the HVc-RA pathways intact.

Functional connectivity from LMAN to HVc

In 4/6 cases in which the correlated activity between HVc and LMAN exhibited a positive peak with a long positive time delay (approximately 60 msec time delay) relative to HVc spikes, a peak with a short negative time delay (approximately -5 msec) was also

observed. The short negative time delay indicates an increase in the probability of firing in LMAN before spikes in HVc, suggesting that there may be a direct feedback connection from LMAN to HVc. Although correlated activity does not necessarily indicate the presence of an anatomical connection, the result mentioned above certainly suggests such a connection, and merits further investigation. A direct anatomical connection from LMAN to HVc has been suggested in canaries (Nottebohm et al, 1982; Okuhata and Saito, 1987). The AFP has been postulated to send a comparison signal between the bird's vocalization and the memorized tutor song (Brainard and Doupe, 2000; Troyer et al, 2000a; b). A connection from the AFP to HVc would provide immediate feedback about such a comparison to the source of motor command in the motor pathway. Although Troyer et al (2000b) has proposed a model for syllable sequence learning that does not require a connection from LMAN to HVc, a feedback signal from the AFP to HVc would help guide learning of the sequence of syllables, since HVc is likely to be a central pattern generator for song sequence in adult zebra finches (Vu et al, 1994a). Injection of retrograde anatomical tracers into HVc, and/or anterograde tracers into LMAN, could help determine the existence of a LMAN projection to HVc. Collision of spontaneous LMAN orthodromic spikes and HVc-stimulated antidromic spikes in the same LMAN neuron would also confirm whether a LMAN to HVc connection exists in zebra finches.

Role of the direct LMAN-RA correlated activity in song learning

As described in Chapter 4, the direct LMAN-RA correlated activity in juveniles had a longer mean time delay, and more jitter in time delays than the direct LMAN-RA correlated activity in adults. The slow and variable timing of RA spike induction by LMAN input in juveniles may be due to the slow kinetics of the NMDA receptors that primarily mediate the LMAN synapses in RA. Indeed, the addition of the conductance of NMDA receptors to fast excitatory conductance (AMPA-type) has been shown to increase the variability of timing of post-synaptic spikes (Harsch and Robinson, 2000). The kinetics of

the NMDA receptors that mediate the LMAN synapses in RA increase during development (White et al, 1999; Stark and Perkel, 1999), consistent with the faster temporal characteristics of the direct correlated activity between LMAN and RA in adults. In adults, similar developmental changes are suggested by studies of LMAN intrinsic receptors (Boettiger, unpublished observations). NMDA receptor activation is also required for song learning during the sensory phase (Aamodt et al, 1996; Basham et al, 1996), and its expression levels in LMAN, Area X are also developmentally regulated (Aamodt et al, 1992; Carillo and Doupe, 1995). One way to test the idea that NMDA receptor kinetics determine the timing of direct LMAN-RA correlated activity is to accelerate the slow NMDA receptor kinetics in juveniles by testosterone treatment. White et al (1999) showed that testosterone treatment of juvenile male zebra finches results in abnormally faster NMDA receptor kinetics of LMAN synapses in RA. If NMDA receptor kinetics are involved in the timing of correlated activity between LMAN and RA, then one would expect that testosterone treated birds would have faster direct LMAN-RA correlated activity, similar to that found in adults. A caveat is that testosterone treatment may disrupt the normal development of numerous aspects of brain function, which may affect the direct LMAN-RA correlated activity. This would make it difficult to attribute changes to one parameter such as NMDA receptor kinetics. Local infusion of testosterone into RA, and/or LMAN, would rule out non-specific effects of testosterone at least outside of the local connectivity of RA and LMAN.

To further examine the correlation between learning, and the timing and strength of the direct LMAN-RA correlated activity, the bird's behavior and environment can be manipulated to delay song learning. Birds isolated from potential tutors have a longer sensory learning phase: isolate birds exposed to a tutor long after the normal sensory period is over are able to incorporate elements from the tutor song (Eales, 1985; 1987). Another behavioral manipulation that delays song learning is blocking the auditory feedback during sensorimotor learning. This results in the delayed crystallization of song in some birds (Konishi, 1965). Isolated or deafened adult birds that exhibit delayed or disrupted learning,

and weaker and slower direct LMAN-RA correlated activity than that in adult normal birds, would provide evidence that the strength and temporal characteristics of the direct LMAN-RA correlated activity are tightly linked to song learning. Moreover, these experiments present an opportunity to delineate whether the changes in the timing and strength of the direct LMAN-RA correlated activity as birds mature simply reflect developmental change, or whether they are specifically correlated with song learning. A caveat is that these behavioral manipulations that disrupt song learning may also delay normal development. Thus, it would be necessary to determine whether LMAN and RA in adult birds that were isolated or deafened as juveniles are similar in size, neuron number and neuronal morphology to those of normal adult birds.

The experiments described above, however, are correlative; they do not establish a causal relationship between song learning, and time and strength of the direct LMAN-RA correlated activity. A more direct test of whether the timing and strength of the direct LMAN-RA correlated activity is important during learning is to manipulate these parameters such that they are abnormal, and determine whether learning is interrupted. Manipulations that would disrupt the correlated LMAN-RA activity, however, may also affect the pattern of activity in LMAN and/or RA, and therefore confound any results. Candidate agents that might decorrelate LMAN and RA activity without affecting their average patterns of activity are neuromodulators. As mentioned in the previous section, neuromodulators such as dopamine may alter the correlation of activity within the AFP, and thus effectively also decorrelate LMAN and RA activity.

Role of direct LMAN-RA correlated activity in adults

The strong direct LMAN-RA correlated activity is consistent with the results that indicate that LMAN still plays a role in vocal plasticity in adults (Morrison and Nottebohm, 1993; Williams and Mehta, 1999; Brainard and Doupe, 2000). As shown in several studies, altered or absent auditory feedback in adults results in the gradual deterioration of the adult

songs (Nordeen and Nordeen, 1992; Williams and McKibben, 1992; Brainard and Doupe, 2000; Leonardo and Konishi, 2000; Lombardino and Nottebohm, 2000), resulting in a poor match between vocal output and the memorized copy of the tutor song. In these cases, LMAN activity is required for the changes in song to occur (Williams and Mehta, 1999; Brainard and Doupe, 2000). The strong direct LMAN-RA correlated activity may thus be involved in the maintenance of adult crystallized song. It would be therefore of interest to measure the direct LMAN-RA correlated activity in adults with degraded songs. If the direct LMAN-RA correlated activity is different, for example, has lower magnitude and slower temporal characteristics, in adults with degraded songs compared to those in normal adults, then this correlated activity may participate in vocal plasticity in adults. This experiment, however, does not distinguish between alterations of the direct LMAN-RA correlated activity actively guiding vocal plasticity in adults, or simply reflecting the state of vocal plasticity.

Auditory responses and selectivity in RA

The auditory responses and selectivity of RA neurons in juveniles share some characteristics with LMAN, and other characteristics with HVc, suggesting that both nuclei contribute to the auditory response characteristics of RA neurons. However, it is not proven that this is the case, nor whether there are any interactions between the LMAN and HVc input to RA in juveniles. It is also possible that one afferent may dominate and mask the contribution of the other input to the auditory responsiveness or selectivity in RA. Similarly, it is unknown whether in juveniles both LMAN and RA afferents are necessary for auditory responsiveness in RA. Thus, determining whether auditory responses are present in RA, and characterizing any auditory responses observed with only LMAN or HVc afferents active, would reveal the relative contribution of LMAN and HVc to auditory responses in juvenile RA. The HVc to RA fiber tract can be damaged, or reversibly inactivated using pharmacological agents, leaving LMAN as the only known source of afferent into RA.

LMAN activity can be silenced by lesions or pharmacological agents to ensure that HVc is the only known afferent to RA. To further isolate the contribution of each isolated pathway from that of intrinsic connectivity in RA, the entire local circuitry within RA can be deactivated using GABA, while recording intracellularly in RA neurons. This would directly measure the excitatory responses of RA neurons that are due to extrinsic afferents from LMAN or HVc.

One caveat in the HVc recordings described in Chapter 5 is that the types of HVc neurons that we were recording from are unknown. The differences between HVc and LMAN auditory responses, and also between HVc and RA responses may no longer be observed if we classify HVc responses as either RA-projecting or Area X-projecting HVc neurons. Mooney et al (2000) found that each type of HVc neuron (RA-projecting, Area X-projecting, and interneurons) has a characteristic spontaneous activity, and differing subthreshold selectivity for bird's own song (BOS) vs. reversed BOS. To clarify the contribution of HVc activity to the auditory responses characteristic in RA, and also LMAN, experiments can be conducted to study the song and order selectivity of each type of HVc neuron, and to compare this to simultaneously recorded single-unit responses in RA or LMAN in the same bird.

The developmental changes in the selectivity of RA neurons, and the comparison of responses and selectivity between LMAN, RA, and HVc indicate that inhibitory responses may shape the selectivity of auditory responses. The inhibitory responsiveness of RA neurons in adults may arise from their intrinsic inhibitory circuitry. In adult LMAN, the intrinsic inhibitory circuitry is necessary for the expression of the high degree of selectivity for BOS over reversed BOS (Rosen and Mooney, 2000). The role of RA inhibitory circuitry in shaping the selectivity of auditory responses can be examined using GABA agonists and antagonists. Similar experiments conducted in juveniles in their sensorimotor phase would determine whether the influence of the inhibitory circuitry on the selectivity of RA auditory responses emerges during development.

An alternative possibility is that the inhibitory responses in RA are shaped by both HVc and LMAN inputs, since these afferents innervate both projection neurons and inhibitory interneurons in RA (Mooney, 1992; Kittelberger and Mooney, 1999; Spiro et al, 1999). These two populations of RA neurons can be distinguished by the shape of their action potentials (Spiro et al, 1999). RA inhibitory neurons synapse onto RA projection neurons; thus, RA projection neurons receive direct excitatory inputs from HVc and LMAN, and also inhibitory inputs from interneurons that are activated by both HVc and LMAN. To isolate the contribution of each pathway, the HVc to RA fiber tract can be blocked to determine the contribution of LMAN; similarly, LMAN can be inactivated to identify the contribution of HVc. The next step would be to identify the contribution of the isolated pathway to the inhibitory responses of RA projection neurons. To accomplish this, the excitatory transmission to RA projection neurons, but not to interneurons, has to be blocked while recording intracellularly from the projection neurons. This can be done by small local infusions of glutamate receptor antagonists through an electrode in close proximity to the recording electrode. RA interneurons have extensive processes that span most of RA (Spiro et al, 1999), and thus some interneurons may be located far away that they are not affected by the local infusion of glutamate receptor antagonists, and are still driven by incoming excitatory inputs. To block excitatory post-synaptic potentials (EPSPs) in the direct LMAN excitatory synapses to RA projection neurons, which are primarily mediated by NMDA receptors, D(-)-2-amino-5-phosphonopentanoic acid (D-APV) can be used, while a combination of D-APV and 6-cyano-7-nitroquinoxaline-2,3 dione (CNQX) would be necessary to block the EPSPs in the direct HVc synapses, which are mediated by both NMDA and non-NMDA receptors (Kubota and Saito, 1991; Mooney, 1992; Stark and Perkel, 1999).

REFERENCES

Aamodt, S. M., Kozlowski, M. R., Nordeen, E. J., and Nordeen, K. W. (1992). Distribution and developmental change in [3-H]MK-801 binding within zebra finch song nuclei. J Neurobiol 23 : 997-1005.

Aamodt, S. M., Nordeen, E. J., and Nordeen, K. W. (1996). Blockade of NMDA receptors during song model exposure impairs song development in juvenile zebra finches. Neurobiology of Learning and Memory 65 (1): 91-98.

Aertsen, A. M. H. J., Gerstein, G. L., Habib, M. K., and Palm, G. (1989). Dynamics of neuronal firing correlation: modulation of "effective connectivity". J Neurophysiol 61 (5): 900-917.

Akutagawa, E., and Konishi, M. (1994). Two separate areas of the brain differentially guide the development of a song control nucleus in the zebra finch. Proc Natl Acad Sci USA 91 (26): 12413-12417.

Alonso, J., Usrey, W. M., and Reid, R. C. (1996). Precisely correlated firing in cells of the lateral geniculate nucleus. Nature 383 : 815-819.

Alonso, J., and Martinez, L. M. (1998). Functional connectivity between simple cells and complex cells in cat striate cortex. Nature Neuroscience 1 (5): 395-403.

Alvarez-Bullya, A., Theelen, M., and Nottebohm, F. (1988). Birth of projection neurons in the higher vocal center of the canary forebrain before, during, and after song learning. Proc Natl Acad Sci USA 85 : 8722-8726.

Alvarez-Bullya, A., Ling, C. Y., and Nottebohm, F. (1992). High vocal center growth its relation to neurogenesis, neuronal replacement and song acquisition in juvenile canaries. J Neurobiol 23 (4): 396-406.

Anokhin, K. V., Mileusnic, R., Shamakina, I. Y., and Rose, S. P. R. (1991). Effects of early experience on c-fos gene expression in the chick forebrain. Brain Res 544 : 101-107.

Barclay, S., and Harding, C. (1988). Androstenedione modulation of monoamine levels and turnover in hypothalamic and vocal control nuclei in the male zebra finch: steroid effects on brain monoamines. Brain Res 459 : 333-343.

Basham, M. E., Nordeen, E. J., and Nordeen, K. W. (1996). Blockade of NMDA receptors in the anterior forebrain impairs sensory acquisition in the zebra finch (Peophila guttata). Neurobiology of Learning and Memory 66 : 295-304.

Bergman, H., Feingold, A., Nini, A., Raz, A., Slovin, H., Abeles, M., and Vaadia, E. (1998). Physiological aspects of information processing in the basal ganglia of normal and parkinsonian primates. Trends Neurosci 21 (1): 32-38.

Bischof, H., and Herrmann, K. (1986). Arousal enhances [14C] 2-deoxyglucose uptake in four forebrain areas of the zebra finch. Behav Brain Res 21 : 215-221.

Bischof, H., and Herrmann, K. (1988). Isolation-dependent enhancement of 2-[14C] deoxyglucose uptake in the forebrain of zebra finch males. Behav Neural Biol 49 : 386-397.

Boettiger, C. A., and Doupe, A. J. (1998). Intrinsic and thalamic excitatory inputs onto songbird LMAN neurons differ in their pharmacological and temporal properties. J Neurophysiol 79 : 2615-2628.

Bolhuis, J. J., Zijlstra, G. G. O., den Boer-Visser, A. M., and Van der Zee, E. A. (2000). Localized neuronal activation in the zebra finch brain is related to the strength of song learning. Proc Natl Acad Sci USA 97 : 2282-2285.

Borst, A., and Theunissen, F. E. (1999). Information theory and neural coding. Nature Neuroscience 2 (11): 947-957.

Bottjer, S. W., Miesner, E. A., and Arnold, A. P. (1984). Forebrain lesions disrupt development but not maintenance of song in passerine birds. Science 224 : 901-903.

Bottjer, S. W., Glaessner, S. L., and Arnold, A. P. (1985). Ontogeny of brain nuclei controlling song learning and behavior in zebra finches. J Neurosci 5 : 1556-1562.

Bottjer, S. W., Miesner, E. A., and Arnold, A. (1986). Changes in neuronal number, density and size account for increases in volume of song-control nuclei during song development in zebra finches. Neurosci Lett 67 : 263-268.

Bottjer, S. W., Halsema, K. A., Brown, S. A., and Miesner, E. A. (1989). Axonal connections of a forebrain nucleus involved with vocal learning in zebra finches. J Comp Neurol 279 : 312-326.

Bottjer, S. W., and Sengelaub, D. R. (1989). Cell death during development of a forebrain nucleus involved with vocal learning in zebra finches. J Neurobiol 20 (7): 609-618.

Bottjer, S. W. (1993). The distribution of tyrosine hydroxylase immunoreactivity in the brains of male and female zebra finches. J Neurobiol 24 : 51-69.

Bourtchuladze, R., Frenguelli, B., Blendy, J., Cioffi, D., Schutz, G., and Silva, A. J. (1994). Deficient long-term memory in mice with a targeted mutation of the cAMP-responsive element-binding protein. Cell 79 (1): 59-68.

Brainard, M. S., and Doupe, A. J. (2000). Interruption of a basal ganglia-forebrain circuit prevents plasticity of learned vocalizations. Nature 404 : 762-766.

Brenowitz, E. A. (1991). Altered perception of species-specific song by female birds after lesion of a forebrain nucleus. Science 251 : 303-305.

Brillinger, D. R., Bryant, H. L., and Segundo, J. P. (1976). Identification of Synaptic Interactions. Biol Cybernetics 22 : 213-228.

Burt, J. M., Lent, K. L., Beecher, M. D., and Brenowitz, E. A. (2000). Lesions of the anterior forebrain song control pathway in female canaries affect song perception in an operant task. J Neurobiol 42 : 1-13.

Canady, R. A., Burd, G. D., DeVoogd, T. J., and Nottebohm, F. (1988). Effect of testosterone on input received by an identified neuron type of the canary song system: a golgi/electron microscopy/degeneration study. J Neurosci 8 (10): 3770-3784.

Carew, T. J. (1996). Molecular enhancement of memory formation. Neuron 16 : 5-8.

Carrillo, G., and Doupe, A. J. (1995). Developmental studies of glutamate receptor and peptide immunoreactivity in the zebra finch song system. Soc Neurosci Abstr 21 (2): 960.

Chergui, K., Nomikos, G. G., Mathe, J. M., Gonon, F., and Svenson, T. H. (1996). Burst stimulation of the medial forebrain bundle selectively increase fos-like immunoreacitvity in the limbic forebrain of the rat. Neurosci 72 : 141-156.

Cole, A. J., Saffen, D. W., Baraban, J. M., and Worley, P. F. (1989). Rapid increase of an immediate early gene messenger RNA in hippocampal neurons by synaptic NMDA receptor activation. Nature 340 : 474-476.

Covey, E., and Casseday, E. C. (1999). Timing in the auditory system of the bat. Annu Rev Physiol 61 : 457-476.

Curran, T., and Morgan, J. I. (1985). Superinduction of c-fos by Nerve Growth Factor in the presence of peripherally active benzodiazepines. Science 229 : 1265-1268.

Dan, Y., Alonso, J. M., Usrey, W. M., and Reid, R. C. (1998). Coding of visual information by precisely correlated spikes in the lateral geniculate nucleus. Nature Neurosci 1 (6): 501-507.

Dave, A. S., Yu, A. C., and Margoliash, D. (1998). Behavioral state modulation of auditory activity in a vocal motor system. Science 282 : 2250-2254.

Doupe, A. J., and Konishi, M. (1991). Song-selective auditory circuits in the vocal control system of the zebra finch. Proc Natl Acad Sci USA 88 : 11339-11343.

Doupe, A. J. (1993). A neural circuit specialized for vocal learning. Curr Op in Neurobiol 3 : 104-111.

Doupe, A. J. (1997). Song- and order-selective neurons in the songbird anterior forebrain and their emergence during vocal development. J Neurosci 17 (3): 1147-1167.

Doupe, A. J., and Solis, M. M. (1997). Song- and order-selective neurons develop in the songbird anterior forebrain. J Neurobiol 33 (5): 694-709.

Doupe, A. J., and Kuhl, P. K. (1999). Birdsong and human speech: common themes and mechanisms. Ann Rev of Neurosci 22 : 567-631.

Doya, K., and Sejnowski, T. J. (1998). A computational model of birdsong learning by auditory experience and auditory feedback. In "Central Auditory Processing and Neural Modeling" (P. W. F. Poon and J. F. Brugge, Eds.), pp. 77-88. Plenum, New York.

Eales, L. A. (1985). Song learning in zebra finches; some effects of song model availability on what is learnt and when. Anim Behav 33 : 1293-1300.

Eales, L. A. (1987). Song learning in female-raised zebra finches: another look at the sensitive phase. Anim Behav 35 : 1356-1365.

Eggermont, J. J., and Smith, G. M. (1996). Neural connectivity only accounts for a small part of neural correlation in auditory cortex. Exp Brain Res 110 : 379-391.

Feller, M. B. (1999). Spontaneous correlated activity in developing neural circuits. Neuron 22 : 653-656.

Fetz, E. E., and Cheney, P. D. (1980). Postspike facilitation of forelimb muscle activity by primate corticomotoneuronal cells. J Neurophysiol 44 (4): 751-772.

Fortune, E. S., and Margoliash, D. (1995). Parallel pathways and convergence onto HVc and adjacent neostriatum of adult zebra finches (Taeniopygia guttata). J Comp Neurol 360 : 413-441.

Foster, E. F., and Bottjer, S. W. (1998). Axonal connections of the high vocal center and surrounding cortical regions in juvenile and adult male zebra finches. J Comp Neurol 397 : 118-138.

Frostig, R. D., Gottlieb, Y., Vaadia, E., and Abeles, M. (1983). The effects of stimuli on the activity and functional connectivity of local neuronal groups in cat auditory cortex. Brain Res 272 : 211-221.

Gentner, T. Q., Hulse, S. H., Bentley, G. E., and Ball, G. F. (2000). Individual vocal recognition and the effect of partial lesions to HVc on discrimination, learning, and categorization of conspecific song in adult songbirds. J Neurobiol 42 : 117-133.

Graybiel, A. M., Aosaki, T., Flaherty, A. W., and Kimura, M. (1994). The basal ganglia and adapive motor control. Science 265 : 1826-1831.

Graybiel, A. M. (1998). The basal ganglia and chunking of action repertoires. Neurobiology of Learning and Memory 70 : 119-136.

Green, D. N., and Swets, J. A. (1966). "Signal detection theory and psychophysics." Wiley, New York.

Greenberg, M. E., Ziff, E. B., and Greene, L. A. (1986). Stimulation of neuronal acetylcholine receptors induces rapid gene transcription. Science 234 : 80-83.

Harsch, A., and Robinson, H. P. (2000). Postsynaptic variability of firing in rat cortical neurons: the roles of input synchronization and synaptic NMDA receptor conductance. J Neurosci 20 (16): 6181-6192.

Herrmann, K., and Arnold, A. P. (1991). The development of afferent projections to the robust archistriatal nucleus in male zebra finches: a quantitative electron microscopic study. J Neurosci 11 (7): 2063-2074.

Hessler, N. A., and Doupe, A. J. (1999a). Social context modulates singing-related neural activity in the songbird forebrain. Nature Neurosci 2 (3): 209.

Hessler, N. A., and Doupe, A. J. (1999b). Singing-related neural activity in a dorsal forebrain-basal ganglia circuit of adult zebra finches. J Neurosci 19 (23): 10461-10481.

Hunt, S. P., Pini, A., and Evan, G. (1987). Induction of c-fos-like protein in spinal cord neurons following sensory stimulation. Nature 328 : 632-634.

Immelmann, K. (1969). Song development in the zebra finch and other estrildid finches. In "Bird vocalizations" (R. A. Hinde, Ed.), pp. 61-74. Cambridge University Press, Cambridge.

Iyengar, S., Viswanthan, S. S., and Bottjer, S. W. (1999). Development of topography within song control circuitry of zebra finches during the snesitive period for song learning. J Neurosci 19 (14): 6037-6057.

Janata, P., and Margoliash, D. (1999). Gradual emergence of song selectivity in sensorimotor structures of the male zebra finch song system. J Neurosci 19 (12): 5108-5118.

Jarvis, E. D., and Nottebohm, F. (1996). Singing induces gene expression in selectied song nuclei of the avian song system. Soc Neurosci Abstr 22 (1): 692.

Jarvis, E. D., and Nottebohm, F. (1997). Motor-driven gene expression. Proc Natl Acad Sci USA 94 : 4097-4102.

Jarvis, E. D., Scharff, C., Grossman, M. R., Ramos, J. A., and Nottebohm, F. (1998). For whom the bird sings: context-dependent gene expression. Neuron 21 : 775-788.

Jin, H., and Clayton, D. F. (1997). Localized changes in immediate early gene regulation during sensory and motor learning in zebra finches. Neuron 19 : 1049-1059.

Johnson, F., and Bottjer, S. W. (1992). Growth and regression of thalamic efferents in the song-control system of male zebra finches. J Comp Neurol 326 : 442-450.

Johnson, F., Sablan, M. M., and Bottjer, S. W. (1995). Topographic organization of a forebrain pathway involved with vocal learning in zebra finches. J Comp Neurol 358 : 260-278.

Jurgens, U., Lu, C.-L., and Quondamatteo, F. (1996). C-fos expression during vocal mobbing in the new world monkey Saguinus fuscicollis. Euro J Neurosci 8 : 2-10.

Kaang, B. K., Kandel, E. R., and Grant, S. G. (1993). Activation of cAMP-responsive genes by stimuli that produce long-term facilitation in Aplysia sensory neurons. Neuron 10 (3): 427-435.

Kaczmarek, L. (1992). Expression of c-fos and other genes encoding transcription factors in long-term potentiation. Behavioral and Neural Biology 57 : 263-266.

Kaczmarek, L. (1993). Molecular biology of vertebrate learning: Is c-fos a new beginning? J Neurosci Res 34 : 377-381.

Katz, L. C., and Shatz, C. J. (1996). Sympatic activity and the construction of cortical circuits. Science 274 : 1133-1138.

Kelley, D. B., and Nottebohm, F. (1979). Projections of a telencephalic auditory nucleus - Field L - in the canary. J Comp Neur 183 : 455-470.

Kirn, J. R., and Nottebohm, F. (1993). Direct evidence for loss and replacement of projection neurons in adult canary brain. J Neurosci 13 : 1654-1663.

Kittelberger, J. M., and Mooney, R. (1999). Lesions of an avian forebrain nucleus that disrupt song development alter synpatic connectivity and transmission in the vocal premotor pathway. J Neurosci 19 (21): 9385-9398.

Kleim, J. A., Lussnig, E., Schwarz, E. R., Comery, T. A., and Greenough, W. T. (1996). Synaptogenesis and Fos expression in the motor cortex of the adult rat after motor skill learning. J Neurosci 16 : 4529-4535.

Knudsen, E. I. (1999). Mechanisms of experience-dependent plasticity in the auditory localization pathway of the barn owl. J Comp Physiol A 185 : 305-321.

Konishi, M. (1965). The role of auditory feedback in the control of vocalization in the white-crowned sparrow. Z Tierpsychol 22 : 770-783.

Konishi, M., and Akutagawa, E. (1985). Neuronal growth, atrophy and death in a sexually dimorphic song nucleus in the zebra finch brain. Nature 315 : 145-147.

Kornhauser, J. M., Nelson, D. E., Mayo, K. E., and Takahashi, J. S. (1992). Regulation of jun-B messinger RNA and AP-1 activity by light and a circadian clock. Science 255 : 1581-1584.

Kossut, M. (1998). Exprerience-dependent changes in function and anatomy of adult barrel cortex. Exp Brain Res 123 (1-2) : 110-116.

Kroodsma, D. E., and Konishi, M. (1991). A suboscine bird (eastern phoebe, Sayornis phoebe) develops normal song without auditory feedback. Anim Behav 42 : 477-487.

Kruijer, W., Cooper, J. A., Hunter, T., and Verma, I. M. (1984). Platelet-derived growth factor induces rapid but transient expression of the c-fos gene and protein. Nature 312 : 711-716.

Kruijer, W., Schubert, D., and Verma, I. M. (1985). Induction of the proto-oncogene fos by nerve growth factor. Proc Natl Acad Sci USA 82 : 7730-7334.

Kubota, M., and Saito, N. (1991). NMDA receptors participate differentially in two different synaptic inputs in neurons of the zebra finch robust nucleus of the archistriatum in vitro. Neurosci Lett 125 : 107-109.

Labiner, D. M., Butler, L. S., Cao, Z., Hosford, D. A., Shin, C., and McNamara, J. O. (1993). Induction of c-fos mRNA by kindled seizures: complex relationship with neuronal burst firing. J Neurosci 13 : 744-751.

Langner, G. (1992). Periodicity coding in the auditory system. Hear Res 60 (115-142).

Leonardo, A., and Konishi, M. (1999). Decrystallization of adult birdsong by perturbation of auditory feedback. Nature 399 (6735): 466-470.

Lewicki, M. S., and Konishi, M. (1995). Mechanisms underlying the sensitivity of songbird forebrain neurons to temporal order. Proc Natl Acad Sci USA 92 : 5582-5586.

Lewicki, M. S. (1996). Intracellular characterization of song-specific neurons in the zebra finch auditory forebrain. J Neurosci 16 (18): 5854-5863.

Lewis, J. W., Ryan, S. M., Arnold, A. P., and Butcher, L. L. (1981). Evidence for a catecholaminergic projection to area X in the zebra finch. J Comp Neurol 196 : 347-354.

Lombardino, A. J., and Nottebohm, F. (2000). Age at deafening affects the stability of learned song in adult male zebra finches. J Neursoci 20 (13): 5054-5064.

Luo, M., and Perkel, D. J. (1999a). Long-range GABA-ergic projection in a circuit essential for vocal learning. J Comp Neurol 403 : 68-84.

Luo, M., and Perkel, D. J. (1999b). A GABAergic, strongly inhibitory projection to a thalamic nucleus in the zebra finch song system. J Neurosci 19 (15): 6700-6711.

Luo, M., Ding, L., and Perkel, D. J. (1999). Topographic mapping throughout the anterior forebrain pathway of the zebra finch song system. Soc Neurosci Abstr 25 (2): 1367.

Maekawa, M., and Uno, H. (1996). Difference in selectivity to song note properties between the vocal nuclei of the zebra finch. Neurosci Letters 218 (2): 123-126.

Margoliash, D. (1983). Acoustic parameters underlying the responses of songspecific neurons in white-crowned sparrow. J Neurosci 3 : 1039-1057.

Margoliash, D., and Konishi, M. (1985). Auditory representation of autogenous song in the song system of white-crowned sparrows. Proc Natl Acad Sci USA 82 : 5997-6000.

Margoliash, D. (1986). Preference for autogenous song by auditory neurons in a song system nucleus of the white-crowned sparrow. J Neurosci 6 : 1643-1661.

Margoliash, D., and Fortune, E. S. (1992). Temporal and harmonic combination-sensitive neurons in the zebra finch's HVc. J Neurosci 12 : 4309-4326.

Marler, P. (1970). A comparative approach to vocal learning: song development in white-crowned sparrows. J Comp Physiol Psychol 71 : 1-25.

McCasland, J. S., and Konishi, M. (1981). Interactions between auditory and motor activities in an avian song control nucleus. Proc Natl Acad Sci USA 78 : 7815-7819.

McCasland, J. S. (1987). Neuronal control of bird song production. J. Neurosci. 7 (1): 23-39.

Mello, C. V., Vicario, D. S., and Clayton, D. F. (1992). Song presentation induces gene expression in the songbird forebrain. Proc Natl Acad Sci USA 89 : 6818-6822.

Mello, C. V., and Clayton, D. F. (1994). Song-induced ZENK gene expression in auditory pathways of songbird brain and its relation to the song control system. J Neurosci 14 : 6652-6666.

Mooney, R., and Konishi, M. (1991). Two distinct inputs to an avian song nucleus activate different glutamate receptor subtypes on individual neurons. Proc Natl Acad Sci USA 88 : 4075-4079.

Mooney, R. (1992). Synaptic basis for developmental plasticity in a birdsong nucleus. J Neurosci 12 (7): 2464-2477.

Mooney, R., and Rao, M. (1994). Waiting periods versus early innervation: the development of axonal connections in the zebra finch song system. J Neurosci 14 (11 Pt 1): 6532-6543.

Mooney, R. (2000). Different subthreshold mechanisms underlie song selectivity in identified HVc neurons of the zebra finch. J Neurosci 20 (14): 5420-5436.

Moore, G. P., Segundo, J. P., Perkel, D. H., and Levitan, H. (1970). Statistical signs of synaptic interaciton in neurons. Biophysical Journal 10 (9): 876-900.

Moratalla, R., Elibol, B., Vallejo, M., and Graybiel, A. M. (1996). Network-level changes in expression of inducible fos-jun proteins in the striatum during chronic cocaine treatment and withdrawal. Neuron 17 : 147-156.

Morgan, J. I., and Curran, T. (1986). Role of ion flux in the control of c-fos expression. Nature 322 : 552-555.

Morgan, J. I., and Curran, T. (1988). Calcium as a modulator of the immediate-early gene cascade in neurons. Cell Calcium 9 : 303-311.

Morgan, J. I., and Curran, T. (1991). Stimulus-transcription coupling in the nervous system: involvement of the inducible proto-oncogenes fos and jun. Annu Rev Neurosci 14 : 421-451.

Mori, K., Nagao, H., and Yoshihara, Y. (1999). The olfactory bulb: coding and processing of odor molecule information. Science 286 : 711-715.

Morris, D. (1970). The comparative ethology of grassfinches and mannikins. In "Patterns of Reproductive Behavior", pp. 399-453. McGraw-Hill, New York.

Morrison, R. G., and Nottebohm, F. (1993). Role of a telencephalic nucleus in the delayed song learning of socially isolated zebra finches. J Neurobiol 24 (8): 1045-1064.

Nastiuk, K. L., Mello, C. V., George, J. M., and Clayton, D. F. (1994). Immediate-early gene responses in the avian song control system: cloning and expression analysis of the canary c-jun cDNA. Mol Brain Res 27 : 299-309.

Nordeen, K. W., Nordeen, E. J., and Arnold, A. P. (1987). Estrogen accumulation in zebra finch song control nuclei: Implications for sexual differentation and adult activation of song behavior. J Neurobiol 18 : 569-582.

Nordeen, K. W., and Nordeen, E. J. (1988). Projection neurons within a vocal motor pathway are born during song learning in zebra finches. Nature 334 : 149-151.

Nordeen, E. J., Grace, A., Burek, M. J., and Nordeen, K. W. (1992). Sex-dependent loss of projection neurons involved in avian song leanring. J Neurobiol 23 (6): 671-679.

Nordeen, K. W., and Nordeen, E. J. (1992). Auditory feedback is necessary for the maintenance of stereotyped song in adult zebra finches. Behav Neural Biol 57 : 58-66.

Nordeen, K. W., and Nordeen, E. J. (1993). Long-term maintenance of song in adult zebra finches is not affected by lesions of a forebrain region involved in song learning. Behav Neural Biol 59 (1): 79-82.

Nottebohm, F., Stokes, T. M., and Leonard, C. M. (1976). Central control of song in the canary, Serinus canarius. J Comp Neurol 165 : 457-486.

Nottebohm, F., Kelley, D. B., and Paton, J. A. (1982). Connections of vocal control nuclei in the canary telencephalon. J Comp Neurol 207 : 344-357.

Okuhata, S., and Saito, N. (1987). Synaptic connections of thalamo-cerebral vocal control nuclei of the canary. Brain Res Bull 18 : 35-44.

Palm, G., Aertsen, A. M. H. J., and Gerstein, G. L. (1988). On the significance of correlations among neuronal spike trains. Biol Cybern 59 : 1-11.

Perkel, D. H., Gerstein, G. L., and Moore, G. P. (1967). Neuronal spike trains and stochastic point processes II. Simultaneous spike trains. Biophysical Journal 7 : 419-440.

Perkel, D. J. (1995). Differential modulation of excitatory synaptic transmission by norepinephrine and baclofen in zebra finch nucleus RA. Soc Nsci Abstr 20 : 165.

Price, P. H. (1979). Developmental determinants of structure in zebra finch song. J Comp Physiol Psychol 93 (2): 260-277.

Rauschecker, J. P. (1999). Auditory cortical plasticity: a comparison with other sensory systems. Trends in Neurosci 22 (2): 74-80.

Raz, A., Feingold, A., Zelanskaya, V., Vaadia, E., and Bergman, H. (1996). Neuronal synchronization of tonically active neurons in the striatum of normal and parkinsonian primates. J Neurophysiol 76 (3): 2083-2088.

Robertson, H. A. (1991). Immediate-early genes, neuronal plasticity, and memory. Biochem Cell Biol 70 : 729-737.

Rosen, M. J., and Mooney, R. (2000). Intrinsic and extrinsic contributions to the auditory selectivity in a song nucleus critical for vocal plasticity. J Neurosci 20 (14): 5437-5448.

Rosenberg, J. R., Amjad, A. M., Breeze, P., Brillinger, D. R., and Halliday, D. M. (1989). The fourier approach to the identification of functional coupling between neuronal spike trains. Prog Biophys Moelc Biol 53 : 1-31.

Rusak, B., Robertson, H. A., Wisden, W., and Hunt, S. P. (1990). Light pulses that shift rhythms induce gene expression in the suprachiasmatic nucleus. Science 248 : 1237-1240.

Ruskin, D. N., Bergstrom, D. A., Kaneoke, Y., Patel, B. N., Twery, M. J., and Walters, J. R. (1999). Multisecond oscillations in firing rate in the basal ganglia: robust modulation by dopamine receptor activation and anesthesia. J Neurophysiol 81 : 2046-2055.

Sagar, S. M., Sharp, F. R., and Curran, T. (1988). Expression of c-fos protein in brain: metabolic mapping at the cellular level. Science 240 : 1328-1331.

Sagar, S. M., and Sharp, F. R. (1990). Light induces a Fos-like nuclear antigen in retinal neurons. Mol Brain Res 7 : 17.

Sakaguchi, H., Wada, K., Maekawa, M., Watsuji, T., and Hagiwara, M. (1999). Song-induced phosphorylation of cAMP response element-binding protein in the songbird brain. J Neuorsci 19 (10): 3973-3981.

Scharff, C., and Nottebohm, F. (1991). A comparative study of the behavioral deficits following lesions of the various parts of the zebra finch song system: Implications for vocal learning. J Neurosci 11 : 2896-2913.

Scharff, C., Nottebohm, F., and Cynx, J. (1998). Conspecific and heterospecific song discrimination in male zebra finches with lesions in the anterior forebrain pathway. J Neurobiol 36 : 81-90.

Schmidt, M. F., and Konishi, M. (1998). Gating of auditory responses in the vocal control system of awake songbirds. Nature Neurosci 1 (6): 513-518.

Sharp, F. R., Sagar, S. M., and Swanson, R. A. (1993). Metabolic mapping with cellular resoultion: c-fos vs. 2-deoxyglucose. Critical Rev in Neurobio 7 : 205-228.

Sharp, P. J., Li, Q., Talbot, R. T., Barker, P., Huskisson, N., and Lea, R. W. (1995). Identification of hypothalamic nuclei involved in osmoregulation using fos immunocytochemistry in the domestic hen (Gallus domesticus), Ring dove (Streptopelia risoria), Japanese quail (Coturnix japonica) and Zebra finch (Taenopygia guttata). Cell and Tissue Research 282 : 351-361.

Shatz, C. J. (1990). Impulase activity and the patterning of connections during CNS development. Neuron 5 (6): 745-756.

Sheng, M., and Greenberg, M. E. (1990). The regulation and function of c-fos and other immediate early genes in the nervous system. Neuron 4 : 477-485.

Sherin, J. E., Shiromani, P. J., McCarley, R. W., and Saper, C. B. (1996). Activation of ventrolateral preoptic neurons during sleep. Science 271 : 216-219.

Simpson, H. B., and Vicario, D. S. (1990). Brain pathways for learned and unlearned vocalizations differ in zebra finches. J Neurosci 10 (5): 1541-56.

Singer, W. (1995). Development and plasticity of cortical processing architectures. Science 270 : 758-764.

Soha, J. A., Shimizu, T., and Doupe, A. J. (1996). Development of the catecholaminergic innervation of the song system of the male zebra finch. J Neurobiol 29 (4): 473-489.

Sohrabji, F., Nordeen, E. J., and Nordeen, K. W. (1989). Projections of androgen-accumulating neurons controlling avian song. Brain Res 488 : 253-259.

Sohrabji, F., Nordeen, E. J., and Nordeen, K. W. (1990). Selective impairment of song learning following lesions of a forebrain nucleus in the juvenile zebra finch. Behav Neur Biol 53 : 51-63.

Solis, M. M., and Doupe, A. J. (1997). Anterior forebrain neurons develop selectivity by an intermediate stage of birdsong learning. J Neurosci 17 (16): 6447-6462.

Solis, M. M., and Doupe, A. J. (1999). Contribution of tutor and bird's own song experience to neural selectivity in the songbird anterior forebrain. J Neurosci 19 (11): 4559-4584.

Solis, M. M. (1999). Influences of Song Experience on the Development of Selectivity in the Zebra Finch Forebrain. Doctoral Thesis. Dept. of Physiology, University of California, San Francisco.

Solis, M. M., Brainard, M. S., Hessler, N. A., and Doupe, A. J. (2000). Song selectivity and sensorimotor signals in vocal learning and production. Proc Natl Acad Sci USA 97 : 11836-11842.

Sompolinsky, H., and Shapley, R. (1997). New perspectives on the mechanisms for orientation selectivity. Curr Op in Neurobiol 7 (4): 514-522.

Spiro, J. E., Dalva, M. B., and Mooney, R. (1999). Long-range inhibition wihtin the zebra finch song nucleus RA can coordinate the firing of multiple projection neurons. J Neurophysiol 81 (6) : 3007-3020.

Stark, L. L., and Perkel, D. J. (1999). Two-stage, input specific synaptic maturation in a nucleus essential for vocal production in the zebra finch. J Neurosci 19 (20): 9107-9116.

Sutter, M. L., and Margoliash, D. (1994). Global synchronous response to autogenous song in zebra finch HVc. J Neurophysiol 72 (5): 2105-2123.

Theunissen, F. E., and Doupe, A. J. (1998). Temporal and spectral sensitivity of complex auditory neurons in the nucleus HVc of male zebra finches. J Neurosci 18 (10): 3786-3802.

Thomson, D. J., and Chave, A. D. (1991). Jackknifed Error Estimates for Spectra, Coherences, and Transfer Functions. In "Advances in Spectrum Analysis and Array Processing" (S. Haykin, Ed.), Vol. 1. Prentice Hall.

Troyer, T. W., Doupe, A. J., and Miller, K. D. (1996). An associational hypothesis for sensorimotor learning of birdsong. In "Computational Neuroscience: Trends in Research 1995" (J. M. Bower, Ed.), pp. 409-414. Academic Press, San Diego.

Troyer, T. W., and Doupe, A. J. (2000a). An associational model of birdsong sensorimotor learning I. Efference copy and the learning of song syllables. J Neurophysiol 84 : 1204-1223.

Troyer, T. W., and Doupe, A. J. (2000b). An associational model of birdsong sensorimotor learning II. Temporal hierarchies and the learning of song sequence. J Neurophysiol 84 : 1224-1239.

Usrey, W. M., Reppas, J. B., and Reid, R. C. (1998). Paired-spike interactions and the synaptic efficacy of retinal inputs to the thalamus. Nature 395 : 384-387.

Vates, G. E., and Nottebohm, F. (1995). Feedback circuitry within a song-learning pathway. Proc Natl Acad Sci USA 92 : 5139-5143.

Vates, G. E., Broome, B. M., Mello, C. V., and Nottebohm, F. (1996). Auditory pathways of caudal telencephalon and their relation to the song system of adult male zebra finches. J Comp Neurol 366 (4): 613-42.

Vates, G. E., Vicario, D. S., and Nottebohm, F. (1997). Reafferent thalamo-"cortical" loops in the song system of oscine songbirds. J Comp Neurol 380 : 275-290.

Vicario, D. S. (1991). Organization of the zebra finch song control system: II. Functional organization of outputs from nucleus robustus archistriatalis. J Comp Neurol 309 : 486-494.

Vicario, D. S., and Yohay, K. H. (1993). Song-selective auditory input to a forebrain vocal control nucleus in the zebra finch. J Neurobiol 24 : 488-505.

Vicario, D. S. (1993). A new brain stem pathway for vocal control in the zebra finch song system. Neuro Report 4 : 983-986.

Vicario, D. S., and Simpson, H. B. (1995). Electrical stimulation in forebrain nuclei elicits learned vocal patterns in songbirds. J Neurophysiology 73 (6): 2602-2607.

Vidyasagar, T. R., Pei, X., and Volgushev, M. (1996). Multiple mechanisms underlying the orientation selectivity of visual cortical neurons. Trends Neurosci 19 (7): 272-277.

Volman, S. F. (1993). Development of neural selectivity for birdsong during vocal learning. J Neurosci 13 : 4737-4747.

Volman, S. F. (1996). Quantitative assessment of song-selectivity in the zebra finch "high vocal center". J Comp Physiol A 178 : 849-862.

Vu, E. T., Mazurek, M. E., and Kuo, Y. (1994a). Identification of a forebrain motor programming network for the learned song of zebra finches. J Neurosci 14 (11): 6924-6934.

Vu, E. T., and Lewicki, M. S. (1994b). Intrinsic interactions between zebra finch HVc neurons involve NMDA-receptor activation. Soc Neurosci Abstr 20 (1): 166.

Wan, X. S. T., Liang, F., Moret, V., Wiesendanger, M., and Rouiller, E. M. (1992). Mapping of the motor pathways in rats: c-fos induction by intracortical microstimulation of

the motor cortex correlated with efferent connectivity of the site of cortical stimulation. Neurosci 49 : 749-761.

White, S. A., Livingston, F. S., and Mooney, R. (1999). Androgens modulate NMDA receptor-mediated EPSCs in the zebra finch song system. J Neurophysiol 82 : 2221-2234.

Wild, J. M. (1993). Descending projections of the songbird nucleus robustus archistriatalis. J Comp Neurol 338 (2): 225-41.

Williams, H., and Nottebohm, F. (1985). Auditory responses in avian vocal motor neurons: a motor theory for song perception. Science 229 : 279-282.

Williams, H. (1989). Multiple representations and auditory-motor interactions in the avian song system. Ann N Y Acad Sci 563 : 148-164.

Williams, H. W. (1990). Models for song learning in the zebra finch: fathers or others? Anim Behav 39 : 745-757.

Williams, H., and McKibben, J. R. (1992). Changes in stereotyped central motor patterns controlling vocalization are induced by peripheral nerve injury. Behav Neural Biol 57 : 67-78.

Williams, H., and Vicario, D. S. (1993). Temporal patterning of song production: participation of nucleus uvaeformis of the thalamus. J Neurobiol 24 (7): 903-912.

Williams, H., and Mehta, N. (1999). Changes in adult zebra finch song require a forebrain nucleus that is not necessary for song production. J Neurobiol 39 : 14-28.

Wong, R. O. L. (1999). Retinal waves and visual system development. Annu Rev Neurosci 22 : 29-47.

Woolley, S. M., and Rubel, E. (1999). High-frequency auditory feedback is not required for adult song maintenance in bengalese finches. J Neurosci 19 (1): 358-371.

Yin, J. C., Wallach, J. S., Del Vecchio, M., Wilder, E. L., Zhou, H., Quinn, W. G., and Tully, T. (1994). Induction of a dominant negative CREB transgene specifically blocks long-term memory in Drosophila. Cell 79 (1): 49-58.

Yu, A. C., and Margoliash, D. (1996). Temporal hierarchical control of singing in birds. Science 273 : 1871-1875.

Zuschratter, W., Gass, P., Herdegen, T., and Scheich, H. (1995). Comparison of frequency specific c-fos expression and fluoro-2-deoxyglucose uptake in auditory cortex of gerbils (Meriones unguiculatus). Euro J Neurosci 7 : 1614-1626.